UNIVERSITY OF SOUTHAMPTON

A Bayesian Belief Network Approach for Modelling Tactical Decision-Making in a Multiple Yacht Race Simulator

By

Thomas Bernhard Spenkuch

Thesis submitted for the degree of Doctor of Philosophy

FACULTY OF ENGINEERING AND THE ENVIRONMENT
FLUID-STRUCTURE INTERACTION RESEARCH GROUP

April 2014

UNIVERSITY OF SOUTHAMPTON

ABSTRACT

FACULTY OF ENGINEERING AND THE ENVIRONMENT
FLUID-STRUCTURE INTERACTION RESEARCH GROUP

Doctor of Philosophy

A BAYESIAN BELIEF NETWORK APPROACH FOR MODELLING TACTICAL DECISION-MAKING IN A MULTIPLE YACHT RACE SIMULATOR

Thomas Bernhard Spenkuch

The importance of human factors has to be taken into account when determining a yacht's performance over a course. The crew's capabilities of technical skills, athletic performance, and his/her ability of making rational decisions under time pressure and in light of uncertainty of the future wind regime are important aspects that will determine the overall performance of a yacht-crew system. This thesis highlights the performance of such a yacht-crew system with a focus on the decision-making process of sailors. Aspects of human behaviour in sport and the decision-making process are explained considering the level of expertise and possible approaches of how to model them are shown. An artificial intelligence AI -system is developed that is capable of simulating the decision-making process of different sailing behaviours/styles as well as different expertise levels of sailors within a dynamically changing yacht racing environment. The constraints of the multiple fleet racing simulator *Robo-Race* (Scarponi 2008) were determined using a series of tests with real sailors identified three important constrains: (1) the predictable behaviour of the AI-yachts, (2) the predictable and unrealistic weather model and (3) the simple model describing the effects of yacht interaction. These restrictions and constraints that limited the real and AI-sailors natural sailing behaviour have been successfully removed in the updated version of *Robo-Race.* The new developed decision-making engine based on Decision Field Theory that uses Bayesian Belief Networks as the perceptual processor showed a clear superiority over the old rule-based decision-making engine. Extensive simulations demonstrate the feasibility of modelling various decision-making processes and therefore different behaviours and expertise levels of sailors. A good comparison was found with that obtained between the *Robo-Race* results and the Olympic fleet racing events.

Table of Contents

List of Figures

List of Tables

DECLARATION OF AUTHORSHIP

I, Thomas Bernhard Spenkuch

declare that the thesis entitled

A BAYESIAN BELIEF NETWORK APPROACH FOR MODELLING TACTICAL DECISION-MAKING IN A MULTIPLE YACHT RACE SIMULATOR

and the work presented in the thesis are both my own, and have been generated by me as the result of my own original research. I confirm that:

- this work was done wholly or mainly while in candidature for a research degree at this University;
- where any part of this thesis has previously been submitted for a degree or any other qualification at this University or any other institution, this has been clearly stated;
- where I have consulted the published work of others, this is always clearly attributed;
- where I have quoted from the work of others, the source is always given. With the exception of such quotations, this thesis is entirely my own work;
- I have acknowledged all main sources of help;
- where the thesis is based on work done by myself jointly with others, I have made clear exactly what was done by others and what I have contributed myself;
- none of this work has been published before submission

Signed: ……..

Date: …….

Acknowledgements

I would like to thank all the people involved in helping me complete this dissertation. In particular I would like to thank my supervisors Prof. Stephen Turnock and Prof. Ajit Shenoi for their grateful guidance and helpful support throughout the entire project.

The human in the loop experiments would not have been possible without the support of Dr. Kenji Takeda who helped to set up the advanced display environment for the yacht fleet simulator experiment in the Flight Simulator Laboratory of the University of Southampton.

Many thanks go to my supervisor, colleagues and friends, Prof. Stephen Turnock, Dr. Kenji Takeda, Dr. Matteo Scarponi, Dr. Rachel Blackburn, Dr. Sally Bennett, Dr. Simon Lewis, Dr. James Roche, Dr. Markus Weinmann, and Dr. Richard Frühmann, for participating in human in the loop experiments.

Finally, I would like to thank my parents and Nina, they are the reason I have made it so far. Without their sacrifices and continual support, it would not have been possible for me to have achieved what I have – Many Thanks.

Nomenclature

Latin Characters:

C	Contrast Matrix	[-]
CD	Drag Coefficient	[-]
CL	Lift Coefficient	[-]
CL, CD	Lift and drag coefficient	[-]
D	Displacement Vector	[m]
E	Expected Preference Value	[-]
L	Sail rig and yacht length	[m]
M	Value Matrix	[-]
M_t	Wind direction within the bend air region	[deg]
P	Probability	[-]
Q	Induced Velocity Vector	[m/s]
R_{bent}	Bent Air Region Radius	[m]
R_{turb}	Turbulent Air Region Radius	[m]
S	Sail Area	[m^2]
T	Time	[s]
U	Velocity	[m/s]
UAW	Apparent Wind Velocity	[m/s]
U_o	Free stream Velocity	[m/s]
$U_{viscous}$	Viscous Velocity	[m/s]
U_θ	Tangential Velocity	[m/s]
V	Valence	[-]
V_A	Apparent Wind Velocity	[m/s]

V_s	Yacht Velocity	[m/s]
V_t	Wind speed within the turbulent and bend air region	[m/s]
V_T	True Wind Velocity	[m/s]
W	Weight Vector	[-]
WD	Wind Direction	[deg]
WS	Wind Speed	[m/s]
YL	Yacht Lengths	[m]
f	factor	[-]
h	Vortex Core Height above Sea Level	[m]
p	percentage reduction for the wind speed in the turbulent region	[-]
q	Variance of the random wind components	[-]
r	radial distance	[m]
u	Velocity	[m/s]
u, v, w	Induced velocities in x-, y-, -z directions	[m/s]

Greek Characters:

$ß_t$	Apparent Wind Angle	[deg]
Γ	Intensity of horse shoe vortex	[1/s]
γ	True Wind Angle, the angle relative to the centreline of the turbulent cone projected by the sailplane	[deg]
$Γ_i$	Vortex strength of element i	[1/s]
δ	Boom angle	[deg]
δ	Boom Angle	[deg]
ε	White Noise	[-]
Θ	Momentum Thickness	[m]
θ	Interval Boundary Angle	[deg]
θ	Weather Model Parameter	[-]
λ	Distance along vortex element	[m]
ρ	Density	[kg/m^3]

ρ_{air}	Density of air	[kg/m^3]
σ_i	Vortex Core Size	[m]
φ	Weather Model Parameter	[-]
ω	Vorticity	[1/s]

Subscripts:

A	Air
app	Apparent
bc	Boundary Condition
fluc	Fluctuating
lat	Lateral
long	Longitudinal
mean	Mean
off45°	Difference between actual angle and 45°angle
ramp	Ramp
t	Turbulent

Glossary of Terms

ACC	America's Cup Class
ADE	Advanced Display Environment
AI	Artificial Intelligence
AoA	Angle of Attack
ARMA	Autoregressive Moving Average
AWA	Apparent Wind Angle
AI	Artificial Intelligence
BBN	Bayesian Belief Network
BDE	Basic Display Environment
CLR	Centre of Lateral Resistance
CFD	Computational Fluid Dynamics
DFT	Decision Field Theory
DoF	Degree of Freedom
DSYHS	Delft Systematic Yacht Hull Series
DNS	Direct Numerical Simulation
EBA	Elimination-by-Aspects
EDFT	Extended Decision Field Theory
EQW	Equal Weight Additive Value
EDFS	Extended Decision Field Theory
FOV	Field of View
FPS	First Person Shooter
HCI	Human Computer Interface
HMD	Helmet-mounted Display
IACC	International America's Cup Class

IMS	International Measurement System
LES	Large Eddies Simulation
LEX	Lexicographic
LLM	Lifting Line Method
ML	Machine Learning
MCD	Majority of Confirming Dimension Rule
MIT	Massachusetts Institute of Technology
NB	Node Bottom
NBI	Node Bottom Image
NT	Node Top
NTI	Node Top Image
NWM	New Wake Model
PID	Proportional Integral Derivative
PM	Philpott Model
RB	Rule-based
RMP	Race Modelling Program
RRS	Racing Rules of Sailing
RAND	Random Choice
RT-VPP	Real Time Velocity Prediction Program
RANS	Reynolds-averaged Navier–Stokes
SAT	Satisfying
TTB	Take The Best
TWA	True Wind Angle
TWS	True Wind Speed
VPP	Velocity Prediction Program
VE	Virtual Reality
VRML	Virtual Reality Modelling Language
WADD	Weighted Additive Value
WSD	Wide Screen Display
YL	Yacht Length

1 Introduction

Sailing is a sport where sailors seek to extract the best performance out of their yacht whilst competing with other crews. The sailors are part of the complex system called a sailing yacht and have to interact with it according to the dynamically changing sailing environment, such as wind and sea state conditions, and opponents. Consequently, the sailor's decisions and behaviours according to these environmental changes are very important in order to perform well and finally to win a race. Strategic and tactical decisions of the sailors are executed by changing the sail setup and rudder angle. Based on their expertise and behaviour, the sailors interpret the changing environment differently, pick up various cues and make a decision followed by an execution of an action. This study examine and simulates the decision-making process of sailors featuring different levels of expertise as well as different sailing behaviours in such a dynamic sports environment and provides a possible way to describe this complex task. Consequently, the following two research questions are crucial for this work: (1) how can an adequate decision-making process be implemented into a multiple yacht fleet racing environment and (2) how can it be tested and evaluated to demonstrate its performance. The challenge consist of the confluence of tactical decision-making, understanding yacht response and performing these tests within an uncertain and fuzzy environment which all rely on the interaction of the sailor with the system.

1.1 Context

A sailing yacht is a complex system consisting of two major components: (1) the actual sailing yacht and (2) the crew controlling it. These two systems have to interact perfectly

with each other and both are at the state of their art in order to win a specific race or more usually a regatta. Regarding the sailing yacht, the hull design and the sail rig have to be designed for this particular campaign using the latest achievements of research. This leads to almost identical performing sailing yachts and puts more pressure on the crew as they have the greatest potential for improvement. This effect even increases if a regatta features just one type of yacht (one design). Consequently to win a race the crew has to make the right strategic and tactical decisions at the right time. Reading a race and the environmental cues influences these decisions and depend on expertise, experience, personality, and attitude.

To overcome the challenge describing the decision-making process and behaviour of sailors in a dynamically changing environment, an appropriate investigation tool in the form of a fleet race sailing simulator has to be used. Numerous test series of America's Cup Class (ACC) yachts were carried out at the University of Southampton and the Wolfson Unit for Marine Technology and Industrial Aerodynamics. Therefore, a variety of different yacht and sail rig data were available and explain the reason the ACC yacht type has been chosen for this work. The America's Cup (AC) is the longest standing sporting trophy in the world and symbolises a lot of prestige and differs from class racing or the Olympics, as it consists of match races where nations from yacht clubs race against each other. Other well known races like the Volvo Ocean race or the Louis Vuitton Cup become more popular and attract more spectators and hence more funding. This leads to a positive side effect providing the teams with more money that goes directly into research to design the best performing yacht. Unfortunately, the most AC challenge, the 33rd that took place in Valencia, Spain in 2010 was more a design competition rather than a sailing competition. The match was sailed in enormous 90ft multihull yachts whereas the challenging team *BMW Oracle Racing* designed a trimaran *USA-17* equipped with a rigid wing sail providing a gigantic thrust throughout the course and led to a safe and unspectacular 2-0 win against the defending team *Alinghi* racing the conventional designed catamaran *Alinghi 5*. The sailing community agreed that this AC challenge went in the wrong direction and should return to its roots focusing on pure sailing and therefore skills of the crew. It looks promising that the participants of the next, the 34th AC challenge took this criticism to heart and agreed to a more sailing skilled based competition.

The 32nd AC challenge which took place in Valencia in 2007 showed an average racing time for finishing the course of around 92 minutes. The corresponding time

differences between winning and losing a race differed from a maximum of 35 seconds down to a minimum of just one second. This can be explained by the highly developed sailing yachts and their marginal differences in terms of sailing performance. Consequently the strategies, tactics, behaviour, decision-making and expertise of the crew are essential for the overall performance of the sailing yacht and can represent the difference between winning and losing.

In contrast to match racing where just two yachts are sailing against each other, fleet races consist of numerous participating yachts racing against each other. In all sailing events, blanketing and covering are important tactical weapons and have to be modelled in an advanced fleet race sailing simulator as it is intended in this study. Therefore, developing a model which describes the complex yacht interaction flow behaviour seems to be essential for this work.

As mentioned earlier, because of the racing rules and the therefore application of similar engineering approaches and tools by the design teams, the differences of the yachts are lessening. Consequently, the most potential to enhance the yacht performance is seen in the performance of the crews. Especially making the right decisions at the right time in terms of changing weather conditions and aggressive opponents are crucial to win a race. Therefore, it would be advantageous for yacht crews to have an advanced tactical training yacht simulator provided which allows them to investigate human behaviour within a fleet racing competition environment. The crews could benefit from the training and preparation for different race scenarios. Furthermore, they could train how to race against an individual crew/sailor or a special type of crew/sailor. This work focuses on these aspects and will be a major step forward in that direction as it finds and describes ways to describe human behaviour within a race or regatta in which the successful yacht-crew-environment interaction and its modelling plays a significant part.

1.2 Aims and Objectives

The overall aim of this project is the successful development and implementation of an advanced method capable to describe the human decision-making process in a complex and dynamically changing yacht fleet racing environment. Furthermore, this study aims to provide a yacht sailing simulator that can be used as a training tool to analyse and to

improve the performance of the athlete. To achieve these aims significant challenges have to be solved that create the objectives of this project and are described as follows:

- Determine the development stage and possible improvements of the sailing simulator *Robo-Race* (Scarponi *et al.*, 2007; Scarponi, 2008) through performing a series of regattas where international experienced sailors race against other yachts crewed by an Artificial Intelligence (AI). This is achieved by carrying out a combination of interviews and questionnaires designed to state the simulator's level and to find possible improvements in terms of yacht dynamics, virtual reality, human computer interaction and display-input device-environments.
- Carry out an investigation with the author's improved version of *Robo-Race* to examine the effect on sailors' performance of enhancing the realism of the simulation through the application of an advanced display-input device-environment consisting of a steering wheel, joystick, 17" flat screen and three projectors.
- Examine how well Computational Fluid Dynamics (CFD) predicts the performance of a sail rig assessed against wind tunnel data. The CFD study is carried out for gaining detailed information about the complex wake flow of a typical sail rig and a pair of in-line upwind sailing yachts used to evaluate a real-time lifting line approach.
- Enhancing the interaction of the yachts in *Robo-Race* by developing, evaluating, and implementing a model based on lifting line theory for modelling covering and blanketing effects for yacht fleet simulation.
- Development of a weather model which captures reasonably well the stochastic nature of the wind environment and its implementation into *Robo-Race.* The model imitates different dynamically changing sailing environments realistically and spectral analysis are carried out and compared to those of recorded data through Fourier Transform calculation.
- Development of a dynamic behaviour and decision-making model that captures different levels of expertise and personalities of sailors. A Decision Field Theory (DFT) approach using Bayesian Believe Networks (BBN) is introduced to deal with decision of a tactical and strategic nature. The derived decisions are based on the yacht's actual race position on the race course, her relative position against multiple opponents and the dynamically changing weather conditions.

The reader has to bear in mind that this work focuses on improvements, applications and models which allow the sailing yacht simulator *Robo-Race* to run in real-time. Therefore, any developed tool in this study has to provide an authentic improvement to the simulator, has to be implementable within a realistic computational budget, and has to provide the best payoff regarding the used computational resource.

1.3 Novelty

A literature review (see Chapters 3 and 4) has shown that simulating human behaviour in a yacht fleet race environment has not been investigated intensively yet. Approaches such as the use of a look-up table for decision-making led to satisfactory results (Scarponi *et al.*, 2007; Scarponi, 2008). The applied human behaviour model in *Robo-Race* (version 2008) consists of a rule-based approach based on questionnaires and can be seen as a regulatory series of if-sentences that are limited by specific rules and regulations. This approach is considered to be valuable and can be used as a starting point to investigate human behaviour but it is also considered to be inappropriate for further steps. It can be criticised as immobile, not 'fuzzy', strict, and becomes very complex the more scenarios are captured and the more yachts are participating in a regatta. It is considered that human behaviour is much more comprehensive and complex especially in a dynamic environment, such as yacht racing. It is further believed that a highly developed human decision-making model cannot be realised using a rule-based approach since this lower level method would not be capable of dealing with all of the challenges.

The novelty of this research consists in developing a yacht fleet racing simulator that is capable of capturing some aspects of human behaviour and high decision-making in a dynamically changing yacht fleet racing environment. One part of originality is achieved by developing a state of the art method for describing human behaviour in sailing regarding the sailor's character and level of expertise and by implementing the corresponding decision-making process successfully in an advanced version of the sailing simulator *Robo-Race*. This study will be the first investigated decision-making study based on what up to six opponents are doing within a realistic yacht fleet racing environment focusing on decisions making and tactical interaction. The corresponding decision-making process can

be described as sensitive where little changes can have a great influence on the results. Therefore, the basis on which the decisions are made have to be described and simulated in an appropriate way. Consequently, a realistic yacht fleet racing environment has been provided where real and artificially intelligence (AI)-based sailors race against each other. This sophisticated environment features a stochastic and natural weather engine as well as a model that describes the complex interaction of yachts realistically since it is a crucial aspect in yacht sailing competitions.

Realising the sophisticated environment led to another part of originality that is expressed by developing a superior model for describing the covering and blanketing effect of sailing yachts based on the lifting line theory assessed against CFD data. A further part of novelty is introduced by the implementation of the stochastic weather model assuring the uncertainty, unpredictability, and dynamic sailing environment.

In summary, the novelty and originality of this work represents the outcome of all these contributions mentioned above leading to a superior yacht fleet racing simulator that provides a dynamically changing and realistic race competition environment. The sophisticated decision-making engine of the simulator is capable of mimicking different sailing styles/behaviours as well as different expertise levels of the sailor/crew and even the simulation of a real human sailor's behaviour would be feasible. To date no similar research investigating and modelling human decision-making in sailing has not been investigated and published as of yet.

1.4 Layout of Thesis

This document is subdivided into three main parts: firstly, the study of relevant available knowledge covered in Chapter 2 to 4. Secondly, the application and implementation of this knowledge to provide a realistic fleet racing environment (Chapters 5 to 7). Thirdly, the development of a sophisticated decision-making engine and its validation throughout extensive studies are shown in Chapters 8 to 9. The thesis is completed by a discussion concluding the achievements of the chosen approaches and potential future projects are highlighted.

The first part starts with an overview of recent studies in the field of human-psychological-physical systems. The general introduction is followed by the individual parts; namely, the description of dynamic models for sailing yachts, followed by a survey of possible sailing simulator setups with respect to human-computer interaction factors and accompanied by the human's behaviour, especially in yacht racing which is covered in the forth section.

In Chapter 2, the document deals with an historical journey about the performance determination of a sailing yacht and available models describing the motion of it. Special attention will be paid on manoeuvring, such as tacking, gybing and speed recovery. Furthermore, the interaction between yachts and models capturing this aspect are also described in this chapter.

The aspects of human behaviour in sport with a special focus on yacht racing will be captured in Chapter 3. Thereby, the decision-making process considering the level of expertise and different approaches of how to model the 'human in the loop' will be discovered. Furthermore, an alternative, such as an intelligent decision-making algorithm is discussed and compared to the rule-based approach in *Robo-Race* (Scarponi, 2008). How to deal with decision-making in Artificial Intelligence (AI) and in the world of sports are described and agent technologies and modelling are highlighted.

Chapter 4 gives the reader an understanding of the recent approaches to determine yacht performance using sailing simulators, where special attention is paid to their capability in modelling yacht-crew systems and human behaviour. For this study, the sailing yacht simulator *Robo-Race* is used and therefore explained in detail (Scarponi *et al.*, 2006; Scarponi *et al.*, 2007; Scarponi, 2008). In short, *Robo-Race* is an unsteady velocity prediction program (VPP) to which behavioural models are added and real sailors can interact with the software as a 'human-in-the-loop'. This is followed by possible human-computer interaction devices and environments, regarding their potential, benefit and drawbacks in order to complete the aspects of hardware and software relevant for this research.

The second section, Chapters 5 to 7, deals with 'human in the loop' studies and resultant improvement for the sailing simulator *Robo-Race*. Chapter 5 describes a series of 'human in the loop' experiments in order to (1) examine the effect on sailor performance by enhancing the realism of the simulation and (2) to determine the level and potential

improvements of the simulator. For the first purpose, two different human interface device/display environments are designed and the effect on the sailor's behaviour and performance sailing upwind races against two computer controlled ACC yachts are compared. For the second purpose, the participants have been observed during these sailing sessions and a subsequent analysis of questionnaires is used as a basis for indicating relevant improvements of *Robo-Race* in order to support the natural behaviour of the sailors.

Chapter 6 deals with the development of one of the most critical constraints of *Robo-Race* regarding the sailors' feedback, the weather model. The sailors rated it to be very predictable and therefore it is replaced by a stochastic and unpredictable weather model which distinguishes between wind speed and wind direction for assuring variations in longitudinal and lateral direction. The dynamic wind environment is ensured by using an autoregressive moving average (ARMA) process for both wind variables whereas this process is coupled with Markov chains for the wind direction to assure wind shifts with variation around a wind mean direction.

As suggested from the research carried out in Chapter 5, Chapter 7 describes the development of an advanced model for simulating interaction of sailing yachts. This model is based on the lifting line theory and completed with a viscous wake model of the sailing yacht. Extensive sensitivity studies investigating the number of used vortex elements are shown and the model's superiority over the previous implemented analytical based wake model is demonstrated in various upwind leg scenarios. The New Wake Model (NWM) benefits from CFD results which are used to support the new covering and blanketing model. The initial strength of the combined main-jib vortex system and its vertical height are determined with use of the CFD studies. A detailed examination of the performance of a typical upwind sail rig arrangement for one or two yachts in-line is performed using a commercial CFD solver and can be found in Appendix A1. Experimental wind tunnel data provided by the Wolfson Unit for Marine Technology and Industrial Aerodynamics are used to validate the calculated CFD results.

In order to improve the physical fidelity of a collapsing asymmetric spinnaker results of dynamic test are used to improve the aerodynamic force model in *Robo-Race*. This led to a

reduction of yacht speed during a gybe which symbolises a closer representation of the real life manoeuvre and can be found in Appendix A2.

The third section starts with Chapter 8 which deals with the simulation of decision-making and tactical interactions in a dynamic yacht fleet racing simulator environment. An introduction to Bayesian Belief Networks (BBN) is given and the gradual development starting with a basic BBN for single yachts towards a superior BBN able to deal with long term goals of a regatta are highlighted. The basic network starts with basic functions focusing on spatial position of a yacht on the race course whereas the superior network also focuses on multiple opponents and the interaction of yachts. The function of the Decision Field Theory (DFT) BBN based decision-making engine is explained and case studies featuring the basic and superior BBN used as the perceptual processor are highlighted. Different sailing behaviours and styles, such as risky, safe and balanced and three different levels of sailing expertise, such as skilled, intermediate, and expert, have been developed and implemented. Extensive sensitivity studies investigating the effect of different weather scenarios and the effect of different starting positions on the performance of the yachts are carried out.

The performance of the new decision-making approach on the race course is shown in Chapter 9. There, yachts controlled by the new decision-making engine, the so called Bayesian-Belief-Network yachts (BBN yachts) had to compete with yachts controlled by the former implemented decision-making engine, the so called rule-based yachts (RB yachts). Two different fleet racing competitions, a small one consisting of four yachts (three BBN and one RB yacht) and a bigger one with seven yachts (three BBN and four RB yachts) have been set up. The fleet racing competitions feature different levels of expertise and the differences in performance between the various BBN yachts among each other and the RB yachts are analysed. At the end of Chapter 9, the two developed fleet racing competition setups are used to provide a link back to real sailing. Therefore, the procedure of the Olympic fleet races have been copied and schematically embedded into the *Robo-Race* framework. The ‘Olympic’ *Robo-Race* results and the Olympic fleet racing competitions are analysed and used to classify the quality of the *Robo-Race* fleet racing simulations.

Finally, this study finishes with Chapter 10 that discusses and summarises the achievements of this project. Thereby, the individual benefit and contribution of each improvement of *Robo-Race* regarding the aims and objectives of this work are highlighted and their contribution to the sailing community is explained. Moreover, further developments of the sailing simulator are highlighted and their individual benefit is discussed.

2 Dynamic Models for Sailing Yachts

This chapter provides a general overview about the mechanics of a sailing yacht, the historical development of sailing simulators, and important tools for a reliable realisation of those. Yacht motion models are described by giving an overview of the existing dynamic models and special manoeuvre challenges like tacking, jibing and rounding the mark are highlighted. Furthermore, special attention is paid to yacht interactions and existing models describing this phenomenon.

2.1 The Sailing Yacht

A sailing yacht can be considered as a system which is driven through the water by various forces. These forces can be classified by different aerodynamic and hydrodynamic forces which act on a sailing yacht.

The flow around a sailing yacht creates different forces. The lift and drag forces are produced by the flow around the sail and always operate at right angles to each other. These aerodynamic forces drive the sailing yacht and therefore the hull, through the water whereby a certain amount of resistance is developed by the hull. The driving force which is generated by the sail has to balance this resistance under equilibrium conditions when the sailing vessel is moving at constant velocity in a given direction.

Figure 1 shows that all resulting forces act along the same line and the sail drive force cannot be generated without an aerodynamic side force, which in turn must be balanced by a hydrodynamic side force. The latter is developed by the keel and the angle of leeway.

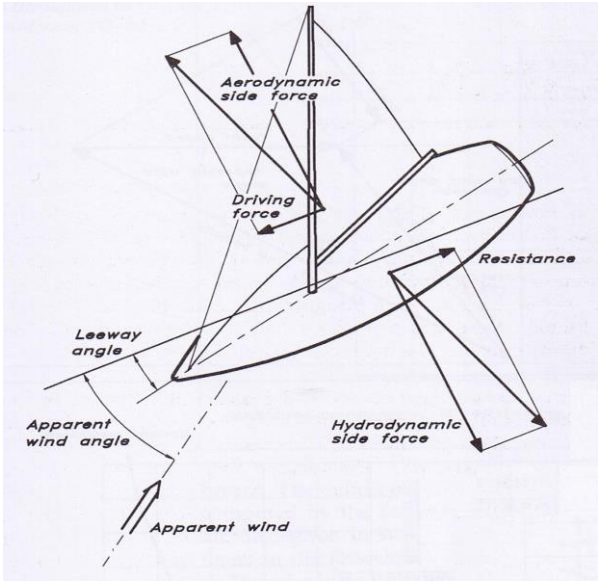

Figure 1: Forces on a sailing yacht, horizontal view (Larrson, 2000)

The following Figure 2 shows the view along the direction of motion. The common used approximation in sailing yacht theory simplifies the acting forces on the sailing vessel. It is assumed that the aero- and hydrodynamic forces act at right angles to the mast. The heeling moment created by the flow around the sail is balanced by the righting momentum from the buoyancy force and the weight.

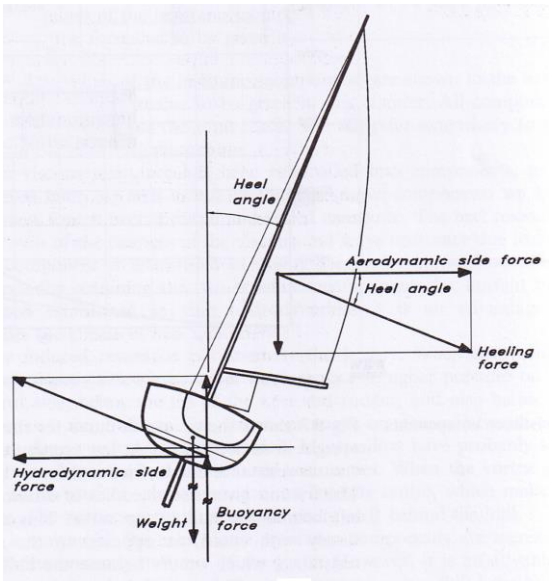

Figure 2: Forces on a sailing yacht, vertical view (Larrson, 2000)

The right-hand rule is a common way to describe the coordinate definitions for a sailing yacht. There, the system is defined as follows: the positive x-direction as towards the bow, the positive y-direction as port, and the positive z-direction upwards (see Figure 3). The motions of the yacht are described considering the coordinate axis as follows (Figure 3):

- Surge is the longitudinal translation
- Sway is the transverse translation
- Heave is the vertical translation
- Roll is the rotation about the x-axis
- Pitch is the rotation about the y-axis
- Yaw is the rotation about the z-axis

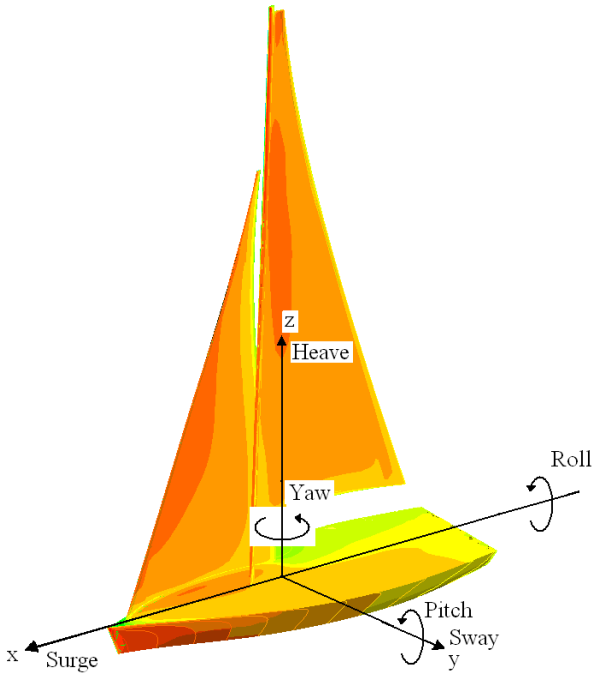

Figure 3: Coordinate system and yacht motion system (Spenkuch, 2006)

2.2 Apparent Wind Angle and Twist

In considering a forward moving sailing vessel, the true wind angle is not the wind angle which acts on the sails. Wind directions are determined relative to the track of the sailing vessel, which due to the acting aero- and hydrodynamic forces is at an angle β, known as the apparent wind angle (AWA) (see Figure 4). The apparent wind vector, V_A, which acts

on the sails of moving sailing yacht is the resultant wind composed of the vectors of the true wind velocity, V_T, and the yacht speed, V_S, as illustrated in Figure 4. This figure also shows that the apparent wind velocity is greater than the true wind velocity. The apparent wind over the sails depends on the following factors:

- The angle between the yacht's course and the true wind direction, γ
- The speed of the yacht, V_S
- Variation in the true wind velocity, V_T, at different heights above the sea
- Rolling of the yacht
- Pitching of the yacht

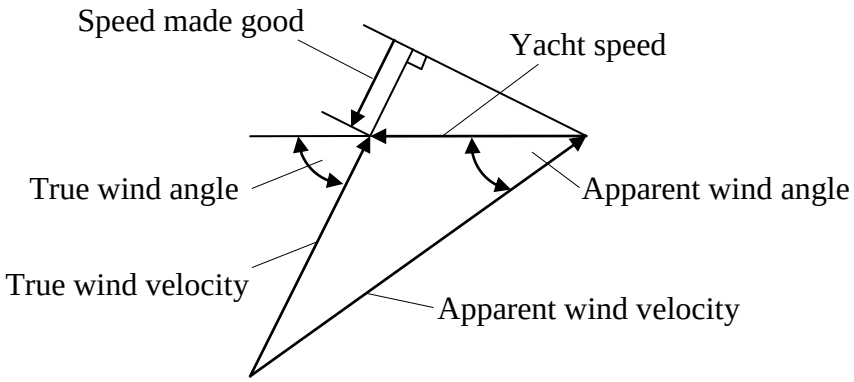

Figure 4: Vector triangle

The wind speed in free air increases with height above the sea or land. The wind gradient occurs due to the friction of the air moving over the surface of the water.

Therefore, the effect of the wind gradient has to be combined with the wind angle triangle that can be seen above in Figure 4. This effect results in a wind profile that changes in magnitude and direction with increasing height (see Figure 5). This updated flow shape is known as the so-called twisted flow. Figure 5 illustrates the twisted flow - blue represents the resultant twisted apparent flow, red the boundary layer effect and green the advance velocity.

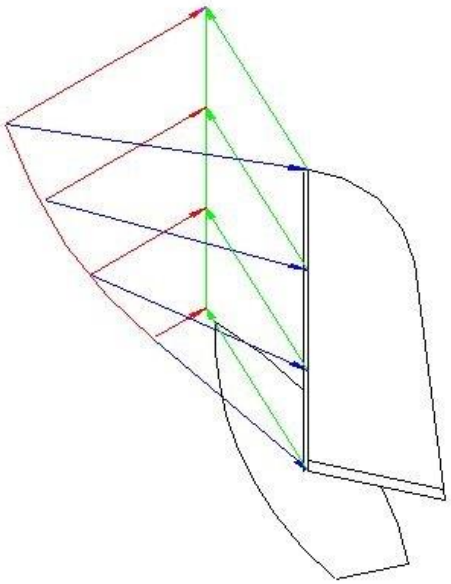

Figure 5: Twisted wind flow (Yacht Research Unit, University of Auckland)

2.3 From VPPs to RMPs and further

The basis of modern sailing simulators was provided in the late 1970's by the Irving Pratt Project realised at the Massachusetts Institute of Technology (MIT). This project tried to predict the surge speed of a yacht based on a limited number of design parameters which can be seen as the first important step of the development of Velocity Prediction Programs (VPPs) and the later sailing simulators (Kerwin and Newman, 1979). The focus on surge speed is straightforward as it is the most evident index for a yacht's performance. The VPP aims to predict the steady sailing condition at any given point of sail and wind speed. Modern VPPs are still using these principles, namely by determining the equilibrium condition for a yacht by iteratively equalising the hydrodynamic and aerodynamic forces acting on the hull and sail rig for every point of sail and wind speed.

One of the important outcomes of the Irving Pratt Project was a VPP that represented the creation of the International Measurement System (IMS) race handicapping system. Over the years, this system was improved and is still being upgraded, by using improved models, for instance the prediction of the hull resistance (Claughton, 1999) and downwind sail flow behaviour.

Another reasonably accurate input to VPP can be made by using Computational Fluid Dynamics (CFD). Due to the great progress of CFD in the recent years, the development of an entirely numerical based VPP is an alternative to conventional-experiment based procedure as it can deliver results with a reasonable degree of confidence (Rosen *et al.*, 2000). The progress in CFD calculations is based on the rapid increase in computational power and the connected realisation of more accurate turbulence models. For instance, the aerodynamic and hydrodynamic forces acting on the hull-sail system are solved by a Reynolds-Average-Navier-Stokes (RANS) turbulence model that was constantly improved (Korpus, 2007). According to Korpus, the use of a numerical solver in conjunction with turbulence models provides a clear advantage in early stages on a project when different new hull and sail designs are compared. The drawback of this method is the requirement for large computational resources which rises for advanced turbulence models. On the other hand, as computation power will increase in future, there is no doubt that models like Large Eddy Simulation (LES), Direct Numerical Simulation (DNS) or a mixture of both will be used as a data source for VPPs and therefore in the evaluation process of different boat designs in the near future.

The next important step in the development of sailing simulators was the implementation of non-deterministic (stochastic) variables to VPPs. For instance, the sea state and wind conditions as they have an important influence in the yacht's performance. Consequently, VPPs were improved by using weather probabilistic models and designed as Race Modelling Programs (RMPs). This application was necessary as an evaluation of a design candidate's performance only based on VPP results is potentially 'inconclusive and possibly misleading for determining the order of merit of two candidate yachts over a series of races' (Lechter *et al.*, 1987). The first 'commercial' use of RMPs was carried out for the America's Cup in 1992 where the *Stars and Stripes* design team combined VPP with weather and sea state data collected over one decade at the race events location (Todter *et al.*, 1993). By focusing on the estimated win/loss percentages for a pair of boats involved in a match-race, the RMP results helped to select the best available boat design.

A further step in the development of VPP was made by Hansen *et al*. (2005) who developed a Real-Time Velocity Prediction (RT-VPP) by applying a procedure for obtaining real-time velocity predictions for a yacht in the wind tunnel while the sails are trimmed. This technique gives a more realistic situation of sail trimming in the wind tunnel

and ‘the performance of a sail is now apparent right away and not only after post processing of the data’ (Hansen *et al*., 2005).

After the major steps mentioned above, researchers ‘opened’ the domain of interest as yacht design and the correspondent yacht’s performance should not only be based on steady state considerations. Therefore, important aspects that occur during a race and influence the overall yacht performance have to be taken into account when determining the performance of a yacht. These aspects, like manoeuvrability, speed recovery, tactics and strategy became objects of research. In recent years researchers dealt with those, namely the evolution of an optimal tacking procedure (Keuning *et al.*, 2005), the simulation of yacht racing on upwind course focusing on the yacht’s motion in waves (Harris, 2005) or the interaction with an adversary (Roncin, 2002).

An advanced approach to close the lack of knowledge of how crew expertise, tactics/strategies influence the yacht performance in a stochastic weather environment was carried out by (Scarponi *et al.*, 2006; Scarponi *et al.*, 2007; Scarponi, 2008). There, a solo yacht racing simulator allowed the systematically investigation of a yacht-crew system by adding behaviour models to VPPs (Scarponi, 2007). It was proven that different crew expertises have a remarkable influence of the overall yacht performance within a race. This yacht-crew simulator system will be explicitly explained in Chapter 4. Furthermore, the studies in yachts motion, manoeuvrability and interaction between yachts mentioned above are explained in the following three subchapters in more detail.

2.4 Dynamic Models

The studies considered earlier indicate that factors like the manoeuvrability, the ability of speed recovering and ground after tacking are important aspects with regard to the dynamic motion of a sailing yacht.

The published work in this area of sailing yacht manoeuvring was done in Japan at the Kanazawa Institute of Technology by the research ground supervised by Professor Y. Masuyama. His paper published in 1993 was the initialisation for this aspect of numerical

modelling of sailing yachts. The presented dynamic model used a set of four partial differential equations and was than evaluated to a set of experimental results gathered from full-scale tests in calm water on a 10.6m cruiser (Masuyama *et al.* 1993). This four Degree of Freedom (DoF) model is built on previous work by Nomoto (Nomoto *et al.*, 1975) and takes into account surge, sway, heel and yaw (see Figure 3). An updated version of this model was presented in 1995, where particular attention was paid to the hydrodynamic derivatives in the equation of motion in order to achieve a more accurate prediction to the experimental results (Masuyama *et al.*, 1995). The scope of this paper was the investigation of the tacking dynamics and the detection of the best available tacking procedure. Furthermore, a second approach to represent the tacking motion of sailing yachts was highlighted, the neural network model, as an alternative to the application of the partial differential equation model. The mathematical model showed good correlation with the experimental results and the mechanism of tacking in detail could be highlighted and furthermore, the most important aspects for an optimal tacking could be found. The neural network model was judge to be improvable as 'the accuracy is not yet sufficient to indicate the delicate differences by the steering procedures' (Masuyama *et al.*, 1995).

A mathematical model for the manoeuvring of a sailing yacht was presented in the Netherlands at the Delft University of Technology by the researchers Keuning *et al.* (2005). This model used the approach of Masuyama described above. The starting point was when the authors published an improved approach of determining the Centre of Lateral Resistance (CLR) of a yacht hull whereby the estimation of the yacht's manoeuvring abilities could be improved (Keuning and Vermeulen, 2002). This work was extended to include a mathematical model for the tacking procedure of a sailing yacht that can be applied to a wide range of yachts (Keuning *et al.*, 2005). In this approach, a set of equations were used containing only coefficients which can be calculated from the yacht's design data. Therefore, experimental results are unnecessary as the so-called 'generic' parameters describing the hull form, appendages, and the sail plan are used from the available data of the Delft Systematic Yacht Hull Series (DSYHS) (Gerritsma *et al.*, 1981). Full scale measurement on tacking manoeuvres for three different yachts and the mathematical model have shown good correlations in the speed and time loss while tacking (see Figure 6).

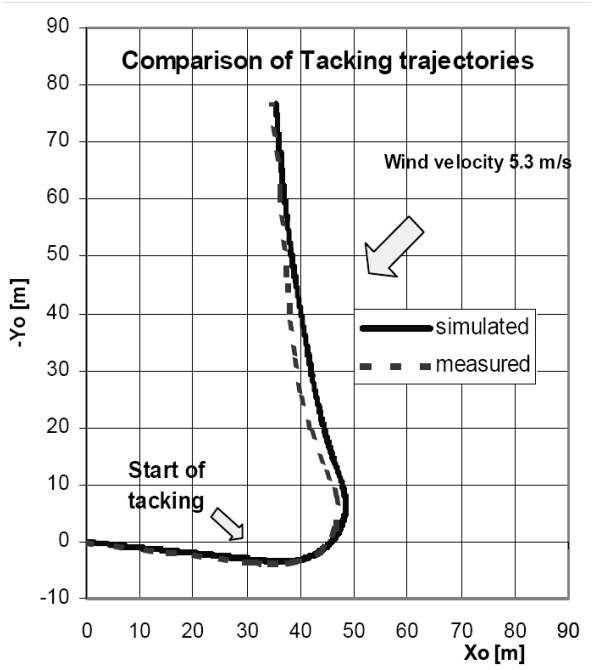

Figure 6: Tacking trajectories of a simulated and measured track of a half-tonner (taken from de Ridder *et al.*, 2004)

With this study 'a reasonably reliable tool for the prediction of the manoeuvring behaviour of a sailing yacht is developed' but it has and will be further refined, as at present the aerodynamic model is not able to distinguish between different sail settings and trimmings accurately (Keuning and Vermeulen, 2007). The subsequent research project of Keuning and Vermeulen (2007) dealt with the calculation of the forces on the keel and rudder of a sailing yacht and the interaction between them. To Keuning's belief, a closer prediction of this phenomenon was necessary. In particular, a good estimation on these forces are required as they influence the yaw moment to a large amount, which in turns provides a more accurate prediction of the yaw balance and the manoeuvring capabilities of the yacht. Based on experimental results, a new formulation for the downwash behind the keel with variable aspect ratio and leeway angle was found which provides a more reliable assessment of the yaw balance. Furthermore, a significant influence of the aspect ratio of the keel on the downwash angle 'seen' by the rudder was also concluded. A publication in 2007 dealt with an improved model in which coefficients were fine tuned to fit the German IACC contender for the optimisation of the tacking procedure (Keuning *et al.*, 2007). The results of the simulations compared with real time measurement data have shown good agreement. The dedicated model in conjunction with experimental data allowed a prediction of the effective attack angle of the rudder in order to find the best tacking

manoeuvre. The research group around Prof. Keuning still works on improvement of their generic mathematical model and therefore, it is has to be regarded as a possible candidate for future work of this research project.

2.5 Yacht Interaction

Two factors have to be regarded when dealing with yacht interaction. On one side the Racing Rules of Sailing (RRS) should be taken into account to ensure a fair race. On the other side, models accounting for blanketing (covering) effects should also be captured when setting up a realistic sailing simulator as those two factors are important strategical and tactical tools for the sailor within a race. Furthermore, simulating yacht interaction improves the level of reality of the sailing simulator more realistic which in turn supports the sailor's natural sailing behaviour.

2.5.1 Racing Rules of Sailing

The conduct of yacht racing and therefore the interactions between two or more yachts within a regatta are regulated through RRS. To the author's believe, simulators capturing all available rules are not present. This is because relatively simple situations, such as port-starboard crossing become very complicated when a crew's individual judgements are taken into account and consequently the opportunities for modelling them are very extensive when considering all possible race situations. Simulators focus on specific rules which are present by a basic set of collision avoidance rules which yielded to satisfactory results (Philpott *et al.*, 2004 and Scarponi *et al.*, 2007). Regarding the latter issue of port-starboard crossing. Scarponi (2007) used an approach which estimated the likelihood of a port-starboard collision by a decision-making tree based on questionnaires and controlled the yacht actions according to the crew's skill setup. Regarding this simple situation, it is quite obvious that sailing yacht designers focused on the hydrodynamic and aerodynamic models and did not focus on the simulation of the RRS when determining the yacht's performance within a regatta.

2.5.2 Blanketing Effect

The wind conditions ‘seen’ on a sailing yacht are affected by the presence of another yacht sailing in close proximity. The perturbations generated by the upwind yacht depend on its sailed course and sail rig. In particular, these perturbations have a great effect on the flow propagating downwind and are therefore an important tactical tool, especially in downwind match racing. Hence, the tactical decisions of both the upwind and downwind yacht are made by maximising blanketing or minimise its damaging effects (Parolini *et al*., 2005). The so-called wind shadow occurs as the flow passing the windward yacht interacts with the wind gradient and alters in a disturbed flow that in turn affects the downwind yacht sailing in this affected region (see Figures 7 and 8).

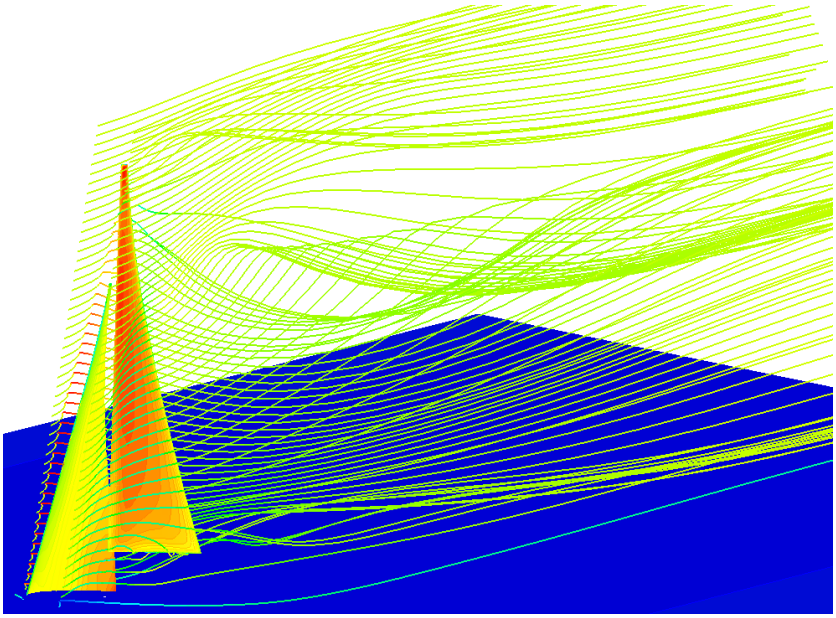

Figure 7: Blanketing effect: local pressure contour on sails and streamlines to identify the vortices in the wake. 3D RANS CFD calculation, 27deg AoA and 10deg heeled yacht (Spenkuch, 2006).

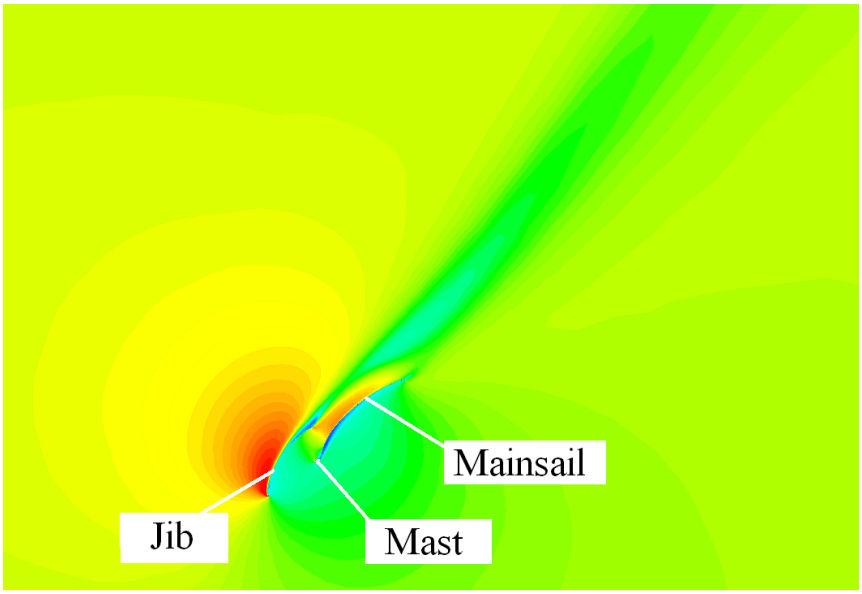

Figure 8: Blanketing Effect: plane section of 3D RANS CFD calculation showing velocity contour, height 1meter, 27deg AoA and 10deg heeled yacht (Spenkuch, 2006)

Philpott *et al.* (2004) presented a blanketing model based on weighting factors which favours the upwind yacht and penalises the blanked yacht. This approach has shown to be a starting point but it is also judged to be too simple since it only models the major effects of yacht interaction. This model will be explained in more detail as it is used in *Robo-Race* (version of 2008) but it will be replaced by a refined model based on lifting line theory (see Chapter 7). Philpott *et al.* (2004) used two different ways of dealing with the physics of covering depending on the point of sail. His model only captures the primary effect on the freestream condition due to the presence of the sail rig constellation. The so-called 'bent air effect' is used for the upwind scenario whereas the 'turbulent air effect' describes the downwind sailing conditions. Both effects are known to propagate downstream and therefore affecting the trailing yacht sailing in the proximity of the upwind yacht.

For the upwind scenario, due to the position of the sails, the flow area of the yacht's leeward side is assumed to be bent with respect to the freestream condition. The bent air region is assumed to be a limited circular area, centred at the end of the boom and spread no further upwind than the position of the bow. Within this region the bent air effect is captured as follows: the flow direction varies linearly according to the distance of the upwind yacht, whereas the freestream flow direction M_t is resumed at the distance R_{bent} from the transom of the yacht.

For downwind sailing, the thrust generated by the sails is mainly due to drag and a region of complex fluid dynamics, the turbulent air region is present on the downwind side

of the sails. The occurring turbulent air effect is modelled by reducing the wind speed regarding the freestream flow speed. The affected truncated area ends at the distance R_{turb} from the yacht and the speed within this region is assumed to resume linearly to the freestream flow speed V_t at R_{turb}.

The wind direction M_t within the bent air region and the wind speed V_t within the turbulent air region are presented as follows in Eqns. (2.1) and (2.2) respectively:

$$\hat{M}_t = M_t + (\beta_t - \delta)\left(1 - \frac{r}{R_{bent}}\right), \tag{2.1}$$

$$\hat{V}_t = V_t + \left(1 - p_{\max}\left(1 - \frac{r}{R_{bent}}\right)\cos^2\left(\frac{\gamma}{\gamma_{turb}}\frac{\pi}{2}\right)\right), \tag{2.2}$$

where, δ stands for the boom angle, $ß_t$ for the apparent wind angle, p_{max} for the maximum percentage reduction for the wind speed in the turbulent region and finally the angle γ relative to the centreline of the turbulent cone projected by the sailplan.

As mentioned above, the drawback of this model is the insufficient accuracy when demanding for a detailed model. This in turn provides a simple coding and furthermore, it is easy to explain to novices who are mostly unfamiliar with the physics of covering.

Another approach to capture the covering issue has been presented by Parolini *et al.* (2005) within the derivation of mathematical models and numerical simulations for the America's Cup yacht. He and the co-authors concentrated on the numerical simulation of the flow around downwind sailing setups. Therefore, the wind shadow region behind an ACC yacht modelled by a hull, mainsail and symmetrical spinnaker are simulated and analysed in detail.

The atmospheric boundary layer research is a large and complicated research area. The reader is referred to Pope (2000) to find more information of turbulent flows and ways of modelling them. Parolini *et al.* (2005) simulated the presence of the atmospheric boundary layer since it affects the true wind speed (TWS). So, the 1/10 law was used to calculate the TWS in this layer (see Figure 5):

$$TWS(z) = TWS(10)\left(\frac{z}{10}\right)^{1/10}, \tag{2.3}$$

where z is the vertical coordinate in meters measured from the static water surface.
The simulations indicated two trailing edge vortices created at the head and bottom of the spinnaker and mainsail which have a dominant effect on the flow. The shadow region generated by the presence of these two vortices extends many boat lengths and is localised by an indicator called 'defect velocity' that is defined as follows:

$$\sqrt{(u_x - u_{bcx})^2 + (u_y - u_{bcy})^2 + u_z^2}, \tag{2.4}$$

where $u_{bc} = (u_{bcx} , u_{bcy} , 0)$ is the inflow boundary velocity.

Simulations carried out by Roncin (2002) demonstrated that the blanketing models based on a horse shoe vortices approach yield good results. The presence of an opponent was represented by a horse shoe vortex with the intensity Γ generated by the lift of the sails.

$$\Gamma = -\frac{Lift}{h \cdot \rho_A \cdot V_{WA}} \tag{2.5}$$

In his study, several investigations have been carried out to adjust the model to the 3D ideal fluid calculations of Caponnetto (1997) which have shown encouraging correlations. The next step was made by investigating a viscous wake component which correlated well with the experimental data (F. and V. Nivelleau, 1994). Finally, these two models were superimposed and yielded to the best results within Roncin's study. The importance of the two components of the final composed model varies according to the distance of the upwind yacht. In its vicinity of the vortex model (a function of the lift) is dominant whereas the viscous model becomes more important further away as the 'smear' increases and the lift decreases.

An advanced approach based on lifting line theory describing the phenomenon of blanketing and covering within a fleet race environment has been developed within this study and is described in Chapter 7.

This chapter gave an overview of the mechanics of a sailing yacht and available models predicting her steady and dynamic performance over a course. Special manoeuvres such as tacking are captured well (Masuyama *et al.* 1995), but they also demonstrate the limitation of describing the physics. The importance of describing the correct simulation of this complex flow behaviour has to be captured in detail in an advanced yacht fleet racing simulator that is capable to deal with the decision-making process of sailors. The behaviour of humans in sport, especially in sailing is shown and discussed in the following chapter.

3 Human Behaviour in Yacht Racing

The fact that a human plays a leading role has to be taken into account when determining a yacht's performance over a course. The sailors' capability of technical skills, athletic performance, and also his/her ability of making rational decisions under time pressure and uncertainness are important aspects as small differences in boat and yacht performances could be observed in latest competitions, such as Olympic Dinghy Sailing or the America's Cup. Considering these aspects, it is obvious that dynamic strategies have to be developed that update the race tactics and race strategy according to changing interaction with other yachts or changing environmental conditions (weather, wind and current) that can lead to the crucial superiority winning a race.

Sailing can be considered as a continuous process which involves a dynamic, interactive process with tactical decisions continued by actions, followed by checking judgments which is followed by new actions. Therefore, sailors' decisions can be regarded as gambling on the environmental changes, determining the payoffs of possible tactical alternatives under an opportunity-cost time pressure aspect (Scarponi, 2008). Several decision-making and cognitive models have been extensively studied in sport psychology, mainly with a novice-expert pattern (Starkes and Ericsson, 2003; Williams *et al*., 1999) and more recent studies considering the performance of athletes have been carried out by (Rulence-Paques *et al*., 2005).

By regarding the objectives of this research and in the light of the above considerations, the development of a reliable and efficient behaviour model capable of dealing with the unpredictable and dynamic nature of sailing, has to be investigated. Therefore, different

approaches of modelling the human behaviour will be considered focusing on their capabilities, opportunities, and possible implementation into a sailing environment.

3.1 Decision-making in Sport

The domain of sports provides numerous different disciplines and therefore a variety of different decision-making aspects. Nevertheless, the following three important aspects can be found in every sporting event and have to be taken into account when regarding the corresponding decision-making process. First, the decision maker, the agent (e.g. sailor, coach) has to be considered. The actual task (tacking, defending) and the temporal context when a decision has to be made (during a race, during a timeout, or in advance) are the other two important aspects playing important roles when describing decision-making in sport.

One crucial fact of decision-making in sports is created by the agents themselves and their task familiarity. The agents are (normally) familiar with the task leading to a natural decision-making which in turn characterises sports decisions as naturalistic (Orasanu and Connolly, 1993).

Another important feature of sport decision is that they are dynamic, meaning that the decision itself develops over time. There, one has to distinguish between internal and external dynamics. The latter describes the change of the environment and therefore the situation itself over time. For instance, the wind or the opponent's position are not static and are always changing during the race. Contrary to this, the internal dynamics consider the subjective decision-making process of the decision maker, i.e. the deliberation. Decision makers do not instantaneously react to the picked up information. They rather collect the environmental information over a period of time (milliseconds to seconds) that in turn needs extra time for the information processing process, the deliberation time.

Third, the majority of sports decisions are made in a framework of high or moderate time pressure. Hence they are made "online" and rarely made in a reflective manner (Johnson, 2006).

Another important feature of sports decision is the variability, meaning that no deterministic prediction from the actual state to response can be made. Therefore,

unpredictability in sports, e.g. the future actions of an opponent in a given situation, is another important key feature describing decisions in sport.

Sailing is a sport discipline with numerous uncertainties due to the opponents' behaviour and the environmental conditions (weather, wind, and current). This becomes obvious, especially during upwind sailing as changing conditions such as wind shifts force the sailor to act accordingly. They have to be interpreted correctly by the sailor to perform the necessary manoeuvre efficiently. Executing a manoeuvre in an unfavourable time period (too early or too late) can yield to a lower surge-speed towards the mark. This leads to a great disadvantage in the race outcome and therefore, the correct estimation of windshifts (strength and duration) is essential for a winning sailing performance and a successful regatta. Therefore, it is a reasonable way to consider the decision-making process in yacht racing as a decision behaviour under opportunity-cost time pressure. Considering this example, it seems to be straightforward to have a closer look at the individual decision-making process of athlete (sailors) which will be done in the next paragraph.

Athletes who have developed expertise in their particular area are capable of thinking effectively about relevant problems in their domain. Research proved that not simply general abilities, such as intelligence or memory, nor the use of general strategies describe the difference between novices and experts. Rather, the fact that experts have acquired extensive knowledge which influences the pick-up of cues and how they organise, represent, and read environmental information makes the difference between them and novices. This, in turn, gives experts an advantage in their abilities to remember, rationalise, and answer queries. The same available environmental information is picked up by novices and experts as experimental results have shown considerable similarities in their visual scanning process, but experts apply a different weightings distribution to the perceptual variables (Araújo *et al*., 2005). Furthermore, experts are more comfortable in executing a task as they tend to be less dependent on opponent information, whereas novices were more active by adjusting and performing technical actions (manoeuvres). Studies comparing experts and novices on decision-making in sport assume that the right decision is recalled from decisions and perceptual information based on memory stored in knowledge pattern (Starkes *et al*., 2003). The research group supervised by Rulence-Paques (2005) stated that athletes' expertise base is obviously organised in a structure and organised in precast

decision-making pattern whose characteristic will influence the athletes' performance. Experimental evidence that expert sailors are able to make better (rational) decisions was demonstrated by Araújo *et al*. (2005) when studying the relationship between decision-making skills and sailing expertise. Hence it is believed that experts can extract the maximal benefit of his/her environment (external information), which is known in advance. Therefore, the reaction time of a tennis player, for instance, can be reduced by cutting the relevant amount of information used for the decision-making process. This strategic improvement is presumably based on the superior application of cues like the opponent's racquet or his/her body motions (Abernethy, 1991). This observation was made by studying boxers where the response of expert boxers was more accurate but the reaction time was equal for all groups of expertise (Ripoll *et al*., 1995). Furthermore, a correlation of the probability of cue utilisation to achieve the (regatta) goals varied considering to the level of expertise (Araújo *et al*., 2005). Araújo showed that as the skill level increases the athlete (sailor) act more prospectively, which in turn, changed the use of one type of information to another which are more suitable for the sailor's goals. In the light of the aspects above, experts in a particular area can be considered as a 'powerful communication system' (Bard *et al*., 1994) that is able to distinguish between plenty of environmental information effectively by picking up cues relevant for a successful performance of their task's objectives.

3.2 Decision-making and Artificial Intelligence

The development of Artificial Intelligence (AI), especially in the computer game sector was and is actually still very dynamic and offers potential ways for capturing human behaviour in a dynamic sailing environment. In the following subchapters topics like Fuzzy logic, Bayesian and Neural Networks, Monte Carlo Simulation, dealing with different characters' moods of humans will be discussed considering the aims and objectives of this project.

In general, the decisions made by the AI in computer games should be:

- Adaptable;
- Realistic;

- True;
- Human like; and
- Enjoyable.

Apart from the latest aspect, these features have been considered when dealing with the development of AI and decision-making in *Robo-Race.* Therefore, the techniques and approaches of researches and game developers dealing with AI decision-making are introduced, examined, and evaluated according to their potential and possible implementation in *Robo-Race*.

Decision-making is a very important element of AI as it is judged according to its performed decisions. An AI that permanently comes to wrong decisions would be characterised as "bad" AI. Hence, the quality of the decision-making has a direct effect on the quality of AI which in turn affects the quality and realism of a simulation (or computer game).

Unfortunately, the game industry neglected the decision-making process of AI's in recent years as they focused more on improving graphics and design. Nowadays, game AI is an important part of a game as Non-player-characters (NPC) control clearly needs some type of AI. Some years ago, standard game AI used finite state machines, search-trees and the A* search algorithm that were widely used in pathfinding. With the popularity of computer games, the demand of a more intelligent, human-like, and realistic AI raised and consequently a diversity of different models were developed and tested in both, research groups and game industry. These changes have emerged numerous approaches and techniques able to respond to the user's actions in order to simulate a more realistic environment. Among these models are genetic and heuristic algorithms, scripting, modified state machines, neural and Bayesian networks.

Most computer games have to face the following three problems which are solved by using game AI: (1) NPC-movement, (2) NPC-decision-making, and (3) NPC-learning. To overcome these challenges an enormous variety of different fields and sub-disciplines of AI has been developed and a selection is given as follows (Rabin, 2002). The reader is referred to (Russell *et al.*, 1995):

- Expert systems imitate and utilize the expertise of human experts within a specified field. The expert's knowledge is simulated within a knowledge base, and executes reasoning automatically according to the knowledge base in response to a query. Expert systems are able to produce similar responses to those given by a human expert.
- Case-based reasoning methods are based on the human character to deal with a new situation by comparing it to the most similar one learned in the past. The methods try to examine a set of inputs that is compared to a stored database which is based on known, mainly historical, sets of inputs and the most suitable outputs in those situations. The advantages of this model are its easy updatability and expansion provided that the model collects automatically new cases whilst running.
- Rule-based models are based on a series of production rules associating actions to conditions. It checks the environmental state to generate an outcome. The advantages of the approach are in its easy implementation, maintaining and analysis.
- Finite-state machines (FSMs) are or were the most common applied game AI technique which consists of a collection of states presenting situations in which the model can exist, with described state "transitions" allowing the model to go into a new state (van den Herik *et al*., 2005). The model's behaviour is described individually for each state. Despite of its simple and intuitive nature, this approach requires a time-consuming development as all possible situations have to be thought of in advance. This fact makes it very inflexible leading to "holes" within the game AI (Spronck *et al.,* 2002) and unrealistic behaviour resulting from unexpected states.
- Production systems consist of a rule database where each rule consists of a conditional statement and a number of related actions executed if the conditional statement is true. Hence such a system can be considered as a number of "if-then" statements with the potential of numerous available solutions since more than one rule can be satisfied parallel which in turn provides potential for solving decision-making conflicts.
- Decision trees come to a decision based on a set of inputs by beginning at the root of a tree. At each intersection point (node) a child node is selected based on the input value which makes it quite similar to "if-then" statements.

- Fuzzy logic differs from traditional logic (0 or 1, true or false) by using real numbers for describing the level of membership in a number of sets.
- Neural networks are used for machine learning (ML) techniques. Based on the design of a human brain, its layout consists of neural interconnections. Neural networks perform by recalculating the internal numeric weights between the interconnected network components again and again. Thereby the neural network learns an (almost) optimal solution for numerous learning situations.
- Belief networks (Bayesian inference) use probability calculation to capture uncertainty and incomplete knowledge of the environment. This technique offers the opportunity to infer the state of the environment and concluding the possible outcome of numerous potential actions.

Approaches dealing with decision-making in simulations are outlined on the following pages. In particular, expert systems and associated decision-making models, such as rule-based and value-driven systems, are highlighted.

Decision models and knowledge based expert systems can be found in the military sector in order to model and improve human decision-making. Therefore, a set of 'human in the loop' simulations have been carried out in recent years, especially for computer guided aircraft models that imitates pilot decision-making in air combat situations. The implemented decision-making models are knowledge based expert systems (e.g. Goodrich and McManus, 1989) or heuristic value driven systems (Lazarus, 1997) or discrete game systems (Austin *et al*., 1990). The systems above use discrete time instants where possible states are calculated by projecting each alternative into the future and by considering the opponent's future state. Then, a score is given to each alternative whereas the one with the highest rating will be executed. To evaluate the possible states, simple rule-based systems use fixed combat geometry rules whereas more powerful systems take use of a predetermined set of questions characterising different (combat) goals. There, the value of each alternative is determined by calculating the weight of the goal individual values. The relative importance of the goal is associated to the weight; the higher the more important it is. An alternative approach evaluating states is the use of explicit functions, such as value functions (Lazarus, 1997). Furthermore, systems with game theoretical approaches using nonlinear scoring function, where one opponent tries to maximise the score and the other tires to minimise it (Austin *et al*., 1990). Despite the high standard of the expert systems

mentioned above, a lack of decision-making under uncertainties can be observed as human preferences and attitude towards risk are not captured. These two aspects have to be implemented into a realistic model dealing with decision-making under uncertainties (Virtanen *et al*., 1999).

A method to overcome this problem is the use of an influence diagram model. A utility function is implemented in the way that tradeoffs between competing alternatives are evaluated by weight parameters in the utility function. This was a great advantage compared to rule-base approaches as the tradeoffs do not have to be expressed explicitly. Another advantage is that it can be built-up, validated, and maintained together with sailors due to simple graphical layout for which no great decision theoretical background is required. Furthermore, sailor's decision-making can be analysed. These facts in turn offer the opportunity to update the decision outcome according to the sailor's preferences and skills easily.

Another alternative to the rule-based system is the value-driven approach. The U.S. Air Force air-to-air combat model BRAWLER showed a successful application of such a hierarchical value-driven methodology in simulating pilot behaviour in air-to-air combat (Lazarus, 1997). There, the selection of an action path consists of: the selection of several alternatives that create the decision space, projection of each alternative into the future, evaluating the future for each alternative using a value function and implementation of the highest scored alternative. The value function performs tradeoffs among conflicting aims by making it sensitive to the goals of a given decision. The value-driven human decision model consists of two loops, an upper and lower one, influencing each other. A possible way of its application was represented in BRAWLER. There, the perception-building process is represented by the upper loop, whereas the lower loop is used for predicting, weighting and finally choosing alternatives. In addition, the projection time for decisions corresponds to the type of decisions, where lower level decisions have shorter projection times than high level decisions.

According to Lazarus (1997), value-driven systems have the following five advantages to rule-based systems:

- In rule-based systems, tradeoffs have to be expressed explicitly whereas in value-driven systems tradeoffs between competing objectives are made naturally.

- In rule-based systems, the complexity of the implementation varies to a power with the number of objectives whereas it varies linearly with the number of objects for value-driven systems.
- In value-driven systems in which various alternatives reflect realistic aspects, exposure to unanticipated conditions often results in reasonable behaviour whereas violation of underlying assumptions yield to unacceptable behaviour for rule-based systems.
- Updating the existing value-driven system can be easily made by adding components to the value function whereas extensive rewrites have to be done in the rule-based system.
- In hierarchical systems, the value-driven system method offers a natural means by which higher level decision makers influence lower level decision makers through the forwarding of weights.

Regarding the highlighted methods and systems above, *Robo-Race* can be classified as a production system based on a rule database. There, each rule consists of conditional statements and a number of related actions are executed if the conditional statements are true. Important studies about modelling adaptive behaviour in sailing were conducted by Scarponi (2008) using *Robo-Yacht*, the precursor of *Robo-Race* (for more information the reader is referred to Chapter 4). There, different heuristics were investigated and their performance under different time-pressure conditions was analysed in order to find the one with the best effort-accuracy trade-off. The decision-making framework of this study was based on research of (Payne *et al.*, 1996) who defined eight different choice rules grouped according to how much information is used and in how the information is used for executing the search task.

Scarponi used a decision matrix that is a well-established technique to define and investigate a decision-making problem to address the predictable nature of yacht races. Two alternatives and four outcomes that correspond to four possible weather situations were taken into account and possible payoffs (distance sailed towards the upwind mark) have been applied for the evaluation. A reduction of the expected payoff was applied when delaying a decision to ensure the opportunity-cost time pressure atmosphere. Monte Carlo simulation was applied for the investigation and three aspects, such as payoffs standard deviation, dispersion in probability, and time pressure level, have been taken into account.

It could be shown that adaptive behaviour in sailing contains a change to more attribute-based strategies and processing smaller amount of information. Adaptive behaviour in this context describes maximising the accuracy whilst being confronted with limited time and cognitive constraints. Furthermore, an unfavourable performance of the effortful, 'breadth-first' strategies, e.g. weighted additive value (WADD), under immense time pressure was observed. In contrast, strategies that are less effortful and attribute-based, e.g. lexicographic (LEX) are recommended for conditions characterised by immense time pressure and high dispersion environment. Readers are referred to (Payne *et al.*, 1996) and (Scarponi, 2008) for more information.

Production systems like the decision maker AI in *Robo-Race* that are based on "if-then" statement system require a time-consuming development when dealing with detailed decision-making analyses. The actual system needs to be able capture various potential race situations making it inflexible and also predictable. A modification or an upgrade to an advanced rule-base system would be possible but comes with a time-intensive development of the existing "if-then" statements. Imagine one wants to add one input layer, such as the feature "opponent" into the decision-making AI, various if-then statements have to be added and most of the existing statements need to be rewritten. If one wants to consider different positions of the opponent relative to the own yacht during different faces of the race, one can imagine that the former simple and intuitive code easily becomes complex and non-transparent. This simple example describes the scenario for one additional feature. The dilemma results from the architecture of the rule-based approach since the complexity of the implementation varies to a power with the number of objectives (Lazarus, 1997). The mentioned complexity and non-transparency enhance the potential of numerous "true" statements that are satisfied simultaneously. This in turn causes conflicts within the AI leading to wrong and unrealistic behaviour, respectively. Nevertheless, the potential conflicts are controllable but come with a large coding input. The limits of this rule-based approach are further pushed or exceeded when mimicking behaviours of real humans or different individual sailor groups as it is intended to realise in this study. Using a rule-based approach for its realisation would be a real and time-intensive challenge that is judged to be ineffective and not seminal.

3.3 Modelling Decision-making in Sports

The key features of sports decision were discussed in Chapter 3.1, where they are described as naturalistic, dynamic, variable , 'online made' and characterised by moderate or high time pressure. These important features have to be kept in mind when developing or choosing a model or method dealing with sport decisions. The model has to be sensitive enough since important, mostly little differences that influence a decision have to be captured correctly. Therefore, it is straightforward that the model deals with relevant variables that enable it to describe, analyse, and predict decisions in a natural environmental context. The following three key questions of both, the environment and the agent have to be considered and evaluated when choosing the right model for the interest of study (Johnson, 2006).

First, the question of static or dynamic modelling has to be posed and can be easily answered for sport decisions since dynamic decisions need dynamic models. The crucial variables driving the model change over time which has to be captured by the model. The modelling of a sequence of events is not feasible by using static frameworks since they consider one discrete static state which does not change even if the environmental state changed. According to Williams *et al.* (1999) and Johnson (2006) 'only a dynamic model can incorporate time course of events that is crucial in sports situations'.

Second, the question of process or outcome orientated modelling. If one wants to study decision modelling, one wants to know how decisions are derived. By only considering variables and the corresponding decision outcomes, one does not enhance the understanding of the underlying process of how decisions are actually made. Only process orientated models can explain this transition of variables to decision outcomes and should be used for modelling decision-making in sport (Alain and Sarrazin, 1990).

Third, the question of probabilistic or deterministic modelling has to be answered. In natural decision-making environments, such as sport, changing conditions and variability are one of the key features causing variable behaviour which in turn require probabilistic models. Contrary to this statement, the majority of implemented decision-making models are deterministic (Fishburn, 1988). For example, this type of model generates the same outputs for predefined inputs or choice potions by associating holistic values for each option. The generated output consists of a set of expected utilities which were derived from holistic values for each option. Now, the option with the highest

expected utility is always chosen (in deterministic models). This type of approach was also used by Scarponi (2008) when investigating adaptive behaviour using pre-described decision rules (highlighted in the previous subchapter).

Considering these three key questions, the majority of sports decisions requires the application of dynamic, probabilistic, and process-orientated approaches. Expect for example, the football coach's choice of the goalkeeper for the penalty shootouts might be satisfactorily modelled by the deterministic weighting and application of static inputs. Therefore, it is important to choose the right model to achieve a matching between the investigated type of behaviour and the used model. The Sequential Sampling Model (SSM) represents such a dynamic, probabilistic, and process-orientated approach and will be introduced in the following paragraph.

SSMs have been successfully applied in the study of judgement, decision-making and perception (Aschenbrenner *et al.*, 1984; Wallten and Barton, 1982; and Link and Heath, 1975). The model uses a basic feature of the human perceptual system, the assumption of selective and limited attention, also known as 'bounded rationality' in decision-making (Simon, 1955). It can be classified as a accumulation-to-threshold model using the following underlying mechanism which is recalled at each moment of the process: Attention changes to a specific dimension of task information (variety, cues) that affect the evaluation of each option (valence) using the actual considered information. As a result, attention changes among dimension over time, causing a change of the accumulated valence that is used to calculate a level of activation (preference) for each option. This process continues until the preference for one option is judged to be 'high enough' by exceeding a threshold of activation.

Now a special type of SSM is introduced, the Decision Field Theory (DFT; Busemeyer and Townsend, 1993; Roe *et al.*, 2001). Similar to other SSM, DFT can be defined as a mathematical tool for developing preferences of a human decision maker where different options are considered. It can be categorised as a cognitive approach built on psychological principles instead of economical ones and can therefore be used to describe psychological human behaviour. DFT offers a mathematical tool which helps to comprehend the cognitive mechanism of the deliberation process of humans in making decisions in an uncertainty rich environment (Busemeyer *et al.*, 1993). DFT provides a probabilistic and dynamic character and therefore differs from earlier mathematical models mentioned above. Due to its character abilities, DFT performs successfully in a wide

variety of cognitive tasks including perceptual discrimination, sensory detection, memory recognition, preferential choice and conceptual categorisation (Lee *et al.*, 2008 and Busemeyer *et al.*, 2002).

DFT features two important assumptions during the derivation of a preference state for each option. First, the psychological property of decay is captured by 'putting more weight' on more recent valences than earlier (in the task) valences when accumulating to produce the overall preference state.

Second, the competition among options, meaning the derivation of a preference for a given option is affected by the presence of other options. Hence, if a decision maker favours a particular option (the corresponding preference raises), the tendency for the other options are suppressed simultaneously (the corresponding preferences become smaller). Also DFT uses a preference threshold that evaluates an option to be 'good enough' to make a decision based on the actual choice.

By modelling the deliberation process rather than just dealing with the outcome, DFT can account for various effects in multi-attribute, multi-alternative choice situations, such as similarity-, attraction-, and compromise effects, without changing any model parameters or mechanisms. The reader is referred to (Johnson, 2006) for a detailed discussion.

Regarding the dynamic nature of decision-making, the effect of time pressure has to be taken into account, especially in sports decisions. Time pressure may cause the selection of an option that is not favoured under conditions without time pressure (Raab, 2001). This effect causes another effect, the 'speed-accuracy tradeoff' which characterises for instance monetary or sports decisions (Schmidt and Lee, 2005). Speed and accuracy have an inverse relationship since the quicker and more impulsive decisions are made, the less accurate they become.

Diederich (2003) and Raab (2001) showed that the effects of speed-accuracy tradeoff and time pressure can be easily and successfully modelled using the DFT model. There, the relationship between time pressure, total amount of information sampled and choice are linked together. This means that an increased time pressure reduces the total amount of sampled information whereas a decision maker in a known time pressured situation tries to decrease the necessary information to obtain a decision. These two important effects of time pressure and speed-accuracy tradeoff can be easily and effectively modelled by lowering the decision threshold.

DFT offers the opportunity to model the individual deliberation process and therefore individual differences of decision-making by altering the related parameters. Research by (Johnson, 2003) showed the successful modelling of impulsive, accountable, and persistent characters.

Another important aspect in sport, the expertise can be easily modelled by using SSM. Experts in sport make both, better and faster decisions compared to those of novices. This experience can be modelled by using different initial preference that results in faster and more accurate responses. The second superiority of experts lies in their use of the available information and the individual knowledge about the task (Chamberlain and Coelho, 1993). This would be modelled by altering the amount of the dimensions of information and the change among them. The experts use their mental resources more efficiently by putting more attention on the crucial task related information. This phenomenon can be easily modelled by decreasing the decay of previously attended information.

Now, one wants to compare the highlighted cognitive model, the SSM with two other popular approaches for studying decision-making, the expected utility and the adaptive decision maker approaches that were earlier highlighted in this chapter. The most popular framework for modelling human behaviour is the expected utility approach that derives decisions by maximising the expected subjective value during a task. Researches have proven that expected utility approaches are not adequate models to describe human behaviour in detail, since they don't capture key features such as dynamic and probabilistic predictions (Johnson, 2006). SSM offers the opportunity to mimic expected utility models by reducing the latter two mentioned key features. This was successfully demonstrated by Busemeyer and Townsend (1993).

The other popular approach is the adaptive decision maker framework. There, it is assumed that the decision maker tries to obtain equilibrium between effort and accuracy, contrary to maximising expected utility like in the approach mentioned above (Payne *et al.*, 1993; Payne and Bettman, 1996). As mentioned earlier in this chapter, Scarponi (2008) used this type of approach to investigate different decision-making strategies, such as the lowest-effort strategy selected by the sailor to achieve a sufficient level of performance. Again, SSM is capable of mimicking the adaptive decision-maker framework by setting up

different parameters resulting in different decision-making strategies. The earlier described effortful, 'breadth-first' strategy, e.g. weighted additive value (WADD) could be easily reproduced by lowering the decision threshold.

Now, one wants to focus on the general modelling of the human decision-making process rather than just regarding the modelling of decision-making in sport. The human decision-making process can be subdivided into three major groups: economical, psychological and synthetic engineering-based decision-making (Lee *et al*., 2008). The first group, economical decision-making, assumes that the decision maker behaves rationally and consequently the corresponding approaches are not able to simulate the cognitive nature of humans, like fatigue, pressure, and memory. To close this gap psychology-based models take utility or subjective values and probabilities into account (Edward, 1962). Those types of approaches are incomplete as they are based on static laboratory decisions that are rarely seen in real life situations (Rothrock *et al.*, 2009). The third, the synthetic engineering-based approach, uses engineering based approaches and techniques to understand and learn attributes of human behaviours in realistic and complex environments. The decision-making is made by a system consisting of modules and sub-modules to which engineering techniques are applied. Consequently, the validation of such a complex model is quite difficult. To overcome the constraints of all three models, a comprehensive model capturing real human decision-making has to be developed by combining all three approaches mentioned above.

This idea was realised by Lee *et al*. (2008) who enhanced the Decision Field Theory (DFT) by using Bayesian Belief Networks (BBNs) as perceptual processor. This update of the DFT model resulted in the Extended DFT (EDFT) and led an efficient handling of dynamically changing environments. Thereby, the approach consists of two major steps. First, the subjective evaluation for the options and the human attention on the interest is updated. The second step uses BBNs to conclude these updates in the dynamically changing environment context. Furthermore, this approach was successfully applied to a human-in-the-loop experiment dealing with a virtual stock market environment. This successful extension of the DFT made it possible to use the probabilistic inference technique of Bayesian networks that is the most powerful one in creating a more human-like reasoning (Touzour, 2002). Bayesian approaches perform various tasks robustly, like

in speech analysis, computer vision, and behavioural imitation (Rao *et al.*, 2004). Research has shown a link between human reasoning and Bayesian statistics (Koerdering and Wolpert, 2004). Moreover, recent results have shown that humans integrate, update, and access knowledge in a logic similar to Bayesian statistics (Griffiths and Tenenbaum, 2006).

Based on these findings, it seems to be a promising way to investigate the application of Bayesian techniques for simulating complex human in a dynamically changing environment in conjunction with the EDFT framework. Consequently, this approach will be explained in more detail as it provides certain advantages on behaviour acquisition (the reader is referred to Chapter 8 for more details).

3.4 Agent Technology and Modelling

To handle the request for autonomous decision-making in a dynamic environment agent technology has been introduced. An agent can be considered as a computer system located in an environment in order to meet its design purposes (Engelbrecht, 2002). Autonomous decisions indicate the capability to detect by itself what actions have to be performed (Wooldridge, 2002). Due to the dynamism of a real environment it is almost impossible to predict all potential situations in advance. The initial setup is an assumption based on unknowns and hence "unexpectedness" is natural for dynamic environments (Picard and Gleizes, 2003). Consequently, the "character" of the agent has to be adaptive in order to perform due to the changing environment and subsequently make improved decisions.

Behaviour modelling and learning are tasks which significantly depend on the problem. Due to the complexity of a dynamic environment it seems to be reasonable to categorise the variety of different behaviours. Based on the psychological hierarchy of human behaviour (Hollnagel, 1994), the behaviours are categorised as follows: strategic behaviour to achieve long-term goals, tactical behaviour to attain mid-term goals, and finally reactive behaviour indicating sensor depending actions. Based on this categorisation the behaviour simulation uses layered approaches which are commonly applied in the field of robotics. For more information the reader is referred to Arkin (1998).

A layered approach inspired by the hierarchical sequence of behaviour (Arkin, 1998) is presented by (Tozour, 2002c) for a First-Person-Shooter (FPS) AI that consists of four basic component layers. In this type of game, human players have to react very quickly to new conditions. The first layer, the movement layer deals with the problem how to move. The second layer, the animation layer is in charge for choosing character animations or playing animation sequences, hence for the environment. The third layer, the combat layer selects the weapons and makes tactical decisions. And finally the fourth layer, the behaviour layer which is responsible for goal decisions and the interaction with other systems to achieve these goals.

Wickramasinghe and Alahakoon (2004) introduced an approach in order to reduce the gap between man and machine by creating agent decisions makers in a more human-like way. Therefore, a novel agent architecture based on psychology, human behaviour and brain study research has been provided in order to account for an autonomous decision-making process of the agent in a dynamic environment. The introduced layer approach simulated a human brain and contains four different layers: inheritance, training, experience and unexpected. Where each individual layer 'corresponds to the behavioural cycle of a human being giving a human oriented architecture to the agent to make autonomous decisions in a dynamic environment' (Wickramasinghe and Alahakoon, 2004). This architecture was implemented in an Evolutionary Artificial Neural Network to represent learning and evolution adaption abilities and was judged to 'have the potential to implement the proposed framework in real life dynamic environments' (Wickramasinghe and Alahakoon, 2004).

Another layered approach not based on the inspiration of the human brain but inspired by different time scales depending on when the decision makers have to make their decisions was introduced by (Adriaans, 2003). In the corresponding paper, the *Robosail* project was described which intended to construct a self-learning steering system for a single-handed sailing yacht. According to the changes in the dynamic environment, the analysis of time scales for the sea-state (hours), veering (10 minutes) and gusts (10 seconds) led to a modular architecture consisting of hierarchical agents operating in different time frames in which the individual decisions are made. Consequently, the decisions made by the agents can be categorised depending on the time frame: Strategic, tactical and reactive behaviour

which correspond to achieve long-term, mid-term goals and execution respectively. The core system consists of the following four agents: skipper, navigator, watchman and helmsman. This agent architecture represents a crew and the corresponding tasks executed by each individual modelled crew members of a modern sailing yacht. This system and its architecture are similar to that of *Robo-Race* that will be explained in more detail in Chapter 4.1.

An additional successful four layered control architecture was introduced by (Stelzer and Jafarmadar, 2007) for controlling an autonomous sailing yacht. The yacht performs autonomous sailing by steering the rudder and sails according to the commands of the control system which consists of the following four layers: strategic long-term routeing, short course routeing, manoeuvre execution, and emergency reflexes. In contrast to *Robosail*, the layers are working in one time frame and are executed in parallel. The hierarchical system layout provided the upper layers with the ability to perform complex and strategic tasks, for instance, long term weather routeing or determining the most suitable time for executing a tack on an upwind leg. Additionally, the information gathered by sensors were passed on to the bottom layers which equipped the yacht with the capability to react directly to unexpected environmental changes like wind gust or static and dynamic obstacle (opponents). Various successful test runs and log file analyses have shown that the yacht performs and steers as expected by sailing experts. This approach delivers an interesting and potential way of combining both a reactive and planner-based methodology but it did not capture the human behaviour aspect since it was not represented in this setup.

Research of Aler *et al.* (2009) dealt with an input-output modelling approach to model human behaviour playing football in a virtual environment called *Robosoccer*. Behaviour cloning techniques have been applied to 'copy' human behaviour to the *Robosoccer* agent. The successful application consisted of the following major steps: first the creation of an interface allowing a human to play *Robosoccer*; second, data gathering (input/output pairs) whilst a human played the video-game. What the player could see on the pitch was considered as the input data, while the corresponding performed action of the player in this specific situation as the output. Then, a machine learning technique was applied to get a classifier studying which action has to be performed in a particular situation (from inputs to

outputs) leading to the new model. Subsequently, this model was implemented into the agent in *Robosoccer* by translating the classifier into the corresponding programming language that controls the agent by what the agent played similarly to the human. Aler *et al*. (2009) focused on low-level-behaviour, for example, looking for the ball, dribbling opponents, conducting the ball to the goal and scoring in the presence of other players. Results showed that the applied approach of behavioural cloning techniques work well for controlling (football) agents by programs that model human play. Human behaviour was represented in a traditional rule-based approach to model human behaviour in AI. The fact that strategical and tactical subjects are not addressed to the agents gives room for improvements. As suggested by the author, cognitive functions, like planning, opponents prediction, and trajectory computation should be applied to the agents to make them more human like (Aler *et al.*, 2009).

An advanced agent orientated approach was carried out by (Kang, 2007). The effect of agent types on team performance was investigated. For that, the impact of two agent types (agent activeness and agent cooperativeness) on team decision efficiency under different degrees of information redundancy by applying a team model of multi-agents called 'Team-Soar' (Kang, 2007) has been conducted. Therefore, the simulated team consisted of four AI agents that were set up differently according to the two levels of agent activeness (active and passive) and three levels of agent cooperativeness (cooperative, neutral, and selfish). It was successfully shown that agent activeness and agent cooperativeness affect the team performance and consequently those attributes can be considered as 'important decision factors of team decision efficiency' (Kang, 2007).

The outlined agent technology and its modelling methodologies represent efficient techniques, approaches, and tools for describing human behaviour. They should provide the reader with some understanding about possible approaches of how to deal with agents in various types of environments. Nevertheless, this topic has to and will be further discussed in the following Chapter 4, but especially in Chapter 8 where a new developed decision-making engine based on Decision Field Theory and Bayesian Belief Networks is explained.

This chapter highlights the description of key features of sports decision that are described as naturalistic, dynamic, variable , 'online made' and characterised by moderate or high

time pressure. These important features have to be captured by a model or method dealing with sports decision, such as the tacking decision on an upwind leg. Possible ways of modelling human behaviour were introduced and potential starting points dealing with the replacement of the rule-based decision-making approach of *Robo-Race* were represented. Considering the discussed limitation and the immense time-consuming effort of extending the existing rule-based decision-making engine in *Robo-Race*, it seems to be straightforward that the 'tactician' of *Robo-Race* has to be redeveloped using a different approach that mirrors the character of sports decisions. Furthermore, it not only has to be capable to account for the detailed description of the decision-making process taking place in the dynamically changing yacht fleet racing environment, but also the definition of individual groups of sailors according to their sailing style and character has to be feasible.

Robo-Race was classified as a production system based on a rule database that would be possible but time-intensive to modify. For instance, the extension "opponent" to the input layer of the existing decision-making AI causes an immense recoding effort. Realising different positions of the opponent relative to the own yacht during different faces of the race result in a complex and non-transparent model. The dilemma comes from the architecture of the rule-based approach since the complexity of the implementation varies to a power with the number of objectives (Lazarus, 1997).

Considering the aim of this study, the biggest disadvantage of rule-based approaches is the delivery of a decision outcome rather than a detailed description of the process of how the decision has been derived. The Decision Field Theory (DFT), a special type of Sequential Sampling Models (SSM), overcomes this limitation and represents a promising matching to sports decision and the project's objectives since its character mirrors a dynamic, probabilistic and process-orientated nature.

The use of sequential sampling models, such as DFT, is recommended by (Johnson, 2006) for describing decision-making in a sporting environment. He justified his statement because the character of those models support dynamic, variable, stochastic processes which typifies decision-making in sport.

Based on the dynamic, unpredictable sport environment that also characterises the decision-making in sailing, the DFT can be seen as a potential candidate for dealing with decision-making in *Robo-Race*. Furthermore, the EDFT using Bayesian belief network seems to be a promising way to account for different behaviours of sailors in a dynamically changing sailing environment.

4 Sailing Simulators and Human Computer Interaction

Considering the objectives of this research, the implementations of human-computer interaction models within a dynamic sailing environment are considered in this chapter. Available sailing simulators created to match different purposes are highlighted whereas the features of *Robo-Yacht* and *Robo-Race* are explained in detail as they play an important role in this research project. Possible human-computer interface (HCI) systems for an active sailing simulator environment are introduced regarding their potential and benefit for enhancing the realism of the simulator.

4.1 Sailing Simulators

The available sailing simulator can be divided into three different categories: first, the 'active' simulators where the sailor plays a physiological active role controlling the yacht. There, the yacht and its rig are reconstructed in order to determine the physiological responses in sailors (Bursztyn *et al.*, 1988) and to analyse sailor's performance (Gale and Walls, 2000). The second category deals with 'passive' simulators where the sailor is not actively involved in the actual process of determining the yacht's performance over a course. This is used, for example in Race Modelling Programs (RMS), where the best yacht design is evaluated under several weather scenarios (Todter *et al.*, 1993). The third category is a mixture of the first two categories in which the sailor can actively interact

with the software but is not physiologically involved in the sailing process (Scarponi *et al.*, 2007).

The development of the active simulators was mainly carried out with dinghy sailing simulators in order to study the physiology of sailors under controlled conditions in a laboratory. The first step in this area was made by Bursztyn *et al.* (1988) who used a dinghy body, able to rotate about the aft and fore role axis. Weights and water pumps were used to equalise the sailor's motions. Simple display devices represented a distance buoy and a sail trim indicator in order to give steering and sheeting cues. Therefore, this simulation provided a starting point whereas this simplified cue displaying environment, the lack of wind-response feedback, and the restricted and simple simulation of tacking limited this setup.

A dinghy simulator for investigating physiological responses on dinghy sailors was developed by Blackburn (1991). An Olympic Laser class Dinghy was suspended such that the hiking moment could be determined. The sailing environment was simulated by using a television replaying a recorded video of a laser sailor sailing in front of the yacht. The actual loads on the mainsail and rudder according to the video were simulated using springs. The sailor had to reproduce the body and arm movements of the 'real' video sailor which in turn made it impossible for the sailor to race his/her own race. This rig setup made it impossible to simulate a tack which provided an unrealistic approach in terms of yacht motion and natural sailing behaviour.

A further step forward was made by Kikuchi and Takashina (1994) who used an improved display environment consisting of a two computer graphic display screen setup at the bow and stern of the single-handed sailboat. The use of a mathematical model to estimate the manoeuvring characteristics of the sailboat in conjunction with the more realistic sailing environment (turning moments on the rudder and boom were created for heeling the vessel) was a first step away from the physiological aspect of the simulators towards to their use as a training tool for teaching the basics of sailing.

An improved apparatus was developed by Walls and Saunders (1994) that was based on research of Bursztyn *et al.* (1988). In the successor, the Olympic Laser class dinghy could rotate freely and weights controlled by a computer were used to balance the

sailor's hiking moment. A computer monitor in front of the dinghy informed the sailor about the actual steering and the trimming of the mainsail.

The next step was made by Gale and Walls (2000) who used the previous described simulator of Walls and Saunders (1994) but increased the level of reality of it. To do so, they applied (1) a mathematical model to describe the dynamics of dinghy sailing yielding a more realistic motion, and (2) an audio and visual feedback consisting of a three-dimensional graphics display to it. The data recorded during an upwind leg were interpreted to evaluate the performance and technique of the sailor by also including mental attributes such as cue processing and decision-making in a quite simple way. The cue recognition was determined by evaluating the time for detecting that a lay line is approached or that a gust will arrive. The decision-making ability focused on handling of gusts and the execution point of the tacks. The simulator simulated successfully dinghy sailing in a laboratory environment and the recorded data analysis allowed it to be used as a training tool since the performance of the sailors could be evaluated.

To the knowledge of the author this simulator designed by Gale and Walls (2000) is the most developed dinghy sailing simulator for determining the sailor's physiological performance in conjunction with a virtual environment. Nevertheless, further improvements on the visual feedback in terms of a more realistic and more detailed presentation of the sailing environment should be carried out in order to enhance the realism of this simulator. Furthermore, the development of a multiple dinghy simulator should be considered as the actual one is only suitable for solo upwind races in which no interactions with opponents are taken into account.

The second category deals with the 'passive' simulations where the sailor does not interact with the software. These programs, referred to as RMPs were already mentioned in Chapter 3.2. Nevertheless, two of them will be highlighted as they play an important role in the latest development of passive sailing simulations.

The approach to model match races around a course that considers different wind and wave conditions was first made by the Stars and Stripes design team (Lechter *et al.*, 1987; Todter *et al.,* 1993). The performance of each yacht candidate was determined by analysing the win/loss probabilities of two yachts over a specific leg of the America's Cup course. The effects of yacht interaction occurring when yachts are very close to each other were taken into account but this phenomenon was just captured to a certain extent and its

whole technical advantage was not reflected in the candidate's performance results. This limitation arose as an equilibrium performance prediction for the yacht's speed and a probability distribution for the wind speed from historical data were used. Therefore, the important ability of acceleration was not taken into consideration which caused a bias in results.

In order to overcome this problem of equilibrium performance prediction, Philpott *et al.* (2004) introduced a fixed-time-increment simulation model for each leg of the course. Therewith, wind fluctuations and interactions between the yachts were taken into account which made it possible to update the yacht's speed dynamically according to the changing weather conditions. Therefore, a dynamic yacht model was introduced to compute the dynamic performance of the yacht that permitted an update of the yacht's speed and location at every time step depending on the local weather condition in vicinity of the yacht. Furthermore, tactical decisions of a helmsman were modelled according to the yacht's position on the course, its relative position to opponents and the changing weather environment. Penalties were applied to possible situations within a match race in order to determine the best tack timing regarding the actual state of the yacht. With these methods, a more accurate simulation model for predicting a match race outcome of two competitive yacht design candidates was developed.

The active and passive simulations determine the individual performance, either the sailor's or the yacht's performance. In order to combine these two categories, an important step forward was taken by Scarponi (2008) who developed a sailing simulator that allowed determining the performance of an active crew-yacht system.

4.2 *Robo-Yacht* and *Robo-Race*

The third category of simulators is represented by *Robo-Race* where a sailor can actively interact with the computer controlled yachts but is not physiologically involved in the regatta. *Robo-Race* is a sailing simulator that takes into account the human factor with respect to strategic decisions during a fleet race. The simulator is designed in a way that one or more users (sailors) can interact with computer controlled ACC-yachts. This setup

provides the recording, analysis, and comparison of the sailors' behaviour, strategies, tactics, and decision-making process. Different models for the yacht-crew interaction have been designed and implemented for the helmsman and the sail tailors, as well as a 'routing engine' which solves problems of a strategic and a tactical nature, like collision avoidance and navigation in wind shifts. The simulator *Robo-Race* is a MATLAB®-Simulink® based tool which is built on the module *Robo-Yacht* which provides the yacht 'physics engine' as well as behavioural models for the automatic crew. A virtual reality environment supports the sailor with a visual real-time feedback of the race state and of his/her yacht within a virtual 3D world.

To simulate fleet races with *N* yachts, *Robo-Race* includes *M* Robo-Yachts which are controlled by the simulator and (*N-M*) human controlled yachts. In order to define a yacht-crew system the setup of the hull, rig and crew parameters for each yacht are required. In addition, two further modules were implemented in order to enhance the realism of the simulation. Firstly, a weather module is used, which prescribes the spatial and temporal variation of the wind speed and direction. Secondly, a race scenario module has been implemented which deals with rule-based routing strategy and an additional library which achieves efficient race tactics and addresses conflicts between tactics and race strategy. An example is tacking onto an unfavoured beat to sail in clean air that is not in the wake of a leading yacht.

The yacht motion is modelled by a four degrees of freedom (DoF) model (surge, sway, yaw and roll) developed by Masuyama (1995) which has proven to perform well for tacking simulations in calm water as the obtained results were in good agreement with those of full scale experiments (see also Chapter 2.4).

4.3 Human-Computer Interfaces

Considering the objectives of the present study, a combination of human-computer interface (HCI) devices that support the natural decision-making process have to be set up and are highlighted in present subchapter. A successful application of HCI needs contributions from researchers in many fields, such as graphic designers, information architects, software developers, hardware designers, system designers and psychologists.

4.3.1 Principles for an interactive system

A high-quality interactive system must be built on fundamental system engineering standards as well as on a reasonable user-interface design. These two important pillars are achievable by setting explicit goals for each category. According to (Shneiderman, 2004) the following aspects of system engineering should be considered when creating an effective system:

- Proper functionality. The initial step is to determine the desired functionality and which tasks and subtasks have to be carried out. Apart from focusing on frequent tasks, the designer should also pay attention to occasional and exceptional tasks for emergency conditions.
- Reliability, availability, security, and data integrity. The second step ensures system reliability which includes specified command functions, data contents must be shown by displayed data and changes such as updates have to be applied correctly. Designers must pay attention to those aspects as user's trust of systems is fragile and difficult to regain for a long time. Furthermore, aspects of privacy, security, and data integrity have to be considered.
- Standardisation, integration, consistency, and portability. This step is necessary as the amount of software packages and users raise and coarse differences between systems can lead to annoying and dangerous errors and finally to an inefficient use.
- Schedules and budgets. This step has to be considered if a project has to be accomplished on schedule and within a certain budget. Additional costs and delayed delivery can threaten a project. For more information, the reader is referred to Shneiderman (2004).

The following five measurable human factors are essential for the evaluation of a successful user-interface (Shneiderman, 1998):

- Time to learn. Regarding the needed time for typical persons of the user community to learn relevant commands to accomplish various tasks successfully.

- Speed of performance. Considering the time to execute the benchmark tasks.
- Rate of errors by users. Taking into account the amount and kinds of errors when users performing the benchmark task.
- Retention over time. Regarding the feasibility of how well users maintain their knowledge after a certain time period. Retention is influenced by time to learn and frequency of use.
- Subjective satisfaction. Considering the aspect of how much users like using different factors of the system. Questionnaires, written surveys and interviews are tools for determining the user's satisfaction.

As these aspects are linked to each other, the designer and project manager must understand the tradeoffs and have to make compromises and choices explicit and in the light of general considerations.

Another important aspect which challenges the interactive designer is the range of human ability. It is important to understand the human psychological process to guarantee that systems are designed to match users' capabilities. Similarly, it is also important to regard human physiological capabilities. Therefore, various physical measurements of static human dimensions and of 'humans in action' have been carried out (Dreyfuss, 1967; Pheasant, 1967; and Bailey, 1996). Since perception plays such an important role, studies investigating the human vision abilities have been realised (Wickens and Hollands, 2000). Therefore, researchers investigated the human response time by varying visual stimuli, or the needed time for humans to adapt to bright or low light.

In order to design an efficient interactive-system a good based knowledge and understanding of cognitive and perceptual abilities of the users are required (Wickens and Holland, 2000). The fact that humans interpret external stimuli rapidly (within milliseconds) and start complex actions makes extensive interactive-computer-systems possible. A classification of human cognitive processes is listed in the journal *Ergonomics Abstracts* and summarised by (Shneiderman, 2004):

- Short-term memory
- Long-term memory and learning
- Problem solving

- Decision-making
- Attention and set (scope of concern)
- Search and scanning
- Time perception

Furthermore, background experience and expertise in the task field and interface domain are important in learning and performance. Task or computer skill knowledge might be helpful for prediction of the user's performance.

Moreover, the user's personality type can also be taken into account by using Myers-Briggs Type Indicator (Keirsey, 1998) based on Carl Jung's theories of personality types: Extroversion vs. introversion, sensing vs. intuition, perceptive vs. judging or feeling vs. thinking are considered and make it therefore interesting for this research project.

Therefore, it has to be investigated how experts and novices differ considering the human cognitive processes and consequently, it has to ensured that the updated version of *Robo-Race* is able to capture most of these significant aspects.

During a system evolution, incremental usability studies and user's acceptance testing have to be carried out. Having built up the initial system successfully, refinements can be performed based on individual interviews and questionnaires. Alongside the system's development and for evolutionary refinements, users' feedback can provide useful knowledge and guidance (Shneiderman, 2004). Based on this insight, a series of runs with different users (sailors) was carried out with *Robo-Race* in the Flight Simulator Laboratory of the University of Southampton in order to get an early feedback and recommendations for improving the existing simulator. This study was carried out by Spenkuch *et al.* (2008) and will be explained in Chapter 5. Furthermore, the corresponding paper presented at the *7th International Conference on the Engineering of Sports*, in Biarritz (France) and is attached to the Appendix.

In order to develop a successful interactive system, a set of theories, principles, and guidelines are available for the designer. Principles such as 'recognise user diversity' or 'use the eight golden rules of interface design' provide helpful and useful guidance during the development process and for evolutionary refinement (Shneiderman, 2004).

Different interaction styles like direct manipulation, menu selection, form fill-in, command language and natural language are available. In order to enhance the realism of the simulation, the direct manipulation is the best approach for this study as users can carry out tasks rapidly and can observe the results instantaneously. The aim of direct manipulation should be that 'the user is able to apply intellect directly to the task the tool itself seems to disappear' (Rutkowski, 1982). Therefore, a visual representation in form of a virtual reality has to be provided which already exists in *Robo-Race*.

Shneiderman (1998) constructed an integrated portrait of direct manipulation with the following three principles:

1. Continuous representation of the objects and actions of interest with meaningful visual metaphors;
2. Physical actions or presses of labelled buttons, instead of complex syntax; and
3. Rapid incremental reversible operations whose effect on the object of interest is visible immediately.

Appling these principles will yield to systems that have the following features:

- Basic functionality will be learned by novices (by possible supervision of more experienced users);
- Experts are able to work fast to perform a wide set of tasks;
- knowledgeable temporary users can keep operational concepts;
- Error messages are seldom required;
- Users have immediate feedback of their actions, and, if the actions are counterproductive for reaching the goal, they can easily reverse the way of their actions;
- Users are less anxious and more confident as the system is understandable and as actions can be undone easily; and
- Users become more confident and master the system because they are the initiators, they feel the control over the system, and they can predict the system's answers.

These points above are important aspects and have to be considered when building a high-quality interactive system. Transferring these aspects to *Robo-Race* lead to the conclusion

that this sailing simulator is built on a promising basis because it is equipped with at least fundamental stages that follow the three principles mentioned above.

4.3.2 Input/output devices

The object of this section is to highlight various input/output devices and discuss some of the factors that have to be considered when selecting the right input/output device setup for *Robo-Race* in order to enhance the realism of the simulation and to support the user's natural sailing behaviour.

An input device transforms information from the user into data for the software in such a way that the computer can perform the desired action. Output devices convert information within a computer system into a perceptible form for humans. The choice and method of use of the device have to be made by focusing on their positive contribution to the applicability of the system. In particular, it should support the user to perform tasks safely, effectively, efficiently and if possible enjoyably. According to Preece (1994), the most appropriate input device will be the one that:

- Matches the physiological and psychological characteristics of the user, their training and their expertise;
- Is appropriate for the tasks that are to be performed; and
- Is suitable for the intended work and environment.

In contrast, the output device should be able to:

- Inform the user about his/her actual state in the file or process;
- Specify how much progress through a process took place;
- Show to the user that it is his/her turn to give some input;
- Approve that input was successful; and
- Inform the user about unsuitable input.

Many types of different input devices are available to suit different situations whereas the usability of an input device depends significantly on its contribution of a suitable feedback. In order to interact with the sailing simulator effectively, various inputs such as discrete

entry device (e.g. keyboard or buttons) and continuous entry devices (joystick, steering wheel and rollerballs) were investigated in order to consider the realism and natural behaviour objectives. It seems to be straightforward to rebuild the reality as realistically as possible when designing a sailing simulator. Therefore, discrete entry devices that just involve sensing one of two discrete positions (on or off) are not suitable for controlling a yacht effectively. Continuous entry devices contribute to a more natural input as they involve sensing in a continuous range which simulates the situation in a more active realistic environment because controlling a yacht is done by continuous movements of the steering wheel more than by pressing buttons.

Similar to the input devices, various types of output devices are available, whereas visual and sound outputs are the most common forms of it. In order to show the computer-generated images, the following displays were available considering the budget and aims of this research project: computer screen monitor, projector, heads-up display, helmet-mounted display. Furthermore, the user can be informed about the consequences of his/her actions by applying a physical output, such as a force feedback to an input device (joystick or steering wheel).

Investigations of different input devices controlling a car and a sailing yacht have been carried out (Andonian *et al.*, 2003 and Spenkuch *et al.*, 2008). Therefore, the performance of the users within the driving and sailing simulator was recorded for different tasks using a joystick or a steering wheel control. For the driving simulator, three driving setups were studied, such as straight-line highway driving, winding country road driving, and evasive manoeuvring. The collected data showed that drivers performed better using the steering wheel in comparison to the joystick. Therefore, the drivers' lane tracking capability was applied for determining the driver's performance. In addition, three different force feedbacks (linear, non-linear speed sensitive, and none) for the joystick have been studied whereas the driver performance improved using the joystick setup with additional force feedback. For the sailing simulator studies, the users had to control an ACC-yacht against two AI-opponents over a course consisting of an upwind leg with subsequent mark rounding. This study will be explained in a detail in Chapter 5 and further information can be found in the Appendix. In short, the user's performance was determined by analysing the needed racing time to finish the course. The joystick setup in conjunction with a

proportional-integral-derivative-controller (PID-controller) yielded poorer performance and a more unrealistic sailing behaviour compared to the steering wheel setup without the PID-controller. Furthermore, the effect of the output environment was investigated in that study by comparing the subjective and objective behaviour of the user within the Virtual Reality environment. Therefore, the computer screen was replaced with a projection environment consisting of three overhead wall-projectors. When the projection environment setup was used, it was clearly observed that the sailors were much more involved, attentive and active in performing the task.

Earlier investigations have been carried out that focused on differences occurring among several visual displays (Johnson *et al*., 1999; Ruddle *et al*., 1999; Patrick *et al*. 2000). Ruddle *et al*. (1999) investigated the differences that arose when participants used a helmet-mounted display (HMD) and a desktop (monitor) display in order to learn the layouts of two large-scale virtual buildings through repeated direct navigational experience. Analysis of the users' behaviour showed that the HMD enhanced an immersive experience that seems to be more real than this one provided by the desktop monitor setup. An experiment that investigated the effects of three visual display setups varying in terms of immersive environment was carried out by (Johnson *et al*., 1999). Therefore, a wide field of view (FOV) HMD, a narrow FOV HMD and a stationary, rear-projection, wide screen display (WSD) have been set up. No significant differences could be determined between the HMD and the WSD used to train soldiers to explore and navigate in an unfamiliar heliport environment. The different display setups did not affect the user's spatial knowledge of the heliport. An alternative to HMDs for virtual environments (VEs) was investigated by Patrick *et al*. (2000) who used a large rear-projection screen. The VE was presented by three different viewing setups: HMD, large projection screen, and desktop monitor. No statistically significant differences in the spatial knowledge learned for the VR could be assessed between the HMD and the large projection screen setup. Furthermore, it was concluded that the large screen projection setup is 'an effective, inexpensive substitute for a HMD' (Patrick *et al*., 2000).

This chapter highlighted suitable human-computer interaction devices for the dynamic sailing environment. Active and passive sailing simulators have been developed to determine the sailor's individual performance. A third category of simulators is identified

by *Robo-Race* where a sailor can actively interact with the computer controlled AI-yachts in a multiple yacht fleet race environment.

A first attempt of how the human (sailor) interact with *Robo-Race* containing a dynamically changing sailing environment is carried out in the next chapter. Potential improvements regarding the realism of the simulation, the hardware, the software, and the display-input-device-environment are highlighted.

5 Robo-Yacht-Sailor Studies

5.1 Experiments with *Robo-Race*

An investigation was carried out with *Robo-Race* with the aim of examining the effect on sailor performance of enhancing the realism of the simulation through use of a wrap around visualisation of the racing course viewed by the helmsman/tactician. For this purpose, the following two human interface device/display environments were designed. Firstly, a Basic Display Environment (BDE) which consists of two screens in conjunction with a joystick. The later is the Advanced Display Environment (ADE) that consists of three projectors with an additional screen and a steering (or helm) wheel as interface device. A number of sailors who were divided according to their sailing skills and their experience with computer game interface devices had to deal with seven upwind races against two computer controlled America's Cup Class (ACC) yachts. This Section is a summary of the most important aspects of the paper presented at the *7th International Conference on the Engineering of Sports* (Biarritz, France) and can be found in the Appendix A1 (Spenkuch *et al.*, 2008).

5.2 The Race Setup

In order to evaluate the performance of sailors a possible methodology is that of using a realistic sailing simulator. Two different display-input device-environments are set up to determine the effect on sailor performance by enhancing the realism of the simulation. A

basic human-computer interaction setup and a more realistic interaction environment between sailor and computer were designed.

The basic device-environment setup consists of a joystick as the only input device and two flat screens (see Fig. 9). The joystick deals with the following two tasks: firstly the adjustment of the default rudder angle given by the PID-controller and secondly the change of the viewpoint distance via zooming. The virtual environment and the onboard instruments are displayed on two flat screens.

An enhanced environment is composed of an additional steering wheel (helm) which controls the rudder angle directly, the joystick for zooming, a 17" flat screen for displaying the onboard instruments and three projectors for displaying the 3D sailing environment on a cluster of screens (see Fig. 10). In addition to the improvement of the visualisation of the simulation, a direct control of the sailing yacht by the sailor is implemented to ensure a direct relationship of the wheel motion to the rudder angle.

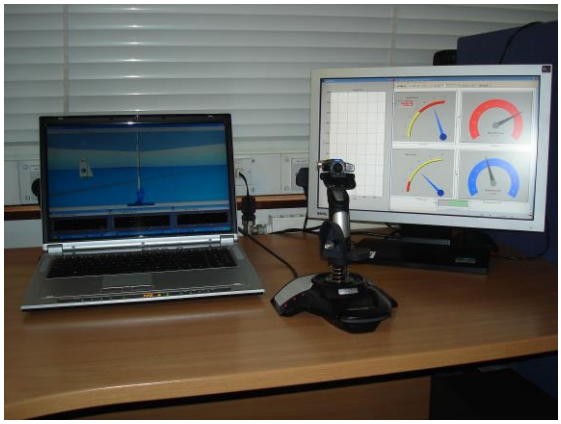

Figure 9: Basic Display Environment (BDE) showing instruments on laptop and VR on standard monitor

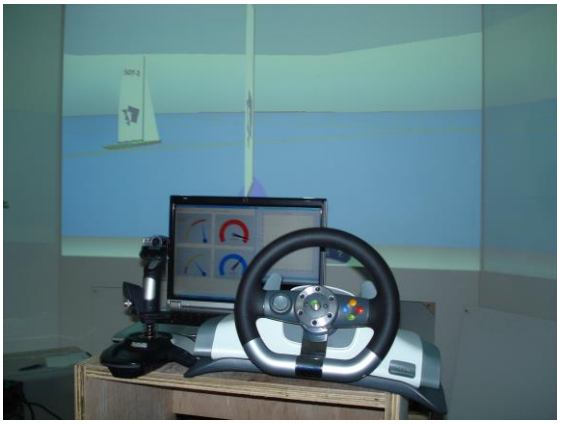

Figure 10: Advanced Display Environment (ADE) showing wheel and curved display panels for VR driven by three data projectors

The task of the sailors consists in racing an upwind leg against two computer driven yachts with the finish occurs at the rounding of the mark (see Fig. 11). The distance between the starting point and upwind mark is ¾ of a nautical mile (or 1389 m). The three ACC yachts start in the same line with a distance of 100 metres between each yacht. Therefore, the starting positions can be classified in three categories as the yacht at the right hand side has the best location (position 1, x = 100) according to the imposed initial heading, followed by the yacht in the middle (position 2, x = 0) and lastly the yacht on the left with the worst

starting position (position 3, x = -100). Furthermore, the history of the stochastic wind conditions remains the same for all races due to the sake of comparability and repeatability of the experiments. The wind speed and wind angle vary about a value of 5 m/s and about ± 20º with an oscillatory pattern. The simulation is run twice as fast as real-time in order to execute more races. The yacht performance is controlled by the parameter which affects the sail setup which consists of a Jib and Mainsail. The sail trim parameter of 1.0 stands for 100% sail drive force whereas the value of 0.9 denotes 90% of the maximum sail drive force (Scarponi, 2008).

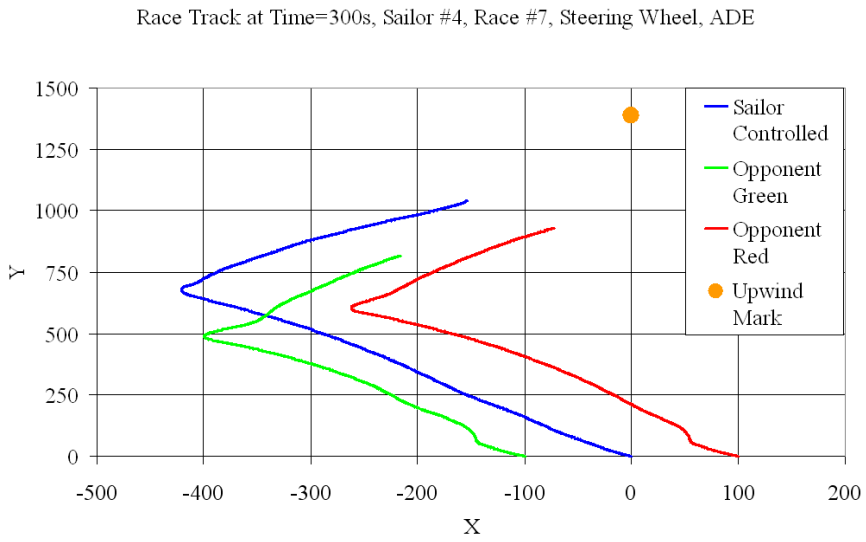

Figure 11:: Example of Race Tracks from Sailor #4, Race #7 using ADE/Steering Wheel, as the two computer controlled yachts respond to the wind shifts the pattern of wind variation can be seen in their course variation

A presentation is given to the sailor at the beginning of each session to ensure that everybody has the same pre-knowledge. This contains an introduction to the sail simulator, an overview of the different input devices, environments, onboard instruments, and finally the task which is required. Two questions are posed to the sailor to determine his/her sailing background and computer game input device experience. Afterwards, a trial is run in order to familiarise the sailor with the simulator, input device, and environment. After the session of seven races, the sailor has to complete a questionnaire which deals with the realism of the simulator, the usability of the input devices and suggestions for further improvements with are listed in chapter 5.5.

Sets of seven races with each sailor in both the BDE and ADE are carried out in order to determine:

- Improvement of the sailor's performance during the session based on experience with a specific input device. Therefore the first and last races of a session are the same without the sailor's knowledge to ensure a natural and unprejudiced behaviour;
- Influence of the sailor's performance when enhancing the realism of the simulation by replacing the joystick through a wheel and the screen for the virtual reality by three projectors-wall environment; and
- Influence of the sailor's performance and behaviour regarding the onboard instrument support under different yacht thrusts. To do so, races #4 and #7 are set-up with/out onboard instruments where all yachts have the same thrust. Furthermore, races #2 and #5 are set-up in the same way whereas the user's yacht is the strongest within the fleet.

5.3 Test Cases

In order to determine the influence of the two different human interface device, the performance of the sailor-simulator-system is investigated. The data analysis is based on several parameters in order to receive trustworthy and reliable results. The performance of the human interface device during the race session, its interaction with the implementation of the sailor's tactics and the sailor's performance improvement during the session considering the two interface devices are determined by regarding the following variables:

- The race time for reaching the upwind mark and the order of arrival at the upwind mark considering the level of sailing expertise and computer game background of the sailor and the used interface device;
- The input error performance during the race session for the joystick setup and steering wheel setup by investigating the clicks on button #5 instead of button #6 and vice versa, and by analysing the wrong steering wheel rotation direction.

As mentioned before, the second objective of the influence of an improved display environment is assessed by analysing the interaction of the sailor with the BDE and the ADE respectively. This data analysis is based on the observation of the sailor's behaviour during the races and the sailor's individual feedback recorded on the questionnaire.

5.4 Summary

The experiments show an important effect on sailor performance when enhancing the realism of the simulation. The improvement of the realism of the simulation was achieved by using two different display setups, the Basic Display Environment (BDE) and Advanced Display Environment (ADE).

In considering the joystick setup which uses the PID-controller no clear picture of the sailors' performance improvement can be drawn. This phenomenon was also observed by (Andonian *et al*., 2003). The results for the joystick show that the setup of the PID-controller and the adjustment of the rudder angle by clicking button#5 and #6 are neither practical nor effective. Furthermore this setup confuses the sailor and constrains his/her natural way of sailing which in turn limits the realism of the simulation. It was observed that even computer game and interface device experienced sailors needed at least three races to reduce their input error whereas other sailors struggled with the correct input until the end of the session.

A completely different picture emerges when using the steering wheel with the direct control of the rudder angle. A clear improvement in the control of the yacht's motion could be observed. This allowed the user to sail the desired course and to apply the arranged tactic and strategy without a limitation caused by the interface device.

An important change of the novices' race behaviour was observed during the sessions. Within the first races the novices adapt to the behaviour of their opponents and then developed their own tactics and strategies which they applied in the following races. They still made wrong tactical decisions due to the lack of specific sailing knowledge and experience, but a significant improvement of the general race performance was observed. Therefore, this simulator with the appropriate steering wheel/ADE setup could be used as an effective training tool for novices.

The effect on the sailor's performance when enhancing the display environment is not measurable, but the observation made during the races and the feedback of the sailors about the realism of the setup is much more positive for the ADE than for the BDE. The improvement of the realism causes a more active and involved behaviour of the sailor within the races. The combination of the ADE and the steering wheel without the use of the

PID-controller has shown to be a good choice to enhance the realism of the simulation which is proven by the results of the steering wheel/ADE runs and the feedback of the sailors who attended this study.

5.5 Recommendations and possible Improvements

The improvements of the realism of the simulation mentioned in the Chapter 5.1 were a good starting point because the functional fidelity of the simulation was enhanced. Araújo *et al*. (2005) stated that sport simulations should be set up in a way such that they allow the user to execute the same actions as those in the real task environment. This means, that the layout of the real and the simulated task can differ as long as the user's activities are consistent. In addition, the validity of the simulation has to be considered as they can influence the sailor's behaviour. Furthermore, environmental constraints have to be taken into account as they influence the realism when unfamiliar human-computer interface need special practise or a visual environment does not deliver adequate feedback because of missing details.

To solve these constraints and to enhance the realism of the simulation which in turn will support the sailor's natural behaviour, the following recommendations and possible improvements were derived from the sailing sessions through questionnaires and individual interviews. They are categorised and prioritised as follows:

- Hardware improvements:
  I. Implementation of a real yacht wheel;
  II. Implementation for adjusting the sails by pressing control buttons or by pulling a rope-based input device;
  III. Use of an apparatus that simulate the yacht's actual heel angle; and
  IV. Use of a head-mounted display device.

- Visual improvements:
  I. Feedback about the actual sail status such as boom position and sail load;
  II. Display of the actual wind conditions within the VR;
  III. Showing the actual heel angle of the yacht with different camera views;

IV. Implementation of waves on the sea surface;
V. Using tools for enhancing the perspective within the three projector environment;
VI. Displaying of important performance indicator such as velocity made good after a tack for example.

- Physics and setup of the simulation improvements:
  I. Improving the interactions of the yacht;
  II. More aggressive opponent setup;
  III. Better variation of windshifts during the session;
  IV. Implementation of a jibing feature and enhancing of downwind capabilities of the computer driven yachts;
  V. Improving the mark reaching and mark rounding of the computer controlled yachts;
  VI. Enhancing the steering wheel rotation according to real yacht steering.

These recommendations and improvements will be discussed throughout the thesis according to their relevance to the project's objectives. Furthermore, their realisation and implementation into *Robo-Race* are highlighted in the following chapters and commented in the future work section.

5.6 Conclusions

The conducted test series with the sailors gave important information of the maturity and constraints of *Robo-Race*. One important constraint, the control and display setup for steering the yacht was solved by applying an advanced display environment in conjunction with a steering wheel which was judged to support the sailor in his/her natural sailing behaviour. The predictable and non-aggressive behaviour of the opponents identified another constrain of *Robo-Race* which is due to the applied rule-based decision-making process. Consequently, this inadequate process has to be replaced and therefore, the focus of work should concentrate on developing a tactician module for *Robo-Race* taking into account the complex and fuzzy inputs of the dynamic fleet racing environment. This important constraint will be described in the Chapter 8. The following Chapter 6 describes the development of a natural and dynamic weather model and its implementation into

Robo-Race. Another important constraint, the model describing yacht interaction was also judged to be inappropriate and has to be replaced in order to simulate this important tactical weapon correctly in a yacht fleet racing environment. Chapter 7 addresses this problem and illustrates the development of an advanced yacht interaction model based on the lifting-line method.

6 A natural and realistic Weather Model for *Robo-Race*

The investigations carried out in Chapter 5 have revealed the constraints of the 'starting' version of *Robo-Race.* Although an important step forward has been made on the hardware side, such as the input and display devices, this chapter starts to focus on the software constraints of the simulator, especially the weather model and its implementation into *Robo-Race*. It seems to be obvious that a simple, predictable weather model will yield predictable, unrealistic and consequently wrong decisions and performance outcomes of the crew as observed in Chapter 5. Furthermore, the one time frame setup used in *Robo-Race,* meaning that the actual weather conditions apply to the entire race course is judged to be a substantial constraint. Consequently, no spatial and therefore temporal differences between two differently positioned yachts on the race course are considered. Therefore, a new developed weather model and the way of its implementation have to overcome these constraints since this study aims to simulate the behaviour and decision-making process of the sailor to a sophisticated level. In order to do so, the characteristics of real weather on the race course have to be simulated correctly at different locations on the race course and various weather scenarios have to be generated easily. Consequently the *new* weather model has to fulfil the following requirements:

- Dynamic and unpredictable
- Probabilistic
- Natural, meaning to capture important real weather features (frequencies)
- Flexible and easy to change

To guarantee to meet these requirements and a sophisticated level of realism, spectral analysis of the generated weather series were carried out and compared to those of recorded weather data through Fourier Transform calculation.

As stated earlier, the new weather model has to be developed in order to enhance the realism of the yacht race simulator. The fact that this simulator deals with short and medium range yacht races also affects the development of the weather model. Longer time-scales of day or seasonal level can be neglected. Hence, the shorter time-scales have to be captured sufficiently, such as wind shifts and turbulence because they play a significant role within a yacht race and have an important influence on the performance of the crew.

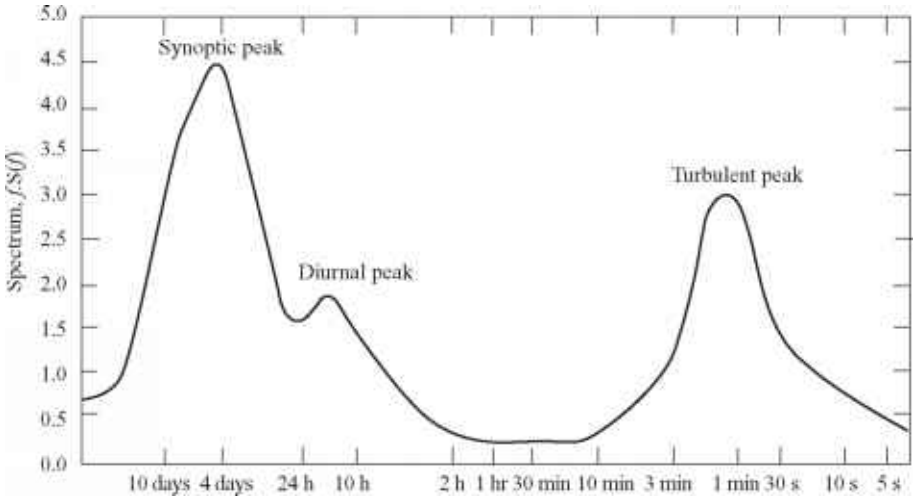

Figure 12: Wind spectrum Farm Brookhaven based on Work by van der Hoven (1957)

Considering the scope of this research project, one has to focus on *turbulent peak* region whereas the low-frequency band located on the left side of Figure 12 showing the *synoptic* and *diurnal* peaks can be neglected. Of particular interest is the modelling of the turbulent peak to a sufficient level that can be seen on the right side of Figure 12 indicating higher frequency fluctuations caused by the presence of hills, trees and buildings for instance.

To develop a new weather model and to implement it successfully into *Robo-Race* the following steps have been taken that also mirrors the structure of the following subchapters:

1. Explanation of the actual used weather model running the weather engine of *Robo-Race.* There, the problems and constraints of the one time frame setup are highlighted and compared to the more advanced setup, the individual yacht time-frame one (see Chapter 6.1).
2. Applying a more sophisticated weather series generated by a more advanced algorithm to the individual yacht time frame setup (see Chapter 6.1).

3. Development of the individual yacht time frame setup where a master and slave yacht methodology has been applied
4. Development of an unpredictable and probabilistic weather model and its extension that different effects can be easily applied, such as a gradual increase of the main wind velocity or the superposition of a sinusoidal wave for instance.

6.1 The Effect of Different Implementation Methodologies

This subchapter compares the originally used with the new developed implementation method (the reader is referred to Chapter 6.2 for a detailed description). Thereby, two evolution steps were considered. Firstly, the introduction of individual yacht time frames and secondly, a realistic natural weather generated by the new weather model. Therefore, three different yacht races are set up to compare

1. The simple weather model with one general time frame for all yachts,
2. The simple weather model with three individual yacht time frames, and
3. The new developed natural weather model (the reader is referred to Chapter 6.3 for a detailed description) with three individual yacht time frames.

The race course itself can be described as a triangular course with three marks (see Figure 13). The start line (horizontal to the final mark) is almost perpendicular to the wind direction (northerly wind) which creates an upwind beat on the first leg. Mark 2, the upwind mark, has to be passed before the yachts are heading down on the first downwind leg to the leeward mark where they have to conduct a gybe. Then, the third leg (second downwind leg) has to be sailed to reach the final mark.

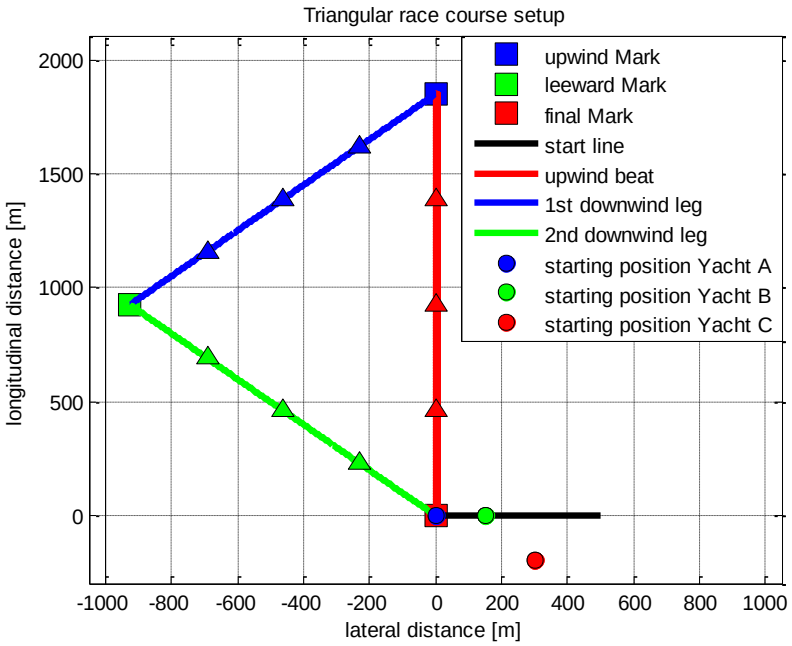

Figure 13: Race course setup showing its triangular shape the corresponding marks and race legs, as well as the start line and the different starting positions of the three yachts.

The distance between the starting line and the upwind mark is one nautical mile (1852 m). The leeward mark is offset to the final mark by half a nautical mile in positive horizontal and negative vertical direction. To examine the effect of the different weather models and the time frame setups, the individual starting positions of the yachts vary in horizontal and vertical direction. The master yacht, *Yacht A*, starts at the final mark (x = 0, y = 0), whereas *Yacht B* starts in the same line with a lateral distance of 100 metres (x = 100, y = 0). *Yacht C* has the worst starting position with a lateral and longitudinal offset of 300 and 200 meters, respectively (x = 300, y = -200). The blanketing effect has been switched off in this chapter in order to simplify the investigations by focusing only on the effect of the different weather frame setups on the reality level of the simulation without any unnecessary disturbances.

For the simple weather model simulation, a wind speed and wind angle varying about a mean value with a sinusoidal oscillatory pattern were set up. The mean wind speed was set to 5 ms^{-1} with a sine wave featuring an amplitude of ± 1.0 ms^{-1} and a frequency of 360º sec^{-1}. The mean wind direction was set to 0º with amplitude of ± 15º and a frequency of 360º sec^{-1}.

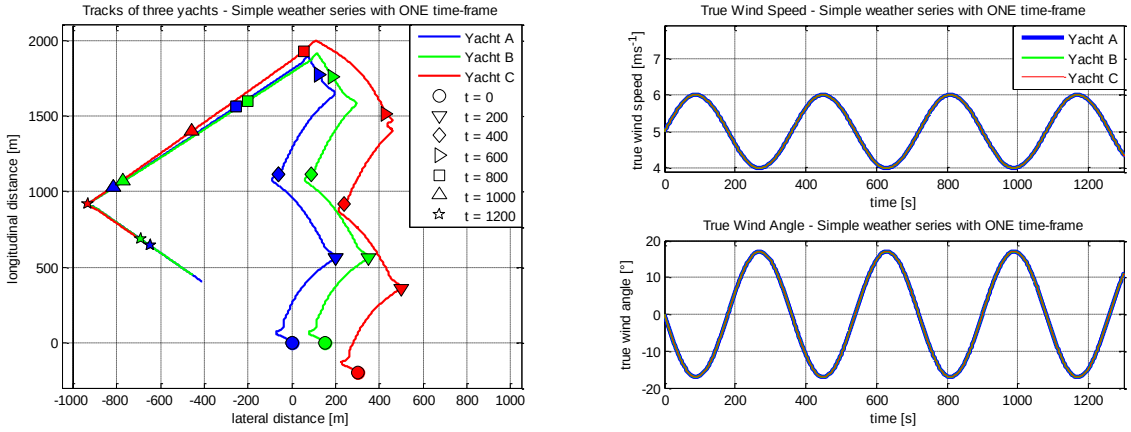

a) **b)**

Figure 14: Yacht race on a triangular race course showing a race with a simple weather model setup and one general time frame. Figure a) on the left, shows the race tracks of the yachts and Figure b) displays the individual wind speeds and wind angles varying about a mean value with a sinusoidal oscillating pattern.

Figure 14 a) shows the race track of the yachts on the course. Although the yachts were placed at different starting positions, they show the same sailing behaviour without considering any spatial and temporal issues. In particular, they conducted identical manoeuvres at the same time on the first three quarters on the upwind beat. This can be explained by examining the individual wind history seen by each yacht being identical due to the one time-frame setup (see Figure 14 b). The sailing behaviour of *Yacht C* differs slightly on the final quarter of the upwind beat since she had to get into position for rounding the upwind mark. *Yacht A* passes it first and kept the lead until the end of the race.

This simulation shows the limitations of the single time frame setup resulting in an unrealistic, unnatural and constraint-rich sailing environment. Consequently, this setup does not provide an environment helping to support natural and realistic sailing behaviour of the computer controlled yachts. The following paragraph highlights the next evolution step of the weather model featuring individual yacht time-frames.

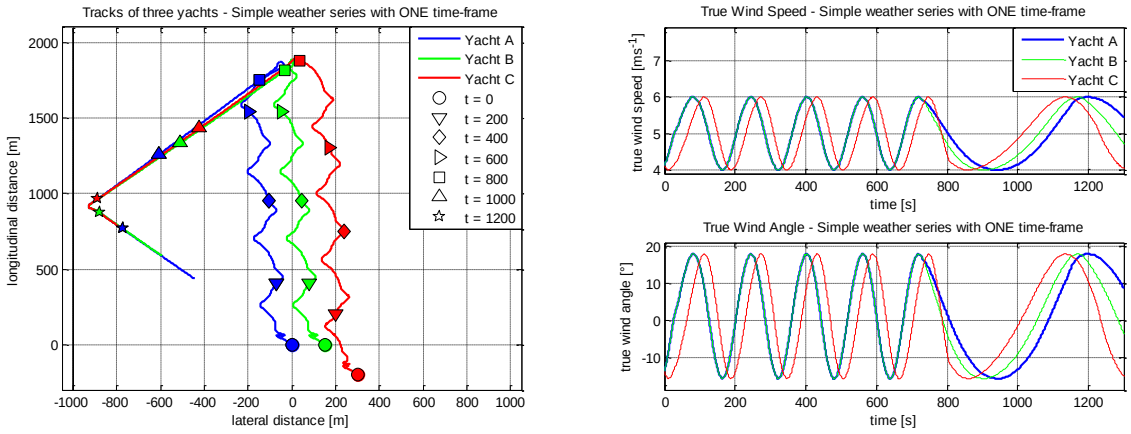

a) **b)**

Figure 15: Yacht race on a triangular race course showing a race with a simple weather model setup and three individual time frames. Figure a) on the left, shows the race tracks of the yachts and Figure b) displays the individual wind speeds and wind angles varying about a mean value with a sinusoidal oscillating pattern.

Figure 15 a) indicates the tracks of the yachts on the race course. Again, the yachts were put at different starting positions but this time they showed a different sailing behaviour on the upwind beat. The yachts conduct the same manoeuvres but at different times. *Yacht A* and *Yacht B* behaved almost identical on the first leg since they experienced the same wind conditions due to their identical longitudinal positions. This picture changes when comparing *Yacht C* with the other two yachts. It can be observed in all figures of Figure 15 that *Yacht C*'s actions were time-delayed which can be explained by her lower longitudinal location on the race course and therefore time-delayed position in the weather series compared to those of *Yacht A* and *Yacht B*. This can be seen for example at t = 400 sec, where *Yacht C* started to tack and the other two yachts had already conducted their tacks several seconds ago. It is also worth pointing out that the frequency of the sine waves in Figure 15 b) were higher when the yachts travelled against the mean wind direction and much lower when they went with the wind on the downwind legs. This phenomenon can be explained by the ratio of the clock and series time-frames as described in Chapter 6.2. Furthermore, it indicates a correct and successful implementation of the individual time-frame setup into *Robo-Race*. This second evolution stage can be seen as an important step forward to provide a more realistic yacht race environment. Nevertheless, it still misses natural and realistic weather statistics. This constraint will be addressed in the next and final evolution stage where a multiple time-frame setup will be combined with a natural and realistic weather series.

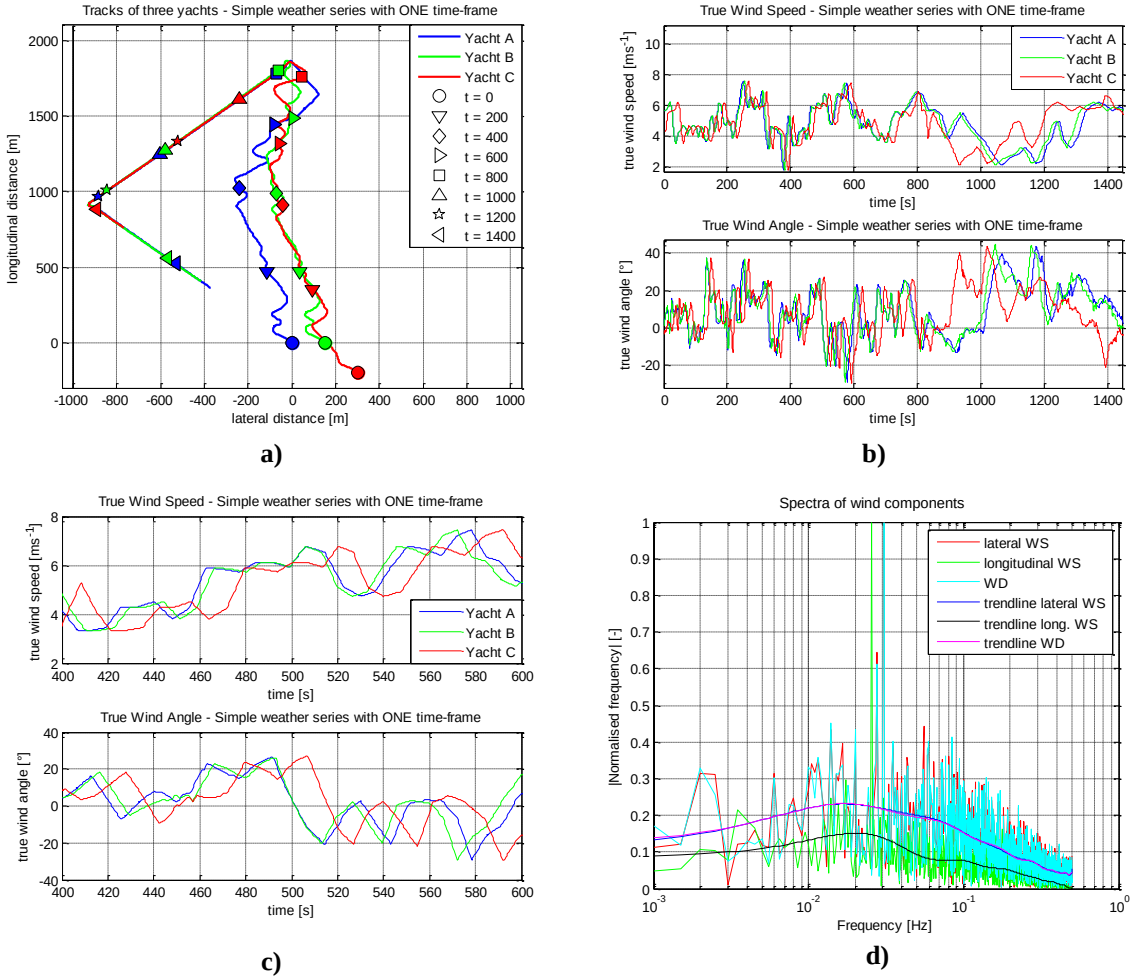

Figure 16: Yacht race on a triangular race course showing a race with the new natural weather model setup and three individual time frames. Figure a) on the top left, shows the race tracks of the yachts. Figure b) and c) displays the individual wind speeds and wind angles varying about a mean value with an oscillating pattern, where Figure c) provides a zoom-in view. Figure d) indicates the spectra of the weather series used for this race.

Figure 16 a) shows the tracks of the yachts on the course. *Yacht A* and *Yacht B* still show a similar sailing behaviour on the first half of the upwind beat but this changes on the second half, where *Yacht B* (green line) is time-advanced to *Yacht A* (blue line). This phenomenon can be also observed in Figure 16 c) where the green line is time-advanced to the blue line from t = 500 sec onwards. This figure also indicates the time-delayed wind history of *Yacht C* that is also observable in Figure 16 b). As it can be seen in Figures 16 a) to c), this setup supports an unpredictable, natural and dynamic yacht race environment indicated by the yacht's dynamic and irregular race tracks. This assumption was further supported by the result of a spectral analysis of the applied weather series indicating a more natural and realistic characteristic of the applied weather series (see Figure 16 d). In particular, this weather series features the two deterministic frequencies of the sinusoidal waves in

longitudinal wind speed and wind direction that are clearly visible in Figure 16 d) as well as the turbulent peak around 0.015 Hz.
It is believed that the final evolution stage provides the necessary features and improvements to eliminate the simulators constraints in supporting to provide a dynamic, natural and unpredictable yacht race environment. Therefore, this setup will be used for further investigations, especially for the development of an advanced artificial intelligence based sailor.

6.2 Implementation into *Robo-Race*

In the previous paragraph, the effects of different yacht time frame setups have been described. Now, one wants to explain the derivation and implementation of the multiple yacht time frame setup into *Robo-Race*. A weather series normally describes the statistics of a stationary observer meaning that he/she does not change the position with time. Since a yacht can be considered as a moving observer, a stationary model has to be transformed into one for moving observer. Thereby, the recording time, the moving velocity of the observer and the introduction of two different time frames are essential for a successful transformation and highlighted below.

The weather system can be considered as a wind field with a mean longitudinal wind speed and changing lateral and longitudinal fluctuations as well as changing wind directions throughout the field. Imagine two stationary anchored yachts which record their individual observed weather at identical time steps Δt for a time period from t_1 to t_2. The two yachts would record the same amount of data samples but different statistics unless the yachts would be exactly located the same position which is most unlikely. This phenomenon can be explained by the variable nature of the real weather components. This feature was captured by the new weather model, by its changing longitudinal and lateral component series. The recorded series would be similar but still different depending on the dynamic lateral wind speed. Imagine *Yacht 1* and *Yacht 2* are facing a wind field travelling from north to south and from east to west, the windward yacht (more easterly) experiences the lateral component of weather series earlier that the leeward yacht (more westerly) just because of her position.

Now, let the two yachts sail from *Mark1* to *Mark2* on an upwind beat, where *Yacht 2* sails twice as fast as *Yacht 1*. The recorded weather conditions on board of each yacht vary in length as well as the statistics itself. The faster *Yacht 2* just recorded half the amount of samples as the slower *Yacht 1*. Due to the different starting positions and therefore different lateral weather conditions, the yachts experienced and consequently recorded similar but different weather data. Hence, the rate the yachts record the observed weather (every Δt) would be the same considering the overall *normal* time-frame. This picture changes if we regard the weather series time-frame in which *Yacht 2* obviously moved twice as fast as *Yacht 1*.

As a result, if a stationary weather series wants to be transformed into one for a moving observer, the corresponding time-frame has to be changed. Let us define two main time-frames: 1) *watch time-frame* and 2) *series time-frame*. The watch time-frame could be considered as the *normal* time that the sailor could read at his watch. The second time-frame, the series time-frame describes how far the yacht has travelled in the weather series generated for a stationary observer. A yacht does not travel with the same velocity in each series of the weather components. This fact requires the calculation of the yacht's position in each individual series component by applying a relation between the watch and the yacht time-frame.

If a wind field moves with the mean longitudinal velocity WS_{mean_y} and a yacht sails at an apparent wind speed WS_{app} relative to it, then the observer experiences the weather series at the rate $WS_{app} \big/ WS_{mean\_y}$. Using the earlier example, *Yacht 2* records a period of time, $x\Delta t$, measured on the crews watch (moving observer), the series time-frame (stationary observer) would be time advanced by

$$\frac{WS_{app}}{WS_{mean\_y}} x\Delta t \tag{6.1}$$

As stated earlier, the yacht's individual apparent wind speed components, WS_{app_x} and WS_{app_y}, relative to the wind field components, WS_{lat} and WS_{long}, are determined by subtracting the yacht's speed vector, V_{yacht} from the resultant mean wind speed vector

WS_{res} (see Figure 17). Thereby, the lateral wind field component consists of WS_{lat} from the series and WS_{WD_x} calculated from the wind direction angle and WS_{long}:

$$WS_{app} = WS_{res} - V_{yacht} = \begin{pmatrix} WS_{app\_x} \\ WS_{app\_y} \end{pmatrix} = \begin{pmatrix} WS_{lat} + WS_{WD\_x} \\ WS_{long} \end{pmatrix} - \begin{pmatrix} V_{yacht\_x} \\ V_{yacht\_y} \end{pmatrix} \quad (6.2)$$

The resultant wind direction angle WD_{res} is calculated by adding the wind angle change caused by WS_{lat} to the wind angle WD_{series} from the wind direction series (see Figure 17).

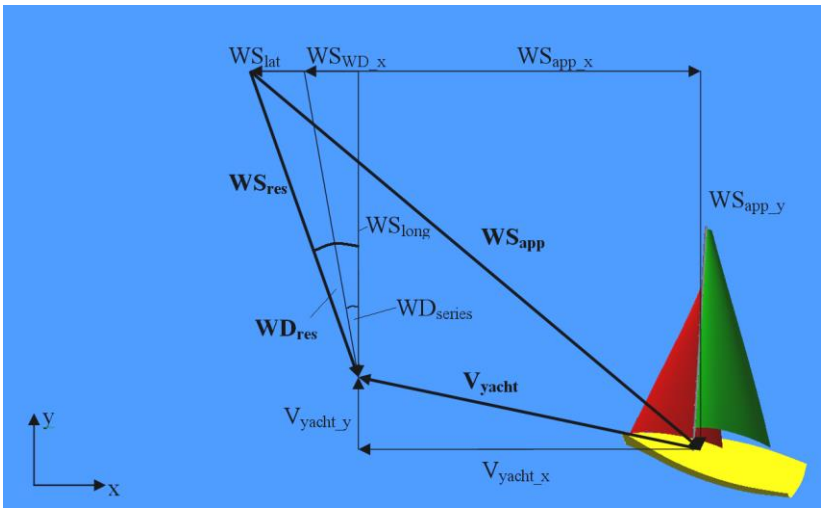

Figure 17: Visualisation of the vector subtraction for calculating the apparent wind WS_{app} showing the required vectors and each individual component.

To get the correct statistics for a moving observer from a weather series of a stationary observer, one have to calculate the corresponding position of the yacht in the stationary weather series. Let t_1 be the time describing the yacht's temporal position in the watch time-frame and T_1 the time describing the yacht's temporal position in the series time-frame, then the corresponding weather statistics for the yacht's position at the next time step t_2 $(= t_1 + \Delta t)$ can be determined by a simple time transformation. Thereby, attention has to be paid to distinguish between the yacht's motion in lateral (V_{yacht_x}) and longitudinal (V_{yacht_y}) direction. The new lateral and longitudinal positions of the yacht in the corresponding weather time series can be calculated by:

$$(T_1 + \Delta T^*)_{WS_{lat}} = \frac{WS_{app\_x}}{WS_{lat}} \Delta t \quad (6.3) \quad \text{and} \quad (T_1 + \Delta T^*)_{WS_{long},WD} = \frac{WS_{app\_y}}{WS_{long}} \Delta t \quad (6.4),$$

where the longitudinal position is used by the longitudinal wind speed as well as the wind direction time series. Before the start of a race, it has to be ensured that the spatial position of the yachts on the course meets the corresponding temporal position in the weather series, meaning for a northerly wind scenario, the more northerly positioned yacht has to be brought forward in the weather series compared to the more southerly located yachts.

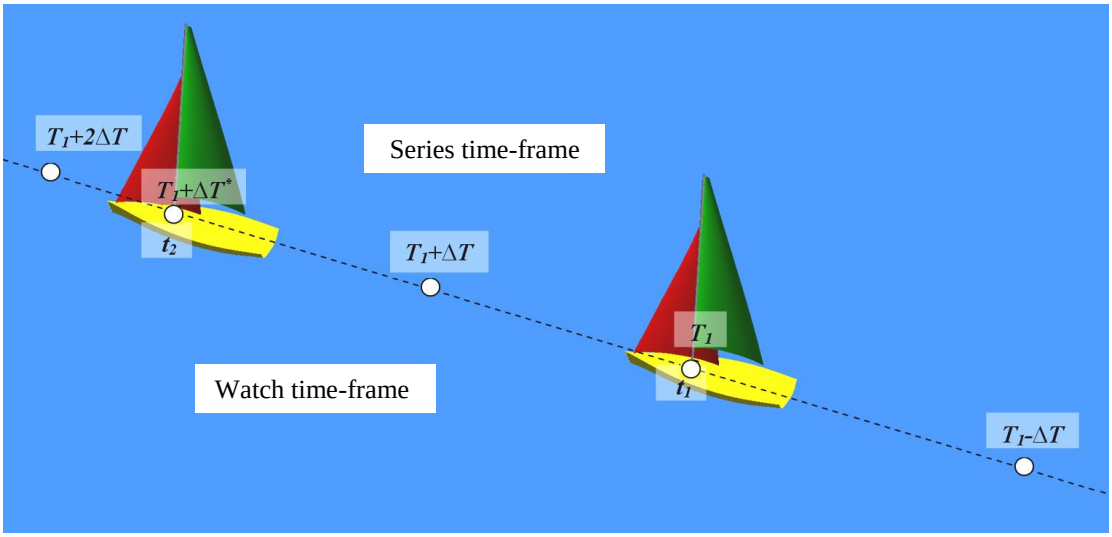

Figure 18: Schematic sketch of a yacht travelling from t_1 to t_2 showing two time-frames, *watch* and *yacht time-frame*, and the necessary statistics required to calculate the opposite statistic of t_2.

As pointed out in Figures 18 and 19, the statistic opposite of the desired time t_2 does not exist as an exact value in the series time-frame and has to be derived from the stationary weather series by linear interpolation between the points $T_1 + \Delta T$ and $T_1 + 2\Delta T$. The opposite statistic of t_2 is named $T_1 + \Delta T^*$. Figure 25 shows a short extract of the wind direction weather series and the important values used in the interpolation process.

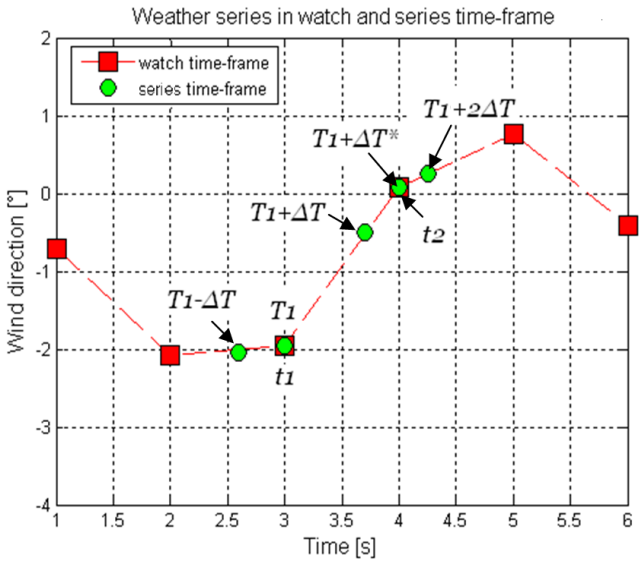

Figure 19: Extract of a wind direction weather series indicating the necessary statistics required to calculate the opposite statistic of t_2.

The implementation of the new weather model into the sailing yacht simulator *Robo-Race* is illustrated in Figures 20 and 21. Figure 20 showing a fleet of three yachts on the right and the *Weather Engine* on the left side.

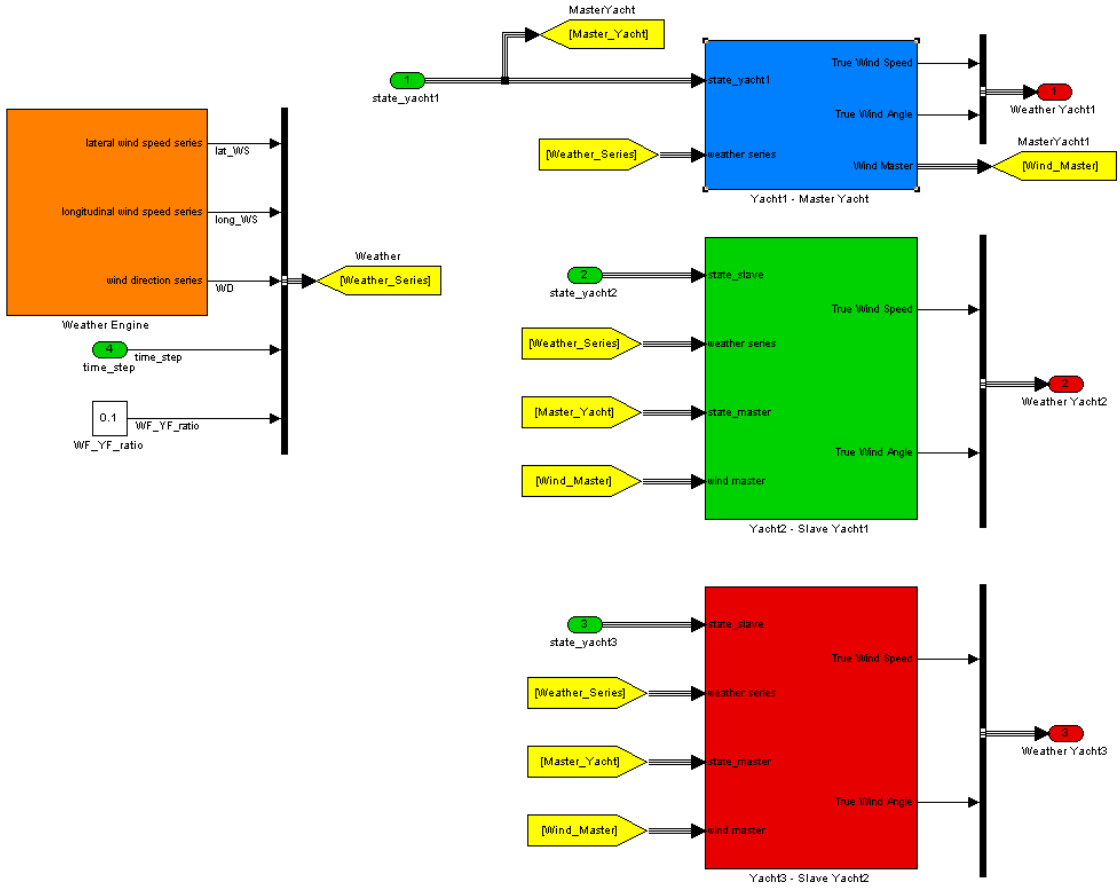

Figure 20: Schematic implementation example of the new weather model into *Robo-Race* showing the *Weather Engine* on the left and a fleet of three yachts on the right.

Depending on the watch time and the position of each yacht on the course, the yachts' individual positions had to be calculated in the three different weather series components using the following procedure. Thereby, two very important points have to be considered: *similarity* and *independency*. Particularly, when yachts are sailing far apart, their observed weather statistics have to be independent and different from each other. This picture changes completely when yachts are sailing closer or very close to another. Then, the yachts experience similar or almost the same wind speeds and directions depending on the distance between them. The point of similarity when yachts are close to another and the point of independency when yacht are far apart are crucial and have to be guaranteed to be captured by the applied implementation method.

Therefore, a *Master Yacht* has been introduced whose position in the weather series components was determined by using Equations 6.3 and 6.4. The other yachts were set to *Slave Yacht* whose individual positions in the weather series are calculated relative to the spatial distance to the master yacht. This method guarantees to deal effectively with the points of similarity and independency. The closer the yachts are sailing to another, the smaller becomes the time difference of the yachts in the weather series and therefore the more similar is the experienced weather of the two yachts and vice versa.

To calculate the temporal distance ΔT_{yachts} of the yachts in the weather series, the spatial distances (lateral and longitudinal) between the yachts on the race course were divided by the actual averaged wind statistics of the two yachts:

$$\Delta T_{yachts_{lat}} = \Delta x \left(\frac{WS_{lat\,Master} + WS_{lat\,Slave}}{2} \right)^{-1} \tag{6.5}$$

$$\Delta T_{yachts_{long}} = \Delta y \left(\frac{WS_{long_{Master}} + WS_{long_{Slave}}}{2} \right)^{-1} \tag{6.6}$$

The *Weather Engine* (see Figure 20) generates a weather series as described in the previous paragraph consisting of 1) a lateral and 2) longitudinal wind speed and 3) a wind direction component. This weather series was the same for all yachts and forwarded to them. Figure 21 shows the inner core of the master yacht using the forwarded inputs to calculate the necessary outputs (*True Wind Speed and True Wind Angle*) required to calculate the yacht's

dynamics in the simulator. Thereby, the yacht's temporal position $T_1 + \Delta T^*$ was used to calculate the corresponding statistics from the stationary weather series via linear interpolation. As mentioned earlier, the temporal weather series position of the master yacht was calculated directly, whereas the other yachts temporal positions were determined relative to it. The corresponding comparison study between the new and the former implemented simpler weather model has been conducted and described in the Chapter 6.1.

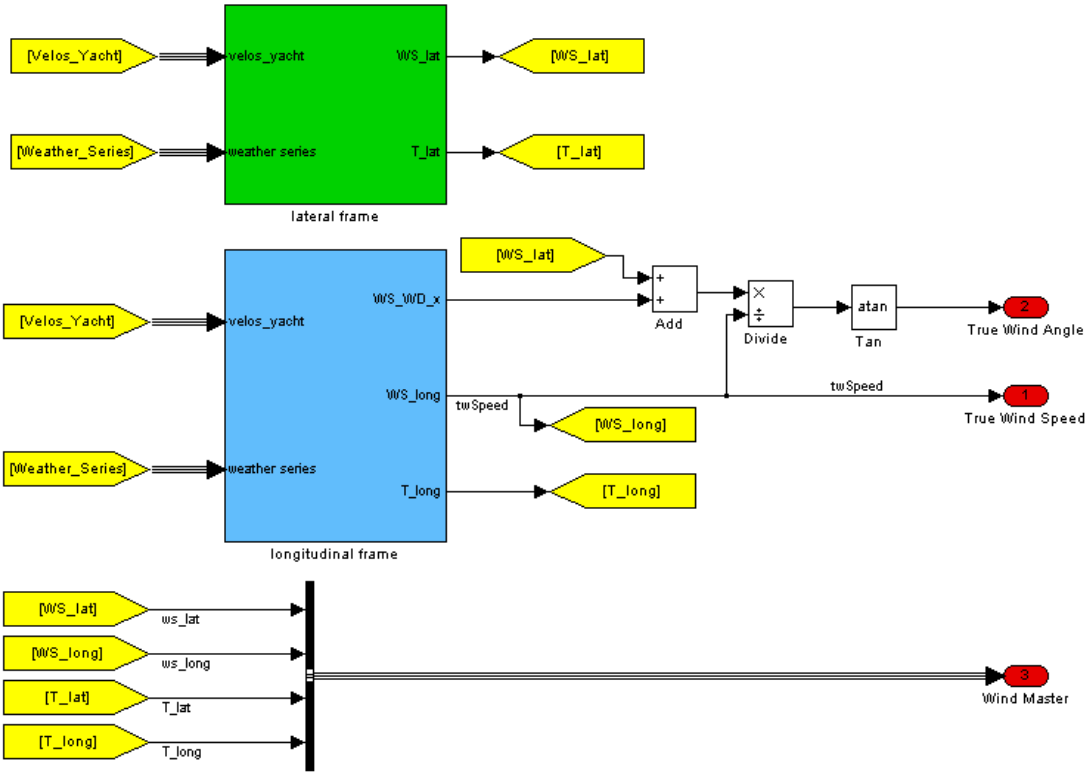

Figure 21: Inner core of the master yacht showing the inputs required for the interpolation process on the left and the outputs on the right. The outputs on the frames have to be further converted to match the notation required by *Robo-Race*.

6.3 An unpredictable and probabilistic Weather Model

The weather model presented in this section was constructed for a stationary observer. The *new* model generates a weather series of the following three components, where the lateral direction is identical to the one shown in Figure 13 but the longitudinal direction points opposite:

- Wind speed component in lateral direction (x-direction)

- Wind speed component in longitudinal direction (y-direction)
- Wind direction where northerly wind (parallel to y-axis) indicates 0°.

The two major wind components are represented by the longitudinal wind speed and the wind direction. The third component, the lateral one, is superimposed to guarantee a variation in lateral direction throughout the wind field. This was realised by applying a level of turbulence (depending on the longitudinal wind speed) with a fluctuation (depending on the wind direction):

$$WS_{fluc\_x} = WS_y \cdot f_{turb} \cdot \frac{WD_{fluc}}{\max\left(WD_{fluc}\right)} \tag{6.7},$$

where WS_y describes the longitudinal wind-speed, f_{turb} the level of turbulence and WD_{fluc} the wind-direction series. The author is aware of the fact that this expression does not hold precisely but considers that it provides a realistic and efficient way to add a varying lateral component to the weather series.

As stated earlier the maximum race time horizon of the simulation was limited to around an hour or two. Therefore, slower meteorological trends dominated by topographical or seasonal facts linking the wind speed with its direction were not considered in this study. Nevertheless, as stated in Philpott *et al.* (2004) the considered meteorological time frame allows the negligence of this correlation yielding a simpler weather model. Simpler in this context does not mean low quality. On the contrary, the *new* weather model represents a highly developed approach to mimic real weather conditions, but this assumption simplifies the development cost noticeably.

A good starting point for generating wind speed series has been introduced by Bossanyi (1985). He used an autoregressive moving average (ARMA) process in his wind-speed prediction models and reached a good level of agreement when comparing it to real data. Philpott *et al.* (2004) judged the ARMA process as an excellent method to describe weather statistics needed for their yacht design sailing simulator research. Therefore, this process has been used as a basis for the advanced wind model since it provides a capable tool to solve the weather model constraints in *Robo-Race*.

The ARMA process is a combination of an autoregressive (AR) and a moving average (MA) model. In this study, an AR model of order two and an MA model of order

one have been applied yielding the following expression for the wind speed fluctuations at time *t*

$$WS_{fluc\_y_t} = \varphi_1 \cdot WS_{fluc\_y_{t-1}} + \varphi_2 \cdot WS_{fluc\_y_{t-2}} + \theta_1 \cdot \varepsilon_{t-1} + \varepsilon_t \qquad (6.8),$$

where ε_t is white noise normal distributed around its mean value of zero. φ_i and θ_1 are parameters of the model set to $\varphi_1 = 0.44$, $\varphi_2 = 0.32$, and $\theta_1 = 1$, respectively. These values have been obtained after a series of sensitivity studies aiming to match the characteristics of the higher frequency spectrum to a sufficient level.

In order to obtain a greater flexibility and therefore a greater variety to the generated weather series, the following effects were superimposed to model generating a fluctuating series by using the ARMA process:

- Mean value
- Ramp
- Sinusoidal wave

All four effects (mean wind-speed excluded) have an individual factor f_i on their side in order to in/decrease the individual influence of the effects on the wind-speed series. This yield the following expression for a wind-speed series

$$WS_y = WS_{mean} + f_{fluc} \cdot WS_{fluc} + f_{ramp} \cdot WS_{ramp} + f_{\sin} \cdot WS_{\sin} \qquad (6.9).$$

The following Figures 22 to 25 illustrate the individual and combined effects on one generated wind speed weather series and its trend after 500,000 executions. Thereby, the flexibility and variation of the model to prefer a single weather scenario has been successfully proven.

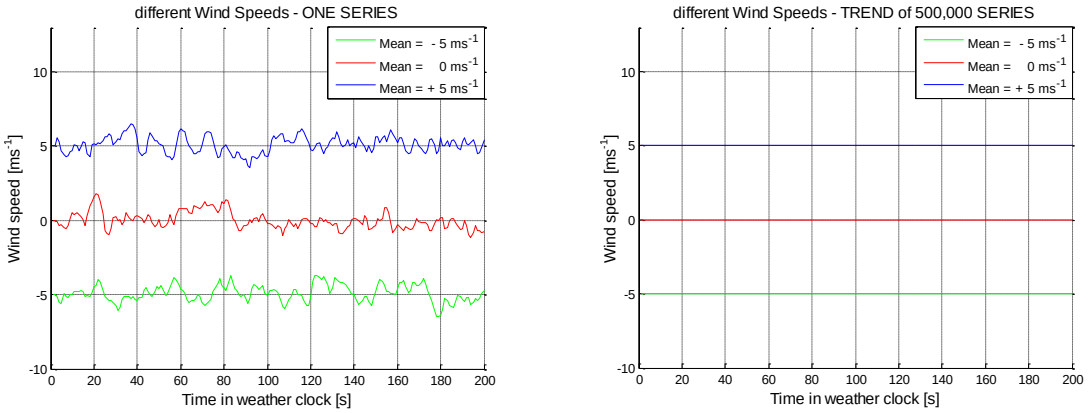

Figure 22: Three different longitudinal mean wind speeds for one series (left) and trend of series for 500,000 replications (right).

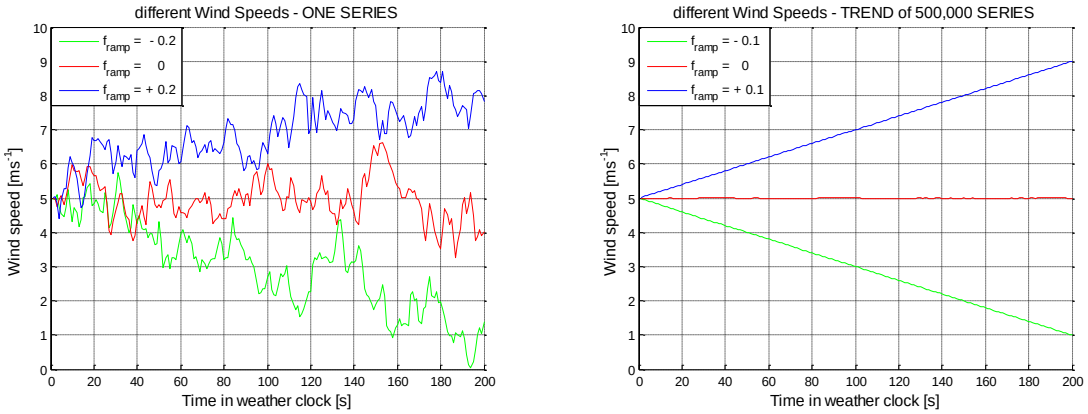

Figure 23: Three different longitudinal wind speed developments with superimposed ramp for one series (left) and trend of series for 500,000 replications (right).

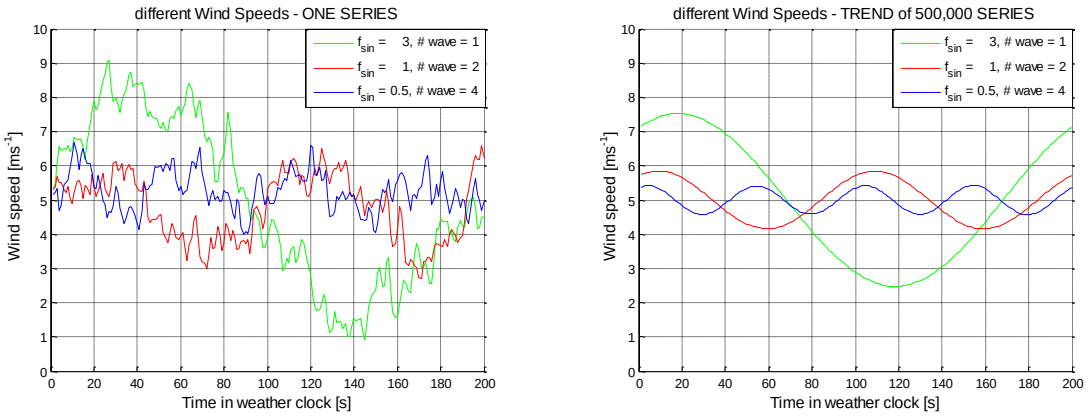

Figure 24: Three different longitudinal wind speed developments with superimposed sinusoidal wave for one series (left) and trend of series for 500,000 replications (right).

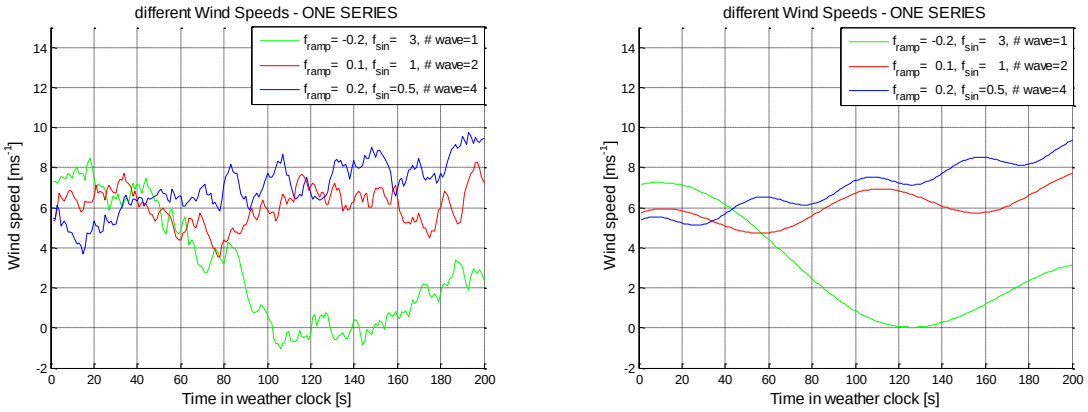

Figure 25: Three different longitudinal wind speed developments with superimposed ramp and sinusoidal wave for one series (left) and trend of series for 500,000 replications (right).

The model to generate a wind direction series turned out to be a bit more complicated since wind shifts which are most important had to be captured which was not guaranteed by just using an ARMA process. As suggested by Philpott *et al.* (2004), the ARMA process was combined with a Markov Chain taking account of wind shifts.

A Markov Chain is a random process in which a mathematical system changes from one state to another. A set of states $S = \{s_1, s_2, \ldots, s_m\}$ is defined and the process starts in one state and successively changes from this state to another, independent on its previous state, making the entire process *memoryless*. Imagine the Markov chain is in state s_i, the process has the option to move to state s_j with the probability p_{ij} or to remain in the actual state with the probability p_{ii} (see Figure 26). These probabilities p_{ij} are called *transition probabilities* and define the so-called *transition matrix T* (size: m x m). A set of possible outputs or emissions has to be defined in an *output matrix* $O = \{o_1, o_2, \ldots, o_n\}$. In this study, two different states (positive and negative) were used and different changes in wind angle were allocated to *O*. The *emission matrix E* (size: m x n) was constructed by the probabilities of the emitting outputs o_i given the model is in state s_i.

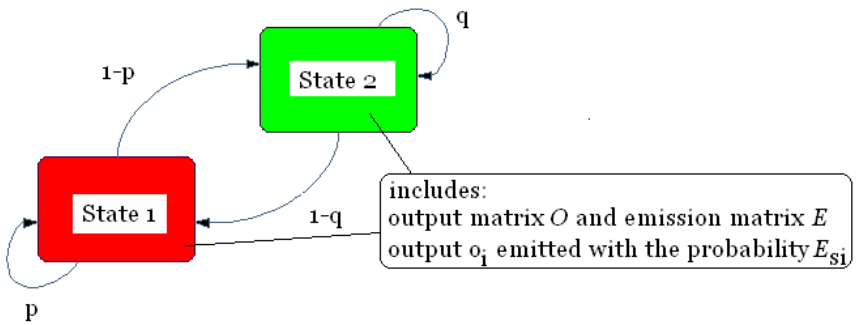

Figure 26: State diagram of the used Markov Chain showing the transition probabilities *p, q* and output matrix *O* and emission matrix *E* within *State1* and *2*.

By combining the ARMA process with the Markov chain, the model is capable of modelling discrete jumps and smaller random variations in the mean wind direction simultaneously which can be expressed by:

$$WD_{fluc_t} = \varphi_1 \cdot WD_{fluc_{t-1}} + \varphi_2 \cdot WD_{fluc_{t-2}} + \theta_1 \cdot \varepsilon_{t-1} + \varepsilon_t \qquad (6.10),$$

where the notation remains the same as in Equation 6.9, whereas the following values were used: $\varphi_1 = 0.4$, $\varphi_2 = 0.05$, and $\theta_1 = 1$, respectively. Again, these values have been obtained after a series of sensitivity studies aiming to match the characteristics of the higher frequency spectrum to a sufficient level.

The basic version of the wind-direction model has to ensure that the distribution for the Markov chain is symmetric about zero. This guarantees a non-influenced wind direction distribution which is important 1) to control the influence of the various superimposed effects successfully and 2) not to favour any wind direction trends unnoticed.

The same effects including the corresponding effect controllers, such as 1) mean value, 2) ramp and 3) sinusoidal wave, were also used to guarantee the flexibility of the wind direction model. The corresponding equation for a wind direction series can be expressed by:

$$WD = WD_{mean} + f_{fluc} \cdot WD_{fluc} + f_{ramp} \cdot WD_{ramp} + f_{\sin} \cdot WD_{\sin} \qquad (6.11).$$

The following Figures 27 to 30 show the individual and combined effects on one generated wind direction weather series and the trend curves after 500,000 executions.

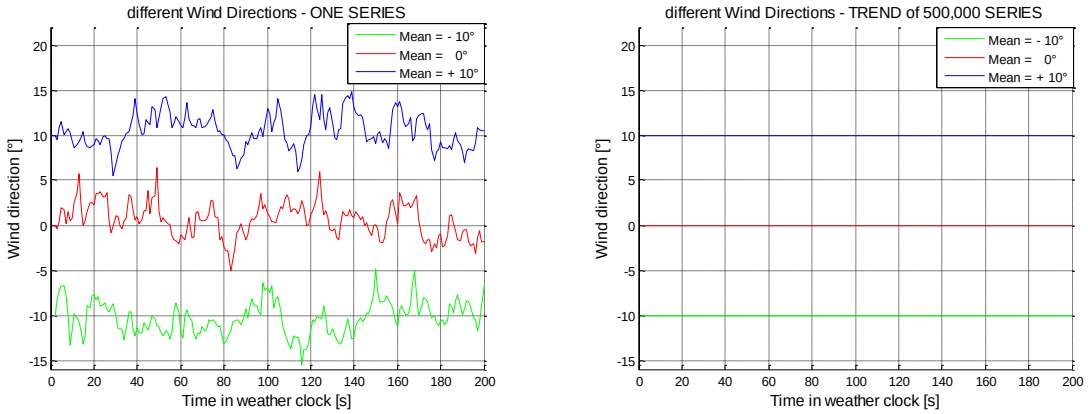

Figure 27: Three different longitudinal mean wind directions for one series (left) and trend of series for 500,000 replications (right).

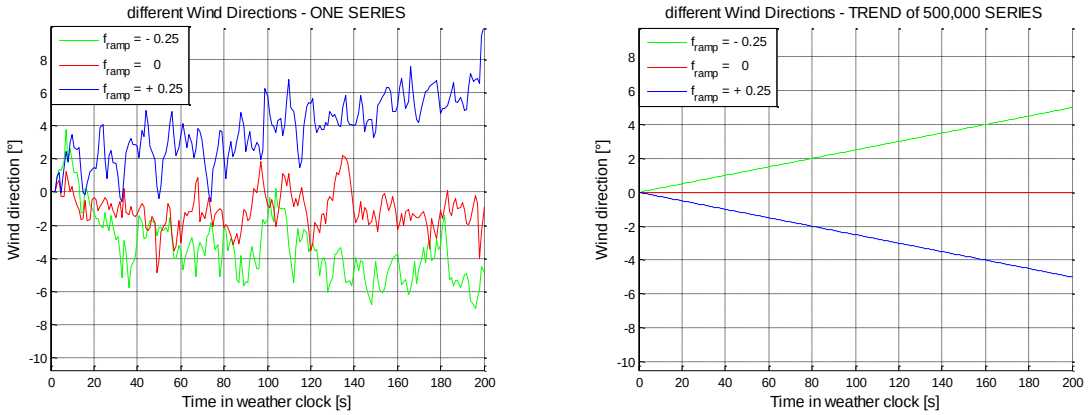

Figure 28: Three different longitudinal wind directions developments with superimposed ramp for one series (left) and trend of series for 500,000 replications (right).

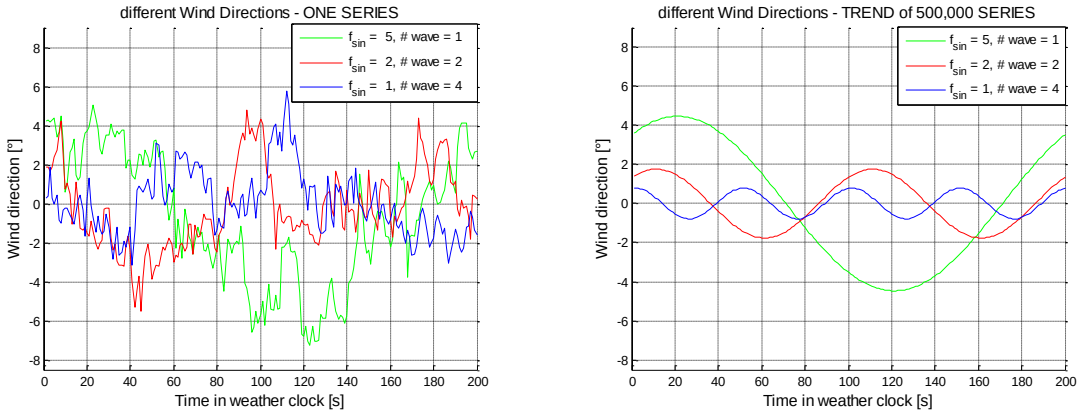

Figure 29: Three different longitudinal wind directions developments with superimposed sinusoidal wave for one series (left) and trend of series for 500,000 replications (right).

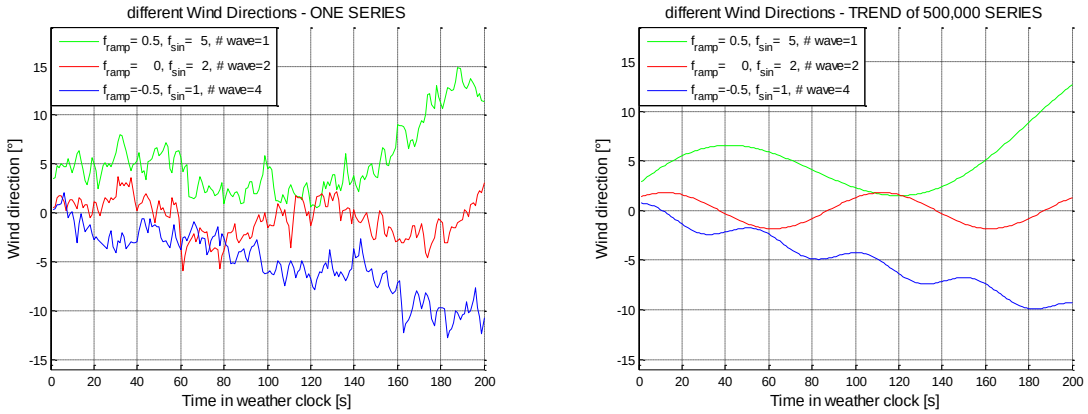

Figure 30: Three different longitudinal wind directions developments with superimposed ramp and sinusoidal wave for one series (left) and trend of series for 500,000 replications (right).

A spectral analysis of the new weather model series has been carried out to ensure its similarity to real weather. As stated earlier, this study focuses on high frequencies around the turbulent peak and the modelling of them. Therefore, the frequency spectra of the longitudinal and lateral wind speed and wind direction for 500,000 weather series have been calculated using a Fourier Transform. The absolute values of the corresponding outcomes were normalised to the maximum frequency of the series and trendlines were introduced to improve the informative value and clarity aspect of the graphs.

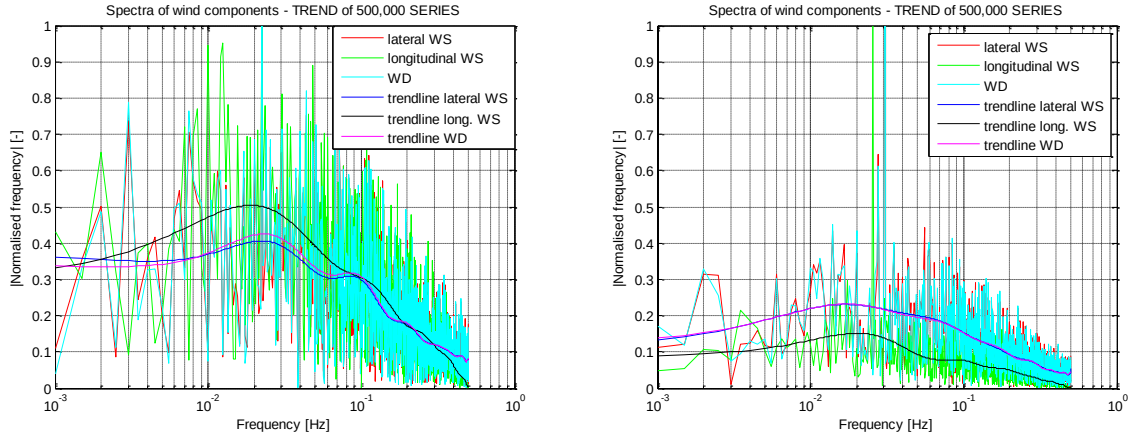

a) b)

Figure 31: Frequency spectra calculated using a Fourier Transform of the longitudinal and lateral wind speed and wind direction for 500,000 weather series without (left) and with (right) two superimposed sinusoidal waves.

Figure 31 a) shows the spectra of a weather series featuring a mean wind speed as the only applied effect on the series. The three trendlines indicate a maximum around 0.015 Hz which is in very good agreement to the location of the turbulent peak in Figure 31. This fact supports the assumption that the new weather model presented in this chapter supports the simulation of the characteristics of real weather. (The reader should not be distracted by

the spikier shape of the maximum which can be explained by the different scale of the x-axis).

Figure 31 b) indicates the spectra of 500,000 weather series featuring the same wind speed setup as the one in Figure 31 a) but with a superimposed effect, two sinusoidal waves. There, two different frequencies of the sine waves were applied to the longitudinal speed component and the wind direction. Their effect on the spectra is visible by two identifiable peaks around 0.03 Hz (see Figure 31 b).

6.4 Conclusions

The study of this subchapter focused on one specific constraint of the sailing yacht simulator *Robo-Race*, the weather engine. The limitations of the original implemented weather model and the superiority of the new weather model were indicated by different test races. In particular, the simulations showed the constraints of the single time-frame setup in conjunction with the simple weather model resulting in an unrealistic, unnatural and constraint-rich sailing environment. By introducing individual yacht time-frames an important step forward has been made providing a more realistic yacht race environment. Nevertheless, the real breakthrough has been achieved by combining the individual yacht time-frame setup with a weather series generated by the new weather model.

During the development of the new weather engine of *Robo-Race*, two important points – similarity and independency – had to be considered meaning the closer the yachts are sailing to another, the smaller becomes the time difference of the yachts in the weather series and therefore the more similar is the experienced weather of the two yachts and vice versa. The new developed methodology to introduce a *Master-Yacht* and to change the other yachts to *Slave-Yachts* provides an effective way to deal with similarity and independency. Thereby, the *Slave-Yacht*s' weather conditions were calculated relative to the spatial distance to the *Master-Yacht*. The conducted simulations comparing the simple weather model to the two development stages of the new weather model showed the successful implementation into *Robo-Race* and the correctness of the *Master-Slave-Yacht* setup.

Furthermore, the simple predictable weather model driving the weather engine has been successfully replaced with a model that supports the dynamic, unpredictable, and

probabilistic nature of real weather. The sufficient level of realism of the new generated weather model was demonstrated by spectral analyses using Fourier Transform. The new weather model features three components, such as wind speed in lateral and longitudinal as well as the wind direction using an ARMA process for the first two and a combination of an ARMA process and a Markov chain for the latter. The flexibility of those components was further improved by applying special effects to it, like a mean value, ramp, sinusoidal wave or a combination of those three. The weather series generated for a stationary observer has been successfully transformed into one for a moving observer by introducing two different time-frames, the so-called clock and series time-frames, to convert the travel spatial distance on the course to a temporal distance within the weather series.

It has been demonstrated by spectral analyses and the results of the conducted simulations that the new developed weather engine supports to provide a dynamic, natural and unpredictable yacht race environment for *Robo-Race*. It is believed that with the implementation of the new weather engine an important step forward has been made to capture reasonable well the stochastic nature of a yacht race environment allowing investigations of behaviour pattern and decision-making processes of sailors to a highly sophisticated level.

7 An Advanced Wake Model for Sailing Yachts

This chapter details the development of an advanced wake model for sailing yachts based on lifting line method. The wake of an upwind sailing yacht is represented as a single heeled horseshoe vortex and image system. At each time step changes in vortex strength are convected into the wake as a pair of vortex line elements. These subsequently move in accordance with the local wind, self-induced velocity and velocity induced by the presence of the wakes of other yachts. A decay factor is used to eventually remove the far wake. The CFD results presented in Appendix A1 are used to capture the initial strength of the combined main-jib vortex system and its vertical height to determine the performance of the wake model. Furthermore, the implementation of the lifting line based model into *Robo-Race* is described.

7.1 Wake Mode

7.1.1 Lifting Line Model – Part I

The objective of the lifting line approach is in capturing the flow interactions between multiple yachts. It is proposed that the use of an appropriate series of vortex line elements with varying vortex strength Γ along the elements can improve the representation of the modification to the local wind strength and direction due to the presence of multiple yachts. The challenge of developing such an approach is to ensure that it is robust and that it requires only a modest increase in computation at each time step. To deal with this

challenge a lifting line approach based on Katz and Plotkin (2001) is used to describe the physical phenomena of blanketing and covering.

At every time step, a horseshoe vortex system with a vortex strength Γ_i is shed according to the actual total lift generated by the sail rig. The vortex strength Γ is calculated using the *Kutta–Joukowski* theorem (Katz and Plotkin, 2001) and expressed by

$$\Gamma = \frac{C_L \cdot S \cdot U}{k \cdot h} \tag{7.1},$$

where h describes the sail rig height and k is a factor which accounts firstly, for the shape difference of a sail compared to a wing and secondly, for the interaction between the main and jib vortex system. The recommended k factor was set at 0.4. Figure 32 shows the generated vortex system. This depends on the actual heel angle of the yacht and is shaped as a horseshoe consisting of four nodes; one node NT_i (Node Top) generated at around 70% of the mainsail height and node NB_i (Node Bottom) generated at the height of the boom. The third and fourth nodes represent the image of node NT_i and NB_i and are referred to NTI_i and NBI_i respectively (Node Image). The horizontal vortex elements created by two successive nodes NT_i and NT_{i-1} have the vortex strength Γ_{i-1}, whereas the first vertical vortex element formed by NB_1 and NT_1 possesses the strength Γ_i.

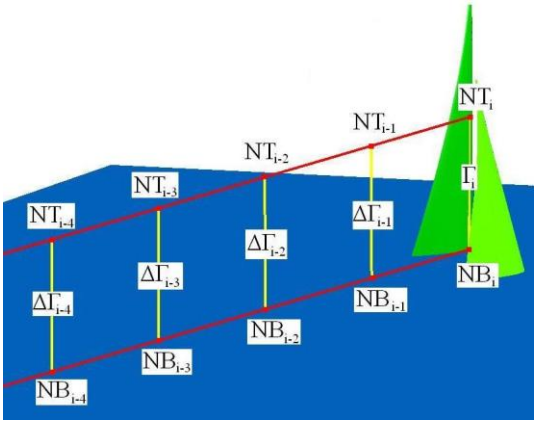

Figure 32: Nomenclature used for the lifting line model describing the vortex system of a sailing yacht, the wake flow field is represented by a series of line element vortices. For reasons of clarity, just the upper part of the vortex system is displayed.

The other vertical elements are generated by a change in lift force and possess therefore the vortex strength $\Delta\Gamma_i$ calculated by the difference of Γ_i and Γ_{i-1}. In order to describe the natural flow behaviour and to assure a robust and consistent computational model, the vortex decay model derived by Morozov using Green's Model of cylindrical vortex decay

is superimposed on the vortex strength along the filaments (Morozov and Kalyadina, 2008). This model considers the viscosity and the turbulence of the flow acting on the vortex trail leading to its dissipation. The vortex strength as a function of time is described by

$$\Gamma(t)=\frac{0.82\frac{q}{l}e^{-0.82\left(q/l\right)\cdot t}}{\frac{1}{\Gamma_0}\left(0.82\frac{q}{l}\right)+\left(C_D\frac{2.09}{8l^2\pi^2}\right)-\left(C_D\frac{2.09}{8l^2\pi^2}\right)e^{-0.82\left(q/l\right)\cdot t}}\cdot\left(1-e^{-r^2/4\nu t}\right) \tag{7.2},$$

where l is the distance of the vortex core and its image, r the viscous core radius of the two cylindrical vortices and ξ_x, ξ_y, ξ_z are random and independent components of the wind velocities. The variance of the random variable is $\overline{\xi_x^2}+\overline{\xi_x^2}+\overline{\xi_x^2}$, and q is defined by

$$q=\sqrt{\overline{\xi_x^2}+\overline{\xi_x^2}+\overline{\xi_x^2}} \tag{7.3}.$$

For this studies reported q was taken as 1 m/s as being representative of the ambient turbulence in the wake behind a yacht and typically l although it varies with heel was of the order of 40 m giving a decay rate of q/l = 0.025. This was found to give reasonable comparable rates of decay of Γ compared to the values found from the CFD studies.

Furthermore, to enhance the model in describing the vortex's nature, a spreading of the vortex core in time is taken into account by using a Gaussian core function with core size σ_p as follows:

$$\sigma_p^2(t)=\sigma_p^2(0)+4\nu t \tag{7.4},$$

where t is the time the vortex exists and ν the kinematic viscosity.

According to Jackson where σ_p /r_c = 0.93 to 0.98 and r_c correspond to the point of maximal tangential velocity (Jackson, 2001)

$$u_\theta(r_c) = \frac{\Gamma(r_c)}{2\pi r_c} \tag{7.5},$$

the vortex spreading can be described as

$$r^2(t) = r^2(0) + 4\nu t \tag{7.6}.$$

The initial radius *r(0)* is calculated by substituting the following result of Jackson (2001)

$$\frac{u_\theta(r_c)h}{\Gamma_0} = 2.08 \text{ to } 2.35 \tag{7.7}$$

into (5) where the value of *2.08* was chosen

$$r(0) = \frac{h}{2.08\pi} \tag{7.8},$$

where *h* is the sail rig height.

For this analysis, the induced velocities at each node due to the presence of the other vortex elements are calculated and the nodes' displacements are determined. Note that this approach also considers the influence of close-by yachts on the vortex elements. At the end of a routine step, the nodes' locations are updated, and the influence of the local wind induced drift is also taken into account.

The induced velocity $d\vec{q}$ of a vortex filament of strength Γ and a segment of length *dl* can be calculated using the Biot-Savart law (Katz and Plotkin, 2001)

$$d\vec{q} = \Gamma \frac{(dl \times \vec{r})}{4\pi r^3} \tag{7.9},$$

Referring Figure 33, and rewriting Equation 7.9 and considering the vortex strength variation of $\Delta\Gamma$ along *dl*, the magnitude of the induced velocity for a Point *P* in space can be expressed as

$$d\vec{q} = \left(\frac{(\Gamma + l\Delta\Gamma)\hat{a} \times \vec{r}}{4\pi r^3} \right) dl \qquad (7.10),$$

or in scalar form as follows

$$| d\vec{q} | = \left[\frac{1}{4\pi} \left(\Gamma - \frac{\Delta\Gamma}{\tan\theta} \right) \sin\theta \right] d\theta \qquad (7.11),$$

where the unit vector $\hat{a}$ is defined as

$$\hat{a} = \frac{N_2 - N_1}{|N_2 - N_1|} = \frac{N_2 - N_1}{L} \qquad (7.12).$$

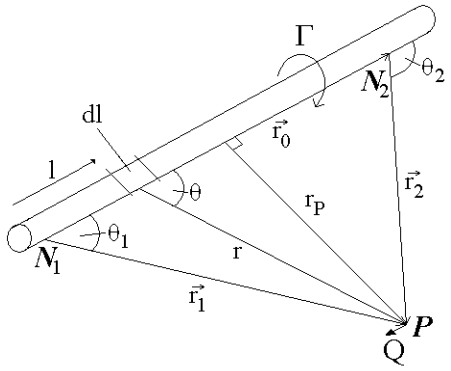

Figure 33: Nomenclature of the distances and angles for the vortex-induced velocity calculation at a point P (Katz and Plotkin, 2001)

Integrating Equation 7.11 from the boundaries θ_1 to θ_2 gives the induced velocity vector $\vec{Q}$ as

$$\vec{Q}_{12} = \frac{\Gamma_1}{4\pi d}(\cos\theta_1 - \cos\theta_2) + \frac{(\Gamma_2 - \Gamma_1)}{4\pi}(\sin\theta_1 - \sin\theta_2) \qquad (7.13),$$

where

$$d = \frac{|\vec{r}_1 \times \vec{r}_2|}{|\vec{r}_0|} \quad (7.14), \quad \cos\theta_i = \frac{\vec{r}_0 \cdot \vec{r}_i}{|\vec{r}_0||\vec{r}_i|} \quad (7.15), \quad \sin\theta_i = \frac{\vec{r}_0 \times \vec{r}_i}{|\vec{r}_0||\vec{r}_i|} \quad (7.16), \text{ and } \quad \vec{r}_0 = \vec{r}_1 - \vec{r}_2 \quad (7.17).$$

In order to represent the physics of an incompressible viscous fluid such as air (assumed that the velocity is Ma < 0.3), the velocity distribution close to the vortex core has to be updated due to viscous effects. Considering a cylinder of radius r_c rotating in such a fluid at an angular velocity ω, the velocity distribution or vortex flow within the radius r_c has to be expressed by the radius r and the angular velocity ω as

$$\vec{Q} = \vec{r}\,\omega \qquad \text{(for } 0<r< r_c\text{)} \qquad (7.18).$$

The affected spherical vortex flow around a node N_i is described by the same equation where r expresses the radius of the sphere.

7.1.2 Viscosity Model – Part II

To represent the viscous effect of the flow passing the yacht, a plane and self-preserved wake depending on the freestream velocity U_0 and the shape of the circulated obstacle is used. Tennekes introduced an approach combining the velocity deficit U_s in the wake to the generated drag of the obstacle (Tennekes, 1972). Following this approach yields

$$\frac{U_s}{U_0} = 1.5791\left(\frac{\Theta}{x}\right)^{1/2} \qquad (7.19), \qquad \frac{l}{\Theta} = 0.252\left(\frac{x}{\Theta}\right)^{1/2} \qquad (7.20),$$

where l describes the half width of the wake at $U = 0.5U_{\max}$, x the local distance along the vortex elements, and y the perpendicular distance to it. The momentum thickness Θ is defined by

$$\Theta = \frac{D}{\rho \cdot U_\infty^2} \qquad (7.21),$$

where D describes the drag per unit length defined by $D = \frac{drag}{h}$, where h is the sail rig height.

Combining Equations 7.19 – 7.21 yields the following equation for expressing the mean speed deficit $\Delta U_{Viscous}$ in a self-preserved viscous wake at any Point *P*

$$\left|\Delta U_{Viscous}\right| = -1.5791\left(\frac{\Theta}{x_P}\right)^{1/2} \exp\left[-\ln 2\left(\frac{y_P}{0.252\left(x_P/\Theta\right)^{1/2}\Theta}\right)^2\right] \qquad (7.22),$$

where x_P and y_P are the distances in x and y direction of Point *P* to the obstacle.

7.3 Wake Model – a Combination of Part I and Part II

The actual wake model can be expressed by a combination of the lifting line model represented in Chapter 7.1.1 and the viscosity model described in Chapter 7.1.2.

Considering the physical flow features, the actual position of Point P in space has to be determined relative to the horseshoe vortex system which represents the yacht's wake. The corresponding searching procedure consists of different criteria starting with the determination of the closest horizontal or vertical vortex element, followed by finding *P's* position relative to this vortex element, whereas the algorithm determines whether the point is in the far-field or within the viscous affected vortex core zone stretched by the spheres around nodes N_i and N_{i-1} and the cylinder between them. According to *P's* position relative to the vortex core the induced velocity is either calculated using Equation 7.18 or Equation 7.23. In considering the whole horseshoe vortex and image system of *M* yachts with all nodes of each yacht shed of at *m* time steps the induced velocity *Q* at a point located in the far-field is calculated by

$$\vec{Q} = \sum_{i=1}^{M}\left(\sum_{n=1}^{m} Q_{VerticalElements} + \sum_{n=1}^{m} Q_{HorizontalElementsBottom} + \sum_{n=1}^{m} Q_{HorizontalElementsTop} + \ldots\right.$$

$$\left. \ldots + \sum_{n=1}^{m} Q_{ImageVerticalElements} + \sum_{n=1}^{m} Q_{ImageHorizontalElementsBottom} + \sum_{n=1}^{m} Q_{ImageHorizontalElementsTop}\right) \qquad (7.23).$$

Equation 7.23 is also used to create the self-relaxing/dynamic moving wake by calculating the induced velocity $\vec{Q}_{Vortex}$ of each individual vortex system node due to the nodes mutual influence and multiplying it with the time step Δt. In addition, taking into account the induced velocity $\vec{Q}_{Yachts}$ generated due to the presence of other yachts, the viscous effect of an upwind yacht, and the nodes' displacement due to the local wind speed. Therefore, the total displacement $\Delta\vec{D}_{N_i,total}$ of a wake's node N_i at a time step is described by the following

$$\Delta\vec{D}_{N_i,total} = \left(\vec{Q}_{Vortex} + \vec{Q}_{Yachts} + \vec{Q}_{Wind}\right)\Delta t \tag{7.24}.$$

Consequently, the updated apparent wind velocity $\vec{U}_{AW}$ seen by a yacht at any point of the flow field can be expressed as follows:

$$\vec{U}_{AW} = \vec{U}_{Viscous} + \vec{Q}_{Yachts} + \vec{Q}_{Vortex} + \vec{Q}_{Wind} \tag{7.25}.$$

7.4 Implementation into *Robo-Race*

The interaction of yachts is an important tactical tool in regattas and particularly in match races such as the America's Cup. Therefore, the yacht interaction model based on Philpott *et al.* (2004) was replaced in *Robo-Race* by the lifting line approach as phenomenon of covering and blanketing has to be presented well in an advanced sailing simulator. Considering two yachts where the upwind yacht is sailing ahead of the downwind yacht. The upwind yacht creates a wake of disturbed turbulent flow affecting the incident flow of its opponent downstream. This interrelationship is expressed in the structure in Figure 34 showing the interaction of three yachts within a race. Furthermore, the principles of the data flow within *Robo-Race* are shown replicating the physical and practical features of yacht interaction.

Figure 34 describes an agent-block in Simulink® that controls the sailing yacht *Yacht A* in *Robo-Race* and the corresponding data flow. Considering *Yacht A* operating in a race with two opponents, *Yacht B* and *Yacht C*, the agent block needs *Yacht A*'s state (own state) and the aerodynamic values as an input to solve the differential equations within the block.

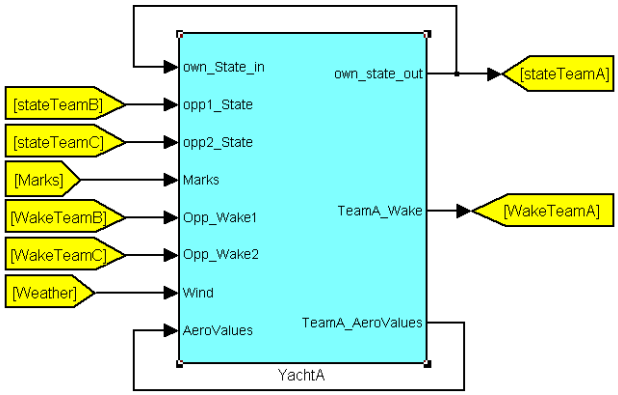

Figure 34: Vortex Principle of yacht interaction and data flow within *Robo-Race* for 3 yachts

Furthermore, the input *Marks* is needed for the navigator to aim towards it whereas a PID-controller controls the rudder angle and the sail settings (Scarponi, 2008). For the wake calculation the state and the wake data of the opponents are needed as well as the weather conditions and the aerodynamic values. The disturbed flow is considered as a function of the generated sail lift which is directly related to the vortex circulation, of the shed height, of the vortex decay rate within the wake, and of the relative position of the yachts to each other (see Equation 7.1).

It can be seen that the block uses the state and wake information of the opponents and the weather data (Wind) as inputs so that the complex and dynamically changing sailing environment is described. The outputs correspond to the state and wake information of *Yacht A* which is forwarded to the other yacht agents. A schematic diagram of how apparent wind angle (AWA), true wind angle (TWA), and true wind speed (TWS) are calculated within the agent-block is given in Figure 35.

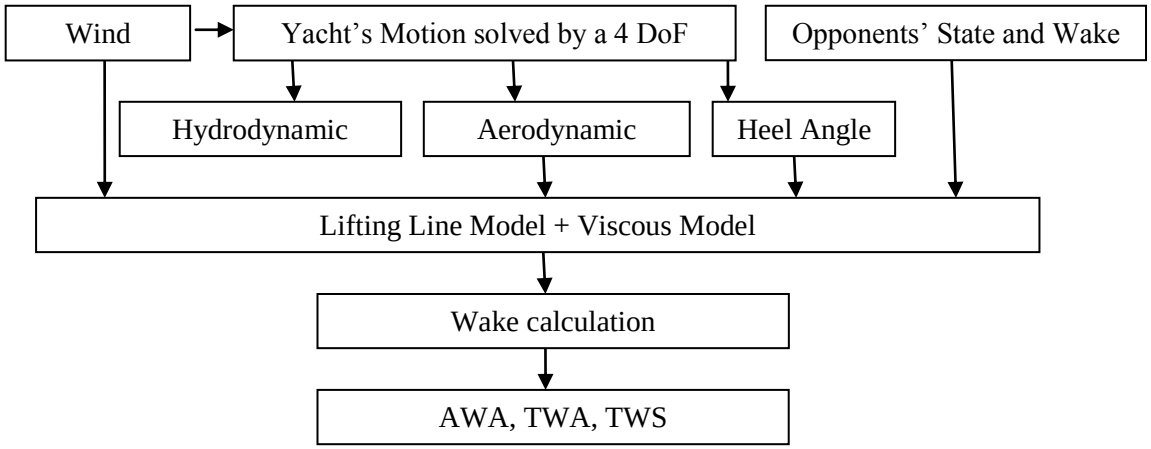

Figure 35: Schematic Diagram showing the data flow starting at the dynamically changing wind environment dictating the acting forces on the yacht which influences together with the opponents the new wake model and hence the new updated wind conditions seen by the yacht

7.5 Evaluation of the Lifting Line Method

A detailed examination of the performance of a typical upwind sail rig arrangement was previously carried out for different heel and yaw angles using a commercial CFD solver (Spenkuch *et al.*, 2008). Experimental wind tunnel data provided by the Wolfson Unit for Marine Technology and Industrial Aerodynamics were used to validate the calculated CFD results. An overview of the CFD simulations is given in Figures 36 and 37. Figure 36 shows the downstream development of the structure of the main vortex. The CFD analysis of a yacht's wake gives important insight in the flow behaviour, especially of the vortex core development downstream of a sail rig. In addition, CFD simulations with two in-line yachts were carried out to provide an initial value for the shed height of the line vortex (around 70% of the mainsail height) and use of the total sideforce for the vortex strength.

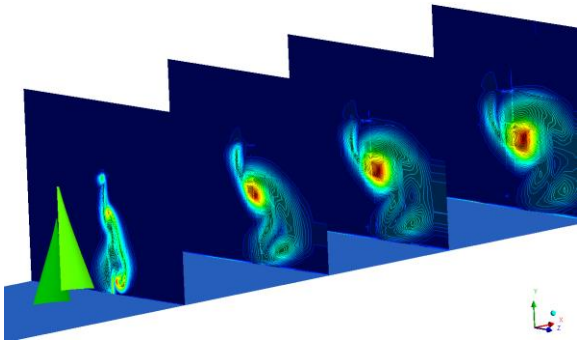

Figure 36: Vortex core development by showing the vorticity contour on surfaces downstream of the sail rig (varying local surface range).

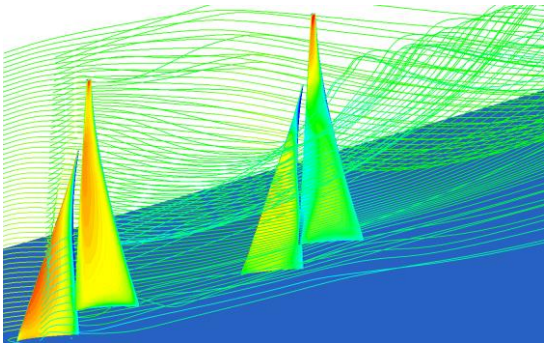

Figure 37: 3D wind tunnel domain mesh with two sail rigs in-line and a distance of 3 sail rig lengths. Varying local pressure contours on downwind sail rig due to the updated flow behaviour. Streamlines to identify the vortices (constant pressure range on both rigs).

For the lifting line method, the complexity of the whole wake flow field is represented by a series of line element vortices in order to generate the same velocity field as calculated from the CFD simulations. The vortex field is simulated by reproducing the predicted vortex core filament from the CFD calculations. This filament is divided into several elements on which a constant vortex strength Γ is implemented. The vortex strength Γ is calculated by using Equation 7.1. A similar formulation is presented by Roncin and Kobus (2004) who investigated the interaction between two yachts by simulating the sail perturbation using a single horseshoe vortex system and a self-preserved viscous plane wake.

Figures 38 and 39 show the velocity distribution in and around the viscous vortex cores for different sail rig arrangements. The results of the tangential velocity of the lifting line approach including the viscous core treatment and the CFD simulations are compared for two different setups with one or two sail rigs with the 27° Angle of Attack (AoA) and 0° heeled sail rig. It is worth noting that the radius of the vortex core is of the order of 30% of the yacht's length (YL) at this stage.

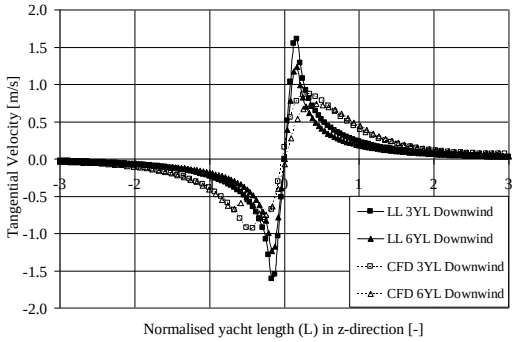

Figure 38: Velocity distribution around the vortex core comparing the lifting line method and the CFD results at 3 and 6 YL downstream

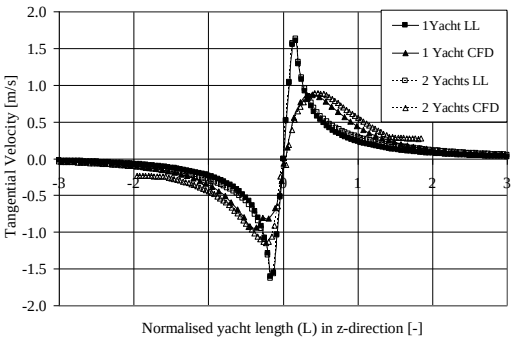

Figure 39: Two yachts setup: Velocity distribution (tangential velocity) in z-direction of the vortex core *2.5 YL* downwind of the sail rig

Figure 38 displays the tangential velocity distribution around the vortex core at *3 YL* and *6 YL* downstream of the sail rig using the lifting line approach and the CFD simulations. The lifting line results for both cases show good agreement with the CFD results for the port side of the vortex core (positive z-direction). On this side almost no difference between the different calculation methods can be seen for a distance of *1.5 YL* away from the vortex centre. Closer to the vortex core an overprediction followed by an underprediction of the lifting line approach was observed but still shows reasonable agreement with the CFD results. A similar development of the tangential velocity can be seen for the starboard side of the vortex core (negative z-direction) where a slight larger difference between the CFD and LLM results were identified. This phenomenon of the asymmetric CFD results could be due to the influence of the wind tunnel side walls.

Calculations of one sail rig and two sail rigs in-line with a distance of *3 YL* between them were carried out and the corresponding results are displayed in Figure 39 showing the tangential velocity at *2.5 YL* downstream of the leading yacht. The influence of the second yacht was predicted in both calculations which results in a slightly lesser tangential velocity. The predicted values of both simulation types showed the same characteristic development from the vortex core centre up to *1.5 YL* away as described in Figure 38.

In general, the lifting line method show good agreement with the CFD results, especially for distances further away than one and a half yacht lengths from the vortex core. It is worth pointing out that the model captures important flow details around the sail rig, such as the upstream influence of a yacht that was neglected in previous models.

The presence of a yacht affects the flow behaviour in its wake in two ways, i.e. a speed change and alteration of local wind directions. An accurate model has to be able to capture both effects. In order to meet this demand the LLM was used to calculate the change in wind direction whereas the viscous wake model was applied to simulate the corresponding influence on the flow speed. This superimposition of the two models ensured that the wake dissipation and the long lasting viscous effect were captured far downstream from the sailing yacht. One can argue that the model is too detailed when the yachts are sailing closed-hauled in a match race as the dissipation is not significant for typical match race distances of a few yacht lengths. But this model has been created for a multiple yacht fleet race where the long lasting flow effects of a leading yacht will affect any following yachts and their behaviour. Figures 40 and 41 show the velocity deficit profile of the viscous wake flow and the calculated flow deflections compared to the free stream flow condition at a height of *0.5 h* in z-direction on different positions downstream of the yacht (*1, 3, 6, 9* and *12YL*). The wake described by the vortex elements has a length of *10* YL, whereas the wake of the Philpott Model (PM) is limited to *8* YL as it was implemented in *Robo-Race*. In addition, the previous implemented blanketing model of Philpott *et al.* is displayed and compared in Figures 40 and 41 (Philpott *et al.*, 2004).

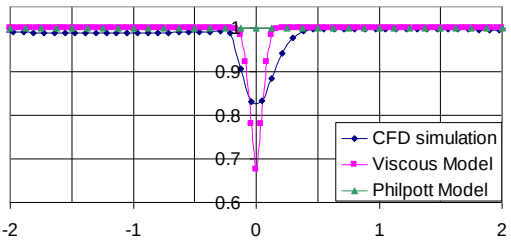

(a) Velocity development at 1 YL downstream

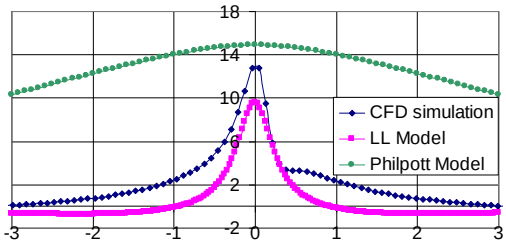

(a) Deflection angle at 1 YL downstream

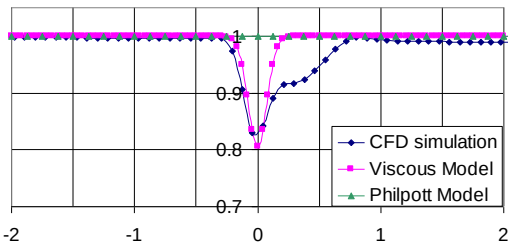

(b) Velocity development at 3 YL downstream

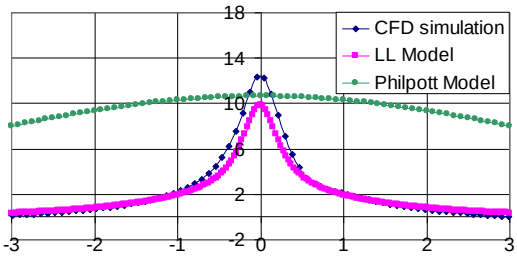

(b) Deflection angle at 3 YL downstream

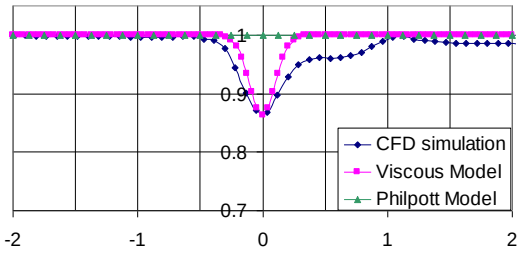

(c) Velocity development at 6 YL downstream

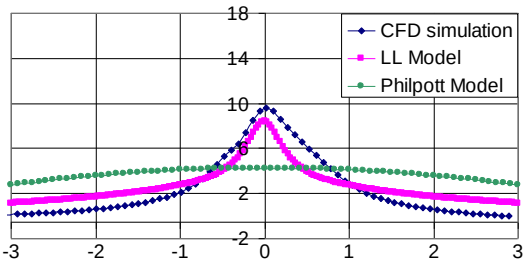

(c) Deflection angle at 6 YL downstream

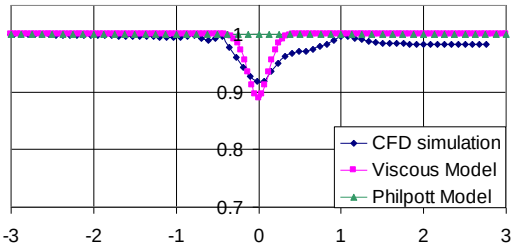

(d) Velocity development at 9 YL downstream

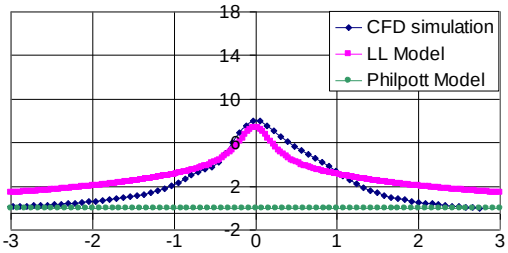

(d) Deflection angle at 9 YL downstream

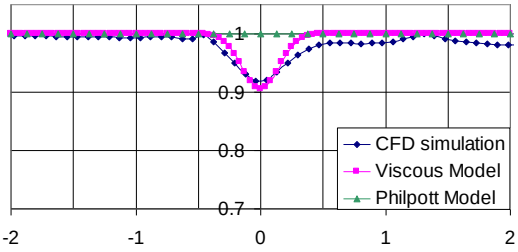

(e) Velocity development at 12 YL downstream

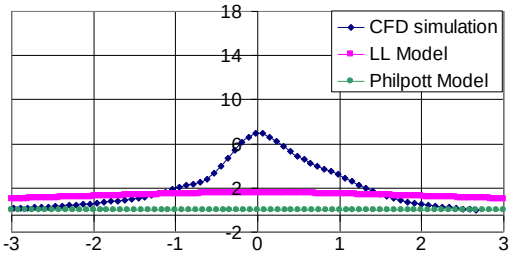

(e) Deflection angle at 12 YL downstream

Figure 40: Velocity development at (a) 1 YL, (b) 3 YL, (c) 6 YL, (d) 9 YL, and (e) 12 YL downstream for CFD, Viscous Model and PM. The velocity deficit starts with a sharp narrow profile and spreads further away from the yacht. The PM does not capture the viscous effect whereby the profile remains untouched.

Figure 41: Deflection angle [°] at (a) 1 YL, (b) 3 YL, (c) 6 YL, (d) 9 YL, and (e) 12 YL downstream for CFD, LLM and PM. Gaussian shaped curves and its maximum are similarly predicted by CFD and LLM whereas the PM does not show these features and consequently over/underpredicts the deflection angle.

The magnitude of the velocity deficit is well predicted by the viscous model compared to the CFD results (see Figure 40). Apart from the distribution at *1 YL* the minimum values are almost identical for both simulation types. The greater spreading of the CFD simulation along the negative x-axis can be explained by the insufficient mesh distribution. The same effect acts along the positive x-axis direction whereby this effect is superimposed by a second effect caused by the jib-mainsail arrangement and their mutual interaction. This effect diminishes further away from the yacht and almost vanishes *12 YL* downstream (see Figure 40 e). The Philpott Model (PM) has no viscous model included which results in an unchanged velocity profile in the yacht's wake.

The deflection angle caused by the presence of the yacht is shown in Figure 41. The magnitude of the maximum deflection angle depends on the applied model type. The characteristic Gaussian shaped development of the deflection angle is well described by the LLM which is also predicted by the CFD simulations. Only the predicted maximum deflection angle and its slightly different development distinguish the LLM from the CFD results. The sudden drop in the LLM results in Figure 41e comes from the limited wake length of *10 YL* and the removal of the influence of any further vortex elements further downstream. A completely different behaviour is seen when considering the PM. There, the maximum values of the deflection angle are well represented up to a distance of 3 *YL* downstream of the yacht. But further away from the yacht the maximum values are underpredicted up to a zero angle change as the wake length is limited to *8 YL*. The characteristic Gaussian shape is not predicted by this model.

It is worth pointing out that the CFD simulations are used to support the new wake model and were not used to adjust the new model. Although the model provides less accuracy than the CFD simulations it captures the most important physical flow changes satisfactorily. Therefore, it represents a real improvement in comparison to the basic PM.

Results showing the performance of the CFD simulation and the lifting line wake model are presented below. Figures 42 and 43 display the contours of the deflection angle of a yacht's steady wake at $z = 0.5$ of the mast height. The displayed wakes start at the stern of the yacht ($x = 1$ and $y = 0$) and the changes in wind angle are plotted in degrees. The contour plots reference frame is identical to the apparent wind angle direction.

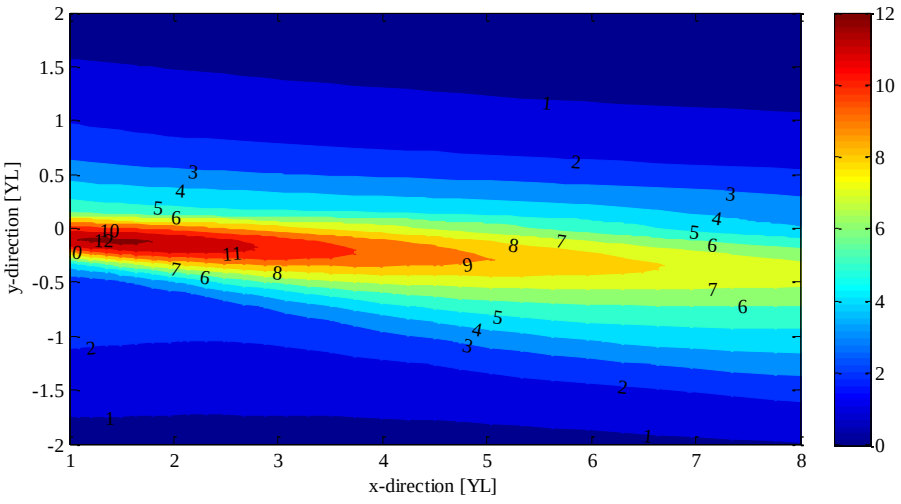

Figure 42: Contour plot of a yacht's steady wake in AWA reference frame – CFD simulation

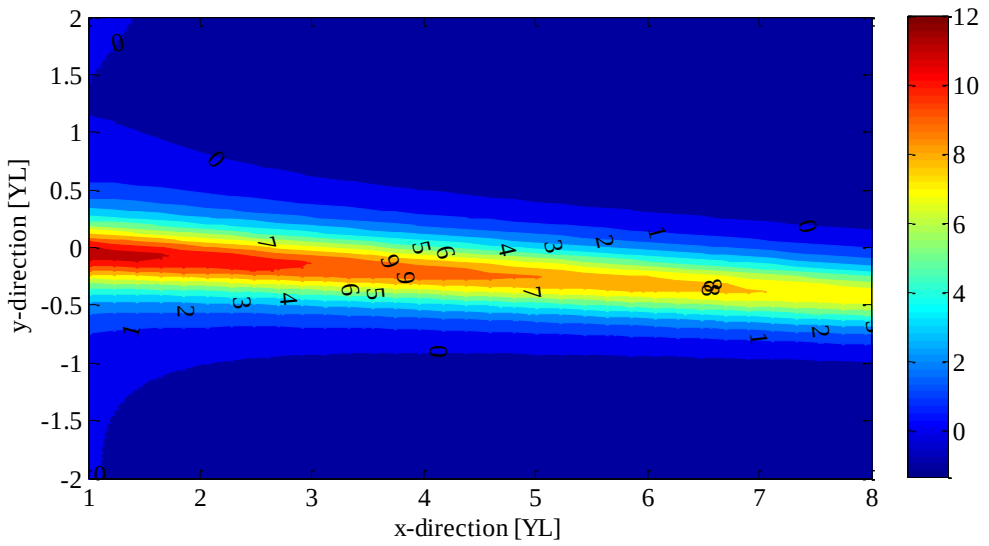

Figure 43: Contour plot of a yacht's steady wake in AWA reference frame – LLM calculation

The results of the CFD simulation are more accurate compared to the LLM (Lifting line method) calculation in the close wake of the yacht (1 to 3 yacht lengths in *x* direction) due to the finer CFD grid resolution compared to the number of applied vortex elements in this region. The behaviour of the wake core width ($-0.5 \leq y \leq 0.5$) along *x* is described well by the LLM and almost no difference to the CFD simulations can be seen. Further away from the vortex core region, the LLM predicts a sharp decline of the deflection angle compared to the CFD simulation which shows a smoother decline perpendicular to the flow direction.

The LLM predicts the wake core region well which is very important as the greatest and most notable changes in velocity and wind angle occur in this area. The changes in the outer region are of secondary order and therefore the missing accuracy of the LLM in this region is of minor relevance as the changes in velocity and wind angle are small and will not influence the tactical decision of the sailors.

The results represented show that the LLM wake model is an improvement to *Robo-Race* as it captures much more detail (angle and velocity changes) compared to the previous implemented model of Philpott *et al.* (2004). Nevertheless, the accuracy of the CFD simulations are not reached but the crucial aspects such as the correct prediction of the velocity and angle changes within the wake core region are captured well by the new yacht interaction model.

7.6 Numerical Investigations – Sensitivity Studies

Two different sensitivity studies have been conducted to investigate the influence on the predicted deflection angle. First, the vortex shed time was changed by using a fixed wake length (*10 YL*) with a varying number of vortex elements of length from e.g. *0.6* to *5.0 YL*. And second, a varying wake length (from *5* to *20 YL*) whereas the vortex shed time has been kept constant (yield *0.9 YL*) and only the number of inscribed wake vortex elements differed (from *6* to *23 YL*). The purpose of this sensitivity study is to find as suitable vortex shed time which provides a good ratio of accuracy to ensure that *Robo-Race* runs simulations with the new wake model in real-time.

7.6.1 Fixed Wake Length (Number of Elements Variation)

Figure 44 shows the change in deflection angle depending on the vortex shed time for different locations downstream of the yacht (*1, 3, 6, 9,* and *12 YL*) whereas the wake length is fixed to *10 YL*. It can be seen that the wake containing 2 horizontal vortex elements (*5 YL*) is insufficiently resolved to capture the physics correctly. Unsurprisingly, close to the start and end points of the elements the results suffer from the lack of resolution. All other shed time setups show almost identical development of the deflection angle up to a distance of *6 YL* downstream of the yacht. The length of the last element and the resulting lack of resolution at the wake's end have a great influence on the predicted deflection angle values (see Figure 44 e). Further downstream of the wake the influence of the vortex elements diminish whereas the coarsest vortex element resolution predicts the greatest values due to the high vortex strength applied to this final element. Based on this the shed vortex element distance of *1.5 YL* is seen to offer the best ratio of accuracy and computational time.

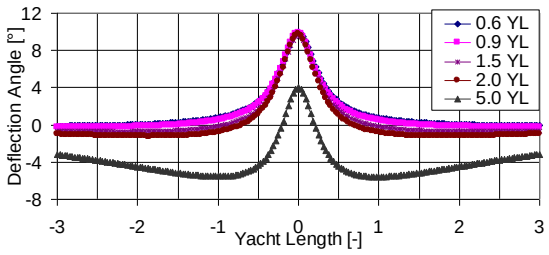

(a) Deflection angle at 1 YL downstream

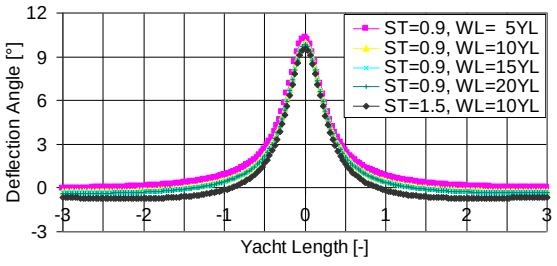

(a) Deflection angle at 1 YL downstream

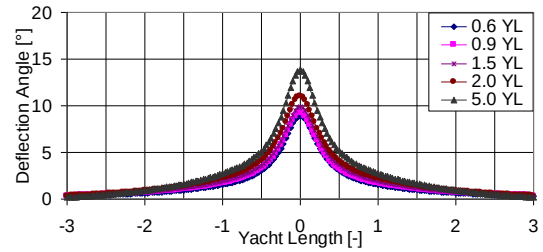

(b) Deflection angle at 3 YL downstream

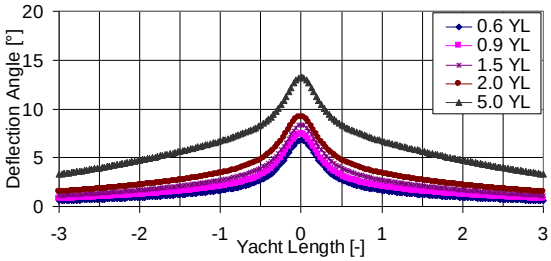

(c) Deflection angle at 6 YL downstream

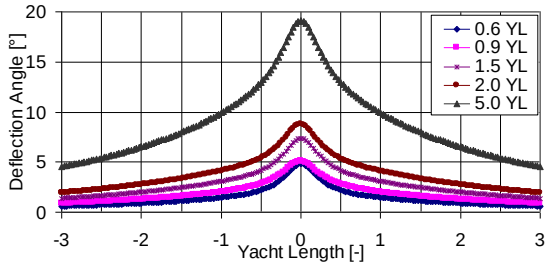

(d) Deflection angle at 9 YL downstream

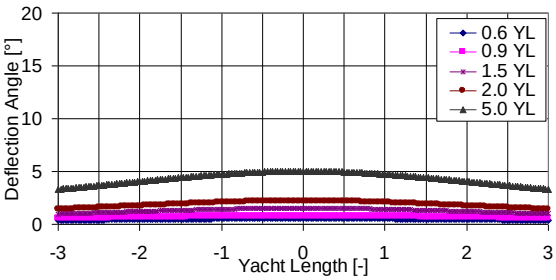

(e) Deflection angle at 12 YL downstream

Figure 44: Sensitivity study considering the deflection angle at (a) 1 YL, (b) 3 YL, (c) 6 YL, (d) 9 YL, and (e) 12 YL. The wake length is fixed to 10 YL with a varying number of inscribed vortex elements

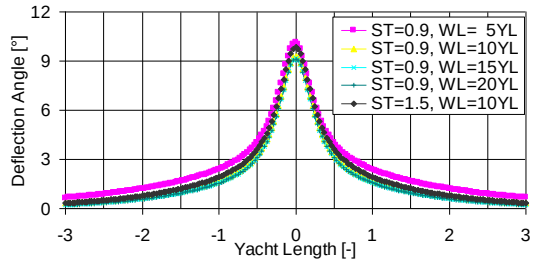

(b) Deflection angle at 3 YL downstream

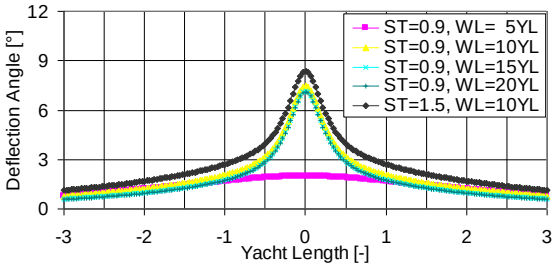

(c) Deflection angle at 6 YL downstream

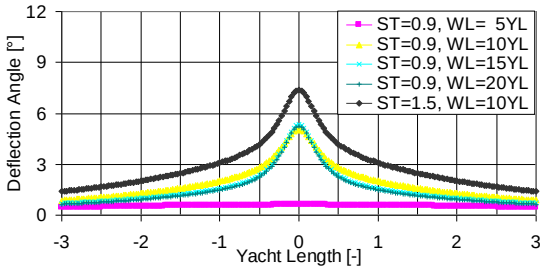

(d) Deflection angle at 9 YL downstream

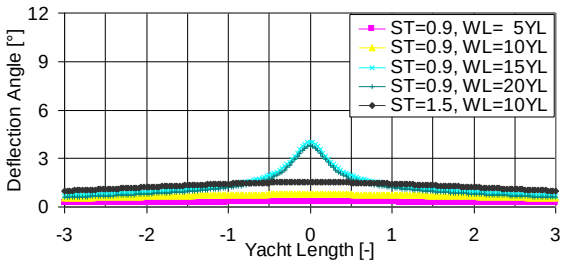

(e) Deflection angle at 12 YL downstream

Figure 45: Sensitivity study considering the deflection angle at (a) 1 YL, (b) 3 YL, (c) 6 YL, (d) 9 YL, and (e) 12 YL. The wake length varies from 5 to 20 YL whereas the vortex shed time has been kept constant

7.6.2 Varying Wake Length (Number of Elements Varies)

Figure 45 shows the change in deflection angle for a constant vortex shed time whereas the wake length varies (*5, 10, 15, and 20 YL*). Furthermore, the data of the chosen shed distance of *1.5 YL* are added for comparison reasons. Almost no difference can be observed

up to a distance of *3 YL* downstream of the yacht (see Figure 45 a and b) and all setups feature the characteristic Gaussian shape for velocity deficit. In Figure 45 c the sudden drop of the *5 YL* long wake data results from the fact that the measurement points are located outside of the describing wake vortex elements. Furthermore, a slight overprediction of the *1.5 YL* shed distance compared to the ones with *0.9 YL* shed distance (with *10, 15, and 20 YL* respectively) increases further downstream (see Figure 45 d) owing to the greater applied vortex strength on its longer final horizontal vortex element compared to the *0.9 YL* shed distance setups. Further downstream at a distance of *12 YL* only the long wakes (*15 and 20 YL*) possess the characteristic Gaussian shape whereas the *1.5 YL* shed distance setup almost produces the same deflection angle values *0.5 YL* away from the vortex centre (x = 0, y = 0, see Figure 45 e).

7.7 Test Cases I: New Wake Model vs. Philpott's Model

In order to evaluate performance and degree of realism of the new wake model (NWM), a series of different upwind race situations were conducted. Therefore the NWM was implemented into *Robo-Race* and comparison studies with the former applied wake model based on Philpott *et al.* have been carried out (Philpott *et al.*, 2004).

Two ACC yachts (YL = 24 m) race on an upwind leg where the following two sailing situations were considered. First, the following yacht, *Yacht B,* sails parallel to the leading yacht, *Yacht A*, which is covering *Yacht B.* Second, after a successful tack of *Yacht B, Yacht A* crosses in a direction perpendicular to *Yacht B*'s wake. In both setups *Yacht A* was sailing on port tack and close hauled. The wind speed was kept at a constant value of 3.93 m/s with wind direction from north to south. To demonstrate the improvement of the NWM, the tracks of the yachts on the course and important data influencing the yachts' performance, such as true wind speed (TWS) components, are displayed for the two wake simulations. The two yachts are run with a PID-controller on the sail settings and the rudder always aiming for an apparent wind angle of 22°.

Figures 46 - 49 show the tracks and the true wind speed history of the two *Yachts A* and *Yacht B* when sailing parallel and closed hauled on an upwind leg. *Yacht A* starts its race at the position x = 0, y = 0 whereas Yacht B starts at x = 27 m and y = -53 m to ensure that *Yacht B* is covered by *Yacht A*. Both yachts start the race simultaneously at t = 0. Immediately after the start the yachts' individual PID-controller search for the quasi-

steady balanced state in which the forces acting on the yachts are in equilibrium. The unbalanced state is visible in the Figures 46 and 47 by the bend in the track shortly after starting the race. The balanced state was reached after about 35 seconds which results in a smooth straight line. The displayed distances between the two yachts are highly dependent on the used wake model which can be seen in Fig. 46 (NWM) and Fig. 47 (PM). The different development of *Yacht B*'s track and consequently also the distance between the yachts can be explained by examining the true wind speed history of the yachts.

As seen in Figure 48, the PID-controller tries to balance the change in TWS which explains the wavy history of the graph. In comparing with Figure 49, which showing the TWS history recorded from the PM, the NWM chart identifies a change in TWS in x- as well as in y-directions, whereas the PM just simulates a change in x-direction. Consequently, the new NWM predicts a change in TWS as well as a change in true wind angle. The different prediction of the TWS-components has a major influence on the yachts performance and hence the travelled distance as the momentum of the yacht depends on the thrust of the sails which in turn is directly depended on the heading and consequently on the amount and the direction of the TWS. As seen in Figure 49 the PM capturing a loss for just one component (x-direction) and overpredicts this loss which increases the distance between the two yachts. That in turn diminishes the blanketing effect of *Yacht A* on *Yacht B* which decreased the damage in TWS over time until *Yacht B* has clean air in her sails. Consequently the distance between the yachts remains constant after around t = 400s. The two yachts are sailing parallel to each other which is the result of the missing TWS y-component. Different to that, the NWM forces *Yacht B* to bear away resulting in a non-parallel track.

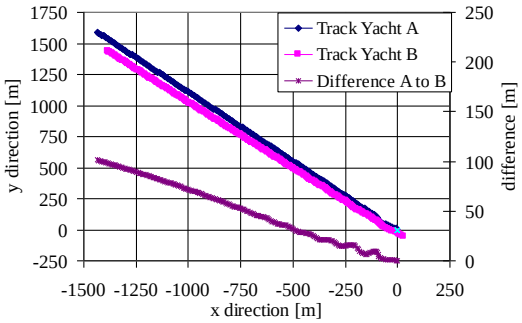

Figure 46: Upwind race using the NWM where the following yacht, *Yacht B*, sails parallel and in the wake of the leading yacht, *Yacht A*. Tracks show that *Yacht B* bears away and that the distance between the yachts increases gradually.

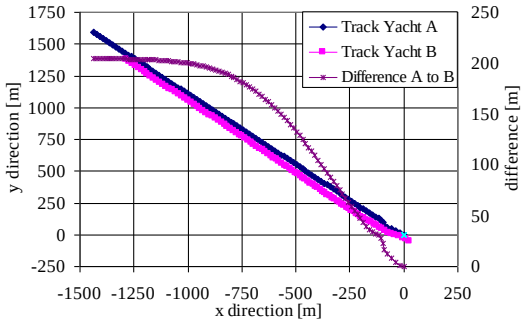

Figure 47: Upwind race using the PM where the following yacht, *Yacht B*, sails parallel and in the wake of the leading yacht, *Yacht A*. Tracks showing parallel yacht tracks whereas the distance between the yachts remains constant after 400 seconds.

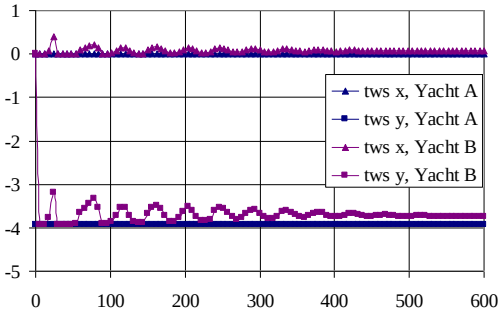

Figure 48: Time history of TWS components in x and y direction using the NWM. A change of TWS for *Yacht A* can be observed for its both components whereas the PID controller tries to balance this change.

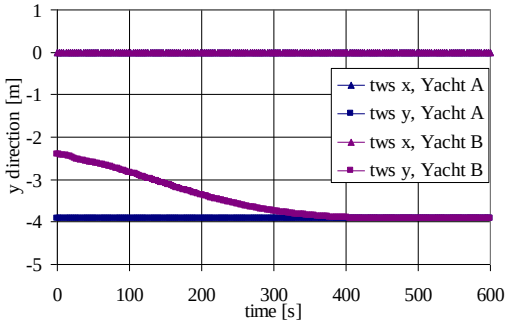

Figure 49: Time history of the TWS components in x and y direction using the PM. Just a change of TWS in x direction can be seen which increases the greater the distance between *Yacht A* and *Yacht B* become.

The track and the TWS histories of the second setup where *Yacht A* crosses the wake of *Yacht B* are displayed in Figures 50 and 51 respectively. *Yacht B*'s position was kept constant to ensure that *Yacht A* crossed Yacht B's wake 2 *YL* downstream and almost perpendicular (see Figure 50). The simulations with the two wake models show completely different behaviours when analysing the TWS histories. For the PM the drop in TWS starts at 187 seconds lasts for 73 seconds and ends with a sudden jump at 260 seconds as the affected blanketing area had been crossed by Yacht A. For the NWM the TWS components show a gradual increase and decrease respectively whereas the minimal and maximal values were reached when *Yacht A* sailed through the centre of *Yacht B*'s wake. As mentioned earlier the values of the TWS components are directly related to the generated sail force (thrust). Hence, we can consider the loss in driving force (momentum) as the integral of the TWS components with respect to time starting and ending at t_1 and t_2 respectively defined by the begin and end of the change of the TWS components. Consequently, the PM overpredicts the loss in TWS leading to an underpredition of the sail thrust which slowed *Yacht A.* In contrast, the influence in TWS using the NWM was limited to 7 seconds causing a natural loss in TWS and consequently in sail thrust as also seen in the good agreement with the CFD results.

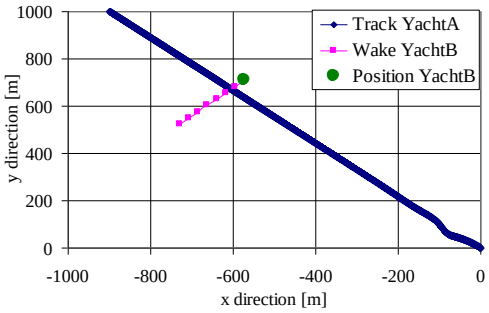

Figure 50: Wake crossing setup. *Yacht A* crosses the *Yacht B*'s wake.

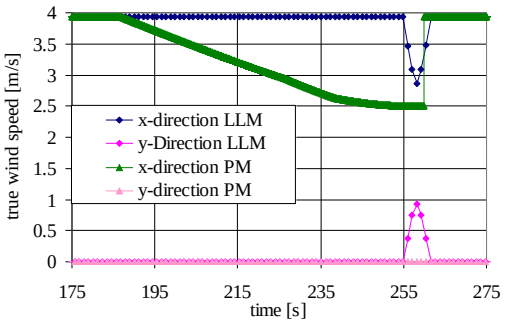

Figure 51: Time history of the TWS components comparing LLM with PM.

7.8 Test Cases II: Real Time Simulations of Tacking Yachts

The effect of the position of a following yacht sitting behind the leading yacht on an upwind leg is investigated in this section. Therefore two upwind yacht fleet simulations with the new wake model (NWM) were conducted and two different wake plots were analysed.

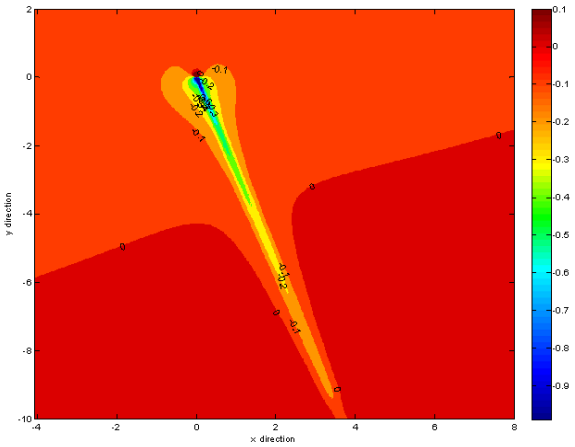

Fig. 52: Wake flow, velocity deficit measured relative to the undisturbed wind flow seen by the yacht. The yacht sailed at an apparent wind speed of 7m/s and was located at x=0, y=0.

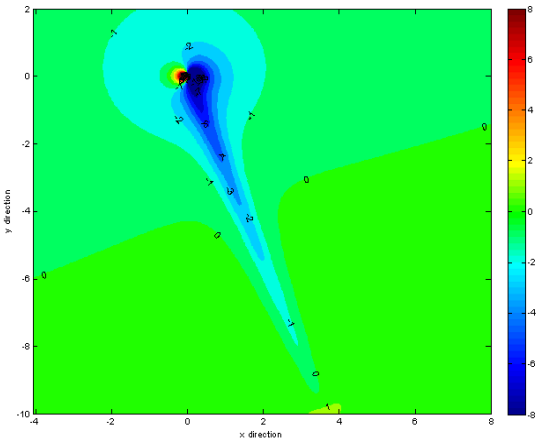

Fig. 53 Wake flow, deflection angle [°] measured relative to the undisturbed wind flow seen by the yacht. The yacht sailed at an apparent wind speed of 7m/s and was located at x=0, y=0.

Two ACC yachts (yacht length, YL = 24 m) race on an upwind leg where the following two sailing situations were considered. First, the following yacht, *Yacht B*, is sailed parallel to the leading yacht, *Yacht A*, which changes course and covered *Yacht B* which in turn reacts to the new situation. Second, the following yacht, *Yacht B*, sailed parallel and in the wake of the leading yacht, *Yacht A*, which bore away putting *Yacht B* closer to its wake centre. This attack was not answered with a counter attack by *Yacht B* which remained in

Yacht A's wake. The wind speed was kept at a constant value of 3.93 m/s with wind direction from north to south. To demonstrate the improvement of the NWM, the tracks of the yachts on the course and important data influencing the yachts' performance, such as true wind speed (TWS) components are displayed. The computer controlled yachts were run with a PID-controller on the sail settings and the rudder always aiming for an apparent wind angle of 22°.

Figure 52 and 53 show the wake contour of a sailing yacht sailing upwind at an apparent wind speed (AWS) of 7 m/s. The yacht is located at x = 0 and y = 0. Figure 52 displays the loss in AWS downstream relative to the AWS seen by the yacht whereas Figure 53 shows the change in wind angle within the yacht's wake. The shape of the affected flow area can be simplified as an acute triangle. The biggest changes in velocity deficit and flow angles occurred in the yacht's close proximity where velocity drops of more than 60% and flow angle changes of more than 8° could be observed. Significant changes in the flow characteristic could be observed up to 6 *YL* downstream in longitudinal yacht direction whereas the affected cross section width was around one *YL* wide.

Within a match or a fleet race sailors try to avoid going into an opponent's wake but often race situations forces the sailor to do so. The contour plots of Figures 52 and 53 provide a helpful tool for sailors making a decision about the location where to sit behind a yacht and areas which should be strictly avoided. Using these contour plots, the described yacht races were set up and the effect of the position of a following yacht in the opponent's wake on TWS and the resultant consequences are shown in Figures 54 to 57.

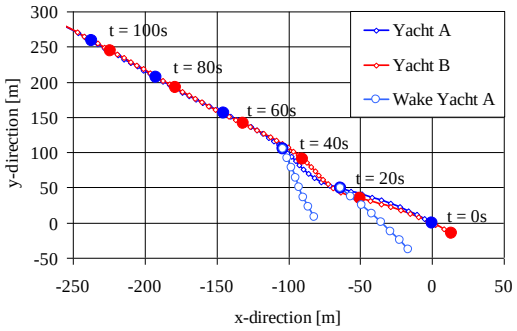

Fig. 54: Upwind race where the following yacht, *Yacht B*, answered *Yacht A*'s manoeuvre and sailed parallel in clear wind of the leading yacht, *Yacht A*. Yachts' positions at diverse points in time are shown as well as *Yacht A*'s wake at these moments.

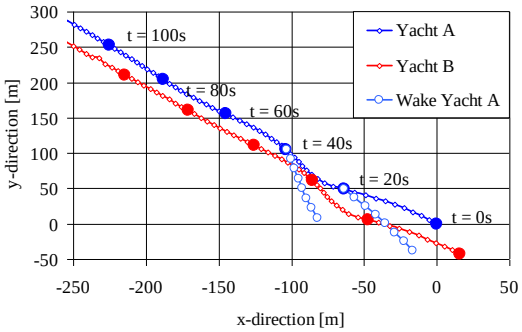

Fig. 55: Upwind race where the following yacht, *Yacht B*, did not answered *Yacht A*'s manoeuvre and sailed in the leading yacht's wake. Yachts' positions at diverse points in time are shown as well as *Yacht A*'s actual wake at these moments.

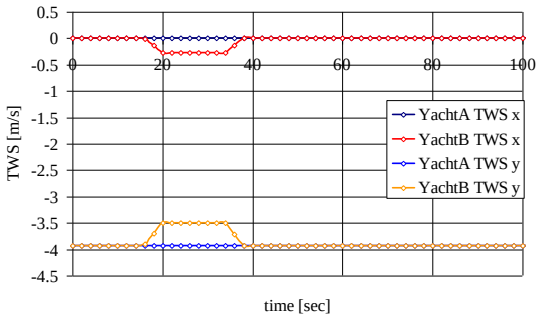

Fig. 56: True wind speed history of the leading yacht, *Yacht A*, and the following yacht, *Yacht B*. The leading yacht had clear wind in her sails resulting in an undisturbed TWS. *Yacht B*'s counter attack guarantied an undisturbed flow in her sail after *Yacht A*'s attack resulting in almost same TWS history as *Yacht A*.

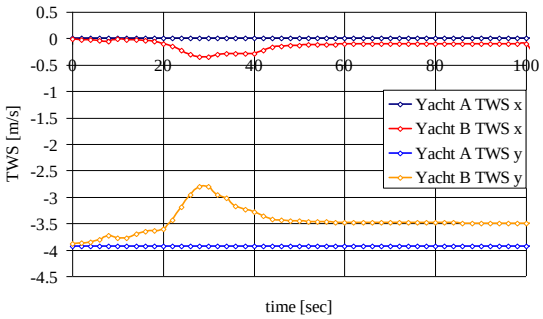

Fig. 57: True wind speed history of the leading yacht, *Yacht A*, and the following yacht, *Yacht B*. The leading yacht had clear wind in her sails resulting in an undisturbed TWS history. *Yacht B*'s history was alternating as it was influenced by *Yacht A*'s wake resulting in a reduced true wind speed.

Figures 54 and 55 display the tracks of *Yacht A* and *Yacht B* on its upwind leg. The position of the two yachts at various times are shown whereas the *Yacht A*'s wake was added to illustrate the relative position of *Yacht B* to *Yacht A*'s wake. In Figure 54, *Yacht A* and *Yacht B* started inline where *Yacht B* was sailing in clear air behind *Yacht A*. After the start, *Yacht A* bore away and came up. This manoeuvre was answered by *Yacht B* which always tried to have clear wind in her sails by avoiding *Yacht A*'s wake. She succeeded as the distance between the yachts stayed almost the same. The clear wind of *Yacht B* can be seen in Figure 56 where almost no difference in TWS of the yachts can be determined after having answered *Yacht A*'s manoeuvre.

Another race situation occurred in Figure 55 where *Yacht B* started its race on the left side (backboard) of *Yacht A*'s wake centre. By not answering *Yacht A*'s manoeuvre correctly *Yacht B* was forced to go through *Yacht A*'s wake which synonymous with a massive TWS loss (see Figure 57).

7.9 Conclusions

A robust covering and blanketing model for yacht fleet race simulations based on lifting line theory is presented in this paper. This new model is capable of representing a complex wake field of a yacht as a series of vortex elements and captures the main features of the flow to a sufficient level of fidelity. The lifting line elements move in accordance with the local wind, self-induced velocity and velocity induced by the presence of the wakes of

other yachts. Furthermore the superposition of the lifting line model and a viscous wake model to calculate the velocity deficit yield important improvements compared to the previous implemented blanketing model of Philpott *et al*. (2004). Detailed CFD analysis of a yacht's wake gave important insight in the flow behaviour, especially of the vortex core development downstream of a single and two in-line sail rigs. Sensitivity studies investigating different lifting line setups with fixed and varying wake lengths were analysed and compared with CFD results and showed good agreement. Studies evaluating the new wake model's performance and degree of realism were carried out in a series of upwind yacht race scenarios and demonstrated a clear improvement in comparison to the previous wake model. This is not only due to the fact that the new model captures the wake flow changes in magnitude and direction, but also the precise prediction of the limited affected blanketed area and hence the authentically simulated loss in sail thrust, make it superior to other models. By implementing this new covering and blanketing model into the sailing simulator *Robo-Race,* it is believed that an important step has been made to enhance the reality of the simulator which in turn supports the sailor in his/her natural sailing behaviour when controlling an ACC-yacht in *Robo-Race.*

8 Bayesian Networks in a Dynamic Yacht Fleet Racing Simulator

This chapter gives an introduction to Bayesian Belief Networks (BBN) and highlights the gradual development of the new decision-making engine starting with a basic BBN for single yachts towards a superior BBN able to deal with long term goals of a regatta. The advanced decision-making engine featuring a new AI decision-making philosophy based on Decision Field Theory (DFT) that uses BBN as a perceptual processor has been implemented into *Robo-Race*. The basic BBN starts with basic functions focusing on spatial position of a yacht on the race course whereas the superior network also focuses on multiple opponents and the interaction of yachts. The function of the DFT-BBN based decision-making engine is explained and case studies featuring the basic and superior BBN used as the perceptual processor are highlighted.

Different sailing behaviours and styles, such as risky, safe and balanced have been developed. Extensive sensitivity studies investigating the effect of different weather scenarios and the effect of different starting positions on the performance of the three sailing behaviours are carried out.

Furthermore, three different levels of sailing expertise, such as skilled, intermediate, and expert, have been developed and implemented. Various sensitivity studies were conducted to determine the effect of the expertise of the sailor on the race course and to analyse the differences in performance between them.

8.1 Introduction

Sailing can be considered as a continuous evolution of the environment which involves a dynamic, interactive process with an overall strategy and tactical decisions continued by actions, followed by checking judgements followed by new actions. Consequently, to win a race by gaining crucial superiority over the opponents, the sailor's strategies and tactical decisions have to be dynamic meaning they have to be updated according to the changing race course environment, such as interaction with other yachts or changing environmental conditions (weather, wind, and current). This becomes obvious, especially on an upwind leg where the changing conditions force the sailor to act accordingly. These changes have to be interpreted driving the subsequent decision-making process of the sailor who has to conduct the necessary decision outcome efficiently. During the decision-making process, the sailor (decision maker) has to look for the probabilities for every possible outcome and payoffs associated with the outcomes of each option. Executing a manoeuvre in an unfavourable time period (too early or too late) can yield lower velocity made good towards the mark leading to a great disadvantage in the race outcome. Therefore, the correct estimation of windshifts (strength and duration) is essential for a winning sailing performance. As a result, the model simulating the sailor's decision-making-process has to be dynamic, adaptive and comprehensive.

As mentioned in Chapter 3, Lee *et al.* (2008) subdivided the human decision-making process into three major groups: economical, psychological, and synthetic engineering-based decision-making. The first group, economical decision-making, assumes that the decision maker behaves rationally and consequently the corresponding approaches are not able to simulate the cognitive nature of humans, such as fatigue, pressure, and memory (Simson, 1955 and Gibson *et al.*, 1997). To close this gap, psychology-based models take utility or subjective values and probabilities into account (Edward, 1962 and Busemeyer *et al.*, 2002). Those types of approach were judged to be incomplete as they are based on static laboratory decisions that are rarely discovered in real life situations (Rothrock *et al.*, 2009). The third group, the synthetic engineering-based category, uses engineering based approaches and techniques to understand and learn attribute of human behaviours in realistic and complex environments (Gonzalez *et al.*, 2003 and Konar *et al.*, 2005). Decision-making is made by a system consisting of modules and sub-modules to which engineering techniques are applied. Consequently, the validation of such a complex

model against real human decisions is quite difficult. To overcome the constraints of all three models, a comprehensive model capturing real human decision-making has to be developed by combining, enhancing, and extending all three approaches mentioned above. This idea was realised by Lee *et al*. (2008) who extended Decision Field Theory (EDFT) by adding a Bayesian belief network to it. Thereby, the Decision Field Theory module calculates the subjective evaluation for the available options and interest on the attributes. The Bayesian Believe Network (BBN) sub-module delivers these updates according to the dynamic environment (Lee 2008). This synthetic engineering-based approach was further enhanced leading to an integrated human decision behaviour model under a Belief-Desire-Intention (BDI) framework. Thereby, BBN and DFT sub-modules were accompanied by a probabilistic depth first search technique to simulate real-time planning and decision-execution tasks of humans under a terrorist bomb attack evacuation scenario.

8.2 Race Preparations

The novel sailor decision behaviour model was implemented into *Robo-Race* as the new 'decision-making engine' solving problems of strategic and tactical nature. As mentioned earlier, this research focuses on tacking decisions. The task of the AI-sailors consists in racing an upwind leg against other computer controlled yachts. The races were finished by rounding the upwind mark. The distance between the start line and upwind mark was set to be two nautical miles (equal to 3704 m). To assure a dynamically changing sailing environment, four different weather scenarios have been developed based on the weather model highlighted in Chapter 6. Attention was also paid to model the mark rounding realistically in order to guarantee fair and reliable simulation results.

8.2.1 Yacht Racing Environment

Four different scenarios have been set up by changing the environmental conditions as well as the types of sailor. The latter were characterised by their personal sailing style/behaviour, such as:

1. Risky/passive

2. Safe/active, and
3. Balanced.

Furthermore, the sailing expertises of the sailors were categorised in:

1. Expert,
2. Intermediate, and
3. Skilled.

The changing environmental conditions were simulated by:

1. The opponents and
2. The weather that was categorised and set up in the following four different scenarios:
    a. Normal,
    b. Calm,
    c. Stormy, and
    d. Variable.

Moreover, different starting position constellations were also investigated which can be subdivided in:

1. Favourable,
2. Neutral, and
3. Unfavourable.

The performance of the individual sailing behaviour have been analysed when the sailors tried to control their yacht as fast as they can to and around the upwind mark depending on their level of expertise, their personal sailing style, and the external conditions.

The race course itself was the same as the one described in Chapter 6.3 which formed a triangle consisting of three marks (see Figure 58). This study focused on the upwind beat and the subsequent mark rounding. Consequently, just the starting line (horizontal through the final mark) and the upwind mark were of interest and used in this study. The complex phenomenon of mark rounding and its simulation will be described in Section 8.7.2.

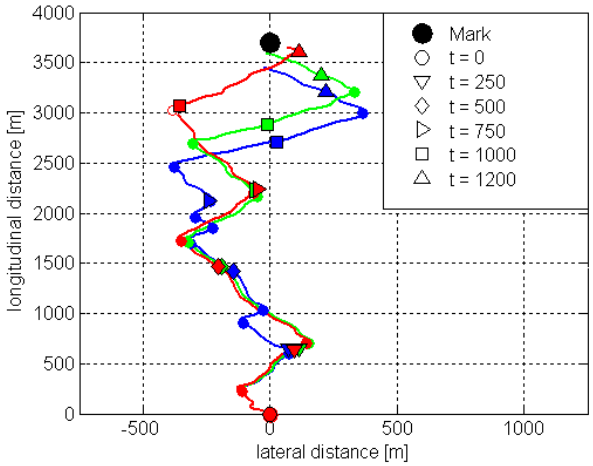

Figure 58: Race course showing the tracks of three yachts on the upwind leg where the yachts start at the final mark (x=0m / y=0m) and race up to the upwind mark (x=0m / y=3704m)

8.2.2 Four different weather scenarios

Four different weather scenarios have been developed for the following investigations. Thereby, the weather model highlighted in Chapter 6 was used as a basis and the following four scenarios have been created by altering the parameters of the basic version:

1. normal,
2. calm,
3. stormy, and
4. variable

As mentioned above, the normal weather setup was a copy of the weather series used in Chapter 6 and therefore featured the characteristics of real weather conditions. The other three setups have been changed accordingly in order to achieve the desired individual features of a weather series.

The calm setup contains higher p1 and p2 values which indicated a low likelihood for the wind statistics to change from one state to the other leading to a less fluctuating wind history (see Figures 59 and 60). This weather character was further intensified by the missing superimposed sinusoidal wave and the lower applied turbulence level.

A completely different picture can be seen when analysing the variable weather setup. There, the characteristic of a weather series have been realised by 1) applying lower p1 and p2 values which increase the likelihood of the state changes in the wind statistics and 2) by stronger and higher frequent sinusoidal waves.

The character of the stormy weather setup was generated by a higher wind speed which was 50% higher compared to the other three setups (8.3 ms^{-1} compared to 5.0ms^{-1}). This wind speed is called *fresh breeze* (Beaufort scale: 5), whereas the other is labelled as *gentle breeze* (Beaufort scale: 3). Moreover, the turbulence level and the amplitude of the sinusoidal waves were increased to match the natural character of stormy weather.

The following Figures 59 and 607 show typical examples of the four different generated wind histories.

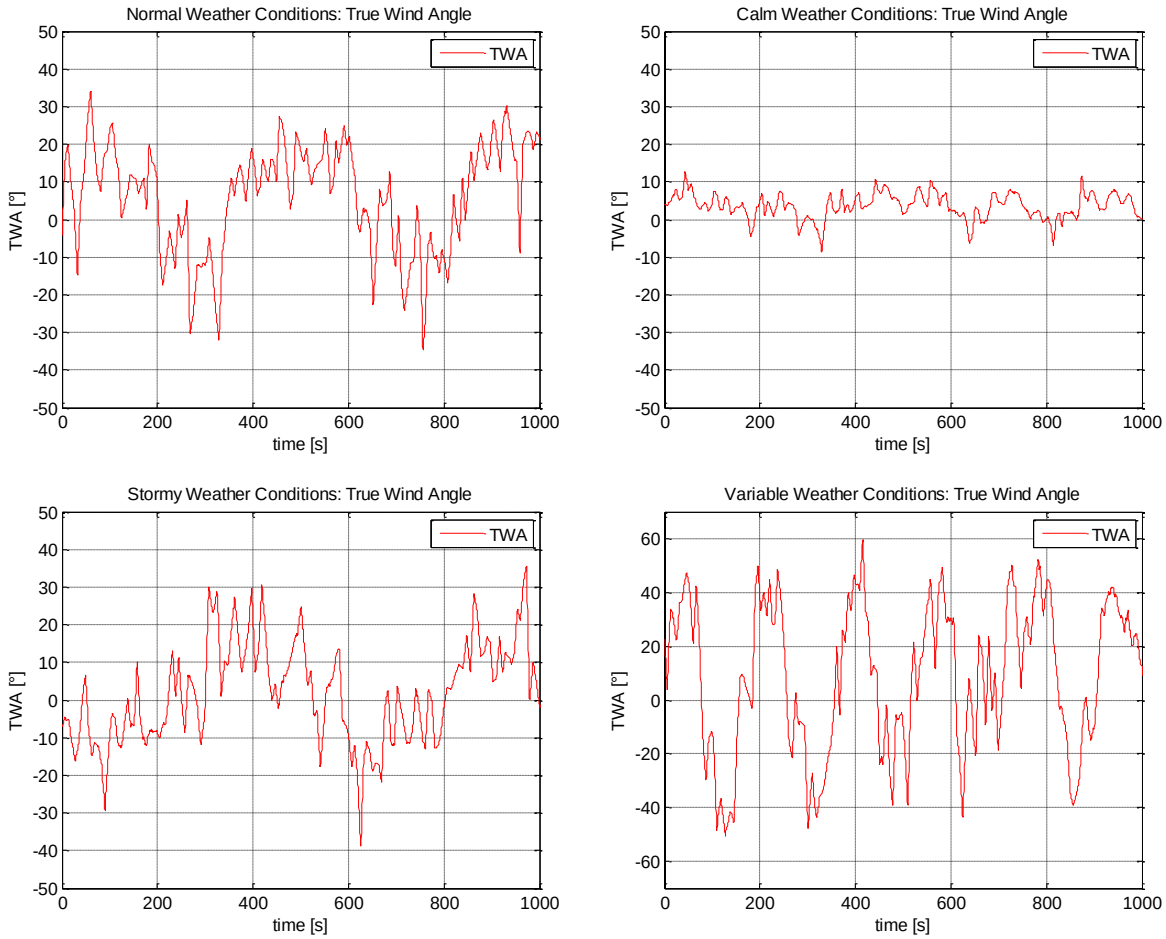

Figure 59: TWA histories of normal, calm, stormy, and variable weather conditions

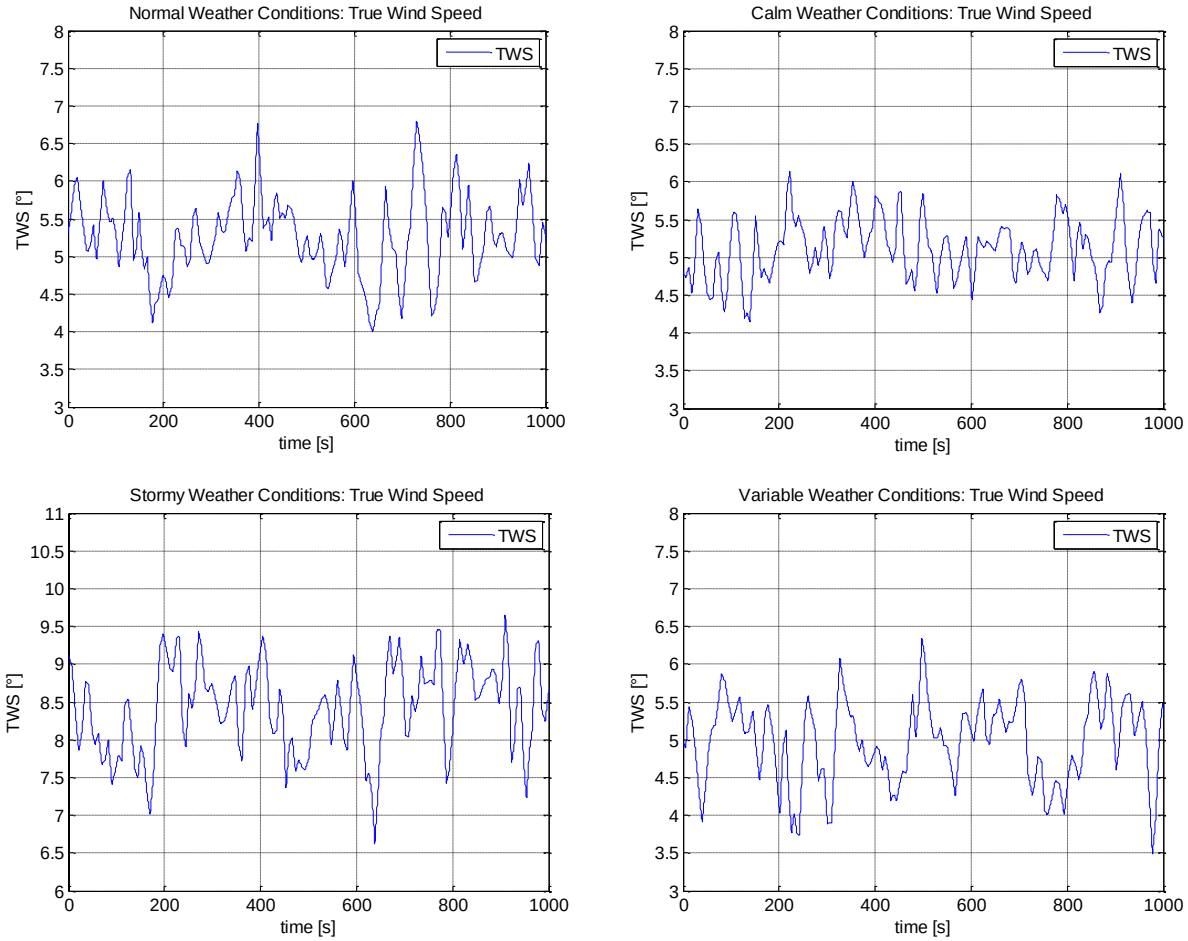

Figure 60 TWS histories of normal, calm, stormy, and variable weather conditions

8.2.3 Mark rounding modelling

To guarantee fair, reliable and meaningful results, the mark rounding part of the race has been modelled for all upcoming races in this study. This approach combines the following advantages:

- the mark rounding can be modelled according to the level of expertise of the sailor
- different mark rounding styles can be investigated and modelled, and
- the results are more transparent, easier to analyse and therefore more meaningful.

A mark rounding zone has been introduced which features a radius of eight yacht lengths (YL) and was centred at the upwind mark position. As soon a yacht enters this circle the following data were recorded to calculate the time the yacht needs to round the mark:

- horizontal and vertical yacht velocities, u_{entry} and v_{entry}.

- zone entrance angle α_{inner} and entry sector

The time a yacht needed for rounding the mark was calculated based on the following procedure and assumptions. It is believed that the ideal incoming angle approaching the upwind mark was 45°. Depending on the sailor's expertise level, the following three different mark rounding styles have been introduced:

- Expert: wide in, tight out
- Skilled: tight in, wide out
- Intermediate: medium in, medium out (see Figure 61)

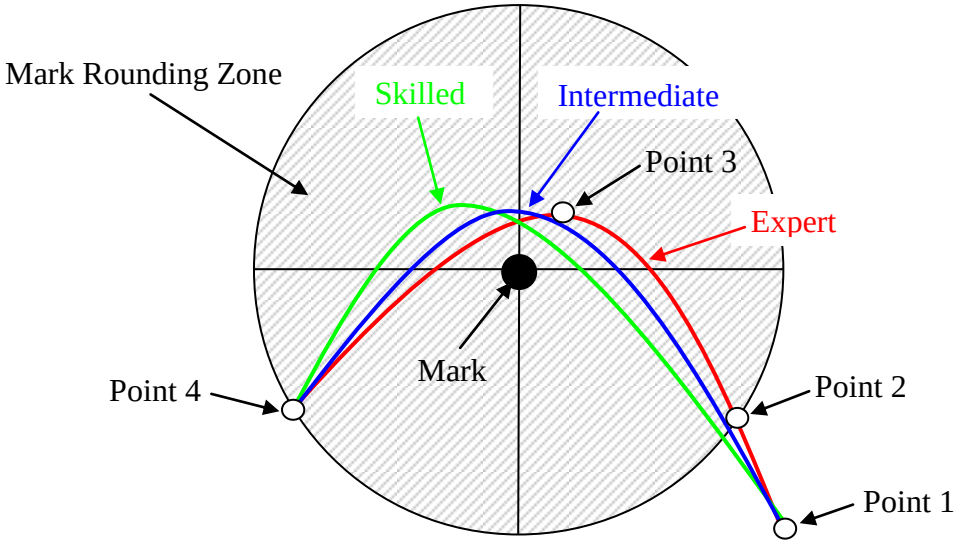

Figure 61: Tracks of three different mark rounding styles

These mark rounding styles not only resulted in different tracks and therefore different distances covered but also in different averaged velocities on the approach-to-the-mark and the sailing-away-from-it stage.

The mark rounding procedure has been divided into three phases: A, B, and C. On phase A, the yacht sails from point 1 to point 2 with the velocities u_{entry} and v_{entry}. At point 2 which is 3 YL away from the mark, phase B begins and the sailor starts to perform his/her individual mark rounding approach depending on his/her level of expertise. As can be seen in Figure 61 these different approaches resulted in different race tracks and therefore different averaged velocities on phase B. Point 3 was defined as the location where the maximum vertical position was achieved and where the first downwind leg of the race begins. It was obvious that phase B influenced phase C and as a result the corresponding tracks and velocities have to be different. The mark rounding modelling and

also the race have been finished as soon the yacht has reached point 4. The corresponding velocities and distances used for the three expertise levels on the different phases can be found in Tables 1-3. To simplify matters and for a broader use for the sailing community the expressions in the table are presented in relation to the entry velocity and the yacht length. The total time needed $T_{Total45°}$ was calculated by adding the individual times of the faces:

$$T_{Total45°} = T_{FaceA} + T_{FaceB} + T_{FaceC} \tag{8.1}.$$

Table 1: Summary of the expert sailor's mark rounding process

Expert	Phase A	Phase B	Phase C	Total
Avg. velocity	v_0	$0.667v_0$	$0.667v_0$	$0.777v_0$
Track distance	$5YL$	$1.25 * 3YL$	$3YL$	$11.75YL$
Time needed	$5 \frac{YL}{v_0}$	$5.625 \frac{YL}{v_0}$	$4.5 \frac{YL}{v_0}$	$15.125 \frac{YL}{v_0}$

Table 2: Summary of the skilled sailor's mark rounding process

Skilled	Phase A	Phase B	Phase C	Total
Avg. velocity	v_0	$0.625v_0$	$0.458v_0$	$0.676v_0$
Track distance	$5YL$	$1.75 * 3YL$	$2.5YL$	$12.75YL$
Time needed	$5 \frac{YL}{v_0}$	$8.4 \frac{YL}{v_0}$	$5.459 \frac{YL}{v_0}$	$18.859 \frac{YL}{v_0}$

The times needed by the intermediate sailor have been calculated by averaging the corresponding times of the expert and skilled sailors (see Table 3).

Table 3: Summary of the intermediate sailor's mark rounding process

Intermediate	Phase A	Phase B	Phase C	Total
Avg. velocity	v_0	$0.646v_0$	$0.562v_0$	$0.727v_0$
Track distance	$5YL$	$1.5 * 3YL$	$2.75YL$	$12.25YL$
Time needed	$5 \frac{YL}{v_0}$	$6.968 \frac{YL}{v_0}$	$4.89 \frac{YL}{v_0}$	$16.858 \frac{YL}{v_0}$

It is obvious that a yacht will also enter the mark rounding zone at another angle that the assumed ideal entrance angle of 45°. Therefore a penalty time $T_{Penalty}$ has been applied that yield the following expression indicating the total time needed for rounding the mark:

$$T_{MarkRounding} = T_{Total45°} + T_{Penalty} \tag{8.2}.$$

To calculate $T_{Penalty}$ it was necessary to know from which direction the yacht entered the mark rounding zone. Therefore, a second zone entrance angle α_{outer} was recorded. This angle referred to an outer zone which features a slightly bigger radius than the mark rounding zone. Having these two entrance angles it was possible to calculate the direction the yacht entered the zone.

Depending on the entrance angle and the entrance direction, the yacht had to perform at least one tack to make it safe around the mark. To achieve a reliable judgement on the necessary tacks, the lower part of the circle has been divided into four evenly spaced sectors. The numbering starts on the lower right side and followed a clockwise direction (see Figures 62 and 63).

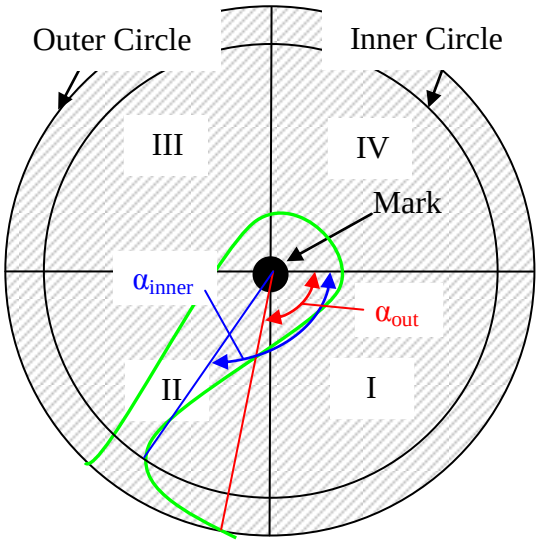

Figure 62: Nomenclature of mark round zone

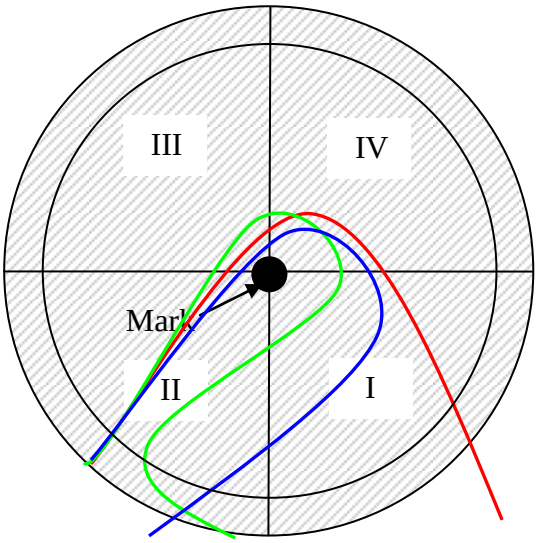

Figure 63: Example of two different mark entrance angles

With this nomination, the yacht's entrance sector was determined and depending on the yacht's entrance direction, the following penalties shown in Table 4 have been applied.

Table 4: Penalty table showing the applied penalties depending on the sailing direction and zone entrance angles where α_{outer} refers to the outer zone and α_{inner} to the mark rounding zone.

	Sector			
	I	II	III	IV
$\alpha_{outer} > \alpha_{inner}$	-	$1 \times T_{Tack} + T_{off45}$	$1 \times T_{Tack} + T_{off45}$	$2 \times T_{Tack} + T_{off45}$
$\alpha_{outer} < \alpha_{inner}$	$1 \times T_{Tack} + T_{off45}$	$2 \times T_{Tack} + T_{off45}$	$2 \times T_{Tack} + T_{off45}$	$3 \times T_{Tack} + T_{off45}$

T_{off45} refers to an extra penalty calculated by the following assumption. It was assumed that the perfect mark rounding approach is based on a 45° entrance angle. Any angle greater than that comes with an extra way and at least one extra tack (see Figure 63). Furthermore, it was believed that the sailor aimed to sail to the 45° line at a distance of 3 yacht lengths away from the mark. For simplification reasons this extra way was assumed to be the chord length c_{3YL} of the segment three yacht lengths way from the mark created by the 45° line and the entrance angle line. Hence, this chord length was calculated by:

$$c_{3YL} = 2 * 3YL * \sin\left(\frac{|\alpha_{45°} - \alpha_{inner}|}{2}\right) \quad (8.3).$$

To get the corresponding time penalty $T_{off45°}$, this extra way c_{3YL} was divided by a percentage of the velocity the yacht entered the mark rounding zone u_{entry}. It was assumed that the yacht's regained velocity after a tack depended on the level of expertise of the sailor and therefore 80%, 70%, or 60% of u_{entry} have been applied as averaged velocities for an expert, intermediate, and skilled sailor, respectively. Hence, the time penalty $T_{off45°}$ can be calculated by:

$$T_{off\,45°} = \frac{c_{3YL}}{x_{expertise} * u_{entry}} \quad (8.4),$$

where $x_{expertise}$ = 0.8, 0.7 or 0.6.

Furthermore, the performance of a tack also depended on the sailor's expertise level and therefore the following time penalties for an extra Tack T_{Tack} indicted in Table 5 have been applied in this study.

Table 5: Penalty table showing the applied penalties for a performed tack

	Expert	Intermediate	Skilled
Time lost during a tack T_{Tack}	10 sec	15 sec	20 sec

Consequently, the total mark rounding time including the corresponding penalties can be written as:

$$T_{MarkRounding} = T_{Total45^\circ} + n_{Tack} * T_{Tack} + T_{off45^\circ} \quad (8.5).$$

where n_{Tack} indicates the number of extra tacks.

8.3 Bayesian Belief Network for Perceptual Processor

The perceptual processor in the dynamically changing environment was simulated by a Bayesian Belief Network (BBN). Two different BBNs (basic and superior) were developed to account for different expertise levels and characters of the sailors. The BBN was chosen as the perceptual processor as it offers the opportunity to combine probability calculation with historical functions. This was achieved by using Bayes' theorem linking prior and conditional probabilities to calculate the posterior probability that will be explained in detail in the following subchapters (Korb and Nicholson, 2004).

8.3.1 An Introduction to Bayesian Belief Network

BBNs are able to deal with uncertainty rich and dynamic environments since they are using the past to conclude possible future actions. Therefore, they represent the logical choice for a perceptual processor in this kind of environment.

Bayes' Theorem is the basis of probabilistic reasoning and offers the opportunity to calculate the probability of an event occurring having a known related piece of information (Tozour, 2002a). It allows reversing the direction of probabilistic statements and is written as

$$P(A|B) = \frac{P(B|A) \cdot P(A)}{P(B)} \quad (8.6),$$

where

$P(A|B)$ = the probabilistic of *A* given that what one knows is *B*,

$P(B|A)$ = the probabilistic of *B* given that what one knows is *A*,

and the independent probabilities:

$P(A)$ = the probability of event *A*, all other things being equal,

$P(B)$ = the probability of event *B*, all other things being equal.

This mathematical theory of Bayes' Theorem is the basis of Bayesian Networks. If one imagine that the events *A* and *B* have a causal bidirectional relationship, one can illustrate those propositions and their interrelationships into a graph. This allows performing probabilistic inference by using the Bayes' Theorem.

Tozour (2002a) gives a comprehensible introduction to BBN by using the following example:

A man at work gets a call from his neighbour telling him that his burglar alarm went off. The man also knows that his alarm system is also sensitive to earthquakes. Consequently, it might have been set off by an earthquake instead of a burglary. The interrelationship of those three propositions can be shown in the following Figure 64.

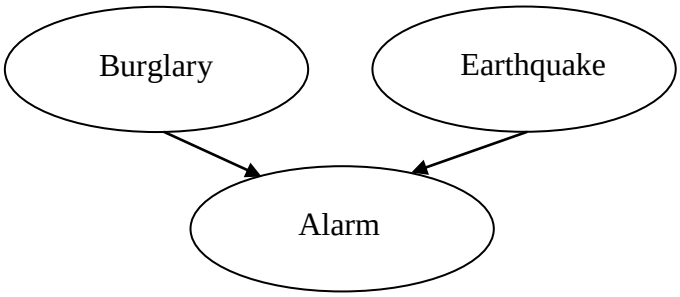

Figure 64: Schematic Bayesian Network

This figure illustrates that both, *Burglary* and *Earthquake* can cause the *Alarm* to ring (= true).

The independent probabilities of a burglary *P(B)* or an earthquake *P(E)* to take place (all other things being equal) can be defined as follows:

Table 6: Probabilities of burglary and earthquake being true

Probability	P(B)	P(E)
Value	0.001	0.002

The following Table 7 illustrates all possible constellations of earthquakes and burglaries as well as the corresponding probabilities:

Table 7: Probabilities of an alarm going off given certain events

Burglary	Earthquake	Alarm
True	True	0.95
True	False	0.94
False	True	0.29
False	False	0.001

Applying Table 6 to Table 7 one can calculate the actual probability of the alarm going off *P(A)* in each possible constellation. To do so, one has to determine the individual probabilities of *P(A)* of each row using the following equation:

$$P(A) = P(B) \cdot P(E) \cdot P(A|B,E) \tag{8.7}.$$

Now, Table 8 can be updated as follows:

Table 8: Actual Probabilities of a burglary and/or earthquake

P(B)	P(E)	P(A)	*n*P(A)
T = 0.001	T = 0.002	0.000002	0.000795
T = 0.001	F = 0.998	0.000938	0.372814
F = 0.999	T = 0.002	0.000579	0.230127
F = 0.999	F = 0.998	0.000997	0.396264
	Sum	0.002516	1

The sum of column *P(A)* in Table 8 indicates the final probability of the alarm going off on any given day to be *P(A)* = 0.25%. This value is also used to clarify the results by normalising the individual *P(A)*, such as 0.000579/0.002516 = 0.230127. Hence, if the alarm went off and we do not have any information about a burglary or an earthquake, there is a 37.28% chance that it was caused by a burglary, a 23.01% chance that it was caused by an earthquake, a 0.0795% chance that it was caused by both and a 39.63% chance that it went off randomly.

Suppose we get the information from the radio that there was an earthquake near the house, the value for *P(E)* can be set to 1. Therefore, Table 9 changes to:

Table 9: Actual Probabilities of a burglary and/or earthquake, *P(E)* is true

P(B)	P(E)	P(A)	*n*P(A)
T = 0.001	T = 1	0.00095	0.003269
T = 0.001	F = 0	0	0
F = 0.999	T = 1	0.28971	0.996731
F = 0.999	F = 0	0	0
	Sum	0.29066	1

Now, the tables highlights that there is 29.07% chance that the alarm went off. A closer look identifies a 99.67% chance that the alarm went off caused by an earthquake and a 0.33% that a burglary happened simultaneously.

Bayesian network development software *Netica* (Korb and Nicholson, 2004) was used to realise these two examples making it easier for the reader to understand the mechanics of Bayesian networks.

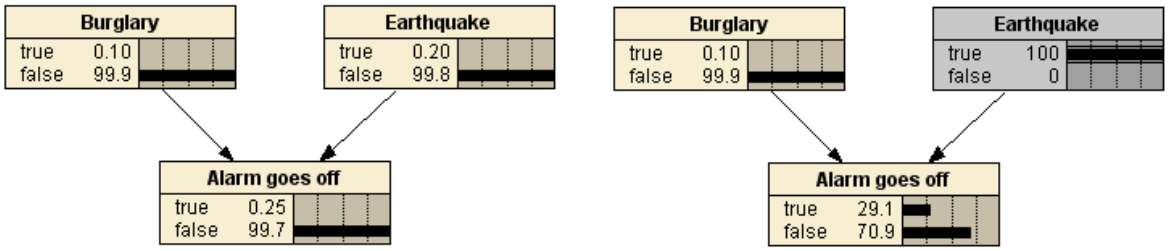

Figure 65: Bayesian Networks showing the final probability P(A) of the alarm going off on any given day to be 0.25% (left side) and P(A) of the alarm going off knowing there was an earthquake near the house to be 29.1% (right side).

Now, two different BBNs, the Basic BBN and the Superior BBN, considering the sailing framework are constructed and highlighted in the following two subchapters. These two BBNs, as well as the ones shown in Figure 65 are created with the software *Netica*. The Basic and Superior *Netica*-BBNs were afterwards recoded in Matlab/Simulink®, extensively tested and implemented in the new decision-making engine of *Robo-Race.*

8.3.2 Basic Bayesian Belief Network

The basic Bayesian Belief Network has been developed to control a yacht on an upwind course whereas in the basic BBN just basic spatial sailing considerations, such as the

yacht's position on the course and its sailing state were taken into account. Therefore, it uses the following four sailing parameters as 'input':

1. The sailing trend regarding the leg coordinate system axis (CSA),
2. Current sailing state,
3. The distance to the leg CSA in x, and
4. Y-direction

These nodes are called *parent nodes*.

As mentioned earlier, the *child nodes* are defined as follows and delivered the necessary output to the corresponding sailing situation:

1. Risk
2. Distance Made Good (DMG), and
3. Weight-Risk.

All nodes and their potential states can be found in Figure 66.

To ensure a stable reasoning, a new leg coordinate system (CS) has been introduced where the yacht's actual position was expressed relative to the positions of the latest past and next mark. Consequently, the actual leg CS has its origin in the latest past mark (here, final mark) and its x-axis vector points towards the next mark (here, upwind mark), whereas the y-axis vector forms a right angle with the x-axis vector and points to its right.

The general Basic BBN with the probabilities of any given race situation can be found in Figure 66, whereas Figure 67 and 68 indicate an un-/favourable race situation, respectively.

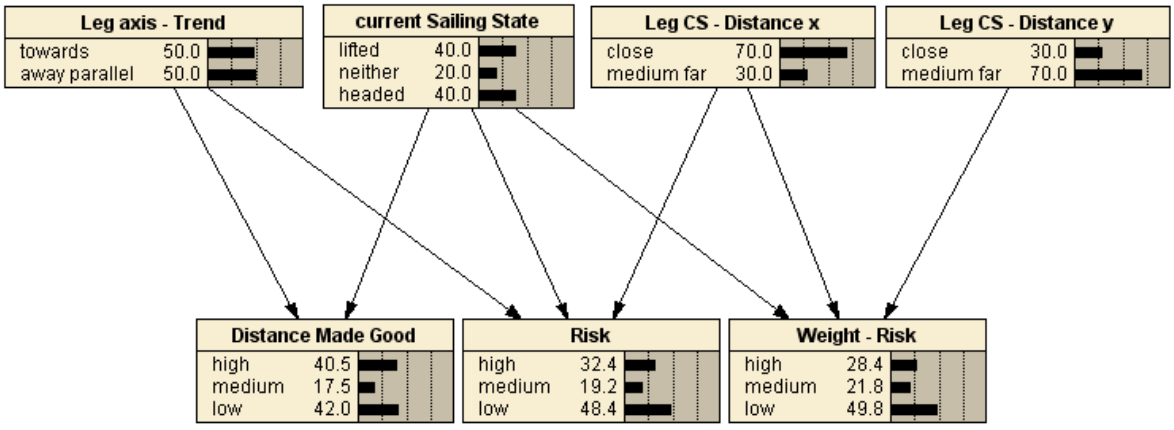

Figure 66: Basic BBN showing the probabilities of any given race situation. The three child nodes *DMG, Risk* and *Weight-Risk* are defined by three states *high, medium,* and *low* and are used as the input of the perceptual processor for calculating the probabilities of *DMG, Risk* and *Weight-Risk* for any option at time *t.*

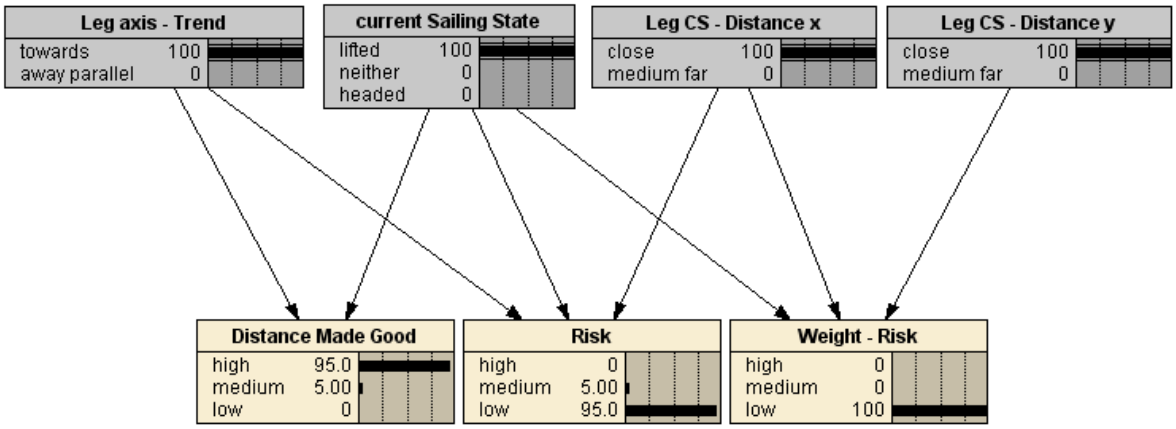

Figure 67: Basic BBN showing the probabilities of a favourable race situation. The yacht is lifted, sails in the vicinity of and towards the leg CS x-axis and close to the upwind mark. Consequently, the DMG towards the mark is high (95%), the risk of the situation is very low (95%) and the sailor's attention on Risk is extremely low (100%).

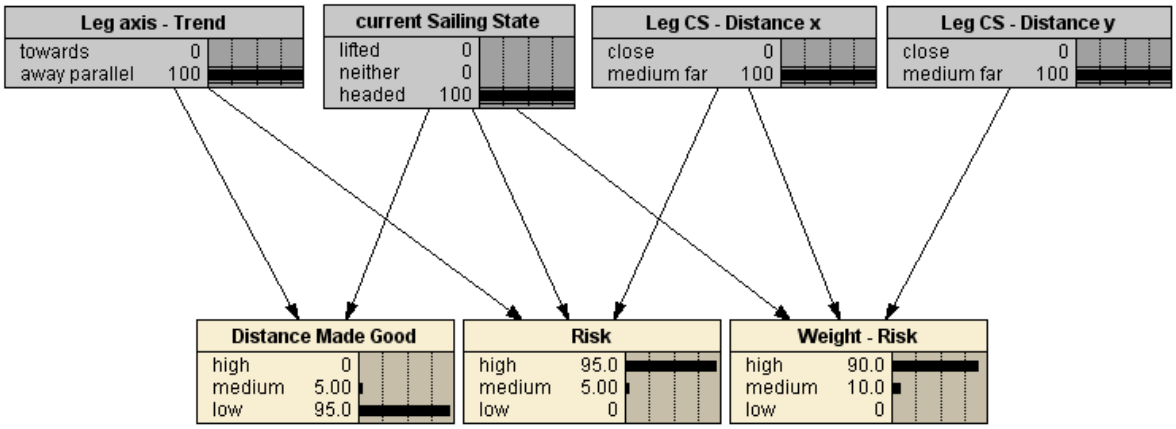

Figure 68: Basic BBN showing the probabilities of an unfavourable race situation. The yacht is headed, does not sail in the vicinity of or towards the leg CS x-axis and is not located close to the upwind mark. Consequently, the DMG towards the mark is low (95%), the risk of the situation is very high (95%) and the sailor's attention on Risk is also high (90%).

8.3.3 Superior Bayesian Believe Network

The superior Bayesian Belief Network features the characteristics of the basic BBN but has been extended by an opponent function. In detail, the Network also focuses on the sailor's hardest opponent considering the relative distance to him/her on the race course. The hardest opponent is defined as the rival that is closest to the sailor regarding the actual ranking list of the regatta. Furthermore, it also takes blanketing into account by distinguishing whether the sailor covers the hardest opponent or the sailor is covered by another yacht. Consequently, the 'input' was extended by the following three parent nodes:

1. Wake

2. Hardest Opponent, and
3. Hardest Opponent-Distance.

The nodes and their potential states can be found in Figure 69.

The general Basic BBN with the probabilities of any given race situation can be found in Figure 69, whereas Figure 70 and 71 indicate an un-/favourable race situation, respectively.

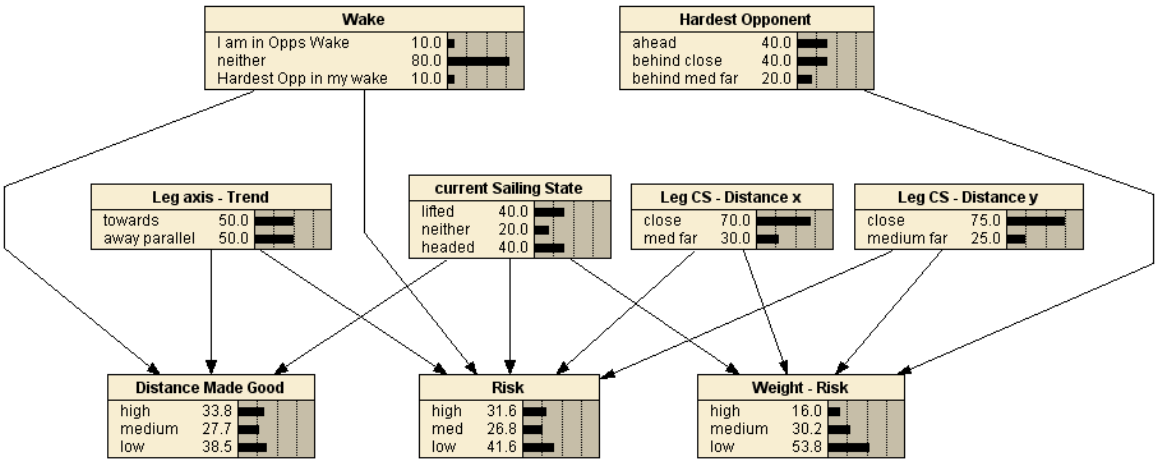

Figure 69: Superior BBN showing the probabilities of any given race situation. The seven parent nodes influence the three child nodes *DMG, Risk* and *Weight-Risk* that are defined by three states *high, medium,* and *low* and are used as the input of the perceptual processor for calculating the probabilities of *DMG, Risk* and *Weight-Risk* for any option at time *t.*

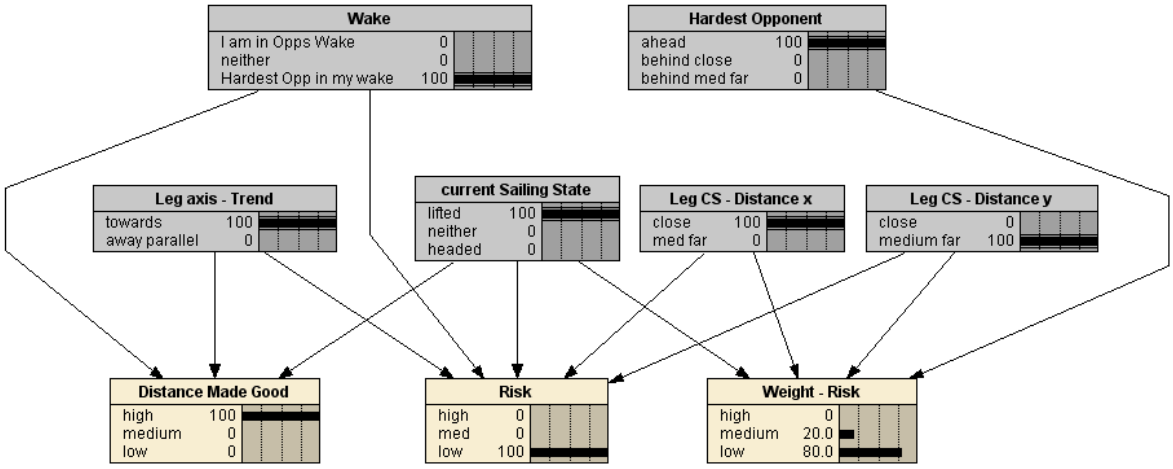

Figure 70: Superior BBN showing the probabilities of a favourable race situation. The sailor's hardest opponent is in his/her wake, the yacht is lifted and sails in the vicinity of and towards the leg CS x-axis but not close to the upwind mark. Consequently, the DMG towards the mark is very high (100%), the risk of the situation is extremely low (100%) but the sailor's attention on Risk is low (80%).

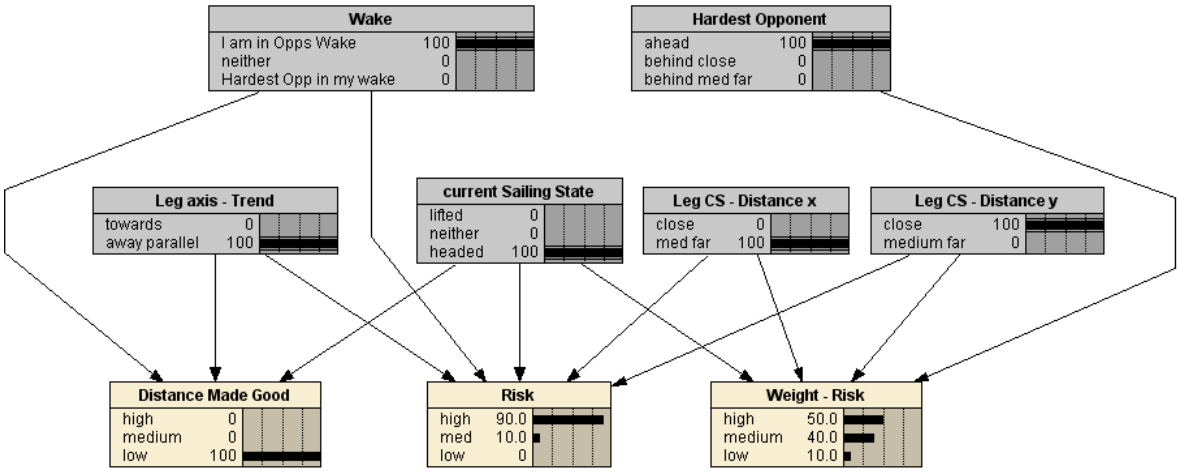

Figure 71: Superior BBN showing the probabilities of an unfavourable race situation. The sailor is blanketed by an opponent, whereas the hardest opponent is ahead. The yacht is headed, does not sail in the vicinity of or towards the leg CS x-axis. Furthermore, she is not located close the leg CS x-distance but also close to the upwind mark. Consequently, the DMG towards the mark is very low (100%), the risk of the situation is very high (90%) and the sailor's attention is mainly on Risk (50%).

The corresponding probability tables of the basic and superior BBNs can be found in Appendix A3. An extract of the *Weight-Risk* node's probability table can be found in Subchapter 8.6 (see Table 12).

8.3.4 The Use of Bayesian Believe Networks

As stated earlier, the BBNs were used to include the sailor's belief on the upwind beat in dynamically changing sailing conditions. Therefore, the BBN uses various environmental information as an 'input' to evaluate:

1. Values for attributes (*Risk* and *Distance Made Good (DMG)*) for the considered options 'to tack' or 'not to tack' and
2. Weights on each attribute, meaning how much attention the sailor puts on each individual attribute represented by the *Risk-Weight* node (see Figures 66 -71).

The following definitions are part of the Decision Field Theory (DFT) that is explained in the following subchapter. The evaluation of the available binary options on each attribute at time *t* are gathered in *M*, which is defined by

$$M = \begin{pmatrix} m^1_{Risk}(t) & m^1_{DMG}(t) \\ m^2_{Risk}(t) & m^2_{DMG}(t) \end{pmatrix} \tag{8.8}.$$

The individual matrix elements $m^i_{Risk}(t)$ and $m^i_{DMG}(t)$ for option *i* were obtained by determining the corresponding values from the BBN nodes *Risk* and *Distance Made Good*, respectively.

In the same way, the weights on each attribute at time *t* was expressed in *W*, which is defined by

$$W = \begin{pmatrix} w_{Risk}(t) \\ w_{DMG}(t) \end{pmatrix} \tag{8.9}.$$

The element $w_{Risk}(t)$ was obtained from the BBN node *Weight-Risk*, whereas

$$w_{DMG}(t) = 1 - w_{Risk}(t) \tag{8.10}.$$

The perceptual processor can be tuned to simulate a category of sailors or even individual sailors by developing the corresponding BBN tables. Therefore, it is possible to mimic the individual behaviour of a sailor by updating the BBN tables that are based on the analysis of real fleet racing events. The probability tables used in this study were developed together with differently experienced sailors starting from novices up to internationally experienced sailors.

8.4 Decision Field Theory

The aim of the work presented here is to develop a comprehensive and successful human decision-making model for dynamically changing frameworks. In particular, this study examines the capability of a DFT based decision-making approach using BBN to model tacking decisions on an upwind beat in dynamically changing yacht racing environments. The novel comprehensive sailor decision behaviour model developed in the following sections is based on the methodology of Lee (2008) and features economical, psychological, and engineering models. The tacking decision has been chosen as it's a very

important and clearly defined yes-or-no decision in sailing and represents a perfect challenge for this study.

In this study, the Decision Field Theory (DFT) was applied to support the real-time planner sub-module. The human deliberation process and the subsequent decision-making were represented by the DFT that is a mathematical tool for developing preferences of a human decision maker where different options are considered. It can be categorised as a dynamic-cognitive approach built on psychological principles instead of economical once and can therefore be used to describe psychological human behaviour. DFT offers a mathematical framework helping to comprehend the cognitive mechanism of the deliberation process of humans in making decisions in uncertainty rich environments (Busemeyer and Townsend, 1993; Busemeyer and Diederich, 2002). DFT provides a probabilistic and dynamic character and therefore differs from earlier mathematical models mentioned above. Due to its character abilities, DFT performs successfully in a wide variety of cognitive tasks including perceptual discrimination, sensory detection, memory recognition, preferential choice and conceptual categorisation (Lee *et al.*, 2008 and Busemeyer *et al.*, 2002).

In DFT, decisions are based on the dynamic development of preference among available options during a deliberation process. This can be mathematically expressed by:

$$P(t+h) = SP(t) + V(t+h) \tag{8.11}.$$

Equation 8.11 represents a human preference state $P(t)$, which is a vector of length m, where m is the number of available options, and t is the time, and h is the time step. $P(t)_i$ depicts the preference for option i. The memory effect is simulated by the stability matrix S, especially by the diagonal elements $s_{i,i}$ which control the growth or decay over time of the preference for option i. The off-diagonal elements $s_{i,j}$ represent the influence of option i on option j, meaning the effect of interaction among the options. Two principles have to be considered when setting up S: 1) in order to achieve a stable linear system described in Equation 8.11, the eigenvalues λ_i of S have to be less than one in magnitude ($|\lambda_i| < 1$) and 2) if the available options are competitive (assumed in this work) the off-diagonal elements $s_{i,j}$ have to be less than zero ($s_{i,j} < 0$ for all $i \neq j$).

The valence term, $V(t+h)$ can be described by

$$V(t+h) = CMW(t+h) \tag{8.12},$$

where the contrast matrix *C* compares the weighted evaluations of each option *MW(t)*. Its diagonal elements $c_{i,i}$ were defined by $c_{i,i} = 1$ and the off-diagonal elements by $c_{ij} = -1 \cdot (n-1)^{-1}$ for all $i \neq j$, where *n* states the number of options. The value matrix *M(t)* simulates the decision maker's subjective evaluation for each option on each attribute. *M* is a *mxn* matrix, where *m* states the number of option and *n* the number of attributes, respectively. The weight vector *W(t)* describes the weight of attention the decision maker considers for each attribute at time *t*. *W* is a vector of length *n*.

For a binary choice problem, such as considered in this work (*to tack* or *not to tack*), *P(t+h)* represents the preference of the decision maker for choosing one option over the other. A positive value of *P(t)* indicates that the sailor (decision maker) favours *to tack*, whereas a negative value of *P(t)* expresses that the other option, *not to tack* is favoured. During the deliberation time, a preference is developed and sequentially updated by the valence term, *V(t+h)*. In detail, the sailor uses objective information (e.g. current sailing state, position on racecourse, relative position of opponents) to derive his/her subjective evaluations for each option (to tack or not to tack) on each attribute (risk, distance made good), which is expressed in *M*. Consequently, the valence changes with time depending on the decision maker's attention fluctuating from one option towards the other and vice versa. The variance can be described as the decision maker's change in developing a decision from a moment to the next. Thereby, the decision maker uses environmental information as well as subjective information stored in his/her memory to evaluate options and its attributes. The sum of the elements of *V(t+h)* is always zero as a preference increase of one option comes with a preference decrease of the alternative options. A decision is derived as soon as the evolution of preferences reaches 1) a specific threshold or 2) a decision criterion for either of the two options (for more information, the reader is referred to Busemeyer (2002), Johnson (2006) and Lee (2008)). Using Equation (8.12) for a binary choice problem in a sailing environment framework yield the following linear system:

$$\begin{pmatrix} p_1(t+h) \\ p_2(t+h) \end{pmatrix} = \begin{pmatrix} s_{11} & s_{12} \\ s_{21} & s_{22} \end{pmatrix} \begin{pmatrix} p_1(t) \\ p_2(t) \end{pmatrix} + \begin{pmatrix} 1 & -1 \\ -1 & 1 \end{pmatrix} \begin{pmatrix} m^1_{Risk} & m^1_{DMG} \\ m^2_{Risk} & m^2_{DMG} \end{pmatrix} \begin{pmatrix} w_{Risk}(t) \\ w_{DMG}(t) \end{pmatrix} \tag{8.13}.$$

To specify such a linear system, one have to start with defining the relevant information dimensions in the task. Using the binary choice problem of performing a tack or not, these dimensions would be 1) *Risk* associated to the actual sailing situation and 2) *Distance Made Good* (DMG) towards the upwind mark. These individual values depend on the sailor's character and form the value matrix *M*. They can be determined by experiments, personal interviews or questionnaires for instance and are highlighted in the following Table 10. There, the cell values of a hypothetical sailor are nominated by the column's maximum to achieve an interval [0; 1].

The subsequent step deals with the definition of the attention weights w_{Risk} and w_{DMG} describing the weight/probability on each attribute at time *t*. The weight vector *W* those values are also obtainable through questionnaires for instance is defined by:

$$W(t) = \begin{pmatrix} w_{Risk}(t) \\ w_{DMG}(t) \end{pmatrix} \tag{8.14}.$$

The contrast matrix *C* for a binary choice problem forms a *2x2* matrix and is defined by:

$$C = \begin{pmatrix} 1 & -1 \\ -1 & 1 \end{pmatrix} \tag{8.15}.$$

Table 10: Attribute matrix of a binary choice problem for a hypothetical sailor

	Risk	DMG
Tack	0.6	0.8
No Tack	1	1
Importance Weight	0.3	0.7

Applying the values of Table 10 to Equation 8.12, the following momentary valances *V(t)* at any given moment with a probability of $q_{Risk} = 0.3$ is

$$V_{Risk}(t) = \begin{pmatrix} 1 & -1 \\ -1 & 1 \end{pmatrix} \cdot \begin{pmatrix} 0.6 & 0.8 \\ 1 & 1 \end{pmatrix} \cdot \begin{pmatrix} 1 \\ 0 \end{pmatrix} = \begin{pmatrix} -0.4 \\ 0.4 \end{pmatrix} \tag{8.16}$$

and with a probability of $q_{DMG} = 0.7$ is

$$V_{DMG}(t) = \begin{pmatrix} 1 & -1 \\ -1 & 1 \end{pmatrix} \cdot \begin{pmatrix} 0.6 & 0.8 \\ 1 & 1 \end{pmatrix} \cdot \begin{pmatrix} 0 \\ 1 \end{pmatrix} = \begin{pmatrix} -0.2 \\ 0.2 \end{pmatrix} \quad (8.17).$$

Depending on the actual focus of attention to *Risk* or *DMG* respectively, one of the two variances/preferences increases at the cost of the other one. Therefore, the sum of the individual valances has to be 0.

The next step deals with the calculation of the new preference state at time *t+h* that is equal to the actual focus of attention to attributes. Firstly, one of the two variances, $V_{Risk}(t)$ and $V_{DMG}(t)$ respectively, is chosen depending on the probabilistic shifts in attention and added to the previous preference state *P(t).*

As mentioned earlier, the memory effect is simulated by the stability matrix *S* that is defined by:

$$S = \begin{pmatrix} 0.9 & -0.2 \\ -0.2 & 0.9 \end{pmatrix} \quad (8.18).$$

Assuming the initial preference is defined to be $P(0) = \begin{pmatrix} 0.05 \\ 0.4 \end{pmatrix}$ telling that the sailor has an initial preference not to tack since his/her actual sailing state is lifted and the yacht is located close to a layline for instance. Hence, the sailor's attention at time *t(1)* is on *DMG* and represented as:

$$P(1) = \begin{pmatrix} 0.9 & -0.2 \\ -0.2 & 0.9 \end{pmatrix} \cdot \begin{pmatrix} 0.05 \\ 0.4 \end{pmatrix} + \begin{pmatrix} -0.2 \\ 0.2 \end{pmatrix} = \begin{pmatrix} -0.24 \\ 0.55 \end{pmatrix} \quad (8.19).$$

If attention at the next moment at time *t(2)* is still on *DMG*, then:

$$P(2) = \begin{pmatrix} 0.9 & -0.2 \\ -0.2 & 0.9 \end{pmatrix} \cdot \begin{pmatrix} -0.24 \\ 0.55 \end{pmatrix} + \begin{pmatrix} -0.2 \\ 0.2 \end{pmatrix} = \begin{pmatrix} -0.53 \\ 0.75 \end{pmatrix} \quad (8.20).$$

If attention at the next moment at time *t(3)* focuses on *Risk* due to environmental changes for instance, then:

$$P(3) = \begin{pmatrix} 0.9 & -0.2 \\ -0.2 & 0.9 \end{pmatrix} \cdot \begin{pmatrix} -0.53 \\ 0.75 \end{pmatrix} + \begin{pmatrix} -0.4 \\ 0.4 \end{pmatrix} = \begin{pmatrix} -0.83 \\ 0.98 \end{pmatrix} \quad (8.21).$$

During the deliberation process, the preferences are changing according to the sailor's attention focus. As mentioned earlier, a decision is derived as soon as the evolution of preferences reaches 1) a specific threshold or 2) a decision criterion for either of the two options. The procedure of how to derive an advanced and stable preference value in a dynamically changing environment is described in the following subchapter.

8.5 The New Decision-Making Engine of *Robo-Race*

As discussed in the previous subchapter, DFT was used to calculate the preference for each option depending on the dynamically changing environment. Subsequently, the preference value has been used to obtain the choice probability of each option by conducting various replication of the DFT process. Lee *et al.* (2008) showed the existence of a converged choice probability at time *t* for a binary choice problem by calculating the minimum amount of time steps required for stabilised preference values. In brief, Lee *et al*. (2008) proved that the difference between the expected preference value *E(P(nh))* and its converged value becomes less than ε ($\varepsilon > 0$) after *n* time steps. The following definitions were used (see Lee e*t al.* (2008) for more detail):

$$n = \frac{\log k}{\log D} \quad (8.22), \qquad D = s_{11} - s_{12} \quad (8.23), \qquad k = \frac{1-D}{\left|E(v_1(h))\right|}\varepsilon \quad (8.24),$$

and

$$E\left(v_1(h)\right) = E\left(w_1(h)(m_{11} - m_{21})\right) + E\left(w_2(h)(m_{12} - m_{22})\right) \quad (8.25).$$

Equation 8.23 represents the difference of the diagonal element s_{11} of the stability matrix S which controls the growth/decay over time of the preference for option *1* and the off-diagonal elements s_{12} represent the influence of option *1* on option *2*, meaning the effect of interaction among the options.

The following section highlights the schematic real-time decision-making algorithm using the BBN-DFT approach as part of the new developed decision-making engine of *Robo-Race*. The algorithm describes how a sailor develops his/her action depending on the environmental conditions (weather and yacht state). The following flow chart represents a schematic overview for a single yacht application (see Figure 72). A more advanced planning algorithm dealing with planning horizons that depend on the sailor's expertise level can be found in Chapter 8.7.1.

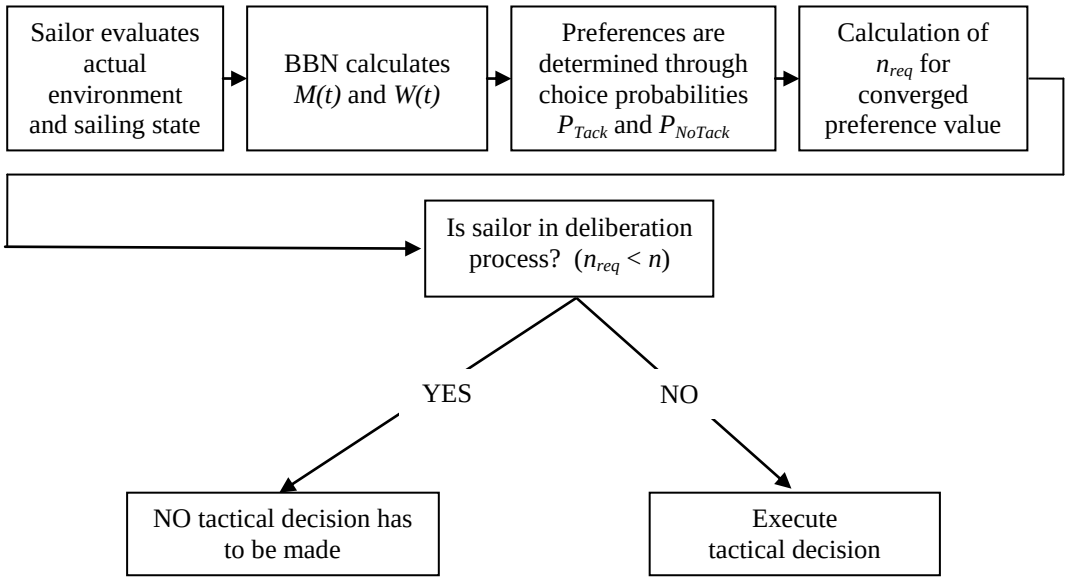

Figure 72: Flowchart showing the schematic decision-making process of a sailor racing a single yacht race.

In this work, the sailor tries to control a yacht as fast as possible on an upwind leg to the upwind mark (see Figure 72). Depending on the environmental conditions, the sailor has to find a possible way towards the upwind mark depending on his/her sailing behaviour and level of expertise (see following subchapters for more details). The lines below describe in detail how decisions were derived within this dynamically changing environment for the basic algorithm driving the decision-making engine:

1. At time *t*, the sailor evaluates the environment according to:

1) the current sailing state (lifted, neither, headed),
2) the sailing trend relative to the leg axis (towards, away-parallel),
3) the x-distance in the leg CS (close, med-far), and
4) the y-distance in the CS (close, medium, far).

2. Based on the sailor's observation skills, the BBN is used to calculate the corresponding value matrix *M(t)*, $M(t) = \begin{pmatrix} m_{Risk}^{Tack}(t) & m_{DMG}^{Tack}(t) \\ m_{Risk}^{NoTack}(t) & m_{DMG}^{NoTack}(t) \end{pmatrix}$, and weight vector *W(t)*, $W(t) = \begin{pmatrix} w_{Risk}(t) \\ w_{Time}(t) \end{pmatrix}$, where $m_{Risk}^{Tack}(t)$ describes the evaluation of the option *Tack* on the attribute *Risk* at time *t*, and $w_{Risk}(t)$ represents the weight the sailor puts on the *Risk* attribute at time *t*.
3. The sailor's preferences are determined using Equation 8.13 with *M(t)* and *W(t)* calculated in the previous step. For each option the choice probabilities P_{Tack} and P_{NoTack} are determined.
4. The number of required time steps n_{req} is calculated using Equation 8.22 to obtain a converged preference value depending on the actual environmental conditions. As long as the sailor does not notice any environmental change, the counter increases the value of *n* by one with every time step. If the sailor picks up a cue showing an environment change, the counter is reset to zero, a new value for *n* depending on the new environmental conditions is computed, and the same process starting with the first step is initialised.
5. If the sailor finds him/herself still within the deliberation process ($n < n_{req}$), no tactical action is undertaken yielding an unchanged course of the yacht.
6. The sailor repeats the above steps until 1) the number of required time steps has been reached or 2) the decision module in *Robo-Race* is set to automatic mark rounding which is initialised as soon as the yacht enters the mark zone (circle of radius of eight yacht lengths around the next mark).

The following paragraphs show examples of the successfully working BBN-DFT algorithm implemented in *Robo-Race* using the described approach above.

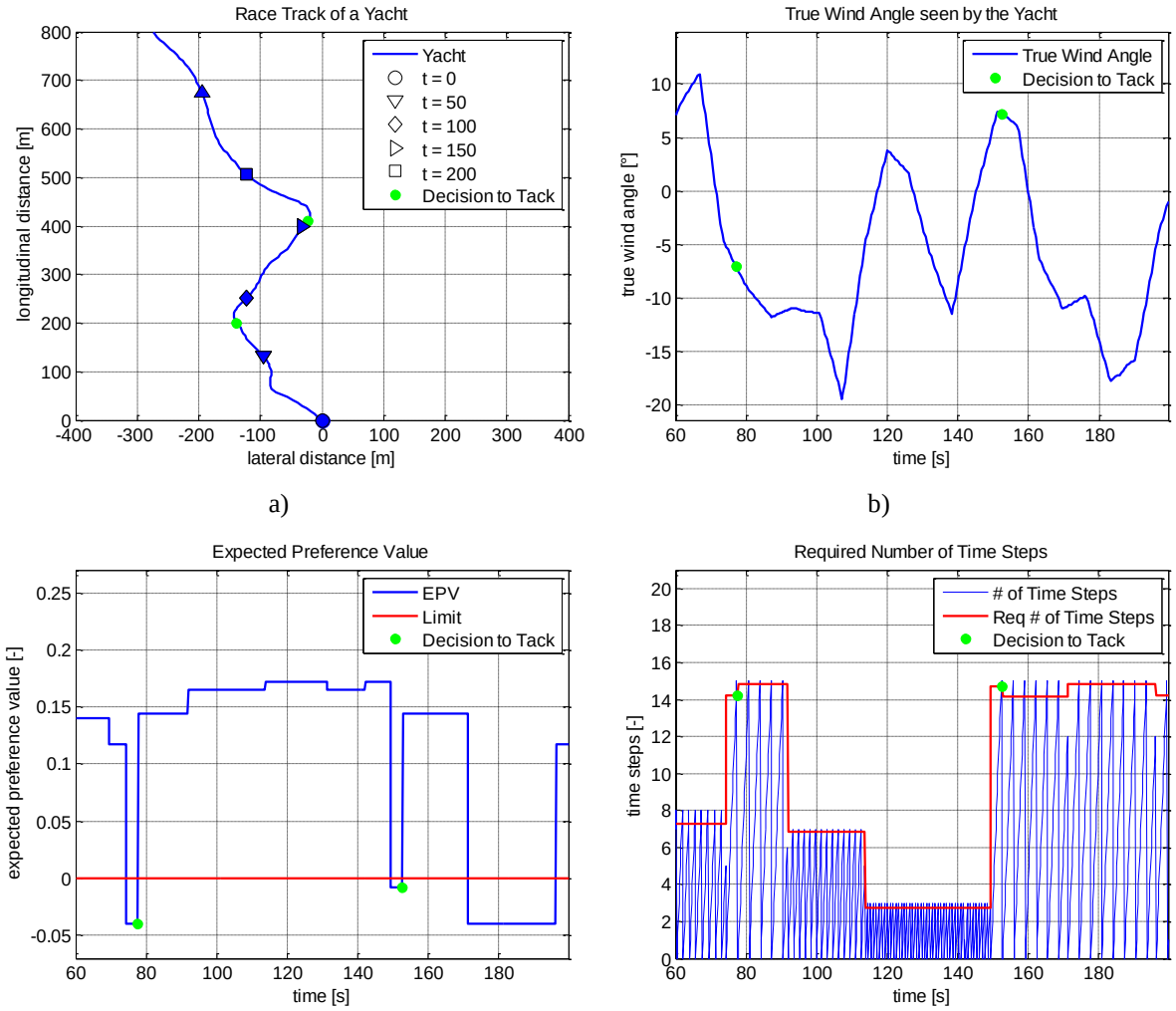

Figure 73: Case study with *Robo-Race* using the new decision-making engine showing the race track (a), the TWA (b), the expected preference values (EPV) (c), and the number of required time steps (d).

Figure 73 a, displays the yacht's track and the location of the tacking decision on the race course. The true wind angle (TWA) is shown in Figure 73 b, the expected preference value in Figure 73 c, and the number of required time steps in Figure 73 d.

As mentioned earlier, the driving forces for a decision were the spatial location of the yacht on the race course, the direction of the yacht and the wind conditions. The TWA development indicates a wind shift between t = 64 sec and t = 108 sec. Corresponding to that, the yachts state changed from lifted to neutral and finally to headed. This has a negative effect on the expected preference value (EPV) which slightly decreased for the neutral state and turned negative for the headed state. Simultaneously to these changes, the number of required time steps to reach a stabilised decision also altered. The first tacking decision was made at t = 78 sec. It is worth clarifying that a decision was made every time

the number of required time steps has been reached. Depending on the EPV the corresponding action was conducted: a positive EPV indicated no changes, whereas a negative EPV indicated the decision to tack. After a tack decision a yacht found itself in the tacking process and could not respond to any new tacking decisions. The time for performing a tack and the subsequent time for equilibrium were assumed to be 50 sec. Therefore, a yacht could not respond to another tack decision whilst completing a tack.

After the conducted tack a negative TWA value indicated a lift and a positive TWA value a header. The latter was reached at t =150 sec which resulted in a negative EPV and the decision to tack once the number of required time steps has been reached (see Figure 73 d). The next negative EPV has been calculated at t = 172 sec that was ignored since the necessary time period after a performed tack has not been reached yet.

After the successful implementation of the new decision-making engine into *Robo-Race* one wants to check its performance and the possibilities to model human behaviour in a dynamically changing yacht racing environment. Therefore, special attention has been paid to the following three aspects:

1. Change of the decision threshold value to derive a decision that affects the speed-accuracy tradeoff of a decision,
2. Change of the stability matrix values that affect the development of preferences over time that in turn affects the memory of the sailor. This feature is later used to model different levels of sailing expertise,
3. Change of the preference table values that affect different behaviour and sailing styles (the reader is referred to the following Chapter 8.6 for more information).

The following Figure 74 show the effect of two differently applied decision thresholds, where the values of *0.13* for *Yacht A* and *0.0* for *Yacht B* have been chosen (see Table 11). The necessary change in the existing algorithm was minor since just the decision thresholds were altered and the code structure itself remained untouched.

The simulation was conducted as a solo-race and therefore the yachts did not influence each other. For reasons of clarity and for a simplified analysis, the two race data were merged in Figure 74 and the actual counted time steps in Figure 74 d) have been left out.

The same procedure has been applied for the stability matrix study highlighted further below (see Figure 75).

Table 11: Decision threshold matrix *Yacht A* and *Yacht B*

	Yacht A	Yacht B
Decision Threshold	0.10	0.0

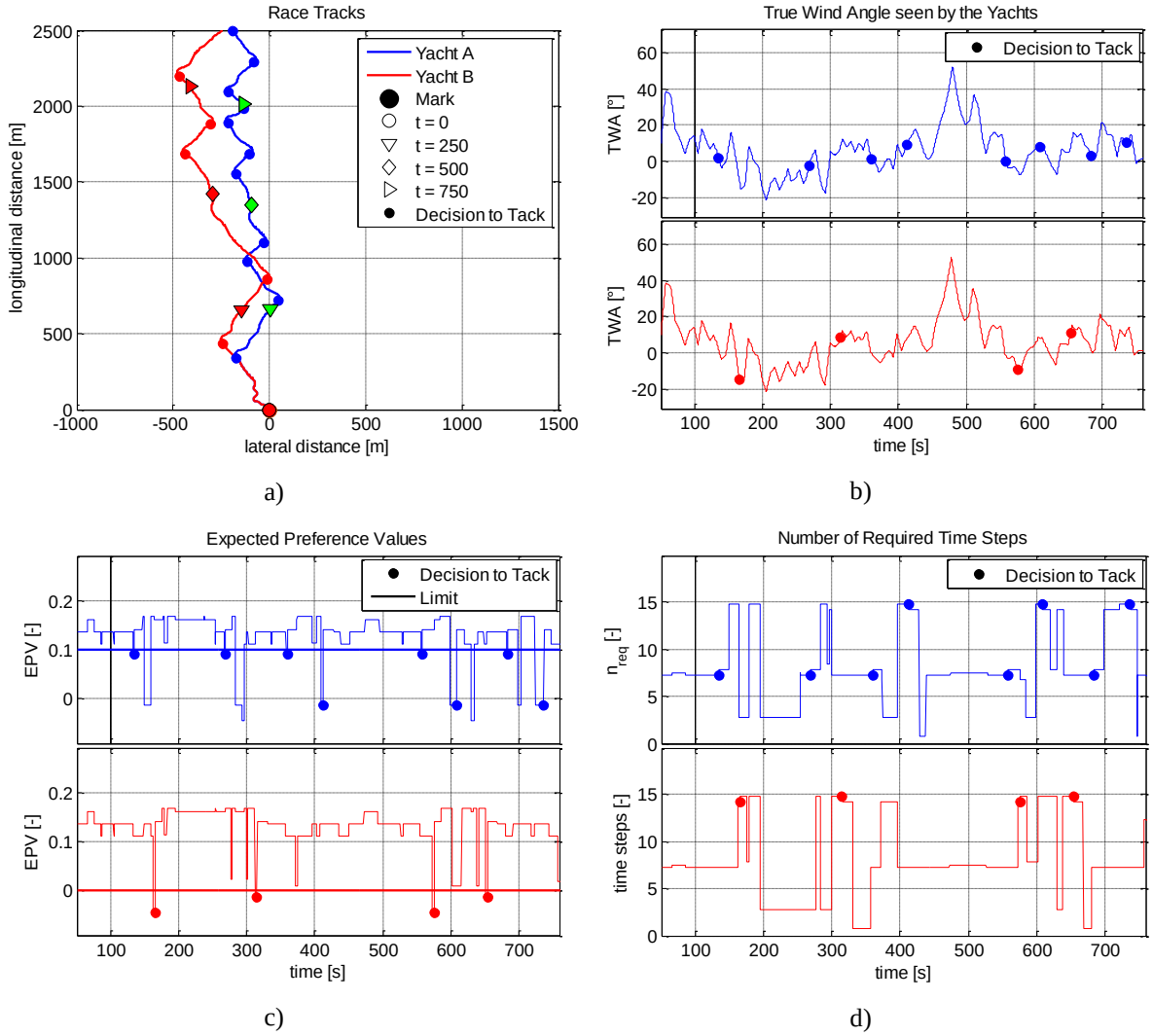

Figure 74: Decision threshold study with *Robo-Race* using the new decision-making engine showing the race track (a), the TWA (b), the expected preference values (EPV) (c), and the number of required time steps (d).

Figure 74 a, represents the race tracks of *Yacht A* and *Yacht B* showing a clear influence of the two differently applied decision thresholds. The track of *Yacht B* indicates a comfortable, more passive sailing style that can be seen in the relatively undisturbed zigzag

track. In contrast to this, *Yacht A* behaved much more actively resulting in a much more interrupted zigzag track on the upwind leg. Figure 74 b, indicates that *Yacht A* performed twice as many tacks compared to *Yacht B* (8 tacks vs. 4 tacks). This phenomenon can be explained by having a closer look to Figure 74 c, showing the EPV development over time and the applied decision thresholds. The crews of the two yachts scan and proceed the environmental information in the same way which can be seen by the identical development of the EPV values before *Yacht A* performed the first tack at t = 134.80 sec (Figure 74 c). After this event *Yacht A* and *Yacht B* did not share the same spatial position anymore and therefore, the EPV values are not identical but they still share the same characteristics.

Figure 74 c, shows the effect of the increased decision threshold of *Yacht A* resulting in quicker and more impulsive decisions of *Yacht A* compared to *Yacht B*. There, the rise of the decision threshold simulated an increase of time-pressure and simultaneously a reduced amount of information necessary to make a decision. This phenomenon can be seen by comparing the number of performed tacks of *Yacht A* and *Yacht B*. Therefore, the effect of time pressure and the related phenomenon of speed-accuracy tradeoff can be easily and successfully modelled by altering the decision threshold in a DFT-framework (Diederich, 2003 and Johnson, 2006).

Now, one wants to change the cell values of the stability matrix *S* to simulate the change over time of preferences that in turn affects the memory of the sailor (see Equation 8.11). Therefore, two yachts, *Yacht A* and *Yacht B*, were set up featuring two differently applied diagonal values of the stability matrix that can be seen in the following Table 12. Similar to the change of the decision threshold values, just the cell values of the stability matrix have been altered whereas the code structure itself remained untouched.

Table 12: Stability matrix for *Yacht A* and *Yacht B*

	Yacht A	Yacht B
s_{11}, s_{22}	0.50	0.90
s_{12}, s_{21}	-0.01	-0.01

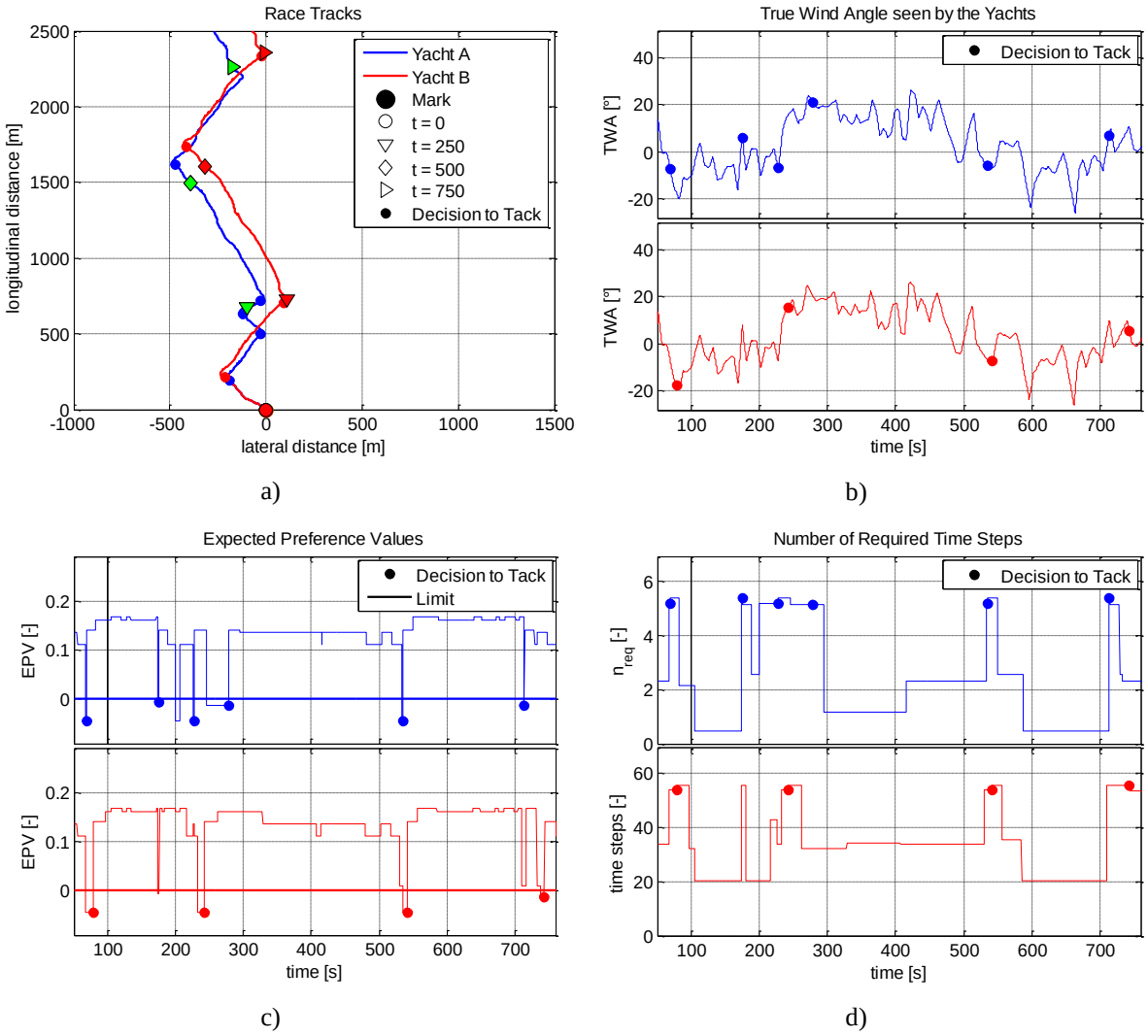

Figure 75: Stability matrix study with *Robo-Race* using the new decision-making engine showing the race track (a), the TWA (b), the expected preference values (EPV) (c), and the number of required time steps (d).

Figure 75 a, highlights the race tracks of *Yacht A* and *Yacht B* showing the effect of the differently applied diagonal values s_{11} and s_{22} of the stability matrix *S*. The track of *Yacht A* shows a more active and quicker sailing style resulting in a more interrupted zigzag track. *Yacht B* in contrast indicates a more confident and calmer sailing style that can be seen in the relatively undisturbed zigzag track. Figure 75 b, indicates that *Yacht B* performed two tacks less than *Yacht A* during the time period of 50 sec to 750 sec (*Yacht A*: 6 tacks vs. *Yacht B*: 4 tacks). This phenomenon can be explained by the number of required time steps which can be found in Table 75c. Due to the fact that *Yacht A* needs up to around 6 time steps to make a decision compared to *Yacht B* that needs around 20 and 60 time steps to decide, *Yacht A*'s crew acts faster and therefore less accurate than the one of *Yacht B*. The quicker decay of previously attended information is modelled by lower s_{11} and s_{22} values

that in turn affect the necessary number of required time steps to make a decision (see Equations 8.22 – 8.24). Consequently, this type of decision is faster but not more accurate nor more sustainable than the one where higher diagonal values have been chosen. For instance, *Yacht B* took more time to make a decision that led to more accurate but slower decisions.

Now, one wants to have a closer look at the first and second tacks of the yachts. *Yacht A* tacks first whereas *Yacht B* needs more information and time to decide leading to a slightly more unfavoured position compared to *Yacht A*. Contrary to that, this type of behaviour prevented her to tack around t = 180 sec since the necessary information to come to a decision, hence the number of required time steps has not been reached. The subsequent weather change forced a reset of the decision-making process and the counter since a new environmental situation emerged. The faster acting *Yacht A* tacked in this situation since the number of required time steps has been reached. The subsequent second weather change forced her to tack again that resulted in the two additional tacks and an unfavoured spatial position compared to *Yacht B*.

Applying higher diagonal values s_{11} and s_{22} of the stability matrix S let to a longer lasting deliberation process and more accurate decisions where the latter represents an important feature of decisions made by experts. The second aspect of expert decisions is speed, meaning the required time to make a decision. This requirement has been realised in Chapter 8.7.1 where a real time planner is used to speed up the deliberation process by looking numerically into the future. The option of applying lower s_{11} and s_{22} values has been refuted for modelling expert decisions since this setup leads to faster but more inaccurate decisions that characterises decisions made by novices and not the one made by experts. Consequently, this fact has been used and applied to the decision-making engine of *Robo-Race* to model the sailing behaviour of novices (see Chapter 8.7).

The effects of speed-accuracy or the influence of preferences over time affecting the memory of sailors and the resulting decision can be easily modelled by changing the corresponding values in the code whereas its structure remains untouched. Realising the same effects just using a rule-based approach would come with a time intensive extension of the existing code since all possible race situations and the related decision outcomes have to be thought of and coded in advance. Therefore, the fine-tuning for a speed-accuracy study would be possible but very time intensive whereas modelling the human

deliberation process is not possible with a rule-based approach since it only deals with decision outcomes and not its derivation. For instance, the derivation of a decision and the consequences could be seen in the second example above where *Yacht B* did not tack since the necessary amount of information has not been reached. To reach this level of detail just using a rule-based approach would be impossible since this approach does not offer an access to the derivation of a decision.

The third described change, the modification of the probabilistic tables of the BBN can be directly made and affects the perceptual processor of the decision maker. This philosophy of modification was used to model individual sailing behaviours that will be explained in detail in the following Chapter 8.6.

8.6 Three Different Sailing Behaviours on the Race Course

8.6.1 Development of Three Different Sailing Behaviours

As mentioned earlier, three different sailing behaviours/styles have been developed for the new decision-making engine of *Robo-Race*, such as

1. risky behaviour leading to a passive sailing style,
2. safe behaviour leading to an active sailing style, and
3. balanced behaviour leading to a deliberate sailing style.

The first, the risky behaviour can be also characterised as passive since the sailor does not react to every environmental change. He/she tries to save time by avoiding tacks, also stays longer on a tack and tries to exceed the limits without missing the next mark.

The second, the safe behaviour can be also described as active since the sailor is prone to respond to every environmental change. His/her first priority is to make it safe to the next mark. Hence, he/she prefers to tack to be on the safe side of the course, meaning the lifted tack. Consequently, the safe sailor does not care too much about the extra time cost caused by a tack. This behaviour yields an active sailing style without exceeding the limits.

The third and last developed behaviour, the balanced behaviour can be considered as a combination of the risky and safe behaviours. It tries to combine the advantages of the

other two leading to a deliberate sailing style. Hence, the sailor reacts carefully to environmental changes, meaning that he/she does not only try to avoid unnecessary actions but also tries to avoid exceeding the limits.

The realisation of the three behaviours has been done by

1. changing the probability tables used by the BBN and,
2. changing the spatial limits and therefore the individual cognitive ability of the sailor.

The following Table 14 shows extracts of important changes made in the probability tables used by the *Weight-Risk* node of the BBN. To keep the altered parameters as little as possible, just the *Risk* and *Weight-Risk* tables have been changed, whereas the *DMG* tables remained the same for all three behaviour types. Furthermore, the following basic rule has been applied for the creation of the different characters of the sailors: The balanced behaviour was considered as the starting point and the risky and active behaviour numbers have been changed by +/- 0.1 where applicable. The entire set of tables has been developed with international experienced sailors and can be found in the Appendix A3.

Table 13: Extract of used BBN probability tables for the Weight-Risk node

Weight-Risk													
P(currentSailing State)	P(Leg CS-Distance x)	P(Leg CS-Distance y)	balanced				safe				risky		
P_cSS_lifted	P_LDx_close	P_LDy_close	0.2	0.4	0.4		0.2	0.4	0.4		0	0.2	0.8
P_cSS_lifted	P_LDx_close	P_LDy_medfar	0	0.2	0.8		0	0.2	0.8		0	0	1
P_cSS_lifted	P_LDx_medfar	P_LDy_close	0.6	0.4	0		0.6	0.4	0		0	0.5	0.5
P_cSS_lifted	P_LDx_medfar	P_LDy_medfar	0	0.3	0.7		0.2	0.4	0.4		0	0	1
P_cSS_neither	P_LDx_close	P_LDy_close	0.7	0.3	0		0.7	0.3	0		0.6	0.4	0
P_cSS_neither	P_LDx_close	P_LDy_medfar	0.3	0.5	0.2		0.2	0.5	0.3		0	0	1
P_cSS_neither	P_LDx_medfar	P_LDy_close	0.8	0.2	0		0.8	0.2	0		0	0.3	0.7
P_cSS_neither	P_LDx_medfar	P_LDy_medfar	0.7	0.3	0		0.7	0.3	0		0.4	0.6	0
P_cSS_headed	P_LDx_close	P_LDy_close	0.8	0.2	0		0.8	0.2	0		0.7	0.3	0
P_cSS_headed	P_LDx_close	P_LDy_medfar	0.3	0.4	0.3		0.4	0.4	0.2		0.1	0.1	0.8
P_cSS_headed	P_LDx_medfar	P_LDy_close	0.9	0.1	0		0.9	0.1	0		0.4	0.6	0
P_cSS_headed	P_LDx_medfar	P_LDy_medfar	0.9	0.1	0		0.9	0.1	0		0.5	0.5	0

By changing the BBN probabilistic tables, the preferences of the sailor for one option over the other (to tack or not to tack) could be influenced. Thereby, the sailor's objective information was used differently to derive a subjective evaluation for each option on each attribute (*Risk*, *DMG*). These preferences could be further influenced by changing the

weight vector to strengthen or weaken the weight of attention the sailor considered for each attribute on a given spatial and environmental state.

The second change was of spatial nature whereby the individual cognitive behaviour of the sailor has been altered. During the decision-making process, the environment was constantly checked by the sailor, which was modelled by the BBN as the perceptual processor. The subjective opinion of where the yacht was actually located on the race course could alter individually. Therefore, a sailor with a risky attitude would consider him-/herself at a *close distance x* away from the leg coordinate system whereas a safe or deliberate sailor would judge the same situation as *medium, far distance x*. Hence the risky sailor acts differently at the same local position as a safe or deliberate sailor would do. The same scenario applied when judging *Distance y* on the leg coordinate system.

The individual spatial cognitive attitude of the three different sailing styles/behaviours was realised by a cone-shaped geometry (see Figure 76). Depending on the behaviour of the sailor the cone featured different radii, where the cone used for the risky setup featured the largest, the safe setup the smallest and the deliberate setup a radius between the two. Table 14 and Figure 76 below describe and illustrate the definition of the cones. Furthermore, not only the direction in x-direction but also the y-direction has been altered for the three behaviour setups.

Table 14: Dimension of the safety zone setup depending on the sailing behaviour

	Risky	Balanced	Safe
Radius top [m]	175	175	175
Radius bottom [m]	550	925	1100
Begin of top zone (distance y – close)	0.70	0.65	0.60

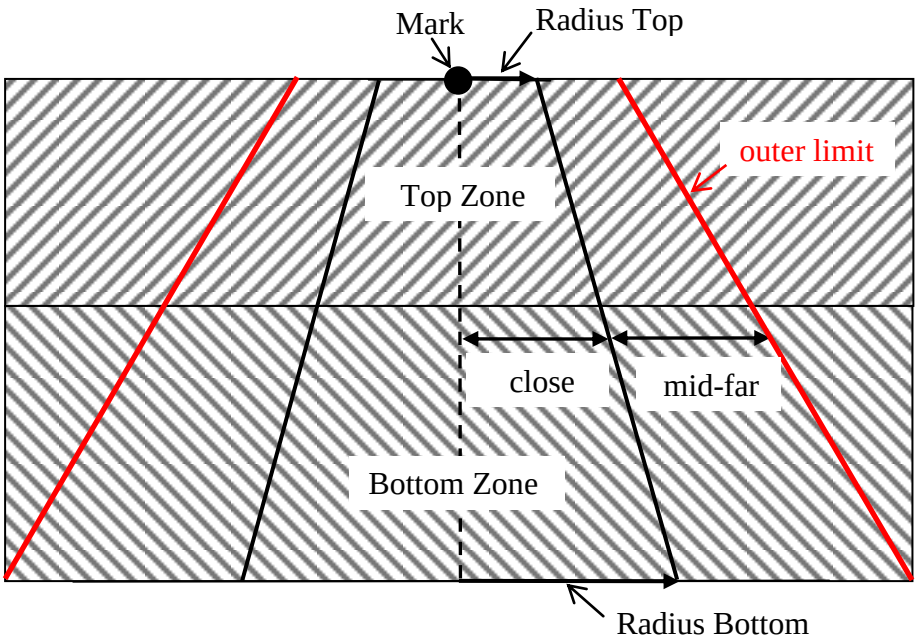

Figure 76: Applied safety zone setup and nomenclature on the race course

The following race to the upwind mark was set up to demonstrate 1) the effect of the modified BBN probability tables and 2) the different cognitive spatial behaviour of the sailors. The individual races have been conducted as solo races without any influences from the opponents and added together for the analysis. The following Figures 77 a – d) display the race tracks, the corresponding true wind angles, the expected preference values and the number of required time steps to obtain a converged EPV.

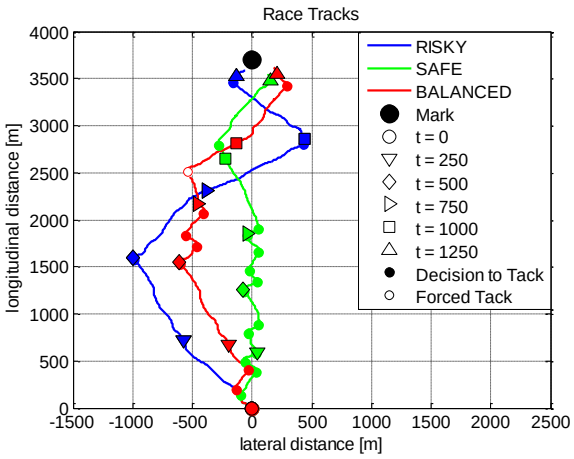

a)

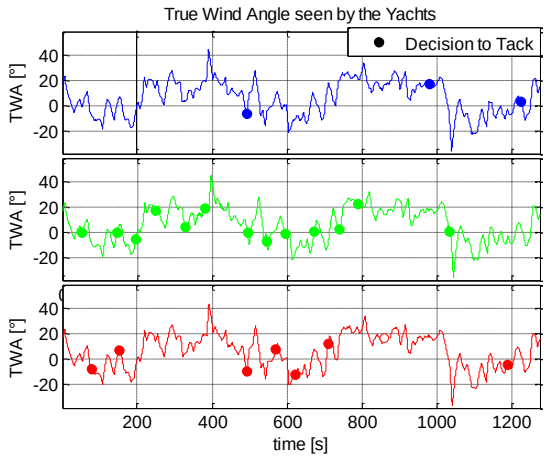

b)

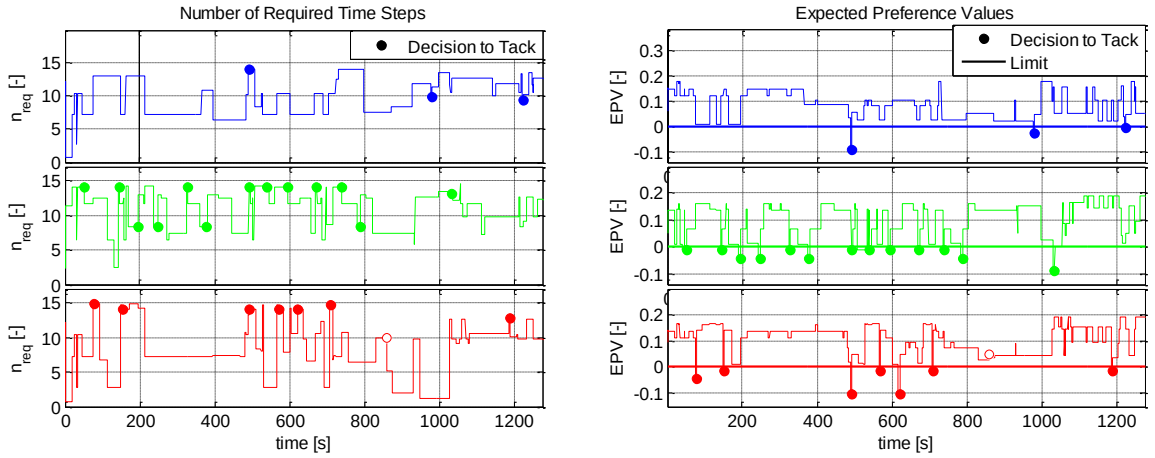

c) d)

Figure 77: Race tracks of behavioural race setup with three yachts (a), the corresponding true wind angles (b), the expected preference values (c), and the number of required time steps to obtain a converged EPV (d).

Figure 77 a, shows three different race tracks with a distinctive signature for every sailing behaviour setup. The track of the risky behaviour indicated a passive sailing style which resulted in an undisturbed clear track with three performed tacks on the upwind leg. The safe behaviour resulted in an active sailing style which can be seen by the interrupted zigzag track with a high number of tacks (13). The balanced behaviour can be considered as a good mixture of both behaviours which can be observed by the race track and the number of performed tacks (8).

The different performances of the sailors can be explained by the different individual use of the available environmental and spatial information. This led to a subjective evaluation for each option on each attribute which in return yield different EPVs which can be clearly observed when analysing the EPV history of the risky and safe sailors for the first 400 sec of the race. The one of the risky sailor showed the characteristic of a sailor who was comfortable with the actual race situation (EPV > 0) and did not see any need to execute a tack. Contrary to that, the sailor featuring the safe behaviour felt quite uncomfortable in a couple of race situations and performed six tacks in the same time period. The balanced sailor was also not pleased with the situation at the first 200 sec of the race and performed two tacks but felt comfortable afterwards. These trends were also observed for the rest of the race whereas the balanced sailor was forced to tack at t = 860 sec since an outer boundary was hit.

Table 15: Results of behavioural race setup

	Risky	Safe	Balanced
Total Race Time [s]	1449	1424.4	1431.6
T zone entrance [s]	1255.6	1276.2	1276
T mark rounding [s]	193.4	148.2	155.6
# of Tacks	5	14	6

It is also worth pointing out that the balanced and safe yachts were best positioned when entering the mark rounding zone. The risky yacht was worse positioned and needed an extra tack which had a negative effect on the mark rounding time (see Table 15).

8.6.2 Sensitivity Studies of Sailing Behaviour Setups

This subchapter investigates the consequences of different sailing behaviours and styles on the race course. Therefore, the above mentioned styles, such as 1) risky, 2) safe and 3) balanced have been used. To keep the changes as little as possible, just one environmental condition, the weather, has been altered, whereas any opponent yachts have not been considered at this stage. Consequently, the basic BBN was set up leading the yacht to concentrate on her spatial position as well as on the changing weather conditions.

The following simulations can be considered as individual solo races since no yacht interaction, blanketing parameters and racing rules have been applied. All three yachts started at identical positions and raced to the upwind mark. The corresponding total race time (TRT) and various other features mentioned below have been recorded. They were used to investigate the decision-making process of different sailing behaviours and styles and their effects on the race course.

Therefore, additionally to the three behaviour styles

- Four different weather scenarios, such as 1) normal, 2) calm, 3) stormy, and 4) variable have been randomly generated and used for the weather engine. Each scenario contained 50 different weather series leading to 200 different weather environments in total.
- These 200 weather series have been used on three different starting positions leading to 600 races in total. The starting positions (SP) have been organised as follows:

Table 16: Starting positions

	SP I	SP II	SP III
x-value	-250	0	250
y-value	0	0	0

The races have been analysed by using following parameters:

- The *ranking*, e.g. how often a yacht became 1st, 2nd, and 3rd.
- The *averaged ranking* calculated by using all 50 races whereas a 1st place counted one point, a 2nd place two and a 3rd place three points.
- The *total race time* including the mark rounding time (see Chapter 8.2.3 for more information).
- The *T zone entrance* meaning the time the yacht entered the mark rounding zone (see Chapter 8.2.3 for more information).
- The *T mark rounding* describing the time the yacht needed for rounding the mark (see Chapter 8.2.3 for more information). In this subchapter here, a unique mark rounding expertise of level two has been applied.
- The *number of executed tacks* averaged over 50 races.
- The *amount of hit outer limit boundaries* also averaged over 50 races.

The following Figures 78 a - d) illustrate typical race tracks of the three applied behaviours sailing in four different weather scenarios. The starting position II has been chosen for this illustration.

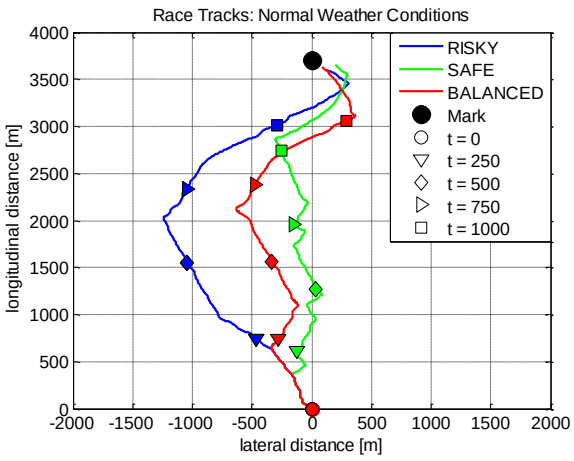

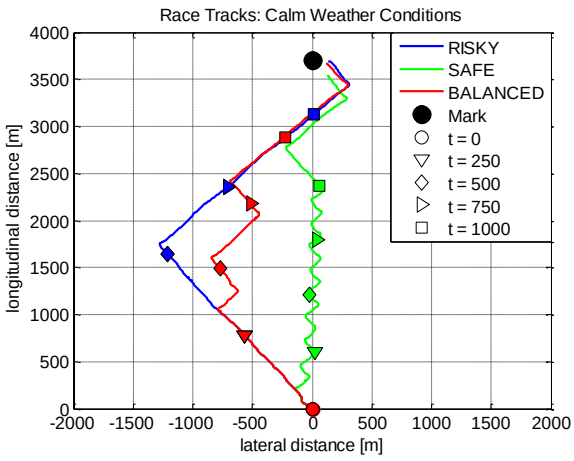

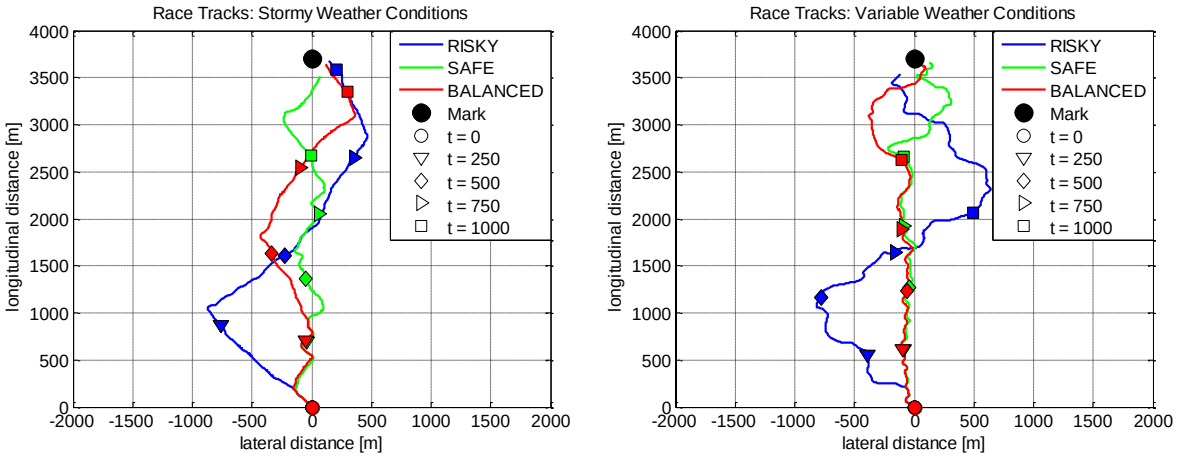

Figure 78: Typical race tracks of behavioural race setup in normal (a), calm (b), stormy (c), and variable (d) weather conditions

Table 17 displays the averaged results of all races conducted in the four different weather scenarios. A detailed description of the runs and the corresponding analysis can be found in Appendix A4.

Table 17: Averaged results of all behavioural races

	Averaged Results over all Weather Setups		
	Behaviour		
Ranking	Risky	Safe	Balanced
1st	40%	14%	46%
2nd	33%	25%	42%
3rd	27%	62%	11%
Avg. Race Time [s]	1419.6	1495	1405.7
Avg. Ranking	1.87	2.48	1.65
T zone entrance [s]	1259.1	1341.6	1256.1
T mark rounding [s]	160.5	153.4	149.6
# of Tacks	3.1	14.6	8
# of Limit	0.4	0	0.3

The best overall performance was achieved by the balanced behaviour that collected the most 1st places (46% won races) and the least 3rd places (11% lost races) leading to an average ranking of 1.65. The second best result was achieved by the risky yacht that won 40% and lost 27% of the races leading to an average ranking of 1.87. The worst average ranking with 2.48 and therefore the worst overall performance was achieved by the safe setup that won just 14% and lost 62% of the races.

This superiority of the balanced yacht was also observed in the fastest averaged total race time of 1405.7 sec which was the fastest of all three, followed by the risky yacht with 1419.6 sec and finished by the safe yacht which needed 1495.0 sec in average.

It is worth pointing out that the risky setup performed the least tacks (3.1 per race), hit the outer limit the most and needed the longest for rounding the mark. These three facts were linked together and can be explained by incapability of the sailor to sail a perfect line towards the mark. This was caused by the fact that the yacht hit the outer boundaries several times which in turn resulted in a bad positioned yacht and unfavourable angles when entering the mark rounding zones and therefore higher more rounding times.

In contrast to the risky behaviour, the safe behaviour had the least amount of hit outer boundaries but the highest number of tacks (14.6 per race) which had a negative effect on the race time. Due to the high number of executed tacks, she was the best positioned yacht when entering the mark zone leading to the lowest mark rounding times of all yachts.

The analysis of the results of all performed simulations of this subchapter demonstrates that the balanced behaviour can be described as a good balanced and effective mixture of the safe and risky sailing behaviours leading to the best performing yacht (the detailed analysis can be found in Appendix A4). The number of performed tacks (8.0 per race) and the mark rounding times were between the one of the risky and safe behaviours. Compared to the other two behaviours she found a good balance between the number of performed tacks and distance made good which classifies a deliberated sailing style.

8.7 Development of Three Different Levels of Expertise

In this work, a skilled sailor featured a planning horizon of one, meaning that he/she reacted immediately after the deliberation process have been finished. The other two sailor types, the intermediate and expert, were able to pick up environmental cues allowing them to read and judge the future weather conditions. The intermediate sailor was equipped with a planning horizon of two, meaning that he/she was capable to judge the yacht's sailing state for the next 30 sec. For the expert sailor, the planning horizon was further extended to three, meaning that the sailor could read the weather conditions for the following 60 sec.

The actions according to the individual planning horizons can be found in the following subchapter.

8.7.1 Real-Time Planner

This section highlights the real-time planning algorithm implemented into the decision-making engine of *Robo-Race*. The algorithm describes 1) how a sailor developed his/her action and 2) came up with a possible future plan depending on the individual planning horizon. This plan was created dynamically based on actual and future environmental conditions (weather and opponents) until the planning horizon limits have been reached. Consequently, the algorithm performs differently for the three types of sailor depending on his/her sailing expertise. The following flow chart in Figure 79 represents a schematic overview for a yacht fleet racing application whereas Figure 80 shows more detailed information of the algorithm architecture used to drive the decision-making engine in *Robo-Race*:

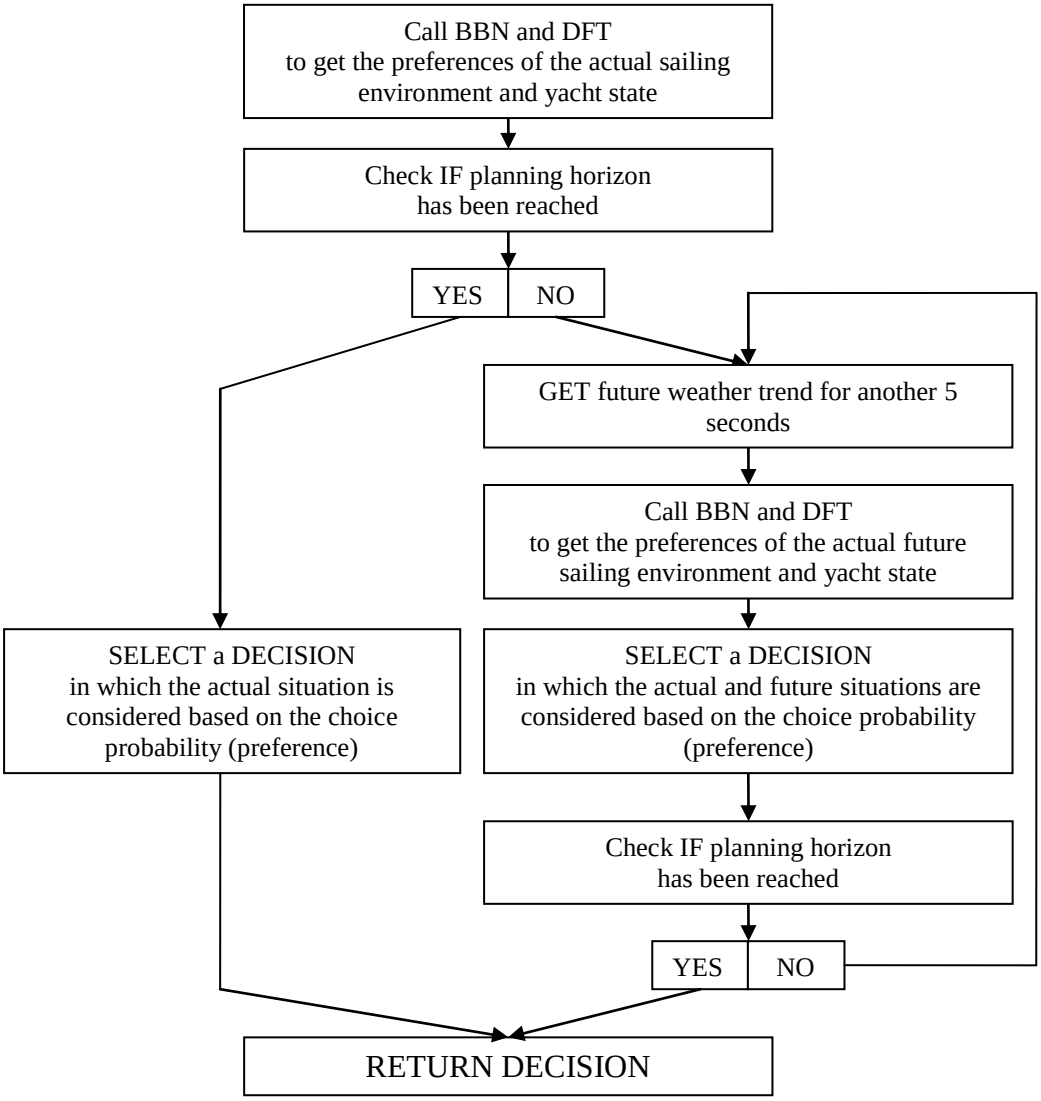

Figure 79: Flowchart showing the schematic decision-making process used within the decision engine in *Robo-Race*.

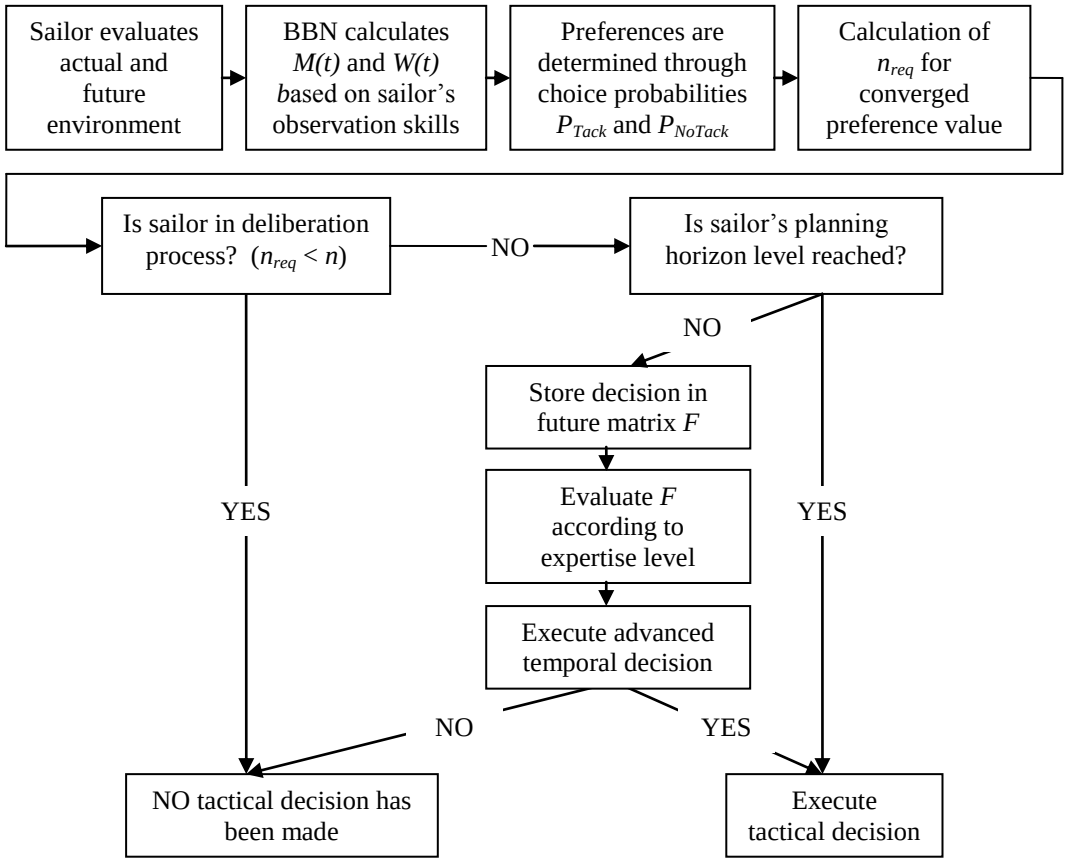

Figure 80: Flowchart showing the decision-making process of a sailor in detail

In this work, the sailor tries to control a yacht as fast as possible on an upwind leg to the upwind mark (Mark2). Depending on the environmental conditions, the sailor has to find the fastest way towards the upwind mark. The following lines describe in detail how decisions were derived within this dynamically changing environment and highlight the corresponding process and plan, respectively:

1. At time *t*, the sailor evaluates the environment according to 1) the current sailing state (lifted, neither, headed), 2) the sailing trend relative to the leg axis (towards, away-parallel), 3) the x-distance in the leg CS (close, med-far), and 4) the y-distance in the CS (close, medium, far). Depending on the perceptual processor level, the evaluation might be extended by 5) the wake option (I am in opponents wake, neither, hardest opponent is in my wake), 6) the relative position of the hardest opponent (ahead, behind), and 7) his/her distance from the sailor yacht (close, med-far).

2. Based on the sailor's observation skills, the BBN is used to calculate the corresponding value matrix *M(t)*, $M(t) = \begin{pmatrix} m_{Risk}^{Tack}(t) & m_{DMG}^{Tack}(t) \\ m_{Risk}^{NoTack}(t) & m_{DMG}^{NoTack}(t) \end{pmatrix}$, and weight vector *W(t)*, $W(t) = \begin{pmatrix} w_{Risk}(t) \\ w_{Time}(t) \end{pmatrix}$, where $m_{Risk}^{Tack}(t)$ describes the evaluation of the option *Tack* on the attribute *Risk* at time *t*, and $w_{Risk}(t)$ represents the weight the sailor puts on the *Risk* attribute at time *t*.
3. The sailor's preferences are determined using Equation 8.13 with *M(t)* and *W(t)* calculated in the previous step. For each option the choice probabilities P_{Tack} and P_{NoTack} are determined.
4. The required number of time steps n_{req} to obtain a converged preference value depending on the actual environmental conditions is calculated using Equation 8.22. As long as the sailor does not notice any environmental change, the counter increases the value of *n* by one with every time step. If the sailor picks up a cue showing an environment change, the counter is reset to zero, a new value for *n* depending on the new environmental conditions is computed, and the same process starting with Step 1 is initialised.
5. If the sailor finds him/herself still within the deliberation process ($n < n_{req}$), no tactical action is undertaken yielding an unchanged course of the yacht.
6. Depending on the planning horizon of the sailor, steps 1 to 5 were repeated every 5 seconds meaning that the sailor checks the future environment in 5 second intervals. The corresponding potential decisions are stored in F (vector of length 60*(planning horizon+1)$^{-1}$, depending on the fact whether the available planning horizon has been provided sufficient time to derive a decision or not.
7. The future vector F is evaluated by the sailor and according actions are undertaken. For example, if F looks like F = [NT_0, NT_5, NT_{10}, NT_{15}, NT_{20}, NT_{25}, NT_{30}, NT_{35}, NT_{40}, NT_{45}, NT_{50}, NT_{55}, NT_{60}], the expert sailor would prefer not to tack at time = 10 sec and 30 sec as the loss of time during the tack would not compensate the little DMG gain between the tacks. Alternatively, if the yacht is actually headed and F indicates a tack at time = 10 sec the sailor would rather tack now giving him/her an advantage over his/her opponents.
8. The sailor repeats the above steps until 1) the number of planning horizon has been reached or 2) the decision module in *Robo-Race* is set to automatic mark rounding

which is initialised as soon as the yacht enters the mark zone (circle of radius of eight yacht lengths around the next mark) which will be explained in the following subchapters.

Experiments conducted by Araújo *et al.* (2005) regarding the available environmental information pick up process of novices and experts shows considerable similarities in the visual scanning process, but differently applied weighting distributions on the perceptual variables. Furthermore, experts were more confident and comfortable in making a decision and executing a task since it is assumed that the right decision is recalled from decisions and perceptual information based on memory stored in knowledge patterns (Starkes *et al.*, 2003). This fact the higher the level of expertise the more confident the decision maker becomes based on extensive knowledge and memory has been simulated by adjusting the stability matrix *S*. It controls the memory effect and affects the number of required time steps for a converged expected preference value. The following setup of *S* has been used:

Table 18: Stability matrix depending on sailing expertise

	Novice	Intermediate	Expert
s_{11}, s_{22}	0.75	0.80	0.85
s_{12}, s_{21}	-0.01	-0.01	-0.01

The higher the s_{ii} value the higher the number of required time steps become (see Figure 81 c). This postponing of a decision had a positive effect on the confidence of the decision maker making the decision which was also observed in the studies of Araújo *et al.* (2005) and Starkes *et al.*, (2003).

The following Figures 81 a) – d) show the results of a race to the upwind mark with three participating yachts. To concentrate on the effect of the real time planner and the modifications of the stability matrix, the races were conducted as solo races and added together for the analysis. Hence no yacht interaction was involved in these races. The following three levels of sailing expertise have been set up and investigated: skilled, intermediate, and expert.

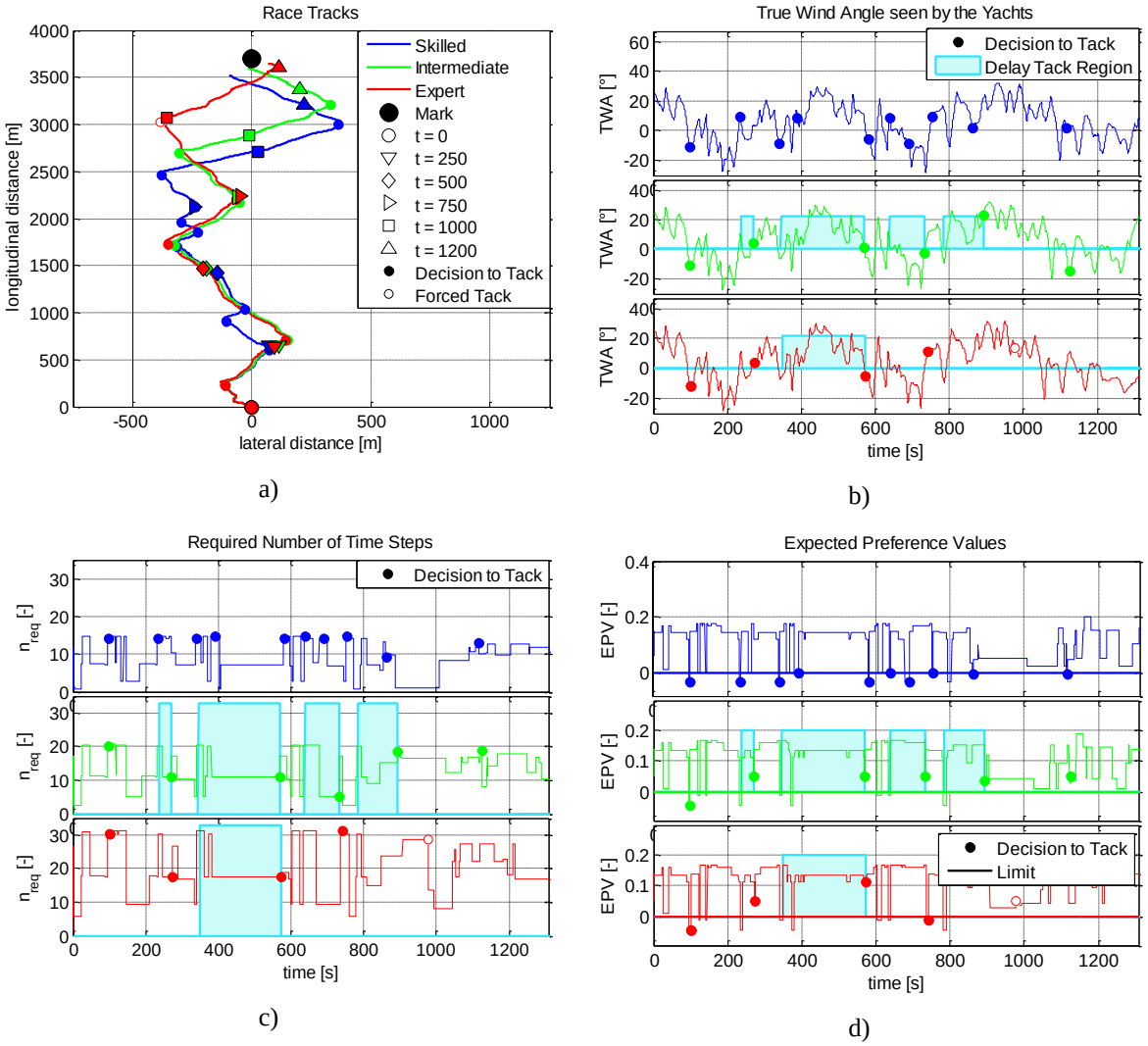

Figure 81: Race featuring different levels of expertise of the sailors showing the race track (a), the TWA (b), the number of required time steps (c), and the expected preference values (d).

Figure 81 a) represents three different race tracks where the one of the higher experienced sailors and the skilled sailor indicated remarkable differences. The tracks of the intermediate and expert sailors were almost identical for the first ¾ of the race with advantages for the expert sailor. These little advantages resulted from his/her ability to postpone the first two tacks by a few seconds compared to the intermediate sailor which had a positive effect on the race time. It is worth pointing out that the intermediate sailor had four delayed tack regions and the expert sailor just one. This can be explained by the expert's ability to overview the following 60 sec which filtered potential tack decisions in the near future in advance. During a delay tack period of the intermediate the averaged EPV for the following 30 sec has been calculated and constantly compared to the actual EPV value. As soon as the situation worsened (EPV averaged over 30 sec less than EPV

actual) the postponed tack will be performed. This situation occurred at t = 474 sec, t = 747 sec, and t = 881 sec. The experts abilities prevented him/her to perform a tack around t = 900 sec. He/she stayed on the tack until the outer limit was hit and performed a forced tack afterwards (see red circle without filling in Figures 82 a) – d). This resulted in a big advantage for the expert and was the key to win this race.

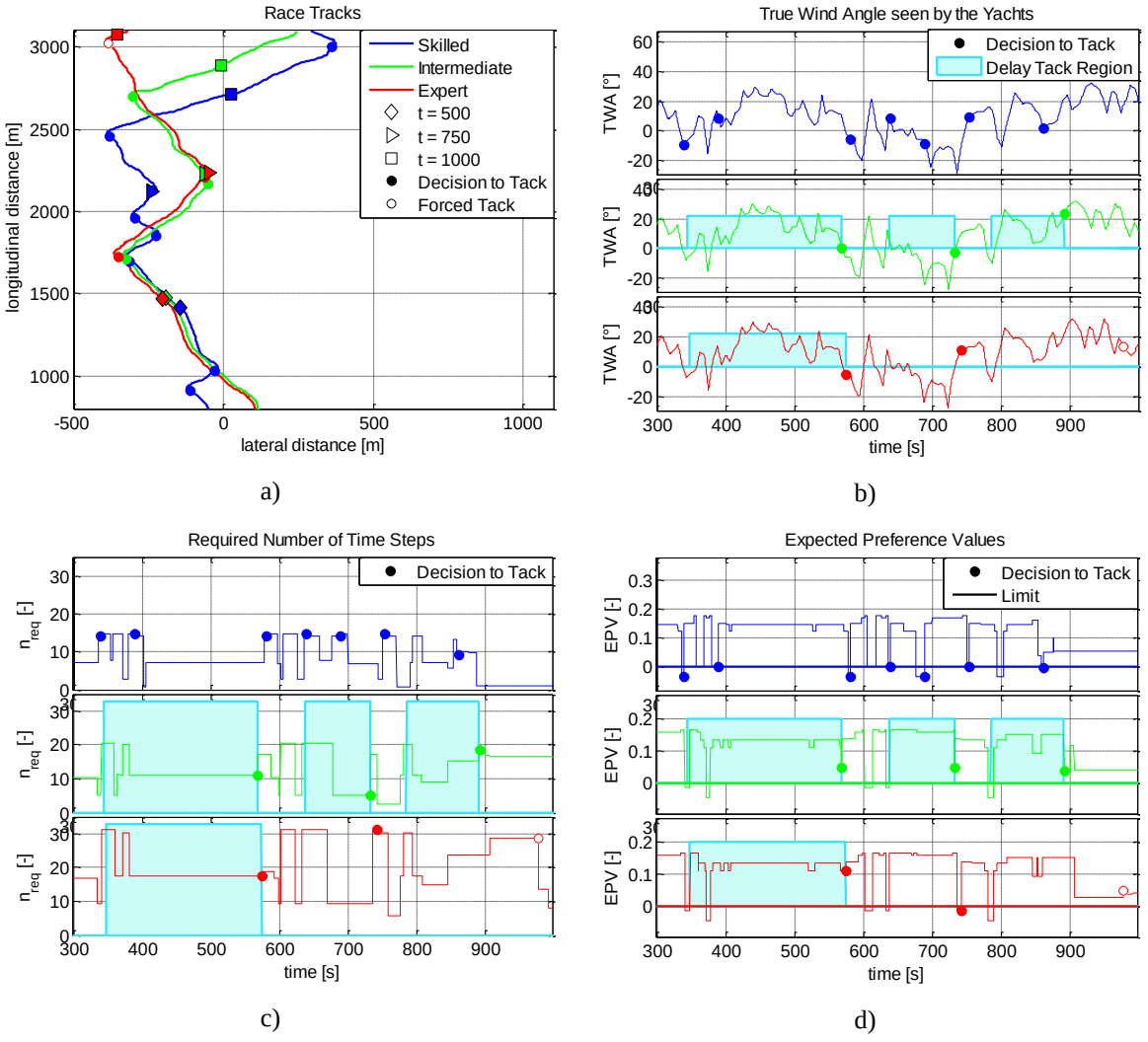

Figure 82: Detailed view of race featuring different levels of expertise of the sailors showing the race track (a), the TWA (b), the number of required time steps (c), and the expected preference values (d).

The following table shows the race times and the number of executed tacks. (A detailed explanation of the derivation and definition of the different race times can be found in the following subchapter 8.7.2).

Table 19: Race times of an expertise dependent sailor setup

	Skilled	Intermediate	Expert
Avg. Race Time [s]	1478.8	1407.4	1393.8
T zone entrance [s]	1310.2	1258	1202.2
T mark rounding [s]	168.6	149.4	191.6
# of Tacks	12	8	8
# of Limit	0	0	0

Table 19 shows a clear superiority of the expert sailor over the two other sailors and a superiority of the intermediate over the skilled sailor which can be seen when analysing the race times. The superiority of a higher expertise levelled sailor over lower ones and the observation that the higher the level of expertise the lower the number of performed tacks became were in very good agreement to studies conducted by Araújo *et al.* (2005). Furthermore, it indicated that the higher the expertise level of the sailor became the more comfortable and confident they felt making the decisions. These facts will be further investigated and discussed at the end of this chapter.

8.7.2 Evolutionary Steps towards a Superior Simulator Setup

The previous Chapters 8.6 und 8.7.1 delivered interesting and promising results indicating that the DFT-BBN based decision-making engine was capable of mimicking different behaviours and sailing styles of a crew. To increase the level of maturity of the simulator the opponents of the sailor were taken into account for the decision-making process. Therefore, the BBN has been expanded by three parent nodes dealing with opponent based issues, such as *wake*, *hardest opponent*, and *hardest opponent distance* (a detailed description can be found in Chapter 8.3.2). The effect on these two updates on the decision-making process will be highlighted and discussed in this paragraph.

To investigate the effect of the hardest opponents feature using the superior BBN setup two upwind races with three participating yachts have been setup. There, one rule-based yacht (Yacht C) and two yachts (Yacht A and Yacht B) using the BBN as the perceptual processor have been set up for this race event. To keep changes as little as possible just one weather scenario featuring a normal weather series has been used but the hardest opponent setup of Yacht B varied. Consequently, the effect of yacht interaction has been taken into

account. To investigate the performance and the effect of the hardest opponent feature, the following setup has been used:

Table 20: Hardest opponent setup in Race 1 and Race 2

	Race 1			Race 2		
Yacht	Yacht A	Yacht B	Yacht C	Yacht A	Yacht B	Yacht C
hardest Opponent	Yacht B	Yacht A	-	Yacht B	Yacht C	-

The yachts started at different staring positions where Yacht A had the best and Yacht C the worst starting position. Yacht B started in the wake of Yacht A and got the opportunity to cover Yacht C on the first leg. The race tracks of Race 1 and the corresponding EPVs of Yacht A and Yacht B can be found on the left side of Figure 83 and Figure 84, whereas the one of Race 2 can be found on the right side.

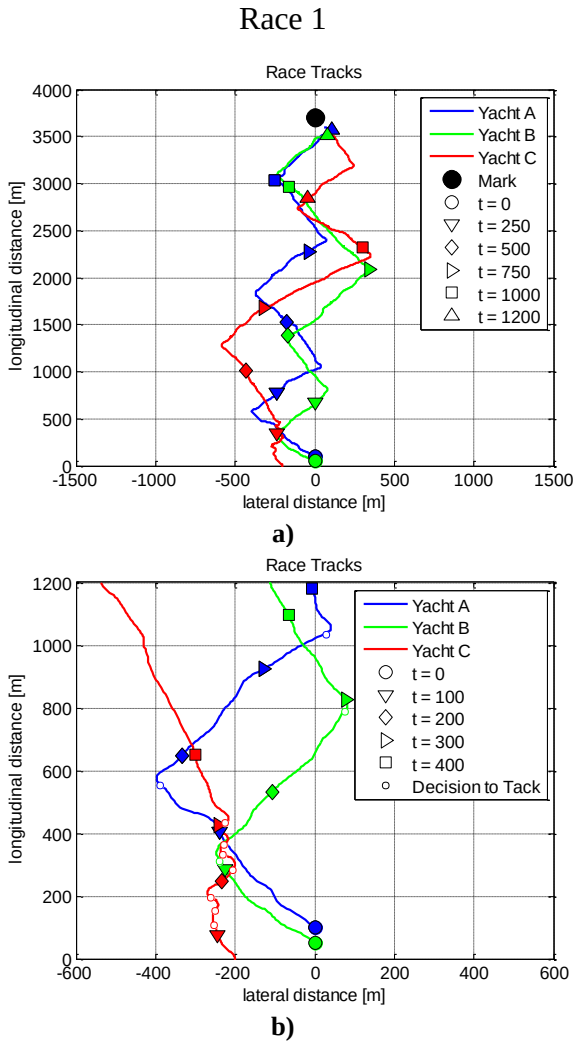

Figure 83: Race tracks of Race 1 showing a general (a) and a closer view of the yachts' way on the course

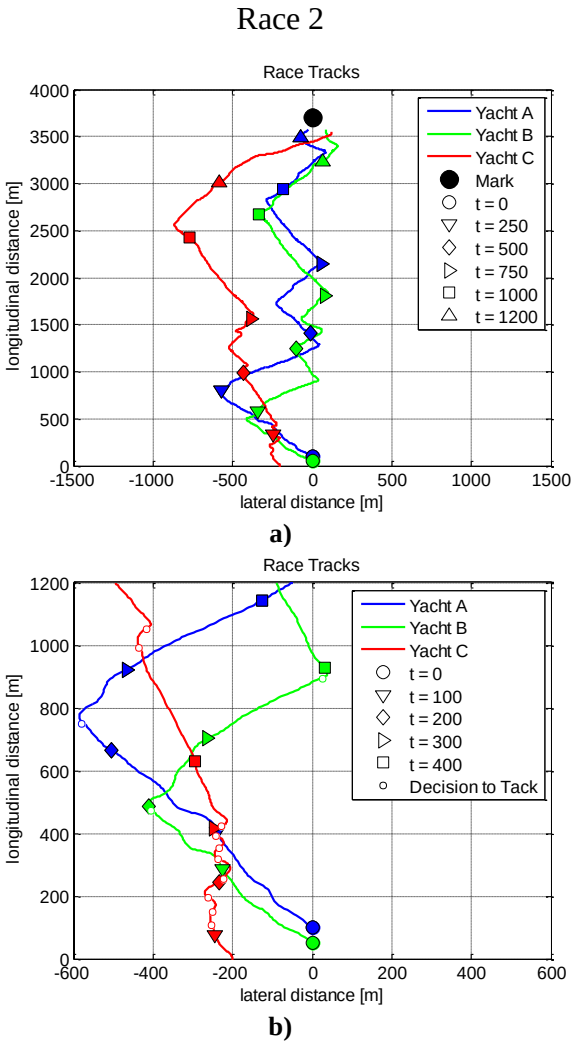

Figure 84: Race tracks of Race 2 showing a general (a) and a closer view of the yachts' way on the course

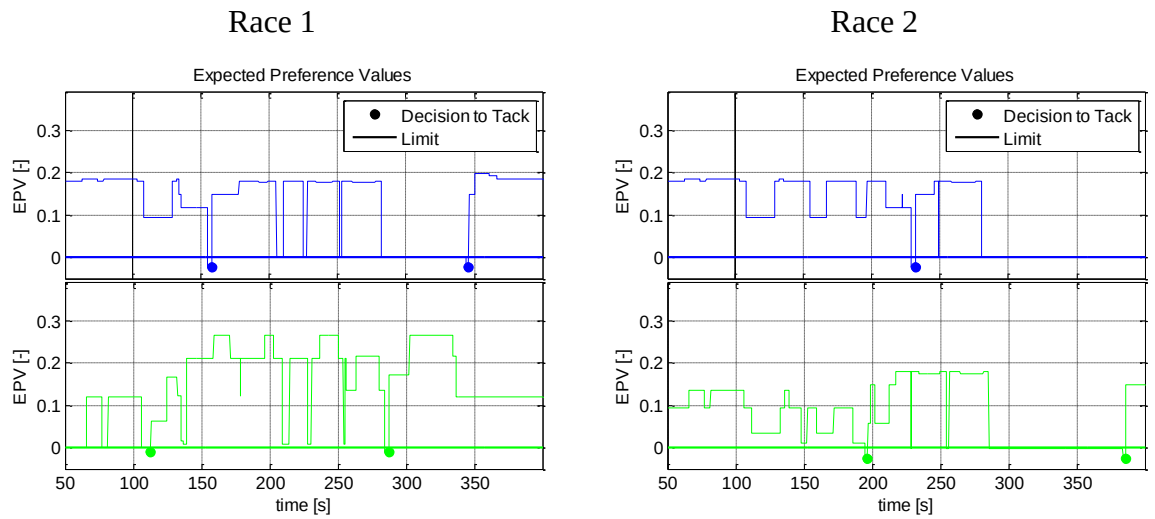

Figure 85: Expected preference value of Yacht A (blue line) and Yacht B (green line) during Race 1 (left side) and Race 2 (ride side)

Figure 83 and Figure 84 indicate different race tracks of the three yachts for the two races and therefore a clear effect of the different hardest opponent setups. In race 1, Yacht B tacked after 117 sec to get out of Yacht A's wake and did not care about Yacht C since Yacht A was set as her hardest opponent. A complete different race track can be seen when analysing the yachts' tracks in race 2. There, Yacht B tacked much later (t = 196 sec) since her hardest opponent was in her wake. This delaying of the tack had also an effect on Yacht A which also wanted to increase her damage to her hardest opponent, Yacht B and delayed her tack. The most challenging situation occurred to Yacht B that had to find a balance between damaging her hardest opponent and not getting too much damage from another yacht. This challenge was mastered by giving Yacht C bad air as long as possible and a subsequent tack once Yacht C has left the wake.

This realistic behaviour of Yacht B has been realised by using the superior BBN setup and the corresponding probability tables which can be found in the Appendix A3. According to the race situation, the sailor applied different weighting distributions to evaluate options and its attributes that yield to a varying EPV development that can be seen in Figure 85. It is also worth pointing out that the rule-based yacht tried to get out of Yacht B's wake and therefore performed seven tacks in the first 300 sec of the races. This inefficient behaviour had a negative effect on her race time and showed the immaturity of Yacht C's behaviour dealing with such a situation. Contrary to her, Yacht B was in a much

more challenging situation but dealt with it much more efficient and realistic that demonstrated the maturity of the new decision-making engine.

8.7.3 The Effect of Sailing Expertise on the Race Course

This paragraph investigates the effect of different sailing expertises on the race course. Therefore, the earlier described levels of expertise, such as 1) skilled, 2) intermediate, and 3) expert have been set up. Similar to the behavioural runs, just one environmental condition, the weather, has been altered, whereas the opponents have not been considered at this stage. Subsequently, the basic BBN was used for this sailing event which can be considered as individual solo races since no yacht interaction, blanketing parameters and racing rules have been applied. Similar to the behavioural runs, all three yachts started at identical positions and raced to the upwind mark. The already introduced recorded times and parameters which support the performance analysis of the yachts have been used for the races:

- The ranking
- The averaged ranking over all races
- The total race time including the mark rounding
- The T zone entrance
- The T mark rounding
- The number of executed tacks averaged over all races
- The averaged amount of how often a yacht hit the outer limit boundaries.

Additionally to the three behaviour styles:

- Four different weather scenarios, such as 1) normal, 2) calm, 3) stormy, and 4) variable have been randomly generated and used for the weather engine. Each scenario contained 50 different weather series leading to 200 different weather environments in total.
- These 200 weather series have been used on three different starting positions leading to 600 races in total. The starting positions (SP) have been organised as follows:

Table 21: Starting positions of expertise based race setup

	SP I	SP II	SP III
x-value	-250	0	250
y-value	0	0	0

- At the analysis two different mark rounding categories have been applied: 1) the mark rounding style correspond to the expertise level of the sailor and 2) one unique mark rounding style, the intermediate one, has been used for all expertise levels of the sailors. This distinction was necessary to analysis the effect of an effective mark rounding performance on the ranking and to obtain clear results that just consider the sailing skills up to the mark rounding zone. This procedure guaranteed that a sailor could not gain any extra advantage over the opponents due to his/her superior mark rounding skills, so just the upwind sailing skills were taken into account at the unique mark rounding skilled analysis.

The Figures 86 a - d) below show typical race tracks of the three expertise levels that sailed in the four weather scenarios. The starting position II has been chosen for these plots.

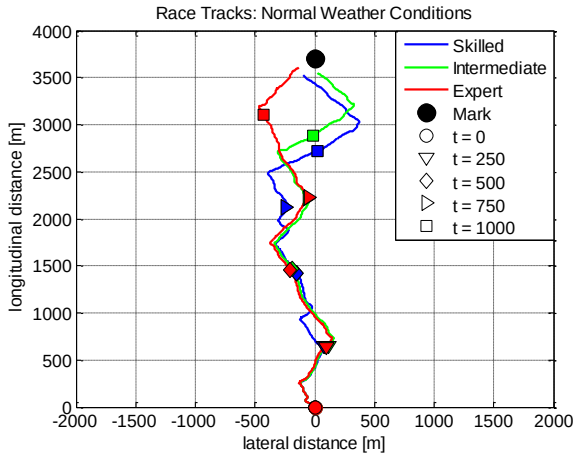

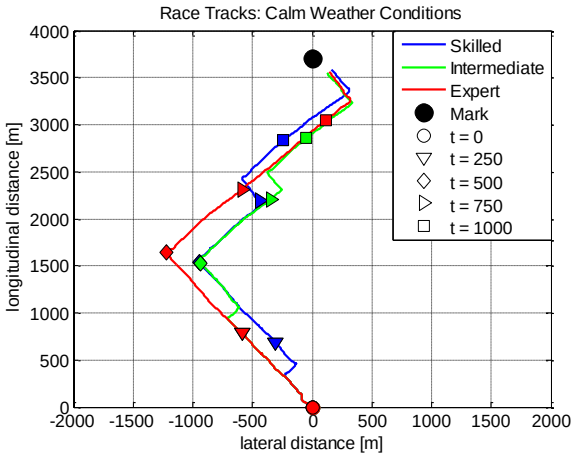

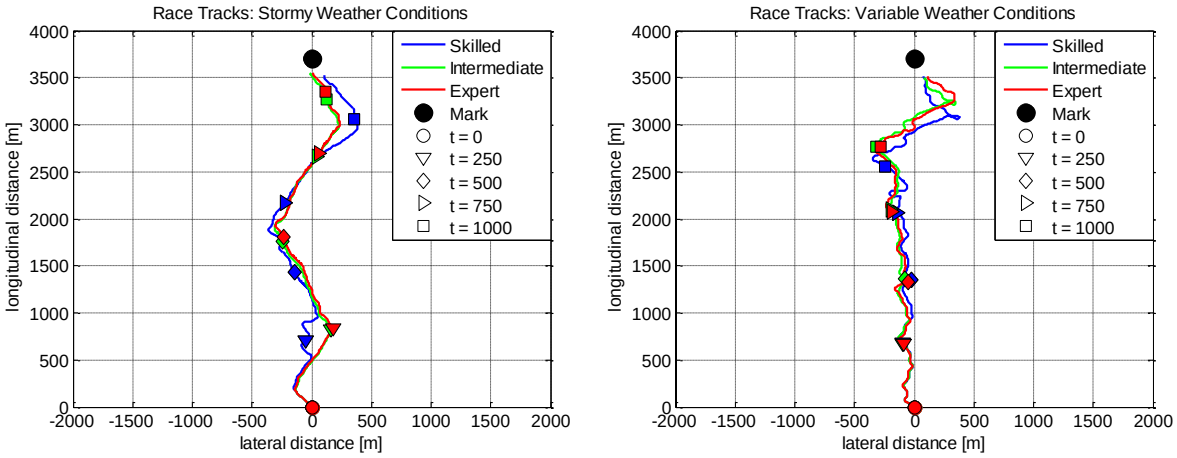

Figure 86: Typical race tracks of expertise based race setup in normal (a), calm (b), stormy (c), and variable (d) weather conditions

Table 22 displays the averaged results of all races conducted for this subchapter. Thereby, all four different weather scenarios and the unique and expertise based mark rounding skills have been considered. A detailed description of the runs and the corresponding analysis can be found in Appendix A5.

Table 22: Averaged results of all four different weather setups with unique (left side) and expertise base mark rounding

	Averaged Results over all Weather Setups			Averaged Results over all Weather Setups		
	Unique Applied Mark Rounding Skills			Expertise Based Mark Rounding Skills		
Ranking	Skilled	Intermediate	Expert	Skilled	Intermediate	Expert
1st	21%	32%	49%	7%	19%	75%
2nd	26%	40%	33%	23%	59%	19%
3rd	53%	29%	18%	71%	23%	7%
Avg. Race Time [s]	1433.9	1407.1	1388.1	1455.3	1407.1	1370
Avg. Ranking	2.32	1.97	1.69	2.64	2.05	1.32
T zone entrance [s]	1283.6	1256.5	1244.6	1283.6	1256.5	1244.6
T mark rounding [s]	150.3	150.6	143.6	171.7	150.6	125.4
# of Tacks	8.5	7.5	7	8.5	7.5	7
# of Limit	0.4	0.3	0.3	0.4	0.3	0.3

Table 22 summarises the trends that were observed during the analysis of the expertise dependent races. The left side of the tables shows the averaged results where the unique mark rounding expertise level has been applied. The right side of the table displays the results where expertise dependent mark rounding skills have been used.

The left side of the table shows a superior performance of the expert, a 2nd place for the intermediate and a 3rd place for the skilled sailor. The expert won the most (49%) and lost the least (18%) races. The opposite can be said for the skilled sailor who won the least

(21%) and lost the most (53%) of the races resulting in the worst performance of the three yachts. The intermediate sailor achieved the 2nd best and a balanced performance by winning 32% and losing 29% of the races.

The expert's constantly good performance led to an average ranking of 1.69, the intermediate achieved 1.92 and the skilled 2.32.

The knowledge about the future wind helped the sailors to avoid unnecessary tacks that had a positive effect on the race times. The ability of the expert sailor to read the near and the remote future (0 - 60 sec) helped him/her to achieve an averaged total race time of 1388.1 sec. The missing knowledge of the remote future increased the race time of the intermediate sailor by 19 seconds to 1407.1 sec. The race time was further increased to 1433.9 sec by the skilled sailor who had not had any knowledge about the future wind.

The right side of Table 27 shows a further increase of the superiority of the expert sailor who extended the lead, whereas the skilled sailor lost more ground in return. The race times of the intermediate sailor did not change since the applied mark rounding setup remained the same for this setup. But the ranking worsened since the expert extended his/her superiority by improving the mark rounding time by 18.7 seconds. In opposite to this, the skilled sailor worsened the mark rounding time by 21.4 seconds. Consequently, this had an effect on the average ranking where the expert improved from 1.69 to 1.32 with 75% won and 7% lost races. Because of the expert's domination, the intermediate sailor worsened his/her performance from 1.97 to 2.05 with 19% won and 23% lost races. The performance of skilled sailor worsened from 2.32 to 2.64 with just 7% won and 71% lost races.

8.8 Conclusions

This chapter shows the development and the implementation of an advanced decision-making engine into *Robo-Race*. The new AI decision-making philosophy based on Decision Field Theory (DFT) using Bayesian-Belief-Network (BBN) as the perceptual processor has been successfully developed for a fleet racing environment. Three different sailing behaviours/styles, such as risky/passive, safe/active and balanced/deliberated have been successfully developed and implemented into *Robo-Race*. The spatial perceptions of the sailor on the course as well as the corresponding probability tables used by the BBN

have been updated that changed the weighting distribution of the sailors to evaluate options and its attributes. Therefore, it was ensured that the sailors used the available environmental and spatial information differently which yield a subjective evaluation for each option on each attribute which in turn created a unique sailing behaviour/style. These facts were in very good agreement with real sailing where sailors picked up the same available environmental information but applied different weighting distributions to the perceptual variables (Araújo *et al.*, 2005 and Starkes *et al.*, 2003).

Furthermore, two higher levels of sailing expertise, such as intermediate and expert, have been successfully developed and implemented into *Robo-Race*. These two expertise levels have the ability to read the future wind based on their experience, where the expert was able to read the wind for the next 60 sec and the intermediate for the following 30 sec. This ability has been used for the real time planner that was included into the decision-making process. Depending on the expertise level's ability to read the future wind different planning horizons have been applied.

Extensive sensitivity studies have demonstrated the successful realisation and implementation of the new developed decision-making engine. This chapter points out that a decision-making engine driven by the DFT approach using BBN as the perceptual processor represents an effective decision-making methodology capable to simulate different sailing behaviours/styles realistically. The implementation of a real time planner into the decision-making process made it possible to simulate higher expertise levels of sailors.

Important effects that influence a decision, such as speed-accuracy or the memory of sailors can be easily modelled by the DFT approach. This was successfully done by changing the corresponding values of the threshold of a decision and the diagonal cell values of the stability matrix *S*. The desired effects were realised by adjusting the corresponding values whereas the code structure remained untouched. Performing such a detailed human decision-making analysis as it was done in this Chapter using a rule-based approach would have come with an immense time-consuming update of the existing code since all possible race situations and the related decision outcomes have to be thought of and coded in advance. The detailed simulations and analyses of the human deliberation process is impossible using a rule-based approach since it only models the decision outcome and not the process of how a decision has been derived.

The successful development and implementation was demonstrated by extensive sensibility studies and realistic and typical behaviours of the different expertise levels could be observed on the race course. The higher expertise levelled sailors for instance executed a lower number and better timed tacks that in return had a positive effect on the race time leading to their superior performance to the skilled sailor. The superior performance of the expert could be explained by the best timed and fewest number of executed tacks. The intermediate sailor performed around half the number of tacks more compared to the expert sailor leading to a worse performance. This can be explained by their different ability to read the future wind. The intermediate sailor was able to read the future for the next 30 seconds but did not know anything beyond this time horizon which indicated a real disadvantage compared to the expert sailor who knew the upcoming wind conditions for the next 60 seconds. This limited time horizon of the intermediate sailor helped to avoid unnecessary tacks in the near future but did not prevent him/her to execute a tack although favourable wind conditions were waiting in the remote future. These observations were in very good agreement with the reality and support once more the successful realisation of describing different levels of expertise of sailors.

Furthermore, three mark rounding styles have been developed to be able to simulate different mark rounding approaches that match the corresponding expertise levels of the sailors. During the analysis two different mark rounding setups have been applied. One setup included the same applied mark rounding expertise level for all sailors whereas the other setup featured a mark rounding expertise level that was equal to the sailing expertise level of the sailors. This double setup strategy made it possible to simulate a more realistic race outcome when the expertise based mark rounding setup has been applied since a more experienced sailor has better mark rounding skills than a less experienced one. The second setup where all sailors featured the same mark rounding expertise level allowed determining the real performance of the sailor on the upwind course since the total race times were not influenced by the superior or inferior mark rounding skills of the sailor. Just having applied the expertise based mark rounding setup one could have argued that the superiority of the expert over the other two sailors or the intermediate over the skilled sailor was just based on the better mark rounding skills. This could be easily refuted by applying the same mark rounding skills for all sailors. Nevertheless, the expert and the intermediate sailors could keep their superiority that was based on a higher developed sailing expertise

with better tactics and decisions when sailing to the upwind mark and not on the better mark rounding skills.

Moreover, the important aspect of yacht interaction has been successfully improved by using a superior BBN dealing with opponent issues. A case study has been carried out that showed the potential of the new AI approach. Challenging situations, such as to find a balance between damaging the hardest opponent and not getting to much damage from another yacht at the same time were solved realistically and effectively. The yacht gave her hardest opponent bad air as long as possible and performed a subsequent tack once her hardest opponent has left her wake.

It is also worth mentioning that the rule-based yacht showed an immature and unrealistic behaviour when she tried to get out of an opponent's wake. She performed various tacks which had a negative effect on the race time. The immaturity of the rule-based yacht and the maturity of the new decision-making engine will be further investigated in the following chapter.

9 Competing Approaches on the Race Course

The previous chapter, Chapter 8 describes the development and the implementation of an advanced decision-making engine. This new AI decision-making philosophy has been embedded in the dynamically changing yacht fleet racing environment of *Robo-Race*. Furthermore, different sailing styles and level of expertise have been developed and implemented.

To find out how this new decision-making approach performs on the race course, different fleet racing competitions have been created. There, yachts controlled by the new decision-making engine, the so called Bayesian-Belief-Network yachts (BBN yachts), had to compete with yachts controlled by the former implemented decision-making engine, the so called rule-based yachts (RB yachts). Two different fleet racing competitions, a small one consisting of four yachts (three BBN and one RB yacht) and a bigger one with seven yachts (three BBN and four RB yachts) have been set up.

During these two fleet racing competitions the different levels of expertise that have been developed in the previous chapter have been implemented to determine their effect on the race course. Furthermore, the differences in performance between the various BBN yachts among each other and the RB yachts are analysed. Also the effect of different expertise levelled BBN yachts (skilled, intermediate, and expert) that participate in the same race with one or more RB yachts is investigated.

To find the right balance between conducted runs and meaningful results, the number of races of a starting position constellation has been limited to 50. Furthermore, just one weather scenario setup, the normal one has been chosen for all races of the two fleet racing competitions.

The races have been analysed by using the following parameters that were identical to the one in Chapter 8 where a detailed description can be found:

- Ranking,

- Averaged ranking,
- Total race time,
- T zone entrance,
- T mark rounding,
- Number of executed tacks,
- Number of hit boundaries also averaged over 50 races.

At the end of this chapter, the two developed fleet racing competition setups are used to provide a link back to real sailing. Therefore, Olympic fleet racing competitions are analysed and used to classify the quality of the *Robo-Race* fleet racing simulations. To provide comparable races, the procedure of the Olympic fleet races have been copied and schematically embedded into the *Robo-Race* framework.

9.1 Fleet Race Events with 4 competing Yachts

As mentioned above, this subchapter deals with the small yacht fleet racing competition consisting of three BBN yachts and one RB yacht. There, the effect and the performance of the new developed decision-making engine are investigated. To achieve reliable results and not a snapshot of a random constellation, four different starting constellations have been set up. The number and the single constellations can be seen in Table 23 and Figure 87. The RB yacht started on the furthest left position and altered to the right until the furthest right position has been reached. The distances between the starting positions were set to be 250 m. The detailed starting positions of the multiple expertise levelled race events can be found in the corresponding paragraph 9.1.4.

Table 23: Starting positions of small fleet race setup

	SP I	SP II	SP III	SP IV
x-value	-375	-125	125	375
y-value	0	0	0	0

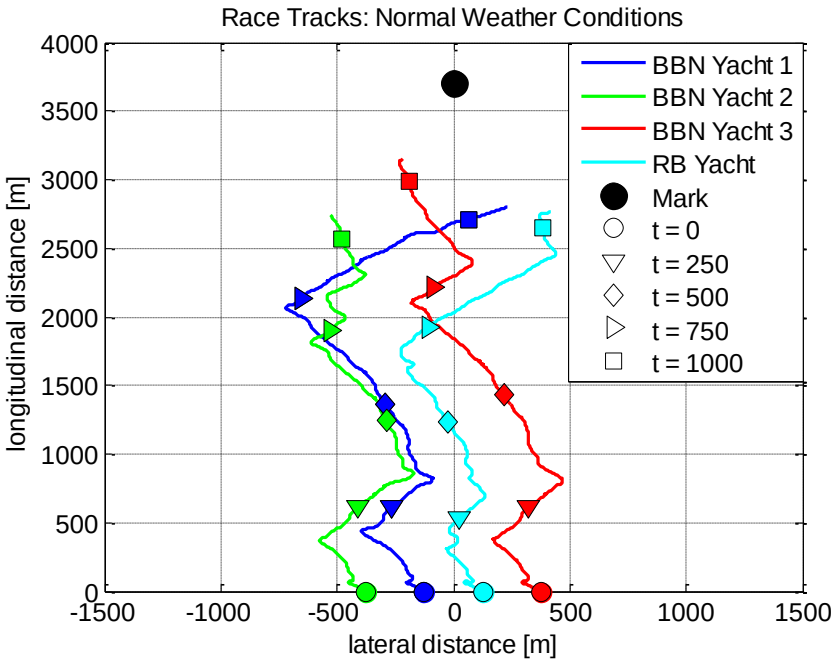

Figure 87: Starting positions and race tracks on the upwind leg of the small fleet race competition with four participating yachts

9.1.1 1st Event: 3 Skilled BBN Yachts vs. 1 RB Yacht

Table 24 below shows the results of the first sailing event where three skilled BBN yachts had to race with one RB yacht.

Table 24: Summary of small fleet race competition: 3 skilled BBN-yachts vs. 1 RB yacht

	Normal Weather Setup											
	Starting Position I				Starting Position II				Starting Position III			
	Expertise Setup				Expertise Setup				Expertise Setup			
Ranking	Skilled	Skilled	Skilled	RB	Skilled	Skilled	Skilled	RB	Skilled	Skilled	Skilled	RB
1st	12	21	16	1	19	16	15	0	19	11	20	0
2nd	13	10	22	5	19	11	18	2	11	12	15	12
3rd	18	14	8	10	9	15	8	18	8	20	5	17
4th	7	5	4	34	3	8	9	30	12	7	10	21
Avg. Race Time [s]	1468.6	1432.7	1431.6	1551.9	1433.2	1451.5	1442.8	1536	1439.3	1465.1	1432.7	1516
Avg. Ranking	2.4	2.06	2	3.54	1.92	2.3	2.22	3.56	2.26	2.46	2.1	3.18
T zone entrance [s]	1295.1	1270.8	1266.7	1379.9	1267.7	1284.6	1281.9	1375.2	1283.4	1292.9	1270	1354.3
T mark rounding [s]	173.5	162	164.9	172.1	165.5	166.9	161	160.8	155.9	172.2	162.6	161.7
# of Tacks	8.8	7.6	8.8	13.9	8	7.9	8.3	15.6	8	8.1	8	16.6

	Normal Weather Setup								
	Starting Position IV					Averaged Results over all Starting Positions			
	Expertise Setup					Expertise Setup			
Ranking	Skilled	Skilled	Skilled	RB		Skilled	Skilled	Skilled	RB
1st	13	11	24	2		32%	30%	38%	2%
2nd	22	10	11	7		33%	22%	33%	13%
3rd	5	19	8	18		20%	34%	15%	32%
4th	10	10	7	23		16%	15%	15%	54%
Avg. Race Time [s]	1462.8	1471.5	1433	1517.9		1451.0	1455.2	1435.0	1530.5
Avg. Ranking	2.24	2.56	1.96	3.24		2.2	2.3	2.1	3.4
T zone entrance [s]	1289.8	1304.3	1262.2	1345.9		1284.0	1288.2	1270.2	1363.8
T mark rounding [s]	172.9	167.2	170.7	172.1		167.0	167.1	164.8	166.7
# of Tacks	8.7	8.7	8.7	15.9		8.4	8.1	8.5	15.5

All three BBN yachts performed better and were always faster than the RB yacht. The superiority of the BBN yachts over the RB yacht can be seen when analysing the total race times which varied between 1431.6 sec and 1471.5 sec for the BBN yacht and between 1516.0 sec and 1551.9 sec for the RB yacht. Consequently, the RB yacht won the least races with three 1st places (1.5%) and lost the most with 108 4th places (54%). An explanation for this bad performance can be found when analysing the number of performed tacks. Depending on the starting position the RB yacht executed between 13.9 and 16.6 tacks which indicated a very active sailing behaviour under these conditions. The skilled yachts in return executed between 7.6 and 8.8 tacks which was around half the number of tacks the RB yacht performed. This well chosen timing and execution of the tacks was the key of success and the base of the superiority of the BBN yachts.

Although the RB yacht performed twice as many tacks than the BBN yachts, she was not better positioned when entering the mark rounding zone apart from one starting constellation where she started from SP II and was fastest with a little lead of 0.2 sec.

At the end of this subchapter a summary table with all averaged results of this event can be found.

9.1.2 2nd Event: 3 Intermediate BBN Yachts vs. 1 RB Yacht

The table below, Table 25 displays the results of the multiple yacht races with three intermediate BBN yachts and one RB.

Table 25: Summary of small fleet race competition: 3 intermediate BBN-yachts vs. 1 RB yacht

	Normal Weather Setup											
	Starting Position I				Starting Position II				Starting Position III			
	Expertise Setup				Expertise Setup				Expertise Setup			
Ranking	Interm	Interm	Interm	RB	Interm	Interm	Interm	RB	Interm	Interm	Interm	RB
1st	27	7	16	0	23	6	21	0	27	7	15	1
2nd	14	12	14	10	11	20	15	4	11	13	14	12
3rd	8	17	11	14	13	18	6	13	9	11	11	19
4th	1	14	9	26	3	6	8	33	3	19	10	18
Avg. Race Time [s]	1394.8	1480.9	1438.6	1532	1416.6	1470.3	1435.9	1550.2	1393.6	1478.4	1446.3	1497.2
Avg. Ranking	1.66	2.76	2.26	3.32	1.92	2.48	2.02	3.58	1.76	2.84	2.32	3.08
T zone entrance [s]	1226.6	1288.5	1266	1360.6	1245.4	1298.5	1259.7	1386.6	1228.1	1301.6	1274.7	1338.3
T mark rounding [s]	168.2	192.3	172.5	171.3	171.2	171.8	176.2	163.6	165.4	176.8	171.7	158.9
# of Tacks	6.8	7.4	7.7	14.5	6.7	7.3	7.5	15.8	6.4	7.7	7.6	16.5

	Normal Weather Setup							
	Starting Position IV					Averaged Results over all Starting Positions			
	Expertise Setup					Expertise Setup			
Ranking	Interm	Interm	Interm	RB		Interm	Interm	Interm	RB
1st	29	7	13	1		53%	14%	33%	1%
2nd	11	13	12	14		24%	29%	28%	20%
3rd	6	17	10	17		18%	32%	19%	32%
4th	4	13	15	18		6%	26%	21%	48%
Avg. Race Time [s]	1397.3	1470.2	1465.2	1504.3		1400.6	1475.0	1446.5	1520.9
Avg. Ranking	1.7	2.72	2.54	3.04		1.8	2.7	2.3	3.3
T zone entrance [s]	1234.1	1303.1	1294.6	1334.6		1233.6	1297.9	1273.8	1355.0
T mark rounding [s]	163.2	167.1	170.6	169.7		167.0	177.0	172.8	165.9
# of Tacks	7	8.1	7.9	17.5		6.7	7.6	7.7	16.1

Similar to the previous races where three skilled BBN yachts were involved, the intermediate yachts performed far better than the RB yacht. Moreover, the intermediate yachts increased the performance and needed 1440.68 sec in averaged to finish a race compared to the skilled BBN yachts that needed 1447.07 sec. Therefore, the intermediate yachts further increased the BBN yachts' superiority over the RB yacht that managed to win just two races (1%) by losing 95 (47.5%). This bad ranking again was caused by the active sailing style of the RB yacht that executed between 14.5 and 17.5 tacks depending on the SP leading to an average of 16.08 tacks for all four races. This was 2.19 times the

amount of executed tacks compared to the intermediate yachts that needed 7.34 tacks in average. As mentioned before, the low amount and the timing of the tacks were the key of the intermediate yachts' superiority over the RB yacht. Due to the intermediate sailor's ability to read the near future wind (up to 30 sec), the tacks were better timed which in return had a positive effect on the race time and enlarged the gap to the RB yacht to around 80 sec that needed 1520.93 sec.

For the sake of clarity, a summary table with all averaged results of this event can be found at the end of this subchapter.

9.1.3 3rd Event: 3 Expert BBN Yachts vs. 1 RB Yacht

Table 26 below shows the results of the fleet races where three expert BBN yachts had to compete with one RB yacht.

Table 26: Summary of small fleet race competition: 3 expert BBN-yachts vs. 1 RB yacht

	Normal Weather Setup											
	Starting Position I				Starting Position II				Starting Position III			
	Expertise Setup				Expertise Setup				Expertise Setup			
Ranking	Expert	Expert	Expert	RB	Expert	Expert	Expert	RB	Expert	Expert	Expert	RB
1st	21	6	23	0	24	2	24	0	22	7	20	1
2nd	17	14	16	3	17	15	15	3	15	13	15	7
3rd	9	14	5	22	4	26	5	15	7	18	3	22
4th	3	16	6	25	5	7	6	32	6	12	12	20
Avg. Race Time [s]	1405.4	1489	1401.7	1534.2	1404.5	1487.7	1400.3	1534	1423.9	1478.5	1425.5	1518.6
Avg. Ranking	1.88	2.8	1.88	3.44	1.8	2.76	1.86	3.58	1.94	2.7	2.14	3.22
T zone entrance [s]	1236.6	1308.3	1231.7	1367.6	1240.6	1312.8	1239.6	1369.1	1246.2	1309.2	1257.1	1353.1
T mark rounding [s]	168.8	180.7	170.1	166.6	163.9	174.8	160.7	165	177.7	169.3	168.5	165.5
# of Tacks	6.4	6.9	6.6	13.7	6.1	6.9	6.9	15.1	6.4	7	6.4	17.5

	Normal Weather Setup							
	Starting Position IV					Averaged Results over all Starting Positions			
	Expertise Setup					Expertise Setup			
Ranking	Expert	Expert	Expert	RB		Expert	Expert	Expert	RB
1st	24	5	20	1		46%	10%	44%	1%
2nd	9	17	19	5		29%	30%	33%	9%
3rd	9	13	5	23		15%	36%	9%	41%
4th	8	15	6	21		11%	25%	15%	49%
Avg. Race Time [s]	1423.3	1467.7	1419.1	1504.4		1414.3	1480.7	1411.7	1522.8
Avg. Ranking	2.02	2.76	1.94	3.28		1.9	2.8	2.0	3.4
T zone entrance [s]	1252.6	1304.1	1249.2	1339.1		1244.0	1308.6	1244.4	1357.2
T mark rounding [s]	170.7	163.7	170	165.3		170.3	172.1	167.3	165.6
# of Tacks	6.8	7.4	7	15.8		6.4	7.1	6.7	15.5

Similar to the simulations where the skilled and the intermediate sailor setups were involved, the expert yachts outperformed the RB yacht by being faster independent from the starting position constellations. This superiority of the BBN yachts can be seen by the poor performance of the RB yacht that won just two (1%) and lost 91 races (40.5%). It is worth pointing out that this expertise setup allowed the RB yacht to finish 2nd 18 times (9%) which was the lowest value of all three expertise setups where the skilled one allowed 26 and the intermediate one 40 2nd places. Depending on the starting position the RB yacht executed between 14.5 and 17.5 tacks which again indicates an active and ineffective sailing behaviour. This led to an averaged tack value of 15.53 per race. In contrast to that, the expert yachts performed between 6.4 and 8.1 tacks per race leading to an average of 6.73 tacks per race which was just 43.4% of the executed tacks of the RB yacht.
All averaged results of this event can be found in a summary table at the end of this subchapter.

9.1.4 4th Event: 3 Multi-Expertise BBN Yachts vs. 1 RB Yacht

The three different levels of expertise BBN yachts, such as skilled, intermediate, and expert had to race against one rule-based (RB) yacht. The starting position constellations of the BBN yachts have been chosen based on the results of the three previous fleet racing competitions. The skilled yacht was always the furthest right BBN yacht, the intermediate sailor the furthest left BBN yacht and the expert sailor was placed between those two. The RB yacht started from the furthest right position (SP I) and changed one position to the right until all four starting positions have been captured. The following Table 32 illustrates the four different starting positions which have been investigated.

Table 27: Starting position constellations with three BBN and one RB-yacht

	SP I	SP II	SP III	SP IV
Race1	Rule-based	Intermediate	Expert	Skilled
Race2	Intermediate	Rule-based	Expert	Skilled
Race3	Intermediate	Expert	Rule-based	Skilled
Race4	Intermediate	Expert	Skilled	Rule-based

The next lower expertise level was set to be the hardest opponent that led to the following constellations:

Table 28: Hardest opponent setup

Yacht	Hardest opponent
Expert	Intermediate
Intermediate	Skilled
Skilled	Rule-based

The following Table 29 shows the results of the multi-expertise BBN yacht simulations.

Table 29: Summary of small fleet race competition: 3 multi-expertise BBN-yachts vs. 1 RB yacht

	Normal Weather Setup											
	Starting Position I				Starting Position II				Starting Position III			
	Expertise Setup				Expertise Setup				Expertise Setup			
Ranking	Interm	Expert	Skilled	RB	Interm	Expert	Skilled	RB	Interm	Expert	Skilled	RB
1st	25	12	13	0	24	11	14	1	21	13	15	1
2nd	13	16	20	1	16	16	12	6	15	15	13	7
3rd	7	19	10	14	7	12	14	17	8	14	16	12
4th	5	3	7	35	3	11	10	26	6	8	6	30
Avg. Race Time [s]	1410.4	1436.2	1437.7	1534.7	1397.7	1448.7	1439.6	1511.6	1422.6	1448	1447.4	1516.5
Avg. Ranking	1.84	2.26	2.22	3.68	1.78	2.46	2.4	3.36	1.98	2.34	2.26	3.42
T zone entrance [s]	1240.5	1262.5	1258	1361.8	1231	1284.6	1266.6	1351.9	1254.7	1280.1	1259.5	1353.4
T mark rounding [s]	169.9	173.8	179.6	172.9	166.7	164.1	173	159.7	167.9	167.9	188	163
# of Tacks	7.2	7.2	9	14	6.8	7.5	8.3	14.9	6.9	7.8	8.4	17.4

	Normal Weather Setup								
	Starting Position IV					Averaged Results over all Starting Positions			
	Expertise Setup					Expertise Setup			
Ranking	Interm	Expert	Skilled	RB		Interm	Expert	Skilled	RB
1st	15	16	18	1		43%	26%	30%	2%
2nd	26	9	5	10		35%	28%	25%	12%
3rd	6	15	10	19		14%	30%	25%	31%
4th	3	10	17	20		9%	16%	20%	56%
Avg. Race Time [s]	1426.2	1453.4	1457.5	1505.3		1414.2	1446.6	1445.6	1517.0
Avg. Ranking	1.94	2.38	2.52	3.16		1.9	2.4	2.4	3.4
T zone entrance [s]	1248.6	1283.9	1296.6	1338.4		1243.7	1277.8	1270.2	1351.4
T mark rounding [s]	177.6	169.5	160.9	166.9		170.5	168.8	175.4	165.6
# of Tacks	7.3	7.6	8.5	16.4		7.1	7.5	8.6	15.7

Similar to the yacht races with unique expertise BBN yachts, the multiple expertise BBN yachts performed far better than the RB yacht. In this constellation, all BBN yachts were faster than and therefore superior over the RB yacht.

This could be clearly seen in the rankings where the RB yacht won three races (1.5%), became 2nd in 24 (12%), 3rd in 62 (31%) and last in 111 (55.5%) races. These numbers led to an average ranking of 3.41.

The best performing yacht was the intermediate BBN one starting from her favourite starting positions (see subchapter 9.1.2) and achieved an average ranking of 1.89. She won 85 (42.5%) and lost 17 (8.5%) races.

The second best performance was the skilled sailor who also started from his/her favourite position and achieved an overall ranking of 2.35 with 60 (30%) won and 40 (20%) lost races.

Close behind was the expert yacht with an average ranking of 2.36. She won 52 (25%) and lost 32 (18%) races. It is worth pointing out that she started from her most disadvantageous starting position (see subchapter 9.1.3) and improved her ranking by 0.4 places (2.76 vs. 2.36) compared to the previous multiple experts vs. one RB-yacht races. Moreover, the total race time dropped from 1480.73 sec to 1446.58 sec which indicated an improvement of 34.15 sec compared to the unique expert BBN races. This can be explained by the presents of lower expertise based opponents (skilled and intermediate) and the fact that this yacht was not set up as hardest opponent in any other yacht setup. Consequently, this yacht was on the safer side than her opponents and did not need to be aware of any extra attacks from her revivals.

Contrary to this, the skilled as well as the intermediate yachts needed around 10 sec (skilled) and 15 sec (intermediate) more compared to the corresponding unique BBN races. This extra time resulted from the hardest opponent setup of the rivals who stayed longer on a tack than necessary in order to increase the damage to her hardest opponent by giving her bad air (see subchapter 8.10).

This fact can be seen as an indicator that the hardest opponent option implemented in the BBN structure worked well and realistically in a multiple fleet race simulation. The sailors paid attention to his/her hardest opponents without losing focus on their overall goal, such as to win the race. Here, the major advantage of the BBN philosophy became visible where a fuzzy but also distinctive character between the different sailing attributes could be found leading to a realistic but also individual sailing style.

The fastest averaged race time of the RB-yacht compared to the unique BBN races can be explained by 1) the worse result of the skilled yacht that resulted from an effective hardest opponent behaviour of the intermediate yacht and 2) the often big spatial

differences of the RB and skilled yacht. Therefore, the latter was not in the range to damage her hardest opponent, the RB-yacht. Nevertheless, the hardest opponent feature worked also in this case which can be seen by the worst average ranking of 3.4 for the RB-yacht in all four expertise race constellations.

9.1.5 Summary of Sailing Events with 4 competing Yachts

Table 30 shows the averaged results over all races of each fleet racing competition highlighted in this subchapter. The results of all three BBN yachts have been averaged for the different expertise levelled setups in order to achieve a clearer picture for the analysis.

Table 30: Summary of all four small fleet race competition: 3 BBN-yachts vs. 1 RB yacht

	Normal Weather Setup								
	Averaged Results over all Races								
	Expertise Setup								
Ranking	Skilled	RB	Intermediate	RB	Expert	RB	Multi BBN	RB
1st	33%	2%	33%	1%	33%	1%	33%	2%
2nd	29%	13%	27%	20%	30%	9%	29%	12%
3rd	23%	32%	23%	32%	20%	41%	23%	31%
4th	15%	54%	18%	48%	17%	49%	15%	56%
Avg. Race Time [s]	1447.1	1530.5	1440.7	1520.9	1435.6	1522.8	1435.5	1517.0
Avg. Ranking	2.21	3.38	2.25	3.26	2.21	3.38	2.20	3.41
T zone entrance [s]	1280.8	1363.8	1268.4	1355.0	1265.7	1357.2	1263.9	1351.4
T mark rounding [s]	166.3	166.7	172.3	165.9	169.9	165.6	171.6	165.6
# of Tacks	8.3	15.5	7.3	16.1	6.7	15.5	7.7	15.7

Table 30 shows a clear superiority of the BBN yachts over the RB yacht. This superiority can be seen by analysing the total race times and the averaged ranking of the yachts. Depending on the level of expertise of the BBN yachts, the gap between the RB and BBN yachts varied between 80.2 sec (intermediates vs. RB) and 87.2 sec (experts vs. RB) which had an immediate effect on the ranking. The averaged ranking of the BBN yachts was always at least one position better than the one of the RB yacht. The BBN yachts achieved an almost constant averaged ranking performance that varied from 2.20 (multi BBN vs. RB) to 2.25 (intermediate vs. RB). The RB yacht's averaged ranking altered from 3.26 to 3.41.

The table also indicates an increase of performance the higher the level of expertise became which can be seen by analysing the averaged total race times of the BBN yachts. The skilled yachts crossed the line after 1447.1 sec, the intermediate yachts after 1440.7 sec

and the expert yachts after 1435.6 sec which is in good agreement to the observations done by Araújo (2005). He also observed a decrease of the total race time the higher the level of expertise became. Moreover, the differences between the single expertise groups shrank the higher the expertise level became. This trend could be also seen in this study where the differences shrank from 6.4 sec (intermediate vs. skilled) to 5.1 sec (expert vs. intermediate).

It is also worth to mention that the higher the level of expertise was the lower the number of tacks became, meaning the sailors made their tacking decision more effectively. The skilled sailors performed 8.30, the intermediate sailors 7.34 and the expert sailors 6.73 tacks per race in average. This dropping number of well timed tacks had a positive effect on the average total race times that has been discussed above.

9.2 Fleet Race Events with 7 competing Yachts

As mentioned earlier, this subchapter deals with the bigger yacht fleet racing competitions where three BBN yachts race against four RB yachts. The superiority of the DFT-BBN controlled decision-making engine could be shown in the small yacht fleet racing competitions. Now, its performance in a bigger fleet racing competition will be determined in this subchapter. The valuable information gathered in previous competitions was used to design an effective but meaningful starting position constellation. Due to the fact that the BBN yachts were all superior over the RB yacht, it was decided to strengthen the position of the RB yachts by giving them predominance over the BBN yachts. Therefore, every BBN yacht was surrounded by two RB yachts which can be seen in Figure 88. The corresponding numbers of the different starting positions are displayed in Table 31 that indicates a difference of 100 metres between two neighbour yachts. A detailed starting position constellation of the multiple expertise levelled race events can be found in the corresponding paragraph 9.2.4.

Table 31: Starting positions at the fleet race competition with 7 participating yachts

	SP I	SP II	SP III	SP IV	SP V	SP VI	SP VII
x-value	-300	-200	-100	0	100	200	300
y-value	0	0	0	0	0	0	0

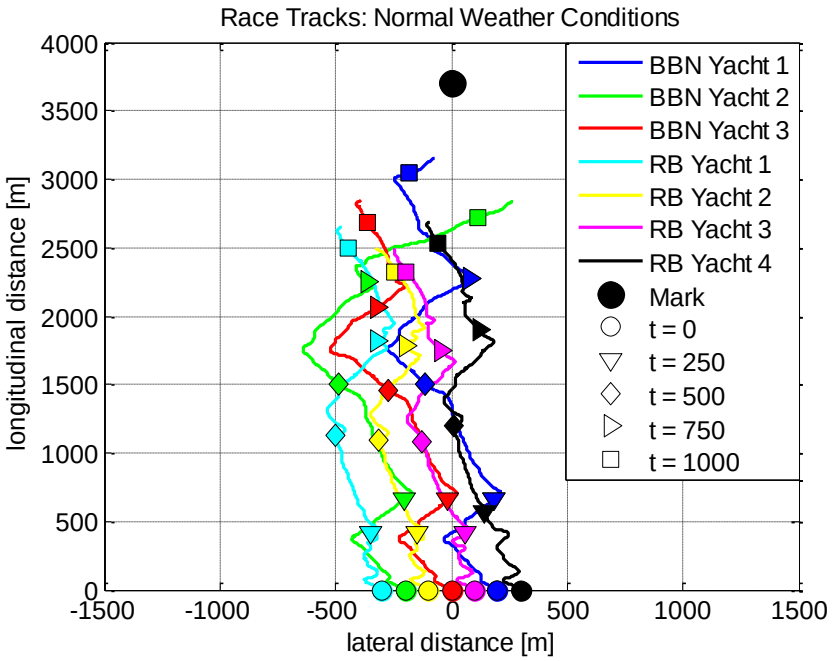

Figure 88: Starting positions and race tracks on the upwind leg of the big fleet race competition with seven participating yachts

9.2.1 First Event: 3 Skilled BBN vs. 4 RB Yachts

Table 32 below displays the results of the multiple yacht fleet races with three skilled BBN and four RB yachts.

Table 32: Summary of big fleet race competition: 3 skilled BBN yachts vs. 4 RB yachts

	Normal Weather Setup								
	Expertise Setup							Averaged Results	
Ranking	Skilled	Skilled	Skilled	RB	RB	RB	RB	Skilled	RB
1st	30	3	10	0	0	0	7	86%	14%
2nd	8	18	13	1	1	3	6	78%	22%
3rd	4	13	8	7	4	4	10	50%	50%
4th	3	3	5	12	11	7	9	22%	78%
5th	1	5	7	9	8	11	9	26%	74%
6th	3	4	5	16	8	10	4	24%	76%
7th	1	4	2	5	18	15	5	14%	86%
Avg. Race Time [s]	1442.9	1531.4	1499.5	1607.7	1628	1631.3	1542.7	1491.3	1602.4
Avg. Ranking	2	3.34	3.18	4.94	5.44	5.32	3.78	2.84	4.87
T zone entrance [s]	1272.1	1351.9	1330	1437.1	1448.4	1450.7	1366.8	1318.0	1425.8
T mark rounding [s]	170.8	179.5	169.6	170.6	179.6	180.6	176	173.3	176.7
# of Tacks	8.5	10.2	9.2	14	15	17.3	16	9.3	15.6

Similar to the multiple yacht races with four participating yachts, the same trends could be observed when analysing the fleet races with seven participating yachts. The skilled BBN yachts outperformed the RB yachts and were clearly superior over them. The skilled yachts achieved an average ranking of 2.84 compared to 4.87 for the RB yachts. Hence, the averaged ranking of the BBN yachts was two places better than the one of the RB yachts.
The BBN yachts' domination was clearer visible when analysing the ranking. The BBN yachts won 43 (86%) races, became 2nd in 39 (78%) and third in 25 (50%) races. In contrast to that, they just lost seven (14%) races, became 2nd last in 12 (24%) races. This picture completely changes when analysing the RB yachts. They won 7 (14%) races, became 2nd in 11 (22%) and 3rd in 23 (46%) races. These numbers of places on the podium were quite small even when there was one yacht more compared to the BBN yachts. Consequently, they had to lose more often and lost 43 (86%) races and became 2nd last in 38 (76%) races.

Again, also in this multiple fleet races, the key of success was the number of executed and well time tacks. The skilled BBN yachts performed 9.30 tacks in average compared to 15.58 tacks the RB yachts needed to sail up to and round the mark. It is also worth pointing out that the fastest skilled yacht was the furthest left BBN yacht with an averaged total race time of 1442.9 sec. In contrast to that, the fastest RB yacht was the one starting from the furthest right position and finished the course in 1542.7 sec which was almost 100 sec slower than the fastest BBN yacht. Furthermore, the average total race time of all RB yachts was 1602.43 sec which was 111.16 sec slower than the average total race time of all three BBN yachts. Or in other words, the RB yachts needed 7.2 % more time than the skilled BBN yachts. It is also worth mentioning that the slowest skilled yacht was still around 11 sec faster than the fastest RB yacht which can be seen as an indicator of the superiority of the BBN yachts, even with their basic setup.

9.2.2 Second Event: 3 Intermediate BBN vs. 4 RB Yachts

Table 33 displays the results of the multiple yacht fleet racing competition with three intermediate BBN and four RB yachts.

Table 33: Summary of big fleet race competition: 3 intermediate BBN yachts vs. 4 RB yachts

	Normal Weather Setup								
	Expertise Setup							Averaged Results	
Ranking	Interm	Interm	Interm	RB	RB	RB	RB	Interm	RB
1st	32	3	11	2	0	1	1	92%	8%
2nd	6	23	11	2	1	1	6	80%	20%
3rd	8	13	9	5	1	1	13	60%	40%
4th	0	5	10	8	6	8	13	30%	70%
5th	1	2	5	11	13	13	5	16%	84%
6th	3	0	2	6	16	15	8	10%	90%
7th	0	4	2	16	13	11	4	12%	88%
Avg. Race Time [s]	1395	1497.5	1486.1	1603	1626.2	1617	1548.6	1459.5	1598.7
Avg. Ranking	1.82	2.92	3.02	5.12	5.62	5.4	4.1	2.59	5.06
T zone entrance [s]	1236	1313.3	1327.4	1430.1	1448	1449.5	1372.4	1292.2	1425.0
T mark rounding [s]	159	184.3	158.8	172.8	178.2	167.5	176.2	167.4	173.7
# of Tacks	7.1	8.5	7.8	13.8	15.5	17.5	16.4	7.8	15.8

The domination of the BBN yachts over the RB yachts was further increased by applying the intermediate sailors to the BBN yachts. They achieved an averaged ranking of 2.59 in comparison to 5.06 achieved by the four RB yachts. This means that a RB sailor finished the races 2.47 places worse compared to an intermediate BBN sailor. This increase of performance of the intermediate sailors can be explained by the lower averaged total race time which dropped from 1491.27 sec (skilled BBN yachts) to 1459.53 sec. This lower race time and the almost constant average race time of the RB yachts of 1598.70 sec increased the gap between the yachts to 132.77 sec, meaning that the RB yachts needed 10.27 % longer than the intermediate ones. The reason for this difference in performance can be found in the number of executed tacks. The intermediate sailors needed less than half the number of tacks the RB yachts needed, 7.80 tacks to 15.80 tacks in average.

It is worth pointing out that the fastest BBN yacht started from SP II whereas the fastest RB yacht began her races from SP VII exactly like in the skilled vs. RB yacht fleet races. Nevertheless, the BBN yacht was much faster and finished her race after 1395 sec and therefore 153.6 sec (or 11%) before the fastest RB yacht. It is also worth mentioning that the slowest intermediate yacht performed more than 50 sec better than the best RB yacht showing again the superiority of the BBN approach.

9.2.3 Third Event: 3 Expert BBN vs. 4 RB Yachts

Table 34 below displays the results of the fleet races where three expert BBN yachts had to compete with four RB yachts.

Table 34: Summary of big fleet race competition: 3 expert BBN yachts vs. 4 RB yachts

	Normal Weather Setup								
	Expertise Setup							Averaged Results	
Ranking	Expert	Expert	Expert	RB	RB	RB	RB	Expert	RB
1st	38	2	8	1	0	0	1	96%	4%
2nd	4	24	12	1	0	0	9	80%	20%
3rd	5	11	16	2	1	4	11	64%	36%
4th	2	7	6	5	10	12	8	30%	70%
5th	1	4	5	9	8	13	10	20%	80%
6th	0	1	1	13	19	8	8	4%	96%
7th	0	1	2	19	12	13	3	6%	94%
Avg. Race Time [s]	1382.2	1464.5	1474.9	1613.6	1616.2	1601.7	1536.8	1440.5	1592.1
Avg. Ranking	1.48	2.88	2.98	5.7	5.62	5.28	4.06	2.45	5.17
T zone entrance [s]	1216.2	1297.6	1301.1	1453.5	1452.2	1439.4	1364.8	1271.6	1427.5
T mark rounding [s]	166	167	173.8	160.1	163.9	162.3	172	168.9	164.6
# of Tacks	6.5	7.6	7.4	14.3	14.7	17	17.3	7.2	15.8

Table 34 indicates an even further increase of the superiority of the BBN yacht over the RB yachts. The BBN yachts were set up to be experts and achieved an average ranking of 2.45 compared to 5.17 achieved by the four RB yachts. These numbers highlight that the expert yachts crossed the finish line 2.72 places before the RB yachts did. The averaged race time of the expert yachts was further improved and dropped from 1459.5 sec (intermediate BBN yachts) to 1440.5 sec, whereas the one of the RB yachts also dropped from 1598.7 sec to 1592.1 sec. This led to a further increased gap of 151.6 sec. In other words, the RB yachts needed 10.52% more time to finish the course.

The expert yachts won 48 (96%) races and became 2nd in 40 (80%) and 3rd in 32 (64%) races. They only lost three (6%) races and became 2nd last twice (4%). As mentioned above the RB yachts could not improve their ranking and won only one (2%) race, become 2nd 9 times (18%) and 3rd 16 times (32%). They lost 47 (94%) races and became 2nd last in 48 (96%) races.

The key to success in the number of executed tacks was further decreased by the expert yachts and resulted in 7.17 tacks in average per yacht per race which was only 45.29% of the amount of performed tacks the RB yachts needed (15.83) to finish a race.

Like in the skilled and intermediate sailor setups, the fastest expert yacht started from SP II whereas SP VII was the location where the fastest RB yacht started from. The fastest expert yacht needed 1382.2 sec and the fastest RB yacht 1536.8 sec to finish a race leading to a gap of 154.6 sec (15.6%). It is also worth pointing out that the slowest expert yacht was 61.6 sec (5.6%) faster than the fastest RB yacht, which once again, proves the superiority of the expert yachts over the RB yachts.

9.2.4 Fourth Event: 3 Multi-Expertise BBN vs. 4 RB Yachts

A skilled, intermediate, and expert BBN yacht had to race against four rule-based (RB) yacht. The starting position constellations of the BBN yachts have been chosen based on the results of the three competitions highlighted above. The skilled yacht was always the furthest right BBN yacht, the intermediate sailor the furthest left BBN yacht and the expert sailor was placed between those two. Each BBN yacht was surrounded by two RB yachts. The following Table 35 illustrates the three different starting positions of the BBN yachts.

Table 35: Starting position constellations of the three BBN yachts

	SP II	SP IV	SP VI
Race	Intermediate	Expert	Skilled

The next lower expertise level was set to be the hardest opponent that yields the following constellations:

Table 36: Hardest opponent setup

Yacht	Hardest opponent
Expert	Intermediate
Intermediate	Skilled
Skilled	Rule-based

The following Table 37 shows the results of the multi-expertise BBN yacht simulations.

Table 37: Summary of big fleet race competition: 3 multi-expertise BBN yachts vs. 4 RB yachts

	Normal Weather Setup								
	Expertise Setup							Averaged Results	
Ranking	Interm	Expert	Skilled	RB	RB	RB	RB	BBN	RB
1st	14	15	19	0	0	0	2	96%	4%
2nd	12	14	11	3	0	3	7	74%	26%
3rd	10	10	8	3	6	4	9	56%	44%
4th	5	5	7	9	8	5	11	34%	66%
5th	5	3	3	9	12	4	14	22%	78%
6th	2	2	1	14	7	19	5	10%	90%
7th	2	1	1	12	17	15	2	8%	92%
Avg. Race Time [s]	1478.1	1467.5	1454.2	1615.7	1633.5	1632.6	1545.4	1466.6	1606.8
Avg. Ranking	2.78	2.54	2.42	5.28	5.42	5.54	4.02	2.58	5.07
T zone entrance [s]	1296.1	1292	1283	1440.4	1456.4	1461.7	1375.6	1290.4	1433.5
T mark rounding [s]	181.9	175.5	171.2	175.3	177.1	170.9	169.9	176.2	173.3
# of Tacks	8.6	8.1	6.7	14.3	16	16.8	15.9	7.8	15.8

Table 37 illustrates the results of the multiple fleet races with seven participating yachts where three differently levelled BBN sailors had to race against four RB yachts. The superiority of the BBN over the RB yachts could be also observed in these races. The average ranking of the BBN yachts reached the value of 2.58 and the one for the RB yachts 5.07 meaning that a RB yacht finished the race 2.49 places behind a BBN yacht. Also the total averaged race time drew a clear picture with 1466.60 sec needed by the BBN yacht to 1606.80 sec needed by the RB yachts.

The BBN yachts won 48 (96%) races, became 2nd in 37 (74%) and 3rd in 28 (56%) races. They lost four (8%) in total and became 2nd last in five (10%) races. A different picture had to be drawn when analysing the RB yachts. They won two (4%) races in total, became 2nd in 13 (26%) and 3rd in 22 (44%) races. Consequently, they lost 46 (92%) and became 2nd last 45 (90%).

Again, the timing and the amount of executed tacks were the key to perform well which was effectively done by the BBN sailors who performed 7.80 tacks in average compared to 15.75 tacks needed by the RB yachts meaning that the latter needed more than twice as many tacks to finish a race.

It is worth pointing out that the final average rankings as well as the total race time were in very good agreement to the level of expertise. The expert achieved an average ranking of 2.42, the intermediate one of 2.54 and the skilled sailor one of 2.78. The same

hierarchy applied to the total average race times where the expert sailor was fastest with 1454.20 sec, the intermediate 2nd fastest with 1467.50 sec and the skilled sailor 3rd fastest with 1478.10 sec.

It is also worth to pay some attention on the starting positions and results in this race series with multiple levelled BBN yacht and the unique BBN yacht series. Comparing these two race setups prove that this simulator can be regarded as a realistic and effective multiple fleet race sailing simulator. The analysis below illustrates and proves the effect and the right implementation of the yacht interaction model, of the decision-making process and of the expertise levels of the sailor setup.

The skilled yacht started from SP VI in this yacht series and achieved an averaged total race time of 1478.10 sec. This was 21.40 sec faster compared to the unique BBN yacht when starting from the same SP (1499.50 sec). Contrary to that, the intermediate yacht decreased her performance from SP II and needed 72.50 sec more in this race series compared to the unique one (1395 sec to 1467.50 sec). In contrast to the intermediate yacht, the expert yacht increased her performance by 10.30 sec to 1454.20 sec in this race series compared to 1464.50 sec in the multiple BBN one. An explanation for this phenomenon, that two yachts improved their performances whereas one yacht worsened can be found when having a closer look on the starting position constellation and the hardest opponent setup.

The expert yacht started in the centre of the starting line (x = 0/ y = 0) and the intermediate yacht was set up to be her hardest opponent. After a while, she could stop paying attention to the surrounding RB yachts since they were far behind because of their active sailing behaviour resulting in too many tacks and lost time. Her hardest opponent, the intermediate yacht, started to her left (backboard) from SP II (x = -200/ y = 0) and followed a similar strategy, such as to stay quite long on the first tack. The intermediate's limitation of not being able to read the future wind from 30 sec onwards, the starting position constellation and the similar strategy resulted in a higher positioned expert yacht on the course. The expert yacht took advantage of his/her ability to forward or postpone a tack more effectively than the intermediate yacht and covered her. The covered yacht tried to escape from the disadvantageous situation which can be seen by an additional executed tack in this race series compared to the unique BBN levelled one (8.1 to 7.1). The coverage and therefore extra tack were the reasons why the intermediate yacht decreased her performance. Contrary to that, the expert yacht decreased her potentially better

performance slightly in order to cause more damage to her hardest opponent but without sacrificing too much race time.

The skilled yacht was set up to be the hardest opponent of the intermediate yacht and took advantage of the intermediate's disadvantageous situation. She was in a lucky position since her hardest rival was fighting with the expert yacht and was therefore not able to cover her too many times. This circumstance had a positive effect on the amount of executed tacks which in return improved the race time as mentioned above.

These multiple BBN yacht races with seven participating yachts demonstrated the sophisticated level the simulator achieved in terms of simulating a natural multiple fleet racing competition. The intermediate yacht served as a good example of demonstration since she found the right balance between losing time on the course and limiting the damage caused by a superior opponent. In addition to that, she managed not to lose too much time and kept up her second place in the hierarchy by performing better than the skilled yacht that had a more advantageous starting position.

This fuzzy but well balanced behaviour demonstrated the great advantage of the DFT-BBN approach. Achieving this level of sophistication using a rule-based approach for driving the decision-making engine of the yachts would be a very challenging and time consuming task since every potential race situation has to be predicted in advanced and needs to be captured by an algorithm.

9.2.5 Summary of Sailing Events with 7 competing Yachts

Table 38 shows the averaged results over all races of each fleet racing competition mentioned in this subchapter. The individual results of all three BBN and four RB yachts have been averaged for the different expertise levelled setups.

Table 38: Summary of all four big fleet race competition: 3 BBN yachts vs. 4 RB yachts

	Normal Weather Setup							
	Averaged Results							
	Expertise Setup							
Ranking	Skilled	RB	Interm	RB	Expert	RB	BBN	RB
1st	86%	14%	92%	8%	96%	4%	96%	4%
2nd	78%	22%	80%	20%	80%	20%	74%	26%
3rd	50%	50%	60%	40%	64%	36%	56%	44%
4th	22%	78%	30%	70%	30%	70%	34%	66%
5th	26%	74%	16%	84%	20%	80%	22%	78%
6th	24%	76%	10%	90%	4%	96%	10%	90%
7th	14%	86%	12%	88%	6%	94%	8%	92%
Avg. Race Time [s]	1491.3	1602.4	1459.5	1598.7	1440.5	1592.1	1466.6	1606.8
Avg. Ranking	2.84	4.87	2.59	5.06	2.45	5.17	2.58	5.07
T zone entrance [s]	1318.0	1425.8	1292.2	1425.0	1271.6	1427.5	1290.4	1433.5
T mark rounding [s]	173.3	176.7	167.4	173.7	168.9	164.6	176.2	173.3
# of Tacks	9.3	15.6	7.8	15.8	7.2	15.8	7.8	15.8

Similar to the feet racing competitions with four participating yachts, the same important trends could be observed in the fleet races with seven participating yachts. All BBN yachts outperformed the RB yachts and were clearly superior over them. This obvious superiority was visible in the total race times and the averaged ranking of the yachts.

The three BBN yachts achieved an averaged ranking performance varying from 2.84 (skilled BBN vs. RB) to 2.45 (expert BBN vs. RB) whereas the RB yachts' averaged ranking altered from 4.87 to 5.17. In other words, a RB yacht finished the race course at least two positions worse than a BBN yacht. Hence, the difference in the classification varied from 2.03 (skilled BBN vs. RB) to 2.72 (expert BBN vs. RB).

The general superiority of the BBN yachts could be further improved by increasing the level of expertise of the sailors. Depending on the level of expertise of the BBN yachts, the differences between the RB and BBN yachts varied from 111.1 sec (skilled vs. RB) to 151.6 sec (experts vs. RB). This improve in performance was based on the number and the timing of executed tacks. It could be observed that the higher the expertise level was set up the more efficient the timing of the tacks became that led to a lower number of executed tacks and therefore to a faster total race time compared to the other two BBN setups. The total race times dropped from 1491.3 sec (skilled) to 1459.5 sec (intermediate) to 1440.5 sec (expert) whereas the number of executed tacks also dropped from 9.3 (skilled) to 7.8 (intermediate) to 7.2 (expert). This trend is in good agreement to the studies conducted by Araújo who also observed a decrease of the total race time the higher the level of expertise became (Araújo, 2005). Similar to the small fleet race competitions and identical to

Araújo's observations, the differences between the single expertise groups became smaller the higher the level of expertise of the sailor became. The triangular relationship between expertise level, total race time, and final ranking and its successful simulation proofs the successful modelling of different levels of expertise in a dynamically changing fleet racing environment. Furthermore, it indicated the sophisticated level of the simulator has reached using the DFT-BBN based decision-making engine.

9.3 Olympic vs. *Robo-Race* Fleet Racing Events

This section uses the fleet racing setups introduced in the previous subchapters and provides a link back to real sailing competitions. Therefore, the Olympic fleet racing competitions taking place around Weymouth and Portland in 2012 have been analysed and used to classify the quality of the *Robo-Race* fleet racing simulations.

In order to compare the results of the *Robo-Race* simulations with real data from the Olympics, the procedure of the Olympic fleet races have been copied and schematically embedded into the *Robo-Race* framework. Therefore, the number of participating yachts has been reduced to 7 for the first 10 races and to 4 in the final race, the medal race. The range of participating yachts at the Olympics depended on the event and varied from 16 (Men's Star) to 49 yachts (Men's Laser) for the first 10 races. The number of starting yachts in the medal races was limited to 10. To guarantee a high index of repeatability the Olympic racing procedure has been identically applied to the *Robo-Race* simulations and yield the following competition:

- A series of 10 fleet races with 7 participating yachts (3BBN and 4 rule-based yachts). Points were awarded in each race: first scored one point, second scored two points and so forth. There have been 10 races for most Olympic events and 15 for the Men's 49er.
- After 10 races, all points were added together whereas points from the worst race were discarded.
- The 4 best teams (at the Olympics 10) then advanced to the medal race. Points were doubled, so first place got two points, second got four and so forth. The final

placing was determined by the points total after the medal race. The team with the lowest number of points was the winner.

To ensure the same high level of variety as at the Olympics, the following aspects have been considered:

- Four different weather characteristics have been applied in the first 10 races of a series. The weather has been set up as normal four times and as calm, stormy, and variable twice each. The medal race took place in normal weather conditions.
- Four different fleet racing events (9 at the Olympics) have been set up, whereas the different *Robo-Race* setups mentioned in the previous subchapter have been used:
    - Fleet race with three skilled BBN and four RB yachts
    - Fleet race with three intermediate BBN and four RB yachts
    - Fleet race with three expert BBN and four RB yachts
    - Fleet race with three different (skilled, intermediate, expert) BBN and four RB yachts

All nine fleet racing events at the Olympics including the two windsurfing events (men's and women's RS:X) have been analysed. At the analysis, attention was paid on essential facts, such as the number of first, second and third places of the best three teams. In addition, the total number of places on the podium has been calculated for each team. For the sake of clarity, the results are presented in total as well as in percentage numbers.

It was not intended to produce an exact copy of the Olympic events. The purpose of this study should demonstrate the sophisticated level of *Robo-Race* by looking on trends in the ranking lists. The hypothesis for sailing is that the true champions will emerge only over a number of races because the dynamic environment of a yacht, such as the local wind conditions and the opponents, can provide such a dominant effect within a race and can therefore distort it. Based on these facts, it was more meaningful to average the results of a series and of all events at the end.

The following Table 39 show the top three teams at the individual Olympic sailing competitions whereas Table 40 displays the averaged results over all sailing events.

Table 39: Results of the individual Olympic fleet racing events

Men's RS:X (38 participating teams)												
Medallist	Team	1st	2nd	3rd	worse	Podium		1st	2nd	3rd	worse	Podium
Gold	Netherlands	7	1	2	1	10		64%	9%	18%	9%	91%
Silver	Great Britain	2	2	2	5	6		18%	18%	18%	45%	55%
Bronze	Poland	0	2	1	8	3		0%	18%	9%	73%	27%
Sum		9	5	5	-	-		82%	45%	45%	-	-

Men's Laser (49 participating teams)												
Medallist	Team	1st	2nd	3rd	worse	Podium		1st	2nd	3rd	worse	Podium
Gold	Australia	4	3	0	4	7		36%	27%	0%	36%	64%
Silver	Cyprus	2	1	0	8	3		18%	9%	0%	73%	27%
Bronze	Sweden	0	0	1	10	1		0%	0%	9%	91%	9%
Sum		6	4	1	-	-		55%	36%	9%	-	-

Men's Finn (24 participating teams)												
Medallist	Team	1st	2nd	3rd	worse	Podium		1st	2nd	3rd	worse	Podium
Gold	Great Britain	2	2	2	5	6		18%	18%	18%	45%	55%
Silver	Denmark	3	2	1	5	6		27%	18%	9%	45%	55%
Bronze	France	0	1	1	9	2		0%	9%	9%	82%	18%
Sum		5	5	4	-	-		45%	45%	36%	-	-

Men's 470 (27 participating teams)												
Medallist	Team	1st	2nd	3rd	worse	Podium		1st	2nd	3rd	worse	Podium
Gold	Australia	5	2	2	2	9		45%	18%	18%	18%	82%
Silver	Great Britain	2	3	2	4	7		18%	27%	18%	36%	64%
Bronze	Argentina	0	2	2	7	4		0%	18%	18%	64%	36%
Sum		7	7	6	-	-		64%	64%	55%	-	-

Men's 49er (20 participating teams)												
Medallist	Team	1st	2nd	3rd	worse	Podium		1st	2nd	3rd	worse	Podium
Gold	Australia	5	2	1	8	8		31%	13%	6%	50%	50%
Silver	New Zealand	2	3	1	10	6		13%	19%	6%	63%	38%
Bronze	Denmark	0	1	2	13	3		0%	6%	13%	81%	19%
Sum		7	6	4	-	-		44%	38%	25%	-	-

Men's Star (16 participating teams)												
Medallist	Team	1st	2nd	3rd	worse	Podium		1st	2nd	3rd	worse	Podium
Gold	Sweden	3	1	1	6	5		27%	9%	9%	55%	45%
Silver	Great Britain	3	4	1	3	8		27%	36%	9%	27%	73%
Bronze	Brazil	3	1	2	5	6		27%	9%	18%	45%	55%
Sum		9	6	4	-	-		82%	55%	36%	-	-

Women's RS:X (26 participating teams)												
Medallist	Team	1st	2nd	3rd	worse	Podium		1st	2nd	3rd	worse	Podium
Gold	Spain	4	2	2	3	8		36%	18%	18%	27%	73%
Silver	Finland	1	1	1	8	3		9%	9%	9%	73%	27%
Bronze	Poland	2	1	2	6	5		18%	9%	18%	55%	45%
Sum		7	4	5	-	-		64%	36%	45%	-	-

Women's Laser Radial (41 participating teams)												
Medallist	Team	1st	2nd	3rd	worse	Podium		1st	2nd	3rd	worse	Podium
Gold	China	3	1	1	6	5		27%	9%	9%	55%	45%
Silver	Netherlands	2	1	2	6	5		18%	9%	18%	55%	45%
Bronze	Belgium	2	1	4	4	7		18%	9%	36%	36%	64%
Sum		7	3	7	-	-		64%	27%	64%	-	-

Women's 470 (20 participating teams)												
Medallist	Team	1st	2nd	3rd	worse	Podium		1st	2nd	3rd	worse	Podium
Gold	New Zealand	3	3	0	5	6		27%	27%	0%	45%	55%
Silver	Great Britain	2	2	0	7	4		18%	18%	0%	64%	36%
Bronze	Netherlands	1	1	1	8	3		9%	9%	9%	73%	27%
Sum		6	6	1	-	-		55%	55%	9%	-	-

Table 40: Results of the averaged Olympic fleet racing events

Overall Averaged Results											
Medallists	1st	2nd	3rd	worse	Podium		1st	2nd	3rd	worse	Podium
Gold	4.00	1.89	1.22	4.44	7.11		35%	17%	11%	38%	62%
Silver	2.11	2.11	1.11	6.22	5.33		19%	18%	10%	53%	47%
Bronze	0.89	1.11	1.78	7.78	3.78		8%	10%	16%	67%	33%
Sum	7.00	5.11	4.11	-	-		61%	45%	36%	-	-

The averaged results show that the gold medallists picked up the most victories (35%), followed by the sliver medallists who achieved the second most victories (19%) and the bronze medallists who won 8% of the races. This picture changed when analysing the other two places on the podium. The silver medallist picked up the most second places (18%) which was slightly more than the gold medallist who achieved to become second in 17% of the races. The bronze medallists ended a race on second position in every 10th race that indicated the lowest value of all medallists. Contrary to this, the bronze medallists achieved the most third places (16%) which was 5% more than the gold and 6% more than the silver medallists.

Based on these numbers it is not a surprise that the gold medallists had the highest appearance in the podium places (62%), followed by the silver medallists (47%). The bronze medallists appeared in the top three in almost every third race (33%).

It is also interesting to see that the top three teams picked up 61% of all potential wins. They also took almost half of the available second places (45%) and 36% of the available third places. A similar decrease in numbers could also be observed when analysing the gold medallists' individual performance. There, the value of the achieved first places was the highest and decreased the lower the positions became (35% to 17% to 10%). The silver medallists' performance showed the same behaviour whereas the value of achieved first

places was lower and almost identical with the one of the achieved number of 2nd places (19% to 18% to 10%). Contrary to this, the bronze medallists achieved their highest value with 3rd places and decreased their performance the higher the positions became (8% to 10% to 16%).

Table 41 below show the results of the four sailing events simulated with *Robo-Race*. The averaged results over all events can be seen in Table 42. It is worth mentioning that all three BBN yachts made it through to the medal race as the top three yachts in every sailing event. They all finished on the podium that should not surprise since this superiority of the BBN yachts could be observed in the previous paragraphs of this chapter.

Table 41: Results of the individual *Robo-Race* fleet racing events

Fleet Race Event with 3 skilled BBN and 4 RB Yachts												
Medallist	Team	1st	2nd	3rd	worse	Podium		1st	2nd	3rd	Worse	Podium
Gold	Yacht C	5	2	4	0	11		45%	18%	36%	0%	100%
Silver	Yacht A	2	4	1	4	7		18%	36%	9%	36%	64%
Bronze	Yacht B	2	3	1	5	6		18%	27%	9%	45%	55%
Sum		9	9	6	-	-		82%	82%	55%	-	-

Fleet Race Event with 3 intermediate BBN and 4 RB Yachts												
Medallist	Team	1st	2nd	3rd	worse	Podium		1st	2nd	3rd	Worse	Podium
Gold	Yacht B	5	2	2	2	9		45%	18%	18%	18%	82%
Silver	Yacht A	2	1	5	3	8		18%	9%	45%	27%	73%
Bronze	Yacht C	1	4	1	5	6		9%	36%	9%	45%	55%
Sum		8	7	8	-	-		73%	64%	73%	-	-

Fleet Race Event with 3 expert BBN and 4 RB Yachts												
Medallist	Team	1st	2nd	3rd	worse	Podium		1st	2nd	3rd	Worse	Podium
Gold	Yacht A	5	4	2	0	11		45%	36%	18%	0%	100%
Silver	Yacht C	3	5	0	3	8		27%	45%	0%	27%	73%
Bronze	Yacht B	2	2	3	4	7		18%	18%	27%	36%	64%
Sum		10	11	5	-	-		91%	100%	45%	-	-

Fleet Race Event with 3 mixed BBN and 4 RB Yachts												
Medallist	Team	1st	2nd	3rd	worse	Podium		1st	2nd	3rd	Worse	Podium
Gold	Yacht B	6	5	0	0	11		55%	45%	0%	0%	100%
Silver	Yacht C	3	4	0	4	7		27%	36%	0%	36%	64%
Bronze	Yacht A	2	1	6	2	9		18%	9%	55%	18%	82%
Sum		11	10	6	-	-		100%	91%	55%	-	-

Table 42: Results of the averaged *Robo-Race* fleet racing events

Averaged Results											
Medallist	1st	2nd	3rd	worse	Podium		1st	2nd	3rd	worse	Podium
Gold	5.25	3.25	2	0.5	10.5		48%	30%	18%	5%	95%
Silver	2.5	3.5	1.5	3.5	7.5		23%	32%	14%	32%	68%
Bronze	1.75	2.5	2.75	4	7		16%	23%	25%	36%	64%
Sum	9.5	9.25	6.25	-	-		86%	84%	57%	-	-

Table 42 show the individual and averaged results of the *Robo-Race* fleet racing events. There, the gold medallists picked up the most victories (48%), followed by the silver medallists (23%) and concluded by the bronze medallist who achieved the least victories (16%). A different trend can be observed when analysing the statistics of the distribution for the second place. The silver medallists picked up slightly more second places than the gold medallists (32% to 30%) whereas the bronze medallists performed worse with 23%. In opposite to this, the bronze medallists achieved the most third places (25%) which was 7% more than the gold and 11% more than the silver medallists.

The gold medallists finished almost every race on a podium place (95%), whereas the silver medallists achieved the second highest appearance with 68%, followed by the bronze medallists with 66%. The best three teams picked up 86% of the potential victories, 84% of the potential second places and 57% of the potential third places.

The individual finishing position distribution for the gold medallists showed an increasing performance the higher the places on the podium became (48% to 30% to 18%). Contrary to that, the silver medallists reached there maximum at the 2nd place (32%), whereas the bronze medallists achieved their highest value at the 3rd place (25%).

The analysis of the Olympic and the *Robo-Race* fleet racing events showed identical important trends. In both events the gold medallists picked up the most 1st places, followed by the silver and bronze medallists. The silver medallists achieved the highest number of 2nd places, followed by the gold and bronze medallists. Furthermore, the bronze medallists picked up the most 3rd places, followed by the gold and silver medallists. Moreover, the gold medallists also achieved the highest, the silver medallists the second highest and the bronze medallists the lowest appearance in the podium places. Another similarity can be observed in the finishing position distribution where the top three teams increased their performance the higher the places on the podium became.

In opposite to these important similarities, the absolute numbers disagree which should not surprise since the number of participating yachts at the Olympic events has been higher than at the *Robo-Race* events. At the Olympics, the number of participating yachts varied from 16 (Men's Start) to 49 (Men's Laser) compared to 7 in *Robo-Race*. At the medal race the number of yachts was reduced to 10 at the Olympics and to 4 in *Robo-Race*. Taking these facts into account it should be straightforward that the absolute numbers in the finishing table of the *Robo-Race* events were higher since the probability of a yacht to reach the top three places increased the fewer the number of participating yachts became. The second aspect was the higher number of potential distortions during a race caused by the increased number of opponents. Because of the higher number of yachts and the higher number of potential distortions, it takes more races for the true champion to emerge which lowers the absolute numbers in the race tables. The same effect could be observed for the silver and bronze medallists who also needed longer to emerge from the rest of the field.

Nevertheless, the analysis of the Olympic and *Robo-Race* fleet racing events showed that the most important trends were identical which could be interpreted as a proof that *Robo-Race* reached a sophisticated level to simulate natural sailing behaviour within a multiple fleet racing environment.

9.4 Conclusions

To find out how the new decision-making approach performed on the race course, different fleet racing competitions have been set up. Three yachts controlled by the new decision-making engine, the so called Bayesian-Belief-Network yachts had to compete with yachts controlled by the former decision-making engine of *Robo-Race*, the so called rule-based yachts. Two different fleet racing competitions, a small one consisting of four yachts (three BBN and one RB yacht) and a bigger one with seven yachts (three BBN and four RB yachts) have been set up and an extensive number of races with varying starting positions and different expertise levels of the sailors have been simulated.

The differences in performance between the various BBN yachts among each other and the RB yachts were analysed as well as the effect of different expertise levelled BBN yachts. The feet racing competitions with four and seven participating yachts showed the

same important trends: All BBN yachts outperformed the RB yachts and were clearly superior over them. This superiority of the BBN yachts could be clearly seen in the total race times and the average ranking of the yachts. During the race events with seven participating yachts a RB yacht finished the race course at least two positions worse than a BBN yacht in average.

The general superiority of the BBN yachts was already visible with the basic BBN setup and could be further improved by increasing the level of expertise of the sailors. Depending on the level of expertise of the BBN yachts, the differences between the RB and BBN yachts varied from 100 sec (skilled vs. RB) to 150 sec (experts vs. RB). The simulations showed that the higher the expertise level was set up the more efficient the timing of the tacks became that led to a lower number of executed tacks and therefore to a faster total race time. This observation was in good agreement to the studies carried out by Araújo *et al.* (2005) who also observed a decrease of the total race time the higher the level of expertise became. Another important trend could be observed in the small and big simulated fleet racing competitions that was also identical to Araújo's study. The differences between the single expertise groups became smaller the higher the level of expertise of the sailor became. The triangular relationship between expertise level of the sailor, the total race time, and the final ranking were successfully simulated which in turn demonstrated the successful and realistic modelling of different levels of sailing expertise in a dynamically changing fleet racing environment using the DFT-BBN approach. This successful modelling of different expertise levels of sailors and the superiority of the BBN yacht compared to the rule-based ones indicated that the simulator using a DFT-BBN driven decision-making-engine worked reliable and has reached a sophisticated level in modelling realistic decision-making processes of sailors.

Furthermore, a successful a link back to real sailing has been done. The Olympic fleet racing competitions have been analysed and compared with fleet racing simulations conducted in *Robo-Race*. The procedure of the Olympic fleet races were copied and schematically embedded into the *Robo-Race* framework. The fleet racing setup with seven yachts has been used for the pre-races whereas the four yacht setup has been used for the medal race.

The analysis of the *Robo-Race* fleet racing events and the Olympics showed important trends that were identical. The gold medallists picked up the most 1st places, followed by the silver and bronze medallists. The highest number of 2nd places was

achieved by the silver medallists, followed by the gold and bronze medallists. Furthermore, the bronze medallists picked up the most 3rd places, followed by the gold and silver medallists. Moreover, the same trends could be observed when analysing the sailors' appearance on the podium. At both events, the gold medallists achieved the highest, the silver medallists the second highest and the bronze medallists the lowest appearance on the podium. Another similarity was observed in the finishing position distribution where the top three teams increased their performance the higher the places on the podium became.

The analysis of the Olympic and *Robo-Race* fleet racing events pointed out that the most important trends were identical which could be interpreted as a further confirmation that *Robo-Race* using the new DFT-BBN decision-making engine reached a sophisticated level to simulate natural sailing behaviour within a multiple fleet racing environment.

10 Conclusions and Further Developments

10.1 Summary

This research project developed an advanced AI-system that is capable to simulate the decision-making process of different sailing behaviours/styles as well as different expertise levels of sailors in a dynamically changing yacht racing environment. This study was based on the research carried out by Scarponi (Scarponi *et al.*, 2006, 2007 and Scarponi 2008) that was a good starting point for simulating the behaviour of sailors. At the beginning of this study the advantages and constraints of the simulator had to be determined and a series of tests with real sailor have been conducted. The feedback of the sailors indicted a predictable behaviour of the AI-yachts as well as of the weather conditions. Therefore, the passed on version of *Robo-Race* had to be updated in order to decrease the restrictions and constraints of the simulator which limited the users in their natural sailing behaviour. The human factor plays an important role when determining the yacht's performance over a course and has to be simulated realistically by using state of the art methods and tools for modelling and analysing human decision-making and behaviour. The major challenge posed in modelling the natural decision-making process of a sailor in this dynamic, ongoing and rich in uncertainties sport discipline. The implementation of an advanced input display environment and the detailed description of yacht interaction were incremental updates that yielded a powerful version of *Robo-Race*.

The implemented decision-making model of the early version of *Robo-Race* consisted of a rule-based approach based on questionnaires and can be seen as a prescriptive series of if-sentences which were limited by little rules and regulations. This approach was considered as a starting point to investigate human behaviour but it was also

judged to be too inappropriate for the purpose of this study as it is immobile, not 'fuzzy', strict and becomes very complex the more scenarios are captured. Therefore, a dynamic model containing a great, almost infinitive number of scenarios had to be considered. The system had to be effective and easy to maintain because the more complex the scenarios are set up the more difficult the modelling of the right decision-making process would become. Moreover, the system had to be able to provide a natural mechanism for modelling different sailing behaviours/styles as well as different levels of sailing expertise. Therefore, a combination of the extended decision field theory using Bayesian Belief Networks (Lee *et al.*, 2008) seemed to be a promising way to bear these challenges.

The successful implementation of the developments mentioned above led to important improvements in the field of modelling the decision-making process of sailors since it allows to:

- understand the interaction of a yacht-crew system within a regatta in detail which in turn yield a more accurate performance prediction of the yacht-crew system depending on the sailor's expertise;
- comprehend the decision-making process and behaviour of sailors according to his/her level of expertise and personality;
- develop a strategical and tactical advantage for a yacht race through the pre-knowledge of possible opponents' actions in the future; and
- enhance the sailor's performance within a regatta by using the latest version of *Robo-Race* as a training tool. It would be possible to race against a specific type of sailor as well as against an individual AI copy of a real sailor who's BBN has been updated according to his/her real sailing behaviour.

10.2 Conclusions

A conducted 'human in the loop' test series with real sailors gave important information of the maturity and constraints of the early version of *Robo-Race*. One important constrain, the control and display setup for steering the yacht was solved by applying an advanced display environment in conjunction with a steering wheel which was judged to support the sailors in their natural sailing behaviour. The predictable and non-aggressive behaviour of the opponents identified another constrain of *Robo-Race* which was due to the applied rule-

based decision-making process. Consequently, this inadequate implemented process had to be replaced and therefore, the focus of work was concentrated on developing an advanced decision-making philosophy for *Robo-Race* taking into account the complex and fuzzy inputs of the dynamic fleet racing environment. Another constraint, the model describing yacht interaction was also judged to be inappropriate and had to be replaced to ensure that this important tactical weapon is simulated correctly.

A first step towards this objective was done by carrying out CFD simulations which were used to support the development of a covering and blanketing model based on lifting line theory. Detailed CFD analysis of a yacht's wake gave important insight in the flow behaviour, especially of the vortex core development downstream of a single and two in-line sail rigs. The robust covering and blanketing model for yacht fleet race simulations capable of representing a complex wake field of a yacht has been successfully developed and implemented into *Robo-Race*. The wake of a yacht was simulated as a series of vortex elements that captures the main features of the flow to a sufficient level of fidelity. The lifting line elements move in accordance with the local wind, self-induced velocity and velocity induced by the presence of the wakes of other yachts. Furthermore the superposition of the lifting line model and a viscous wake model to calculate the velocity deficit yield important improvements compared to the previous implemented blanketing model of Philpott *et al.* (2004). Studies evaluating the new wake model's performance and degree of realism were carried out in a series of upwind yacht race scenarios and demonstrated a clear improvement in comparison to the previous wake model. This is not only due to the fact that the new model captures the wake flow changes in magnitude and direction, but also the precise prediction of the limited affected blanketed area and hence the authentically simulated loss in sail thrust makes it superior to other models. By implementing this new covering and blanketing model into the sailing simulator *Robo-Race,* it is believed that an important step has been made to enhance the reality of the physical aspects of the simulator. This improvement provided a more realistic sailing environment for the AI-sailors which in turn support their natural sailing behaviour when controlling a yacht in *Robo-Race.*

The second step dealt with the development of a weather model which captures reasonably well the stochastic nature of the wind environment and its implementation into *Robo-Race.*

The limitations of the original implemented weather model and the superiority of the new weather model were indicated by different test simulations. In particular, the simulations showed the constraints of the single time-frame setup in conjunction with the simple weather model resulting in an unrealistic, unnatural and constraint-rich sailing environment. By introducing individual yacht time-frames an important step forward has been made providing a more realistic yacht race environment. Nevertheless, the real breakthrough has been achieved by combining the individual yacht time-frame setup with a weather series generated by the new weather model.

During the development of the new weather engine of *Robo-Race*, two important points – similarity and independency – had to be considered meaning the closer the yachts are sailing to another, the smaller becomes the time difference of the yachts in the weather series and therefore the more similar is the experienced weather of the two yachts and vice versa. The new developed methodology to introduce a *Master-Yacht* and to change the other yachts to *Slave-Yachts* provides an effective way to deal with similarity and independency. Thereby, the *Slave-Yacht*s' weather conditions were calculated relative to the spatial distance to the *Master-Yacht*. The conducted simulations comparing the simple weather model to the two development stages of the new weather model showed the successful implementation into *Robo-Race* and the correctness of the *Master-Slave-Yacht* setup.

Furthermore, the simple predictable weather model driving the weather engine has been successfully replaced with a model that supports the dynamic, unpredictable, and probabilistic nature of real weather. The sufficient level of realism of the new generated weather model was demonstrated by spectral analyses using Fourier Transform. The new weather model features three components, such as wind speed in lateral and longitudinal as well as the wind direction using an ARMA process for the first two and a combination of an ARMA process and a Markov chain for the latter. The flexibility of those components was further improved by applying special effects to it, like a mean value, ramp, sinusoidal wave or a combination of those three. The weather series generated for a stationary observer has been successfully transformed into one for a moving observer by introducing two different time-frames, the so-called clock and series time-frames, to convert the travel spatial distance on the course to a temporal distance within the weather series.

It has been demonstrated by spectral analyses and the results of the conducted simulations that the new developed weather engine supports to provide a dynamic, natural

and unpredictable yacht race environment for *Robo-Race*. It is believed that with the implementation of the new weather engine an important step forward has been made to capture reasonable well the stochastic nature of a yacht race environment allowing investigations of behaviour pattern and decision-making processes of sailors to a highly sophisticated level.

The third important step of this research project was the development and the implementation of an advanced decision-making engine. The new AI decision-making philosophy based on Decision Field Theory (DFT) using Bayesian-Belief-Network (BBN) as the perceptual processor has been successfully developed for a fleet racing environment and three different sailing behaviours/styles, such as risky/passive, safe/active and balanced/deliberated have been successfully developed and implemented into *Robo-Race*. The spatial perceptions of the sailor on the course as well as the corresponding probability tables used by the BBN have been updated that changed the weighting distribution of the sailors to evaluate options and its attributes. Therefore, it was ensured that the sailors used the available environmental and spatial information differently which yield a subjective evaluation for each option on each attribute which in turn created a unique sailing behaviour/style. These facts are in very good agreement with real sailing where sailors picked up the same available environmental information but applied different weighting distributions to the perceptual variables.

Furthermore, two higher levels of sailing expertise, such as intermediate and expert, have been successfully developed and implemented into *Robo-Race*. These two expertise levels have the ability to read the future wind based on their experience, where the expert was able to read the wind for the next 60 sec and the intermediate for the following 30 sec. This ability has been used for the real time planner that was included into the decision-making process. Depending on the expertise level's ability to read the future wind different planning horizons have been applied.

Extensive sensitivity studies have proven the successful realisation and implementation of the new developed decision-making engine demonstrated that the DFT approach using BBN as the perceptual processor represents an effective decision-making philosophy that is capable to simulate different sailing behaviours/styles realistically. The extension of a real time planner into the decision-making process made it also possible to simulate higher expertise levels of sailors. An extensive number of races with varying

starting positions and different expertise levels of the sailors have been simulated using two different fleet racing competitions, a small one consisting of four yachts (three BBN and one RB yacht) and a bigger one with seven yachts (three BBN and four RB yachts). The fleet racing competitions with four and seven participating yachts showed the same important trends: All BBN yachts outperformed the RB yachts and were clearly superior over them. This superiority of the BBN yachts could be clearly seen in the total race times and the average ranking of the yachts. During the race events with seven participating yachts a RB yacht finished the race course at least two positions worse than a BBN yacht in average. The general superiority of the BBN yachts was already visible with the basic BBN setup and could be further improved by increasing the level of expertise of the sailors. The simulations also showed that the higher the expertise level was set up the more efficient the timing of the tacks became that led to a lower number of executed tacks and therefore to a faster total race time. This observation was in good agreement to the studies carried out by Araújo *et al.* (2005) who also observed a decrease of the total race time the higher the level of expertise became. Another important trend could be observed in the small and big simulated fleet racing competitions that was also identical to Araújo's studies: The differences between the single expertise groups became smaller the higher the level of expertise of the sailor became.

The triangular relationship between expertise level of the sailor, the total race time, and the final ranking were successfully simulated which in turn demonstrated the successful and realistic modelling of different levels of expertise in a dynamically changing fleet racing environment. This successful modelling of different expertise levels of sailors and the superiority of the BBN yachts over the rule-based yachts indicated that the new version of *Robo-Race* using the DFT-BBN driven decision-making engine has reached a sophisticated level in modelling realistic decision-making processes of sailors.

Important effects that influence a decision, such as speed-accuracy or the memory of sailors can be easily modelled by the DFT approach. This was successfully done by changing the corresponding values of the threshold of a decision and the diagonal cell values of the stability matrix *S*. The desired effects were realised by adjusting the corresponding values in the code whereas its structure remained untouched. Realising the same effects just using a rule-based approach would come with a time intensive extension of the existing code since all possible race situations and the related decision outcomes have to be thought of and coded in advance. A detailed simulations and analyses of the

human deliberation process is impossible using just a rule-based approach since it only models the decision outcome and not the process of how a decision has been derived. This represents the great advantage of the DFT model since it simulates the derivation of a decision through describing the deliberation process and the corresponding preferences of a decision maker. Therefore, it is possible to describe the factors that influence a decision which in turn makes it easy to mimic distinctive decision environments, such as time-pressure or the individual influence of a decision maker's memory. This comprehensive tool made it possible to simulate a mature behaviour when two important task aims collide, such as damaging my hardest opponent without threatening my overall aim namely to sail as fast as possible to the upwind mark. There, the DFT-BBN driven decision-making engine found a realistic and efficient compromise within this race situation. Another mature and realistic behaviour could be demonstrated when getting out of an opponent's wake. Contrary to this efficient behaviour, the rule-based yacht showed immature and unrealistic manoeuvres when trying to get out of an opponent's wake by performing various tacks which had a negative effect on the race time. The immaturity of the rule-based yacht and the maturity of the new decision-making engine could be demonstrated by these race situations and the finishing tables in Chapter 9.

Furthermore, a successful a link back to real sailing has been done by comparing fleet racing simulations conducted in *Robo-Race* with the Olympic fleet racing competitions of 2012. The procedure of the Olympic fleet races was copied and schematically embedded into the *Robo-Race* framework. The seven yacht fleet racing setup has been used for the pre-races and the four yacht setup for the medal race.

The analysis of the Olympic and *Robo-Race* fleet racing events showed that important trends, such as the number of first places of the gold medallist or the appearance of each medallist on the podium were in good agreement. This once more points out that *Robo-Race* reached a sophisticated level in describing and mimicking decision-making and behaviours of sailors independent from their expertise level.

10.3 Further Developments

The simulator already reached an advanced level in different categories. Nevertheless, important improvements are still possible regarding

- the physical model of the yacht's motion and hull shape
- the virtual environment
- the AI setup to mimic a real sailors behaviour

The published evidence in Masuyama *et al.* (1995) and the research done by Spenkuch *et al.*, (2008) drew the conclusion that the four degrees of freedom model capturing surge, sway, heel and yaw proved to be appropriate for the purpose of this study since the dynamic behaviour of the yacht and the model's sensitivity to the behaviour of the crew can be judged to be sufficient. Nevertheless, other models that were introduced by Harris (2005) to simulate a yacht racing on an upwind leg by taking into account the yacht's motion in a seaway should be kept in mind. In particular, Keuning's generic mathematical model could be considered as an alternative to Masuyama's model since its implementation would offer the following advantages:

- the model has proven to perform well (Keuning *et al.* 2005, 2007) and is still topic of research. The research team around Keuning is progressively improving the model. Hence, the implemented model can upgraded according to the progress of this research group;
- due to the generic-based model, different hull shapes and therefore different sailing yachts could be implemented in *Robo-Race*. Consequently, the sailing simulator would be based on parameters describing a boat's hull and the corresponding equation of motion. Various boat types could be simulated easily and more potential research projects, such as the investigation of the effect of different yacht types on the behaviour of the sailor, or the determination of the best suited yacht for a special type of sailor would be possible for example; and
- a reliable mathematical model for the tacking manoeuvre could be implemented which also focuses on downwash of the rudder which in turn change the effective angle of attack of the rudder. Therefore, the tacking manoeuvre would be captured in more detail that in turn would enhance the physics of the simulation.

In addition, the motions of the actual steering wheel have to be updated to those of a real yacht steering wheel by using a transfer function. Therefore, the incoming signal from the steering wheel will be weaken or amplified by the function and subsequently transmitted as the desired rudder angle input to the corresponding Simulink® block. Furthermore, as the

actual steering wheel is featured with a force feedback option, the force action on the rudder will be passed on to the steering wheel to provide the sailor with an actual feedback of the acting rudder forces.

The representation of relevant environmental wind and sea conditions would be also important when conduction human-in-the-loop experiments. The actual wind conditions could be displayed on the sea surface by a combination of: (1) adjustable arrows indicating the wind velocity and direction and (2) dynamic moving shades that denote upcoming gusts.

Another important aspect is the implementation of waves within the virtual reality of *Robo-Race* that could not be realised in the limited time scale of this project. In order to enhance the layout and resolution within the VR, the environment of Microsoft's Flight-Simulator® would be a suitable option as its VR already includes waves and could be linked to *Robo-Race*. This job could be carried out as a potential third year project. Therefore, a combination of the Flight-Simulator® environment and Matlab®/Simulink® has to be set up. This has to be done in the way that the yacht's dynamics are calculated by Matlab®/Simulink® which will be used for 'moving' the yacht through the virtual environment generated by Flight-Simulator®. This setup might be too computational-intensive for a conventional workstation that cannot deliver the required real-time simulations. Therefore, a splitting of the computational work on two computers, one for the Matlab®/Simulink®- process and the other one for generating Flight-Simulator® environment can be considered by following the example of Andonian *et al.* (2003).

The author believes that applying these improvements will lead to an even more realistic version of *Robo-Race* in terms of yacht dynamics and virtual environment. Consequently, this updated version would have solved the most important environmental constraints of the existing version of *Robo-Race* which in turn enhances the realism of the simulation and would support the natural behaviour of the real sailors.

References

Abernethy, B., 'Visual Search Strategies and Decision-Making in Sports'. Int. Journal of Sport Psychology, 22, pp.189-210, 1991.

Aschenbrenner, K. M., Albert, D., Schmalhofer, F., 'Stochastic choice heuristics'. Acta Psychologica, 56(1-3), pp. 153-166, 1984.
Adriaans, P., 'From Knowledge-Based to Skill-Based Systems: Sailing as a Machine Learning Challenge'. Springer Berlin/Heidelberg, Vol. 2838, pp. 1-8, 2003.

Alain, C., Sarrazin, C., 'Study of decision-making in squash competition: A computer simulation approach'. Canadian Journal of Sport Sciences, 15(3), pp. 193-200, 1990.

Aler, R., Valls, J.M., Camacho, D., Lopez, A., 'Programming Robosoccer agents by modeling human behavior', Expert Systems with Applications, Vol. 36 (2, Part 1), pp. 1850-1859, 2009.

Andonian, B., Rauch, W., Bhise, V., 'Driver Steering Performance Using Joystick vs. Steering Wheel Controls'. SAE World Congress, 2003-01-0118, 2003.

Araújo, D., Davids, K., Serpa, S., 'An Ecological Approach to Expertise Effects in Decision-Making in a Simulated Sailing Regatta'. Psychology of Sport and Exercise, 6, pp. 671-692, 2005.

Arkin, R.C., 'Behavior-Based Robotics', MIT Press, 1998.

Austin, F., Carbone, G., Falco, M., and Hinz, H., 'Game Theory for Automated Maneuvering During Air-to-Air Combat', Journal of Guidance, Control, and Dynamics, Vol. 13, No. 6, pp. 1143-1149, 1990.

Bailey, R. W., 'Human Performance Engineering: Using Human Factors/Ergonomics to Achieve Computer Usability', 3rd edition, Prentice-Hall, Englewood Cliffs, 1996.

Banks, D. and Singer, B., 'A predictor-corrector technique for visualizing unsteady flow'. IEEE Transactions Visualization and Computer Graphics 1, pp. 151-163, 2000.

Banks, J., Webb A., Spenkuch, T., Turnock, S.R., 'Measurement of dynamic forces experienced by an asymmetric yacht during a Gybe, for use within sail simulation software', 8th International Conference on the Engineering of Sport, Vienna, Austria, 2010.

Bard, C. et al., 'Relationship Between Perceptual Strategies and Response Adequacy in Sport Situations'. Int. Journal of Sport Psychology, 25, pp. 266-281, 1994.

Blackburn, M. J., 'A 90 Minute Dinghy Sailing Race Simulation: Physiological Responses to Discontinuous Isometric Exercise', Honours Thesis, University of Canberra, 1991.

Bossanyi, E. A., 'Short-term stochastic wind prediction and possible control applications', Proceedings of the Delphi Workshop on Wind Energy Applications, 1985.

Bursztyn, P.G., Coleman, S.G., Harrison, J.J.H., 'Laboratory Simulation and the Demands of Single-handed Dinghy Racing', Journal of Physiology, Vol. 400, 14 pages, 1988.

Busemeyer, J.R. and Diederich, A., 'Survey of decision field theory', Mathematical Social Science 43, pp. 345-370, 2002.

Busemeyer, J.R. and Townsend, J.R., 'Decision field theory: a dynamic-cognitive approach to decision making in an uncertain environment', Psychological Review 100, pp. 432–459, 1993.

Caponnetto M., 'The aerodynamic interference between two boats sailing close-hauled', Int. Shipbuild. Progr., 44, no.439, pp. 241-256, 1997.

Chamberlain, C. J., Coelho, A. J., 'The perceptual side of action: Decision-making in sport'. In J. L. Starkes, F. Allard (Eds.), Cognitive issues in motor expertise, Amsterdam, Netherlands: Elsevier Science, pp. 135-157, 1993.

Claughton, A. R., Wellicome, J. F., Shenoi, R. A., 'Sailing yacht design: Theory', 2nd edition, Addison Wesley Longman, Southampton, UK, 2006.

Claughton, A.R., 'Developments in the IMS VPP Formulations'. The 14th Chesapeake Sailing Yacht Symposium, pp. 1-20, 1999.

Collie, S. and Gerritsen, M., 'The Challenging Turbulent Flow Past Downwind Yacht Sails and Practical Application of CFD to Them.' 2nd High Performance Yacht Design Conference Auckland, 2006.

Diederich, A., 'MDFT account of decision making under time pressure'. Psychonomic Bulletin and Review, 10(1), pp. 157-166, 2003.

Dreyfuss, H., 'The Measure of Man: Human Factors in Design', 2nd Edition, Whitney Library of Design, New York, 1967.

Edward, W., ‘Subjective probabilities inferred from decisions’, Psychological Review 69, pp.109-135, 1962.

Engelbrecht, A.P., ‘Computational Intelligence: An Introduction’, Hoboken, N.J.: J. Wiley & Sons., 2002.

Fishburn, P. C., ‘Expected utility: An anniversary and new era. Journal of Risk and Uncertainty’, Vol. 1, pp. 267-284, 1988.

Gaillarde, G., de Ridder, E., van Walree, F., Koning J., ‘Hydrodynamic advice of Sailing Yachts through Seakeeping Study’, The 18th Chesapeake Sailing Yacht Symposium, pp. 107-116, 2007.

Gale, T. J., Walls J. T., ‘Development of a Sailing Dinghy Simulator’, Simulation, Vol. 74, No. 3, pp. 167-179, 2000.

Gerritsma, J., Onnink, R., Versluis A., ‘Geometry, resistance and stability of the Delft systematic yacht hull series’, International Shipbuilding Progress, Volume18, n° 238, pp. 276-297, 1981.

Gibson, F.P., Fichman, M., Plaut, D.C., ‘Learning in dynamic decision tasks: computational model and empirical evidence’, Organizational Behavior and Human Decision Processes, Vol. (71), pp. 1-35, 1997.

Gonzalez, C., Quesada, J., ‘Learning in dynamic decision making: the recognition process’, Computational & Mathematical Organization Theory, Vol. (9), pp. 287-304, 2009.

Goodrich, K.H., and McManus, J.W., ‘Development of a Tactical Guidance Research and Evaluation System (TiGRES)’, Proceedings of the 1989 AIAA Guidance, Navigation, and Control Conference, AIAA Paper 89-3312, 1989.

Griffiths, T.L. and Tenenbaum, J.B., ‘Statistics and the Bayesian mind’, Significance, Vol. 3(4), pp. 130–133, 2006.

Hansen, H., Hochkirch, K., Richards, P., ‘Advances in the Wind Tunnel Analysis of Yacht Sails’, 26th Symposium on Yacht Design and Construction, 2005.

Hanson, D.T., ‘An investigation of the dynamic effects of tacking and jibing on sailing yachts’, MSc Thesis, Ship Science, University of Southampton, 2005.

Harris, D.H., ‘Time Domain Simulation of a Yacht Sailing Upwind in Waves’, The 17th Chesapeake Sailing Yacht Symposium, pp. 13-32, 2005.

Hollnagel, E., ‘Human Reliability Analysis: Context & Control’, Academic Press, 1994.

Jackson, W., (editor), 'Wake Vortex Prediction – an overview', prepared for Transportation Development Centre Transport Canada, 2001.

Johnson, D. M., Stewart II, J. E., 'Use of Virtual Environments for the Acquisition of Spatial Knowledge: Comparison Among Different Visual Displays', Military Psychology, 11(2), pp. 129-148, 1999.

Johnson, J. G., 'Incorporating motivation, individual differences, and other psychological variables in utility-based choice models'. Utility Theory and Applications (Pubblicazione n. 7). Dipartimento di Matematica applicata Bruno de Finetti, Università di Trieste, Italy, pp. 123–142, 2003

Johnson, J. G., 'Cognitive modeling of decision making in sports', Psychology of Sport and Exercise, Vol.7 (6), pp. 631-652, 2006.

Kang, M., 'The effects of agent activeness and cooperativeness on team decision efficiency: A computational simulation study using Team-Soar', International Journal of Human-Computer Studies, Vol. 65 (6), pp. 497-510, 2007.

Katz, J., Plotkin A., 'Low-speed Aerodynamics', 2nd edition, Cambridge University Press, UK, 2001.

Keirsey, D., 'Please Understand Me II: Temperament, Character, Intelligence', Prometheus Nemesis Books, Del Mar, CA, 1998.

Kerwin, J.E., Newman, J.N., 'A summary of the H. Irving Pratt Ocean Race Handicapping Project', The 4th Chesapeake Sailing Yacht Symposium, 1979.

Keuning, J.A., Vermeulen, K.J., 'Further Analysis of the Forces on Keel and Rudder of a Sailing Yacht', The 18th Chesapeake Sailing Yacht Symposium, pp. 49-62, 2007.

Keuning, J.A., Vermeulen, K.J., 'On the Balance of Large Sailing Yachts', The International HISWA Symposium of Yacht Design and Construction, 2002.

Keuning, J.A., Vermeulen, K.J., de Ridder, E.J., 'A generic mathematical model for the manoeuvering and tacking of a sailing yacht', The 17th Chesapeake Sailing Yacht Symposium, pp. 143-163, 2005.

Kikuchi, M. and Takashina, J., 'Development of Marine Simulator for Singlehanded Sailboat', MCMC'94, pp 287-300, 1994.

Körding, K.P. and Wolpert, D.M., 'Bayesian integration in sensorimotor learning', Nature, Vol. (427), pp. 244–247, 2004.

Konar, A. and Chakraborty, U.K., 'Reasoning and unsupervised learning in a fuzzy cognitive map', Information Sciences, Vol. (170), pp. 419-441, 2005.

Korb, K.B., Nicholson, A.E., 'Bayesian Artificial Intelligence', CRC Press, 2004.

Korpus, R., ‘Performance Prediction without Empiricism: A RANS-Based VPP and Design Optimization Capability’, The 18th Chesapeake Sailing Yacht Symposium, pp. 77-94, 2007.

Larrson, L., ‘Principles of Yacht Design’, International Marine/Ragged Mountain Press, 2000.

Lazarus, E., ‘The Application of Value-Driven Decision-Making in Air Combat Simulation’, Proceedings of the 1997 IEEE International Conference on Systems, Man, and Cybernetics, Vol. 3, pp. 2302-2307, 1997.

Lechter, J.S., Jr., Marshall, J.K., Oliver III, J.C., Salvesen, N., ‘Stars and Stripes’, Scientific American, 257(2), pp. 34-40, 1987.

Lee, S., Son, Y.-J., Jin J., ‘Decision field theory extensions for behavior modeling in dynamic environment using Bayesian belief network’, Information Sciences, Vol. 178 (10), pp. 2297-2314, 2008.

Lee, S., Son, Y-J, Jin, J, ‘Decision field theory extensions for behavior modeling in dynamic environment using Bayesian belief network’, Information Sciences, Vol.178 (10), pp. 2297-2314, 2008.

Lesieur, M., Begou, P., Comte, P. and Métais, O., ‘Vortex recognition in numerical simulations’, ERCOFTAC, Bulletin No. 46, pp. 25-28, 2000.

Link, S. W., Heath, R. A., ‘A sequential theory of psychological discrimination’. Psychometrika, 40, pp. 77-105, 1975.

Masuyama, Y., Fukasawa, T., Sasagawa, H., ‘Tacking simulations of sailing yachts - numerical integration of equations of motions and application of neural network technique’, The 12th Chesapeake Sailing Yacht Symposium, pp. 117-131, 1995.

Masuyama, Y., Nakamura, I., Tatano, H., and Takagi, K., ‘Dynamic performance of a sailing cruiser by full scale sea tests’, The 11th Chesapeake Sailing Yacht Symposium, pp. 161-179, 1993.

Masuyama, Y., Tahara, Y., Fukasawa, T., Maeda, N., ‘Database of Sail Shapes vs. Performance and Validation of Numerical Calculation for Upwind Condition’, The 18th Chesapeake Sailing Yacht Symposium, pp. 11-31, 2007.

Morozov, V.V. and Kalyadina, T.V., ‘Green’s model of cylindrical vortex decay’, Computational Mathematics and Modeling, Vol. 19 (2), pp. 186-194, 2008.

Newman, B. and Low, H. ‘Two-dimensional impervious sails: experimental results compared with theory’, Journal of Fluid Mech., Vol. 144, pp. 445-462, 1984.

Nivelleau V. and F., ‘Sillage aérodynamique du voilier – Cartographie générale du sillage - Etude locale (girouette)- interaction de deux voiliers‘. St Cyr l’Ecole, 1994.

Nomoto, K., and Tatano, H., 'Balance of helm of sailing yachts', 4th HISWA Symposium on Yacht Design and Yacht Construction, Amsterdam, 1975.

Orasanu, J., Connolly, T., 'The reinvention of decision-making', Decision-making in action: Models and methods, pp. 3-20, 1993.

Parolini, N. and Quarteroni, A., 'Mathematical models and numerical simulations for the America's Cup', Comput. Methods Appl. Mech. Engineering 194, pp. 1001-1026, 2005.

Patrick, E., Cosgrove D., Slavkovic, A., Rode, J. A., Verratti, T., Chiselko, G., 'Using a Large Projection Screen as an Alternative to Head-Mounted Displays for Virtual Environments', CHI Letters, Vol. 2, Issue 1, pp. 478-485, 2000.

Payne, J. W., Bettman, J. R., Johnson, E. J., 'The adaptive decision maker'. Cambridge: Cambridge University Press, 1993.

Payne, J.W., and Bettman, J.R., 'When time is money: decision behaviour under opportunity-cost time pressure', Organizational Behaviour and Human Decision Processes, Vol.66 (2), pp.131-152, 1996.

Pemberton, R.J., Turnock, S.R., Dodd, T.J., Rogers, E., 'A Novel Method for Identifying Vortical Structures'. Journal of Fluids and Structures, Vol. 16(8), pp. 1051-1057, 2002.

Pheasant, S., 'Bodyspace: Anthropometry, Ergonomics and the Design of the Work', 2nd Edition, Taylor and Francis, London, UK, 1996.

Philpott, A., Henderson S.G., Teirney, D.P., 'A simulation model for predicting yacht match-race outcomes', Operations Research, Vol.52 (1), pp. 1-16, 2004.

Picard, G. and Gleizes, M.P., 'An Agent Architecture to Design Self-Organizing Collectives: Principles and Application', Adaptive Agents and Multi-Agent Systems, Springer, 2003.

Pope, S.B., 'Turbulent Flows', Cambridge University, Cambridge, England, ISBN: 0521598869, 2000.

Preece, J., et al., 'Human-Computer Interaction', ISBN 0-201-62769-8, Addison-Wesley, 1994.

Raab, M., 'T-ECHO: Model of decision making to explain behavior in experiments and simulations under time pressure'. Psychology of Sport and Exercise, 3, pp. 151–171, 2001.

Rabin S., 'AI Game Programming Wisdom', Charles River Media, 1st edition, ISBN 1584500778, 2002.

Rao, R.P.N., Shon, A.P., and Meltzoff, A.N., 'A Bayesian Model of Imitation in Infants and Robots', in Dautenhahn, K. and Nehaniv, C. (editors), 'Imitation and Social Learning in Robots, Humans, and Animals: Behavioural, Social and Communicative Dimensions', Cambridge University Press, 2004.

Ridder, E. J., Vermeulen, K. J., Keuning J. A., ,A Mathematical Model for the Tacking Maneuver of a Sailing Yacht', The International HISWA Symposium on Yacht Design and Yacht Construction, pp. 1-27, 2004.

Ripoll, H., 'The Understanding-Acting Process in Sport: The Relationship Between the Semantic and the Sensorimotor Visual Function', Int. Journal of Sport Psychology, 22, pp. 221-243, 1991.

Roe, R. M., Busemeyer, J. R., Townsend, J. T., 'Multi-alternative decision field theory: A dynamic connectionist model of decision-making'. Psychological Review, 108, pp. 370–392, 2001.

Roncin, K., 'Simulation dynamique de la navigation de deux voiliers en interaction', PhD Thesis, Laboratoire de mécanique des fluides, ECN, 2002.

Roncin K., Kobus J. M., 'Dynamic simulation of two sailing boats in match racing', Sports Engineering, Springer London, Vol. 7(3), pp. 139-152, 2004.

Rothrock, L. and Yin, J., 'Integrating compensatory and noncompensatory decision making strategies in dynamic task environments', in: Kugler, T., Smith, C., Connolly, T., Son, Y., (Eds.), Decision Modeling and Behavior in Uncertain and Complex Environments, Springer, pp. 123–138, 2009.

Ruddle, R. A., Payne, S. J., Jones, D. M., 'Navigating Large-Scale Virtual Environments: What Differences Occur Between Helmet-Mounted and Desk-Top Displays', Presence, Vol. 8, No.2, pp. 157-168, 1999.

Rulence-Paques, P., Fruchart, E., Dru, V., and Mullet, E., 'Cognitive algebra in sport decision making', Theory and Decision, 58, pp.387-406, 2005.

Russell, S. J. and Norvig, P., 'Artificial Intelligence: A Modern Approach', Prentice Hall, 1995.

Rutkowski, C., 'An introduction to the Human Applications Standard Computer Interface, Part 1: Theory and principles', BYTE, Vol. 7, No. 11, pp. 291-310, 1982.

Scarponi M., 'Including Human Performance in the Dynamic Model of a Sailing Yacht: A Combined Ship Science – Behavioural Science Approach Towards a Winning Yacht-Sailor Combination', PhD Thesis, Università di Perugia, 2008.

Scarponi, M., Shenoi, R.A., Turnock, S.R., Conti, P., 'A combined ship science behavioural science approach to create a winning yacht-sailor combination', SNAME, The 18th Chesapeake Sailing Yacht Symposium, pp. 1-10, 2007.

Scarponi, M., Shenoi, R.A., Turnock, S.R., Conti, P., 'Interactions between yacht crew systems and racing scenarios combining behavioural models with VPPs', Proc. of The 19th HISWA Symposium on Yacht Design and Yacht Construction, pp.83-97, 2006.

Schmidt, R. A., Lee, T. D., 'Motor control and learning: a behavioral emphasis'. Champaign, IL: Human Kinetics, 2005.

Shneiderman, B., 'Designing the User Interface, Strategies for Effective Human-Computer Interaction', 3rd Edition, ISBN 0-201-69497-2, Addison-Wesley, 1998.

Shneiderman, B., 'Designing the User Interface, Strategies for Effective Human-Computer Interaction', 4th Edition Preview, ISBN 0-321-19785-2, Addison-Wesley, 2004.

Simon, H.A., 'A behavioral model of rational choice', The Quarterly Journal of Economics 69, pp. 99-118, 1955.

Spenkuch, T., 'Effect of heel on sail rig performance using CFD: a quantified evolution of the ability of CFD to capture this behaviour', MSc Thesis, University of Southampton, UK, 2006.

Spenkuch, T., Turnock, S.R., Scarponi, M., Shenoi, R.A., 'Development of a sailing simulator environment for assessing and improving crew performance', 7th International Conference on the Engineering of Sport, Biarritz, France, 2008.

Spronck, P., Sprinkhuizen-Kuyper, I., Postma, E., 'Improving Opponent Intelligence through Machine Learning', Proceedings 3rd International Conference on Intelligent Games and Simulation, 2002.

Starkes, J., Ericsson, K. A., 'Expert performance in sport: Recent advances in research on sport expertise', Champaign, IL: Human Kinetics, 2003.

Stelzer, R. and Jafarmadar, K., 'A layered system architecture to control an autonomous sailboat', Towards Autonomous Robotic Systems (TAROS 2007), Aberystwyth, UK, pp. 153-159, 2007.

Teeters, J., Ranzenbach, R. and Prince, M., 'Changes to Sail Aerodynamics in the IMS Rule'. The 16th Chesapeake Sailing Yacht Symposium, 2003.

Tennekes, H. and Lumley, J.L., 'A First Course in Turbulence', MIT Press, Cambridge, 1972.

Todter, C., Pedrick, D., Calderon, A., Nelson, B., Debord, F., Dillon, D., 'Stars and Stripes Design Program for the 1992 America's Cup', The 11th Chesapeake Sailing Yacht Symposium, pp. 207-222, 1993.

Tozour, P., 'Introduction to Bayesian Networks and Reasoning under Uncertainty', AI Game Programming Wisdom, 2002a.

Tozour, P., ‘Building an AI Diagnostic Toolset’, AI Game Programming Wisdom, 2002b.

Tozour, P., ‘First-Person Shooter AI Architecture’, AI Game Programming Wisdom, Charles River Media, pp. 387–396, 2002c.

van den Herik, H.J., Donkers, H., Spronck, P.H.M, ’Opponent Modelling and Commercial Games’, Symposium on Computational Intelligence and Games, 2005.

Van der Hoven, I., ‘Power Spectrum of Horizontal Wind Speed in the Frequency Range from 0.0007 to 900 Cycles Per Hour’, Journal of Meteorology, Vol. 14, No. 2, pp. 160-164, 1957.

Virtanen, K., Raivio, T., and Hämäläinen, R.P., ‘Decision Theoretical Approach To Pilot Simulation’, Journal of Aircraft, Vol. 36, No. 4, pp. 632-641, 1999.

Walls, J. T., and Saunders, N. R., ‘Evolution of the Dinghy Simulator, A Tool for Sports Specific Testing’, Proceedings of the Australian Physiological and Pharmacological Society, Vol. 25, No. 2, 1994.

Wallsten, T. S., Barton, C., ‘Processing probabilistic multidimensional information for decisions’. Journal of Experimental Psychology: Learning, Memory, & Cognition, 8, pp. 361-384, 1982.

Wickens, C. D., Hollands, J. G., ‘Engineering Psychology and Human Performance’, Prentice-Hall, Englewood Cliffs, NJ, 2000.

Wickramasinghe, L.K. and Alahakoon, L.D., ‘A Novel Adaptive Decision Making Agent Architecture Inspired by Human Behavior and Brain Study Models’, Fourth International Conference on Hybrid Intelligent Systems (HIS'04), pp.142-147, 2004.

Williams, M., Davids, K., Williams, J., ‘Visual perception and action in sport’, London: E&FN Spon., 1999.

Wooldridge, M. and Jennings, N.R., ‘Intelligent agents: theory and practice’, The Knowledge Engineering Review, Vol. 10(2), pp. 115-152, 1995.

Yacht Research Unit, http://www.engineers.auckland.ac.nz/~dpel004/yru/html/Wind-tunnel/theory.html, University of Auckland, Sept. 2005.

Appendix

A1 CFD Studies for Yacht Interaction

As suggested in the previous Chapter 5, this chapter describes the development of an advanced model for simulating the interaction of sailing yachts. An introduction to the CFD studies carried out in order to develop a covering and blanketing model for yacht fleet race simulations is given. Therefore, a detailed examination of the performance of a typical upwind sail rig arrangement was performed for different heel and yaw angles using a commercial CFD solver. Experimental wind tunnel data provided by the Wolfson Unit for Marine Technology and Industrial Aerodynamics were used to validate the calculated CFD results. The CFD procedure adopted is explained in the following paragraphs.

A1.1 Sloop Rig Model

The Wolfson Unit for Marine Technology and Industrial Aerodynamics evaluated a sailing yacht at the University of Southampton in the low speed section of a wind tunnel (4.6m width by 3.7m height). The model was mounted on a six-component balance attached to a turntable and suspended from the balance in a tank of water (Teeters *et al.*, 2003). Different sail setups and heel angles were tested. The experimental data obtained from these wind tunnel tests were used to carry out a validation study into the influence of heel upon the performance of a sloop rig (see Figure 89).

(a) side view

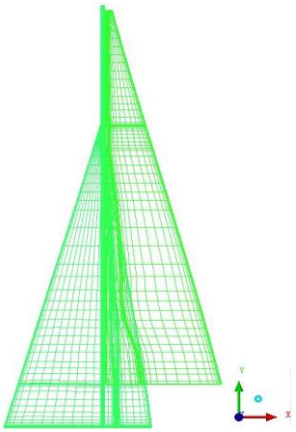

(b) surface mesh (medium)

Figure 89: Views of experimental test (a) and corresponding computational sail rig mesh (b)

The dimensions for the jib and mainsail surfaces are defined by five sections beginning at the foot (0%) and increasing in steps of 25% up to the top (100%). Each sail section shape is defined by its camber, draft, and front and back percentage (see (Spenkuch, 2006) for further information). The angle of the sail towards the mast angle varies for each section to create the span-wise distribution of the sail twist in order to model more realistic sailing conditions. The foot length of the jib and the mainsail are 774 mm and 667 mm respectively. The height of the jib is 1618 mm and the mainsail is 2000 mm high comprising a total sail area A made up of 0.665 m^2 (jib) and 0.720 m^2 (mainsail). Figure 6 shows the sail rig surfaces with a superimposed viscous grid of medium density.

The following 3D simulations with different incidence and heel angles are executed to determine the effect of heeled sails. The comparison with the experimental data shows the level of accuracy of the CFD calculations and gives an idea of the accuracy of the viscous wake analysis. The lift and drag coefficients of the sail rig are used for the validation and defined further below (see Equations A.1 and A.2).

For the viscous sail wake analysis, the criteria of maximum vorticity (Lesieur *et al.*, 2000) and minimum pressure (Banks and Singer, 1995) are used for the identification of the position of the vortex cores. Different surfaces parallel to the inlet and outlet wall of the wind tunnel are introduced downstream of sail rig beginning at the stern of the yacht and continued by 0.5, 1.5, 3.5, 6, 9 yacht lengths behind it for the small domains and 12, 15, 18 yacht lengths for the big domain. On those surfaces the vorticity ω is calculated and defined as the curl of the velocity (see Equation A.3):

$$Cl = \frac{Lift}{0.5\rho u_\infty^2 A} \qquad \text{(A.1)}, \qquad Cd = \frac{Drag}{0.5\rho u_\infty^2 A} \qquad \text{(A.2)},$$

$$\vec{\omega} = \vec{\nabla} \times \vec{u} \qquad \text{(A.3)},$$

where A is the sail area of 1.385 m^2.

Two additional analysis surfaces are introduced 0.2 sail rig lengths upwind of the rig in order to determine the flow angle 'seen' by the rigs.

A1.2 Initial Investigations and Setup

All meshes and simulations for this study were carried out using the software packages of ANSYS® ICEM CFD 11.0 and ANSYS® CFX 10.0. As stated in (Parolini and Quarteroni, 2005), the Shear Stress Transport (SST) offered the best performance for the available computational power and is the applied turbulence model for all calculations within this study, whereas the fluid air is set up as an ideal gas.

Wind tunnel tests on 2D impervious sails carried out by Newman and Low (Newman and Low, 1984) were used to investigate three different mesh types (structured, unstructured and hybrid) at four different mesh densities around typical sail sections with the effect on lift, drag, reattachment and separation locations analysed. The similar Reynolds numbers of 1.2×10^5 (Newman and Low) and 1.71×10^5 (Wolfson Unit data) provide confidence that the flow conditions and behaviour are similar. Further 2D investigations using a cut of the sail rig at the height of 5% of the luff of the mainsail were carried out to determine an appropriate mesh technique, a time step value for the unsteady runs and the difference of the steady and unsteady simulation approach. The structured meshes utilised an H-block topology for each sail with features such as clustering at the leading/trailing edges, boundary layer mesh around the sails to ensure a y+-value of 1 and an O-grid around the mast (see Figures 90 and 91). Detailed information about this mesh sensitivity study can be found in (Spenkuch, 2006).

A structured 2D mesh of 163,900 cells was found to give an acceptable level of fidelity without requiring a too large a 3D mesh. The results of the 2D slice mesh sensitivity study were used to build a 3D mesh around the jib-mainsail-mast configuration. Supplementary investigations into the boundary layer growth on the wind tunnel working section walls

were made to find a method whereby these could be treated with a 'free-slip' condition and yet any axial pressure gradient effects could be captured.

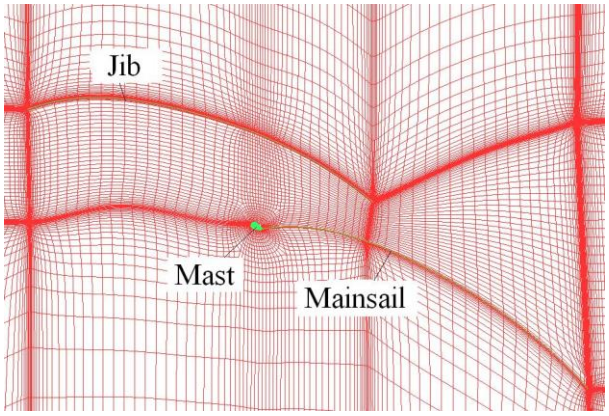

Figure 90: Smooth structured mesh of medium density

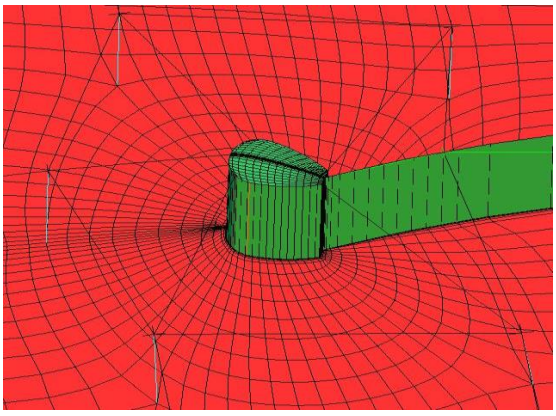

Figure 91: Smooth structured mesh of medium density with O-mesh around the mast (view at mast and mainsail)

For the 3D simulations three structured meshes were chosen, consisting of the wind tunnel domain including the jib, the mainsail and the mast. The applied block topology offers the opportunity to split the blocks around the sail rig in such a way that an approximation to a rotary disc was created in order to adapt the mesh easily to the actual heel and wind incidence angles. The wind tunnel domain is split in 576 blocks; 6 in x-, 8 in y- and 12 in the z-direction. The large number of blocks is due to the need to split the domain 12 times in z-direction to assure that the blocks are correctly associated to the complex twisted sail rig structure. Three structured meshes with the same features as the 2D meshes described above were created for the grid validation investigation (see Table 43).

The following boundary conditions are set up:

- velocity inlet at the wind tunnel inlet, pressure outlet at the wind tunnel outlet;
- no-slip wall condition at the jib, mainsail, mast, wind tunnel bottom; and
- free slip wall condition at the wind tunnel ceiling and side walls (the wind tunnel is reduced by the same amount of the boundary layer thickness on these walls in order to apply these saved cells around the sail rig).

Table 43: Mesh sensitivity study, individual C_D and C_L for the jib and mainsail. A practical restriction of 4 million cells limited further mesh sensitivity studies with finer meshes. 27° AoA and 0° heeled sail rig.

Grid Density	Number of	Jib	Mainsail

	Cells	C_D	C_L	C_D	C_L
Coarse	851,469	0.123	0.934	0.209	0.505
Medium	1,692,787	0.111	0.94	0.207	0.508
Fine	3,374,461	0.102	0.93	0.21	0.516

The velocity of the flow through the wind tunnel domain was 7 m/s that correspond to a Reynolds Number of 1.71×10^5. Two different series of runs were carried out to investigate the effect of the heeling angle and the angle of attack (AoA) on sailing performance. These were:

1. to investigate the influence of the angle of attack, the angle of attack varies whereas the heel angle remains constant (AoA varies in values of 23°, 27°, 32° and the heel angle is kept constant at 0°, 30°);
2. to investigate the influence of the heel angle, the heel angle varies whereas the angle of attack remains constant (AoA remains constant at 27° and the heel angle varies in values of 0°, 10°, 20°, 30°).

In order to complete the detailed wake analysis and to ensure that the size of the wind tunnel domain was sufficient, a larger domain (8.5 sail rig lengths width by 24 sail rig lengths by 2 sail rig lengths height) was generated using 1.8 million cells (Figure 92).

Furthermore, to gain useful information for the evaluation of the lifting line model, a multiple fleet race environment is set up by using an extended wind tunnel domain (2.5 million elements) with two sail rigs in-line and a distance of three sail rig lengths between the up and downwind yacht (Figure 93).

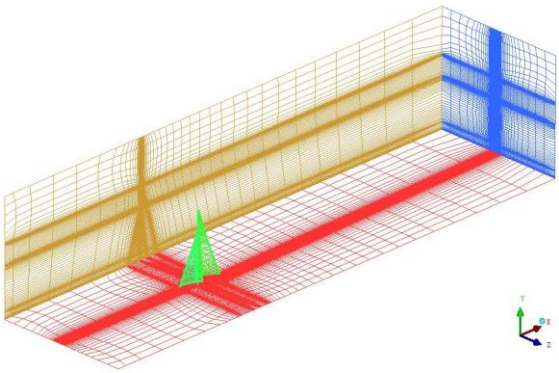

Figure 92: 3D wind tunnel domain mesh of middle density with sail rig located 3 sail rig lengths downstream of the inlet and 10 sail rig length upstream of the outlet

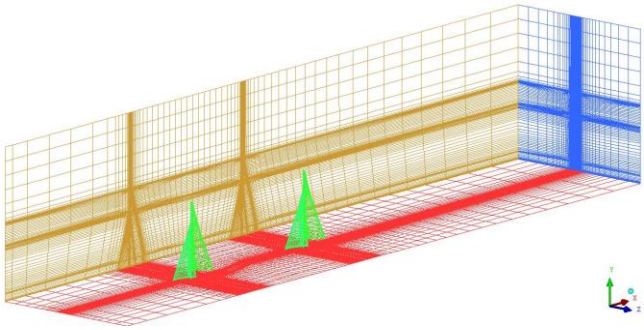

Figure 93: 3D wind tunnel domain mesh with 2 sail rigs in-line, whereas a distance of 3 sail rig lengths is implemented between the yachts.

A1.3 CFD Results for one Yacht

Figure 94 shows the experimental and CFD results for a varying heel angle where the AoA is kept at a constant 27°. It can be seen that C_L and C_D decrease approximately linearly to a heel angle of 20° and increase for the 30° heeled sail rig. Fig. 94 illustrates the same development of the CFD and experimental data as the heel angle increases. It can be seen that CFD is able to capture the flow behaviour observed during the wind tunnel tests in the Wolfson Unit. Generally, an overprediction of the drag coefficient is observed which can be explained by: (1) a general overprediction of drag by the SST model with (2) the use of an insufficiently fine mesh of middle density due to the lack of computational power.

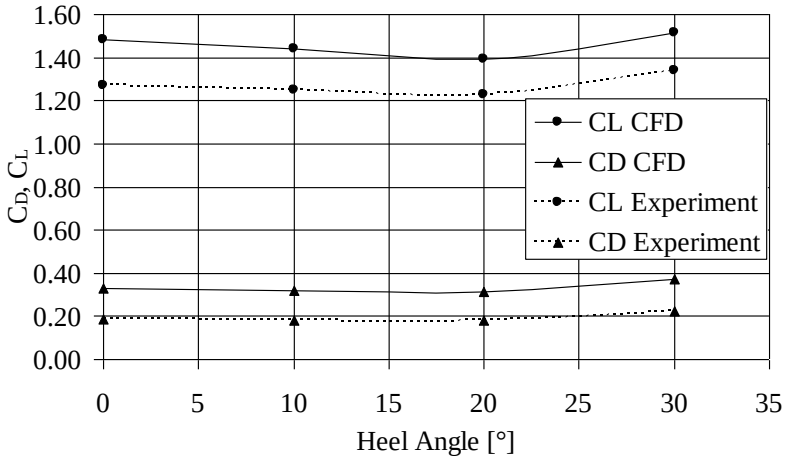

Figure 94: C_D and C_L for experimental data and CFD results. Different heel angles are investigated where the AoA remains constant at the value of 27°.

Figure 95 below displays the CFD results with and without the hull, and the experimental data of the Wolfson Unit. The presented experimental values are obtained by easing the position of the sails (de-powering of the sails) whereas the hull and the wind direction remained constant. The best fit lines describe the efficiency of the sail rig height where lines of shallow slope identify greater efficiency than the steep ones as their lift to drag ratio increases.

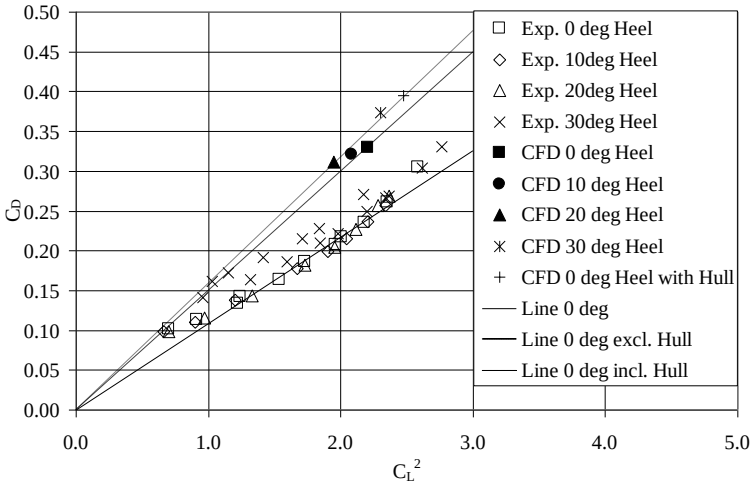

Figure 95: Experimental and CFD data for 27° AoA including hull

The added lines in Figure 95 above show a difference between the efficiency of the 0° and 30° heeled sails for the experimental results as the efficiency increases for the 30° heeled case. This can be viewed as a reduction in the induced drag for the heeled case (Claughton *et al*, 2006). The same behaviour is observed for the CFD results as the lines of best fit identify a loss of efficiency for the 30° heel angle compared to the 0° heel angle simulation. Furthermore, not only is the notable change of the shift in the lines captured by the CFD calculation, but also the fact that the three data points for 0°, 10° and 20° cases are comparable as can also be seen from the experimental results. The effect of the hull on the performance of the sailing yacht is also evident. The slope of the corresponding line is steeper than that of those without the hull. This loss of efficiency can be explained considering Figure 97, where a flow 'jump' over the hull is observed. This 'jump' makes the flow less efficient by changing the pressure distribution of the jib and mainsail in an unfavourable way, especially at the foot.

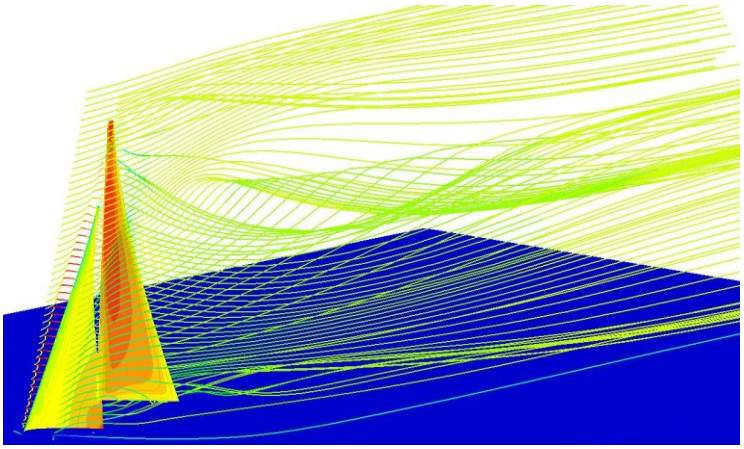

Figure 96: Local pressure contour on sails and streamlines to identify the vortices in the wake. 27° AoA and 10° heeled sail rig.

Three main vortices are generated by the sail rig; two smaller ones at the top of the mast and at the end of the foot of the mainsail and a large vortex around the top region of the jib and mainsail (see Figures 97 and 98). The two smaller vortices decrease in strength rapidly and are almost negligible after 3-4 yacht lengths downstream of the sail rig.

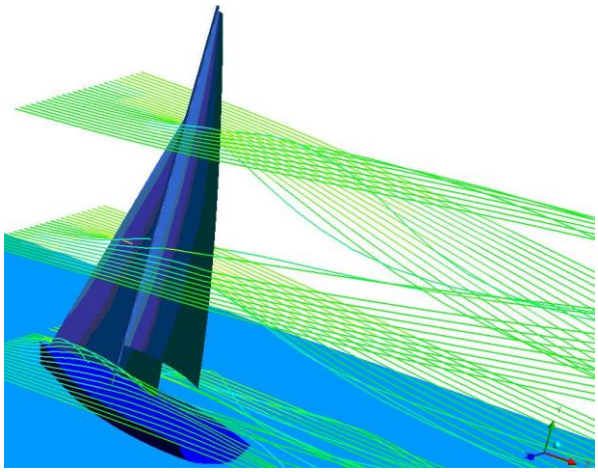

Figure 97: Streamlines around sailing yacht to show the updated flow behaviour downwind as the flow has to 'jump' over the hull. 27° AoA and 0° heel angle.

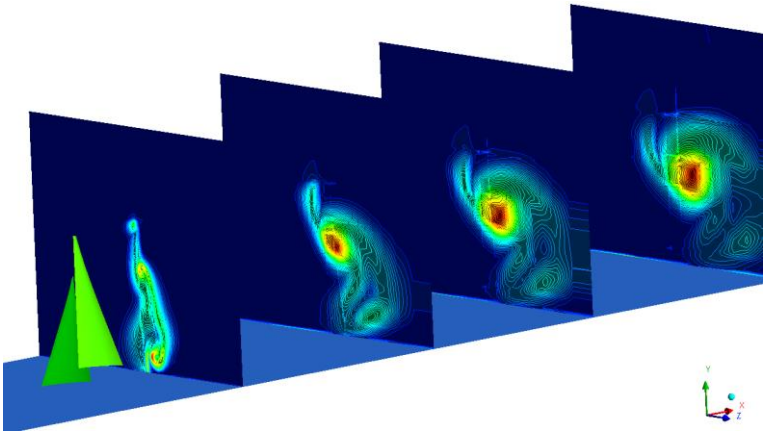

Figure 98: Vortex core development by showing the vorticity contour on surfaces downstream of the sail rig (varying local surface range).

A1.4 CFD Results for two Yachts

The blanketing and covering effects on the downwind yacht due to the presence of the upwind yacht can be seen in Figure 99 and is also clearly visible on the sails' lift and drag coefficients. Table 44 displays the C_L and C_D values of the jibs and mainsails for the two

yachts. The drag on the jib for the downwind yacht increases (plus 35%) whereas the lift decreases in value of 22%. For the mainsail both coefficients decrease in value, whereas the favourable decline of 11% for C_D is accompanied by a 22% loss in lift.

Table 44: C_L and C_D values of the upwind and downwind sail rigs considering the individual sails.

	Jib		Mainsail	
	C_D	C_L	C_D	C_L
Upwind Yacht	0.122	1.038	0.214	0.525
Downwind Yacht	0.165	0.806	0.190	0.412
Difference [%]	35.39	-22.31	-11.01	-21.62

Table 45: Ratio of C_L and C_D of the upwind and downwind sail rigs considering the individual and combined sails.

	C_L/C_D		
	Jib	Mainsail	Combined
Upwind Yacht	8.539	2.459	5.499
Downwind Yacht	4.900	2.166	3.533
Difference	-42.62	-11.92	-35.76

Table 44 shows the loss in performance for the downwind yacht by displaying the ratio of C_L to C_D. The individual sail ratio decreases in value by 43% for the jib and 12% for the mainsail and results in a combined loss for the sail rig of almost 36%. The presence of the upwind yacht alters the flow behaviour significantly whereas the flow angle 'seen' by the downwind yacht is changed by 9.95° considering the 'undisturbed' flow acting on the upwind rig. It should be noted that these values are not directly comparable to those in Table 45 due to the presence of the tunnel walls. Also, in an actual sailing environment the sailing conditions of the downwind yacht would be adjusted. Nevertheless, the loss in performance is real.

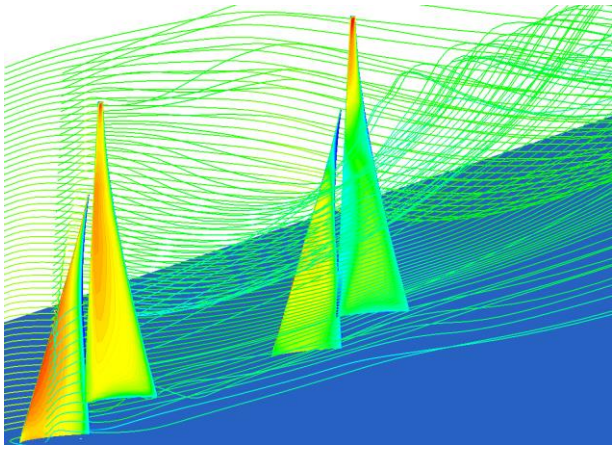

Figure 99: 3D wind tunnel domain mesh with two sail rigs in-line and a distance of 3 sail rig lengths. Varying local pressure contours on downwind sail rig due to the updated flow behaviour. Streamlines to identify the vortices (constant pressure range on both rigs).

A1.5 Results and Discussion

Figure 100 below displays the development of the maximum vorticity of the dominant vortex downstream of the sail rig. It can be observed that the vorticity values have different starting values and decrease exponentially. The varying vorticity starting values can be explained by the difference in sail lift which differs according to the actual incidence angle. The steep decrease in vortex strength continues up to the value of 2 yacht lengths downstream and decelerates thereafter. Furthermore, it can be seen that the exponential decrease in vortex strength (vorticity) does not vary much for the different sail rig setups and wind conditions. The simulation using the large (big) domain illustrates the development of the vortex strength further downstream and continues the exponential vorticity decrease of the smaller domain simulations.

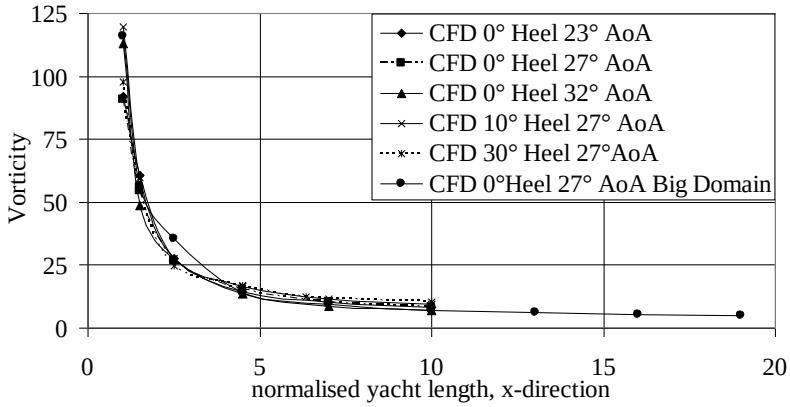

Figure 100: Vorticity development downstream of the sail rig, *0* in x-direction describes the bow and *1* the stern of the sailing yacht, CFD results for different heel and incidence angles using small and big domains.

Figure 101 shows the vertical and tangential tracks of the vortex cores at different locations downstream of the sail rig. It can be observed that the filaments of the vortex cores start at around 70% of the mainsail height, whereas the highest shed off value is reached at 32° AoA. Afterwards, the vortex core filaments decrease to a minimum that occurs at around 57% in vertical and 13% horizontal direction for all runs using the small domain expect for the 30 heeled sail rig setup (60% and 18%, respectively). Subsequently, the vortex cores gain between 3% and 5% in height, whereas the simulation with 32° AoA achieves the greatest increase.

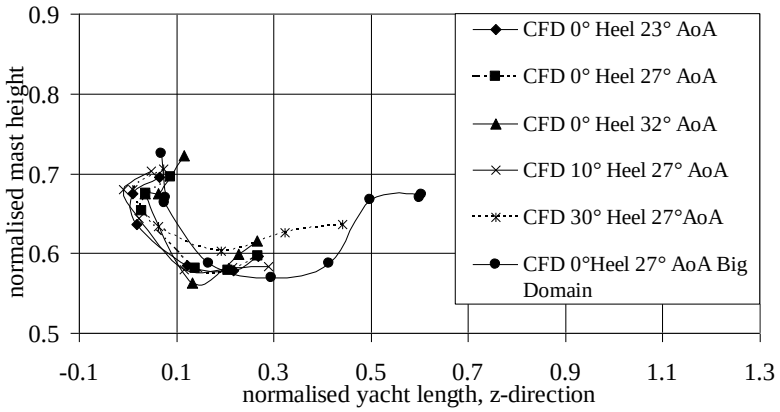

Figure 101: Vortex core tracks within the sail rig wake downstream; the line starting points begin at around 70% of the normalised mainsail height and describe the position of the vortex cores at the stern of the yacht.

Furthermore, the vortex core of the 30° heeled sail rig covers the greatest horizontal distance of all sail rig setups. The big domain simulation shows a slightly different behaviour as the vortex is less influenced by the wind tunnel side walls. The vortices have more space for their development and moves further away from the sail rig. Therefore, the location of the minimum is altered and occurs at around 30% in horizontal direction. Subsequently, the vortex cores increase in height and remain at a horizontal value of 67% for 12, 15 and 18 sail rig lengths downstream of the yacht. Moreover, an almost identical horizontal and vertical location of the vortex cores 15 and 18 sail rig lengths downstream can be observed.

A1.6 Conclusion

This study clearly demonstrates that the effect of heel angle is captured by the RANS-equations using the SST model. The aim of showing the effect of heel on sail rig performance was achieved and the trends of the computed results show good agreement with experimental data. Moreover, the special flow behaviour for the 30 degrees heeled sail rig is well predicted as the flow around the sails is correctly calculated and the difference between the 20 and 30 degrees heel angle is clearly visible, as also observed by experiment. The only disadvantage is the overprediction of the drag coefficient in the simulations. This can be solved by using more computing power. Furthermore, for a more detailed wake analysis, a Statistical Identification Method such as *VORTFIND* has to be considered for

identifying the vortex cores as the used vorticity maxima and pressure minima methods have difficulties in identifying weak vortices in the presence of a shear flow (Pemberton et *al*, 2002). Detailed CFD analysis of a yacht's wake gave important insight in the flow behaviour, especially of the vortex core development downstream of a sail rig. Furthermore, CFD simulations with two in-line yachts were carried out to provide an initial value for the shed height of the line vortex and use of the total sideforce for the vortex strength. Nevertheless, the wake examination, especially the vortex analysis, led to important results that can be used for the development of a more detailed model to capture blanketing and covering within a fleet race.

A2 The asymmetric Gybe Model

During downwind sailing a yacht can alter direction by gybing through the wind. This requires the spinnaker sail to be collapsed and filled on the other side of the yacht. In order to improve the physical fidelity of this process in *Robo-Race* model scale tests of a yacht with an asymmetric spinnaker were performed. These dynamic tests were performed in the University of Southampton 3.8m x 3.8m low speed wind tunnel using controlled motion of the model yacht and dynamometer system passing through a constant wind to determine the dynamic heel and drive forces experienced during a gybe. Due to the trimming of the sails the drive force reduces significantly compared to the equivalent quasi-static approximation as the bow passes through the wind. A relationship was developed to modify the existing quasi static drive force data in *Robo-Race* (Banks *et al.*, 2010). This relationship was applied as a thrust correction factor to account for the dynamic effects when simulating a gybe and is explained below.

To modify the data in *Robo-Race* a relationship had to be developed to represent the experimental data. The wind tunnel data was normalised to match the *Robo-Race* data at the beginning of the gybe. The ratio between the drive force of the normalised wind tunnel data and the quasi static data used in *Robo-Race* was then calculated. This ratio was then used by *Robo-Race* as a thrust correction factor to modify the calculation of drive force, to match the trends determined from wind tunnel testing. By incorporating this, *Robo-Race* could determine the dynamic drive force experienced when gybing for apparent wind angles within the range 130 to 230 degrees. The Thrust Factor is set to 1 when not gybing, when outside this apparent wind angle range or when a gybe has not been initiated or is complete.

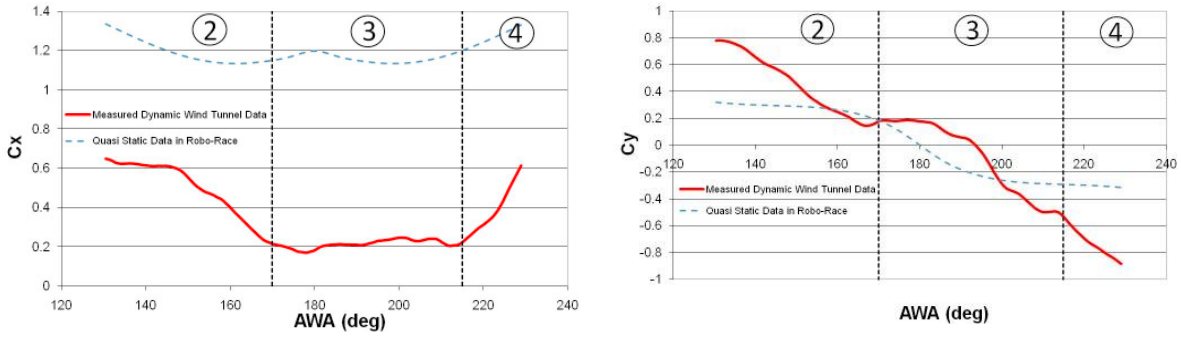

Figure 102: Non-dimensional drive and heel force coefficients (Cx and Cy) for the wind tunnel data, with wake blockage corrections applied, and the quasi static force coefficients used by *Robo-Race*.

To see what impact this modification had on a yacht within *Robo-Race*, a simulation of a yacht gybing with just an asymmetric spinnaker was completed both with and without the Thrust Correction Factor. Figure 103 compares the aerodynamic drive force generated in both cases with experimental data. It can clearly be seen that the drive force calculated with a Thrust Correction Factor agrees much more closely with the wind tunnel data. However it should be noted that unlike the experimental testing the apparent wind speed (AWS) in *Robo-Race* varies throughout the gybe. This is the reason why the drive force increases coming out of the gybe, where the AWS has increased due to the vessel slowing down.

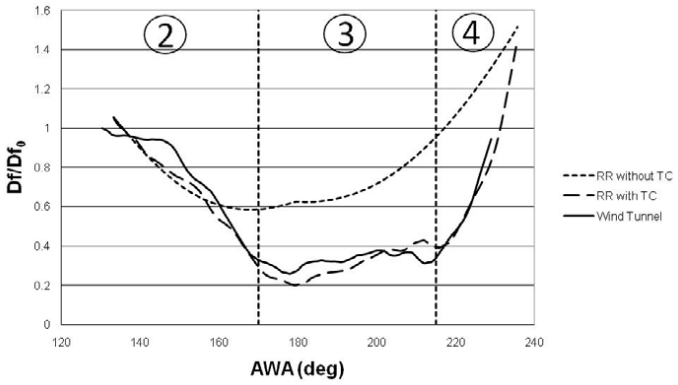

Figure 103: Drive force Df, non-dimensionalised by the initial drive force Df_0 at 130 deg AWA, recorded from a *Robo-Race* simulation with and without the Thrust Correction (TC) applied, plotted alongside the corrected wind tunnel data.

In Figure 104 the impact of this reduction in drive force on the vessels speed, and hence position, can clearly be seen. As you would expect the momentum of the yacht ensures there is little difference going into the gybe between the two simulations. This momentum also delays the point where the minimum surge speed occurs until the yacht has almost

completed the manoeuvre. The use of the thrust correction factor results in a loss of ground of approximately 5m after 40 seconds.

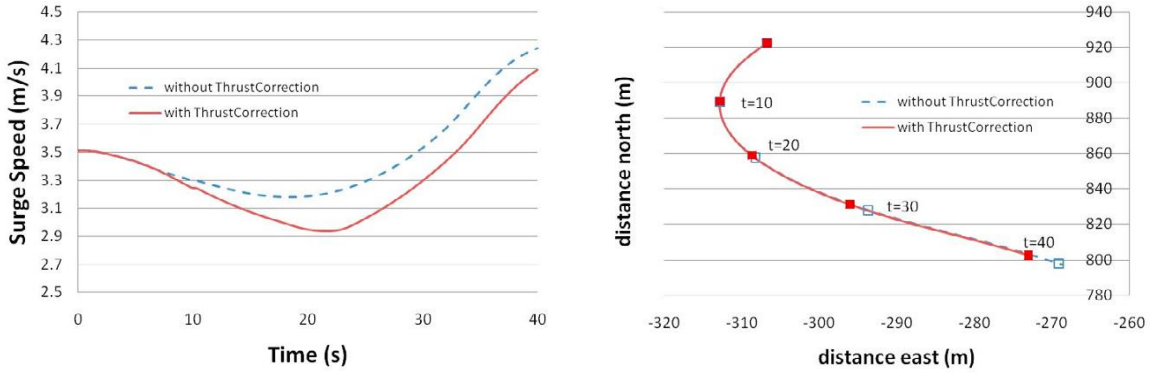

Figure 104: The impact of Thrust Correction on vessel surge speed, and track, with respect to time (t) in seconds. The simulation was performed in a northerly wind of 5 m/s.

The use of the wind tunnel data and their successful modification and implementation into *Robo-Race* led to a significant improvement of the aerodynamic force model in the sail simulation software.

A3 Probability Tables

This section shows the probability tables used by the basic and the superior Bayesian Belief Networks.

Table 46: Probability table used by the basic BBN: Risk node

Risk														
P(LegAxis-Trend)	P(currentSS)	P(LegAxis-Distx)	P(LegAxis-Disty)	balanced				safe				risky		
P_LAx_towards	P_cSS_lifted	P_LDx_close	P_LDy_close	0	0.1	0.9		0	0.1	0.9		0	0.1	0.9
P_LAx_towards	P_cSS_lifted	P_LDx_close	P_LDy_medfar	0	0	1		0	0	1		0	0	1
P_LAx_towards	P_cSS_lifted	P_LDx_medfar	P_LDy_close	0.1	0.2	0.7		0.1	0.2	0.7		0.1	0.2	0.7
P_LAx_towards	P_cSS_lifted	P_LDx_medfar	P_LDy_medfar	0	0.1	0.9		0	0.1	0.9		0	0.1	0.9
P_LAx_towards	P_cSS_neither	P_LDx_close	P_LDy_close	0.1	0.3	0.6		0.1	0.3	0.6		0.1	0.3	0.6
P_LAx_towards	P_cSS_neither	P_LDx_close	P_LDy_medfar	0	0.2	0.8		0	0.2	0.8		0	0.1	0.9
P_LAx_towards	P_cSS_neither	P_LDx_medfar	P_LDy_close	0.1	0.4	0.5		0.1	0.4	0.5		0.1	0.4	0.5
P_LAx_towards	P_cSS_neither	P_LDx_medfar	P_LDy_medfar	0	0.3	0.7		0	0.3	0.7		0	0.3	0.7
P_LAx_towards	P_cSS_headed	P_LDx_close	P_LDy_close	0.3	0.3	0.4		0.3	0.3	0.4		0.3	0.3	0.4
P_LAx_towards	P_cSS_headed	P_LDx_close	P_LDy_medfar	0	0.4	0.6		0	0.4	0.6		0	0.4	0.6
P_LAx_towards	P_cSS_headed	P_LDx_medfar	P_LDy_close	0.4	0.4	0.2		0.4	0.4	0.2		0.3	0.3	0.4
P_LAx_towards	P_cSS_headed	P_LDx_medfar	P_LDy_medfar	0	0.5	0.5		0	0.5	0.5		0	0.4	0.6
P_LAx_awayPar	P_cSS_lifted	P_LDx_close	P_LDy_close	0.6	0.3	0.1		0.6	0.3	0.1		0.4	0.2	0.4
P_LAx_awayPar	P_cSS_lifted	P_LDx_close	P_LDy_medfar	0	0.1	0.9		0	0.1	0.9		0	0.1	0.9
P_LAx_awayPar	P_cSS_lifted	P_LDx_medfar	P_LDy_close	0.7	0.3	0		0.7	0.3	0		0.7	0.3	0
P_LAx_awayPar	P_cSS_lifted	P_LDx_medfar	P_LDy_medfar	0.5	0.4	0.1		0.5	0.4	0.1		0.5	0.4	0.1
P_LAx_awayPar	P_cSS_neither	P_LDx_close	P_LDy_close	0.5	0.3	0.2		0.6	0.4	0		0.5	0.3	0.2
P_LAx_awayPar	P_cSS_neither	P_LDx_close	P_LDy_medfar	0.6	0.4	0		0.6	0.4	0		0.6	0.4	0
P_LAx_awayPar	P_cSS_neither	P_LDx_medfar	P_LDy_close	0.7	0.3	0		0.7	0.3	0		0.7	0.3	0
P_LAx_awayPar	P_cSS_neither	P_LDx_medfar	P_LDy_medfar	0.6	0.4	0		0.6	0.4	0		0.6	0.4	0
P_LAx_awayPar	P_cSS_headed	P_LDx_close	P_LDy_close	0.7	0.3	0		0.8	0.2	0		0.6	0.3	0.1
P_LAx_awayPar	P_cSS_headed	P_LDx_close	P_LDy_medfar	0.8	0.2	0		0.8	0.2	0		0.8	0.2	0
P_LAx_awayPar	P_cSS_headed	P_LDx_medfar	P_LDy_close	1	0	0		1	0	0		1	0	0
P_LAx_awayPar	P_cSS_headed	P_LDx_medfar	P_LDy_medfar	0.8	0.2	0		0.8	0.2	0		0.8	0.2	0

Table 47: Probability table used by the basic BBN: DMG node

Distance Made Good												
P(P(LegAxis-Trend)	P(currentSS)	balanced				safe				risky		
P_LAx_towards	P_cSS_lifted	0.9	0.1	0		0.9	0.1	0		0.9	0.1	0
P_LAx_towards	P_cSS_neither	0.7	0.3	0		0.7	0.3	0		0.7	0.3	0
P_LAx_towards	P_cSS_headed	0.5	0.5	0		0.5	0.5	0		0.5	0.5	0
P_LAx_awayPar	P_cSS_lifted	0.5	0.3	0.2		0.5	0.3	0.2		0.5	0.3	0.2
P_LAx_awayPar	P_cSS_neither	0.2	0.6	0.2		0.2	0.6	0.2		0.2	0.6	0.2
P_LAx_awayPar	P_cSS_headed	0	0.1	0.9		0	0.1	0.9		0	0.1	0.9

Table 48: Probability table used by the basic BBN: Weight-Risk node

Weight-Risk													
P(currentSS)	P(LegAxis-Distx)	P(LegAxis-Disty)	balanced				safe				risky		
P_cSS_lifted	P_LDx_close	P_LDy_close	0.2	0.4	0.4		0.2	0.4	0.4		0	0.2	0.8
P_cSS_lifted	P_LDx_close	P_LDy_medfar	0	0.2	0.8		0	0.2	0.8		0	0	1
P_cSS_lifted	P_LDx_medfar	P_LDy_close	0.6	0.4	0		0.6	0.4	0		0	0.5	0.5
P_cSS_lifted	P_LDx_medfar	P_LDy_medfar	0	0.3	0.7		0.2	0.4	0.4		0	0	1
P_cSS_neither	P_LDx_close	P_LDy_close	0.7	0.3	0		0.7	0.3	0		0.6	0.4	0
P_cSS_neither	P_LDx_close	P_LDy_medfar	0.3	0.5	0.2		0.2	0.5	0.3		0	0	1
P_cSS_neither	P_LDx_medfar	P_LDy_close	0.8	0.2	0		0.8	0.2	0		0	0.3	0.7
P_cSS_neither	P_LDx_medfar	P_LDy_medfar	0.7	0.3	0		0.7	0.3	0		0.4	0.6	0
P_cSS_headed	P_LDx_close	P_LDy_close	0.8	0.2	0		0.8	0.2	0		0.7	0.3	0
P_cSS_headed	P_LDx_close	P_LDy_medfar	0.3	0.4	0.3		0.4	0.4	0.2		0.1	0.1	0.8
P_cSS_headed	P_LDx_medfar	P_LDy_close	0.9	0.1	0		0.9	0.1	0		0.4	0.6	0
P_cSS_headed	P_LDx_medfar	P_LDy_medfar	0.9	0.1	0		0.9	0.1	0		0.5	0.5	0

Table 49: Probability table used by the superior BBN: Risk node

Risk							
P(LegAxis-Trend)	P(currentSS)	P(LegAxis-Distx)	P(LegAxis-Distx)	Wake	balanced		
P_LAx_towards	P_cSS_lifted	P_LDx_close	P_LDy_close	P_Im_In_OW	0	0.1	0.9
P_LAx_towards	P_cSS_lifted	P_LDx_close	P_LDy_close	P_W_neither	0	0.1	0.9
P_LAx_towards	P_cSS_lifted	P_LDx_close	P_LDy_close	P_HO_in_MW	0	0.1	0.9
P_LAx_towards	P_cSS_lifted	P_LDx_close	P_LDy_medfar	P_Im_In_OW	0	0	1
P_LAx_towards	P_cSS_lifted	P_LDx_close	P_LDy_medfar	P_W_neither	0	0	1
P_LAx_towards	P_cSS_lifted	P_LDx_close	P_LDy_medfar	P_HO_in_MW	0	0	1
P_LAx_towards	P_cSS_lifted	P_LDx_medfar	P_LDy_close	P_Im_In_OW	0.1	0.2	0.7
P_LAx_towards	P_cSS_lifted	P_LDx_medfar	P_LDy_close	P_W_neither	0.1	0.2	0.7
P_LAx_towards	P_cSS_lifted	P_LDx_medfar	P_LDy_close	P_HO_in_MW	0.1	0.2	0.7
P_LAx_towards	P_cSS_lifted	P_LDx_medfar	P_LDy_medfar	P_Im_In_OW	0	0.1	0.9
P_LAx_towards	P_cSS_lifted	P_LDx_medfar	P_LDy_medfar	P_W_neither	0	0.1	0.9
P_LAx_towards	P_cSS_lifted	P_LDx_medfar	P_LDy_medfar	P_HO_in_MW	0	0.1	0.9
P_LAx_towards	P_cSS_neither	P_LDx_close	P_LDy_close	P_Im_In_OW	0.1	0.3	0.6
P_LAx_towards	P_cSS_neither	P_LDx_close	P_LDy_close	P_W_neither	0.1	0.3	0.6
P_LAx_towards	P_cSS_neither	P_LDx_close	P_LDy_close	P_HO_in_MW	0.1	0.3	0.6
P_LAx_towards	P_cSS_neither	P_LDx_close	P_LDy_medfar	P_Im_In_OW	0.9	0.1	0
P_LAx_towards	P_cSS_neither	P_LDx_close	P_LDy_medfar	P_W_neither	0.9	0.1	0
P_LAx_towards	P_cSS_neither	P_LDx_close	P_LDy_medfar	P_HO_in_MW	0.9	0.1	0
P_LAx_towards	P_cSS_neither	P_LDx_medfar	P_LDy_close	P_Im_In_OW	0.1	0.4	0.5
P_LAx_towards	P_cSS_neither	P_LDx_medfar	P_LDy_close	P_W_neither	0.1	0.4	0.5
P_LAx_towards	P_cSS_neither	P_LDx_medfar	P_LDy_close	P_HO_in_MW	0.1	0.4	0.5
P_LAx_towards	P_cSS_neither	P_LDx_medfar	P_LDy_medfar	P_Im_In_OW	0	0.3	0.7
P_LAx_towards	P_cSS_neither	P_LDx_medfar	P_LDy_medfar	P_W_neither	0	0.3	0.7
P_LAx_towards	P_cSS_neither	P_LDx_medfar	P_LDy_medfar	P_HO_in_MW	0	0.3	0.7
P_LAx_towards	P_cSS_headed	P_LDx_close	P_LDy_close	P_Im_In_OW	0.3	0.3	0.4
P_LAx_towards	P_cSS_headed	P_LDx_close	P_LDy_close	P_W_neither	0.3	0.3	0.4
P_LAx_towards	P_cSS_headed	P_LDx_close	P_LDy_close	P_HO_in_MW	0.3	0.3	0.4
P_LAx_towards	P_cSS_headed	P_LDx_close	P_LDy_medfar	P_Im_In_OW	1	0	0
P_LAx_towards	P_cSS_headed	P_LDx_close	P_LDy_medfar	P_W_neither	1	0	0
P_LAx_towards	P_cSS_headed	P_LDx_close	P_LDy_medfar	P_HO_in_MW	1	0	0
P_LAx_towards	P_cSS_headed	P_LDx_medfar	P_LDy_close	P_Im_In_OW	0.4	0.4	0.2
P_LAx_towards	P_cSS_headed	P_LDx_medfar	P_LDy_close	P_W_neither	0.4	0.4	0.2
P_LAx_towards	P_cSS_headed	P_LDx_medfar	P_LDy_close	P_HO_in_MW	0.4	0.4	0.2
P_LAx_towards	P_cSS_headed	P_LDx_medfar	P_LDy_medfar	P_Im_In_OW	0.8	0.2	0
P_LAx_towards	P_cSS_headed	P_LDx_medfar	P_LDy_medfar	P_W_neither	0.8	0.2	0
P_LAx_towards	P_cSS_headed	P_LDx_medfar	P_LDy_medfar	P_HO_in_MW	0.8	0.2	0
P_LAx_awayPar	P_cSS_lifted	P_LDx_close	P_LDy_close	P_Im_In_OW	0.6	0.3	0.1
P_LAx_awayPar	P_cSS_lifted	P_LDx_close	P_LDy_close	P_W_neither	0.6	0.3	0.1
P_LAx_awayPar	P_cSS_lifted	P_LDx_close	P_LDy_close	P_HO_in_MW	0.6	0.3	0.1
P_LAx_awayPar	P_cSS_lifted	P_LDx_close	P_LDy_medfar	P_Im_In_OW	0	0.1	0.9
P_LAx_awayPar	P_cSS_lifted	P_LDx_close	P_LDy_medfar	P_W_neither	0	0.1	0.9
P_LAx_awayPar	P_cSS_lifted	P_LDx_close	P_LDy_medfar	P_HO_in_MW	0	0.1	0.9
P_LAx_awayPar	P_cSS_lifted	P_LDx_medfar	P_LDy_close	P_Im_In_OW	0.7	0.3	0
P_LAx_awayPar	P_cSS_lifted	P_LDx_medfar	P_LDy_close	P_W_neither	0.7	0.3	0
P_LAx_awayPar	P_cSS_lifted	P_LDx_medfar	P_LDy_close	P_HO_in_MW	0.7	0.3	0
P_LAx_awayPar	P_cSS_lifted	P_LDx_medfar	P_LDy_medfar	P_Im_In_OW	0.5	0.4	0.1

P_LAx_awayPar	P_cSS_lifted	P_LDx_medfar	P_LDy_medfar	P_W_neither	0.5	0.4	0.1
P_LAx_awayPar	P_cSS_lifted	P_LDx_medfar	P_LDy_medfar	P_HO_in_MW	0.5	0.4	0.1
P_LAx_awayPar	P_cSS_neither	P_LDx_close	P_LDy_close	P_Im_In_OW	0.5	0.3	0.2
P_LAx_awayPar	P_cSS_neither	P_LDx_close	P_LDy_close	P_W_neither	0.5	0.3	0.2
P_LAx_awayPar	P_cSS_neither	P_LDx_close	P_LDy_close	P_HO_in_MW	0.5	0.3	0.2
P_LAx_awayPar	P_cSS_neither	P_LDx_close	P_LDy_medfar	P_Im_In_OW	0	0.2	0.8
P_LAx_awayPar	P_cSS_neither	P_LDx_close	P_LDy_medfar	P_W_neither	0	0.2	0.8
P_LAx_awayPar	P_cSS_neither	P_LDx_close	P_LDy_medfar	P_HO_in_MW	0	0	0.8
P_LAx_awayPar	P_cSS_neither	P_LDx_medfar	P_LDy_close	P_Im_In_OW	0.7	0.3	0
P_LAx_awayPar	P_cSS_neither	P_LDx_medfar	P_LDy_close	P_W_neither	0.7	0.3	0
P_LAx_awayPar	P_cSS_neither	P_LDx_medfar	P_LDy_close	P_HO_in_MW	0.7	0.3	0
P_LAx_awayPar	P_cSS_neither	P_LDx_medfar	P_LDy_medfar	P_Im_In_OW	0.9	0.1	0
P_LAx_awayPar	P_cSS_neither	P_LDx_medfar	P_LDy_medfar	P_W_neither	0.9	0.1	0
P_LAx_awayPar	P_cSS_neither	P_LDx_medfar	P_LDy_medfar	P_HO_in_MW	0.9	0.1	0
P_LAx_awayPar	P_cSS_headed	P_LDx_close	P_LDy_close	P_Im_In_OW	0.7	0.3	0
P_LAx_awayPar	P_cSS_headed	P_LDx_close	P_LDy_close	P_W_neither	0.7	0.3	0
P_LAx_awayPar	P_cSS_headed	P_LDx_close	P_LDy_close	P_HO_in_MW	0.7	0.3	0
P_LAx_awayPar	P_cSS_headed	P_LDx_close	P_LDy_medfar	P_Im_In_OW	0.7	0.3	0
P_LAx_awayPar	P_cSS_headed	P_LDx_close	P_LDy_medfar	P_W_neither	0.7	0.3	0
P_LAx_awayPar	P_cSS_headed	P_LDx_close	P_LDy_medfar	P_HO_in_MW	0.7	0.3	0
P_LAx_awayPar	P_cSS_headed	P_LDx_medfar	P_LDy_close	P_Im_In_OW	1	0	0
P_LAx_awayPar	P_cSS_headed	P_LDx_medfar	P_LDy_close	P_W_neither	1	0	0
P_LAx_awayPar	P_cSS_headed	P_LDx_medfar	P_LDy_close	P_HO_in_MW	1	0	0
P_LAx_awayPar	P_cSS_headed	P_LDx_medfar	P_LDy_medfar	P_Im_In_OW	1	0	0
P_LAx_awayPar	P_cSS_headed	P_LDx_medfar	P_LDy_medfar	P_W_neither	1	0	0
P_LAx_awayPar	P_cSS_headed	P_LDx_medfar	P_LDy_medfar	P_HO_in_MW	1	0	0

Table 50: Probability table used by the superior BBN: DMG node

Distance Made Good					
P(LegAxis-Trend)	P(currentSS)	Wake	balanced		
P_LAx_towards	P_cSS_lifted	P_Im_In_OW	0.9	0.1	0
P_LAx_towards	P_cSS_lifted	P_W_neither	0.9	0.1	0
P_LAx_towards	P_cSS_lifted	P_HO_in_MW	0.9	0.1	0
P_LAx_towards	P_cSS_neither	P_Im_In_OW	0.7	0.3	0
P_LAx_towards	P_cSS_neither	P_W_neither	0.7	0.3	0
P_LAx_towards	P_cSS_neither	P_HO_in_MW	0.7	0.3	0
P_LAx_towards	P_cSS_headed	P_Im_In_OW	0.5	0.5	0
P_LAx_towards	P_cSS_headed	P_W_neither	0.5	0.5	0
P_LAx_towards	P_cSS_headed	P_HO_in_MW	0.5	0.5	0
P_LAx_awayPar	P_cSS_lifted	P_Im_In_OW	0.5	0.3	0.2
P_LAx_awayPar	P_cSS_lifted	P_W_neither	0.5	0.3	0.2
P_LAx_awayPar	P_cSS_lifted	P_HO_in_MW	0.5	0.3	0.2
P_LAx_awayPar	P_cSS_neither	P_Im_In_OW	0.2	0.6	0.2
P_LAx_awayPar	P_cSS_neither	P_W_neither	0.2	0.6	0.2
P_LAx_awayPar	P_cSS_neither	P_HO_in_MW	0.2	0.6	0.2
P_LAx_awayPar	P_cSS_headed	P_Im_In_OW	0	0.1	0.9
P_LAx_awayPar	P_cSS_headed	P_W_neither	0	0.1	0.9
P_LAx_awayPar	P_cSS_headed	P_HO_in_MW	0	0.1	0.9

Table 51: Probability table used by the superior BBN: Weight-Risk node

Weight-Risk						
P(currentSS)	P(LegAxis-Distx)	P(LegAxis-Distx)	Wake	balanced		
P_cSS_lifted	P_LDx_close	P_LDy_close	P_HO_ahead	0.2	0.4	0.4
P_cSS_lifted	P_LDx_close	P_LDy_close	P_HO_b_close	0.2	0.4	0.4
P_cSS_lifted	P_LDx_close	P_LDy_close	P_HO_b_medfar	0.2	0.4	0.4
P_cSS_lifted	P_LDx_close	P_LDy_medfar	P_HO_ahead	0	0.1	0.9
P_cSS_lifted	P_LDx_close	P_LDy_medfar	P_HO_b_close	0	0.1	0.9
P_cSS_lifted	P_LDx_close	P_LDy_medfar	P_HO_b_medfar	0	0.1	0.9
P_cSS_lifted	P_LDx_medfar	P_LDy_close	P_HO_ahead	0.6	0.4	0
P_cSS_lifted	P_LDx_medfar	P_LDy_close	P_HO_b_close	0.6	0.4	0
P_cSS_lifted	P_LDx_medfar	P_LDy_close	P_HO_b_medfar	0.6	0.4	0
P_cSS_lifted	P_LDx_medfar	P_LDy_medfar	P_HO_ahead	0	0.3	0.7
P_cSS_lifted	P_LDx_medfar	P_LDy_medfar	P_HO_b_close	0	0.3	0.7
P_cSS_lifted	P_LDx_medfar	P_LDy_medfar	P_HO_b_medfar	0	0.3	0.7
P_cSS_neither	P_LDx_close	P_LDy_close	P_HO_ahead	0.7	0.3	0
P_cSS_neither	P_LDx_close	P_LDy_close	P_HO_b_close	0.7	0.3	0
P_cSS_neither	P_LDx_close	P_LDy_close	P_HO_b_medfar	0.7	0.3	0
P_cSS_neither	P_LDx_close	P_LDy_medfar	P_HO_ahead	0	0.1	0.9
P_cSS_neither	P_LDx_close	P_LDy_medfar	P_HO_b_close	0	0.1	0.9
P_cSS_neither	P_LDx_close	P_LDy_medfar	P_HO_b_medfar	0	0.1	0.9
P_cSS_neither	P_LDx_medfar	P_LDy_close	P_HO_ahead	0.8	0.2	0
P_cSS_neither	P_LDx_medfar	P_LDy_close	P_HO_b_close	0.8	0.2	0
P_cSS_neither	P_LDx_medfar	P_LDy_close	P_HO_b_medfar	0.8	0.2	0
P_cSS_neither	P_LDx_medfar	P_LDy_medfar	P_HO_ahead	0.5	0.3	0.2
P_cSS_neither	P_LDx_medfar	P_LDy_medfar	P_HO_b_close	0.5	0.3	0.2
P_cSS_neither	P_LDx_medfar	P_LDy_medfar	P_HO_b_medfar	0.5	0.3	0.2
P_cSS_headed	P_LDx_close	P_LDy_close	P_HO_ahead	0.8	0.2	0
P_cSS_headed	P_LDx_close	P_LDy_close	P_HO_b_close	0.8	0.2	0
P_cSS_headed	P_LDx_close	P_LDy_close	P_HO_b_medfar	0.8	0.2	0
P_cSS_headed	P_LDx_close	P_LDy_medfar	P_HO_ahead	0.5	0.3	0.2
P_cSS_headed	P_LDx_close	P_LDy_medfar	P_HO_b_close	0.5	0.3	0.2
P_cSS_headed	P_LDx_close	P_LDy_medfar	P_HO_b_medfar	0.5	0.3	0.2
P_cSS_headed	P_LDx_medfar	P_LDy_close	P_HO_ahead	0.9	0.1	0
P_cSS_headed	P_LDx_medfar	P_LDy_close	P_HO_b_close	0.9	0.1	0
P_cSS_headed	P_LDx_medfar	P_LDy_close	P_HO_b_medfar	0.9	0.1	0
P_cSS_headed	P_LDx_medfar	P_LDy_medfar	P_HO_ahead	0.9	0.1	0
P_cSS_headed	P_LDx_medfar	P_LDy_medfar	P_HO_b_close	0.9	0.1	0
P_cSS_headed	P_LDx_medfar	P_LDy_medfar	P_HO_b_medfar	0.9	0.1	0

Table 52: Extract of probability tables used by the superior BBN setup

Risk							
P_LAx_awayPar	P_cSS_neither	P_LDx_close	P_LDy_medfar	P_Im_In_OW	0.6	0.2	0.2
P_LAx_awayPar	P_cSS_neither	P_LDx_close	P_LDy_medfar	P_W_neither	0.2	0.2	0.6
P_LAx_awayPar	P_cSS_neither	P_LDx_close	P_LDy_medfar	P_HO_in_MW	0	0.2	0.8
P_LAx_awayPar	P_cSS_headed	P_LDx_close	P_LDy_medfar	P_Im_In_OW	0.4	0.3	0.3
P_LAx_awayPar	P_cSS_headed	P_LDx_close	P_LDy_medfar	P_W_neither	0.6	0.3	0.1
P_LAx_awayPar	P_cSS_headed	P_LDx_close	P_LDy_medfar	P_HO_in_MW	0.1	0.2	0.7

Distance Made Good							
P_LAx_awayPar	P_cSS_neither	P_Im_In_OW			0.3	0.4	0.3
P_LAx_awayPar	P_cSS_neither	P_W_neither			0.5	0.4	0.1
P_LAx_awayPar	P_cSS_neither	P_HO_in_MW			0.7	0.3	0
P_LAx_awayPar	P_cSS_headed	P_Im_In_OW			0	0.2	0.8
P_LAx_awayPar	P_cSS_headed	P_W_neither			0.2	0.2	0.6
P_LAx_awayPar	P_cSS_headed	P_HO_in_MW			0.4	0.2	0.4

Weight - Risk							
P_cSS_neither	P_LDx_close	P_LDy_medfar	P_HO_ahead		0.4	0.2	0.4
P_cSS_neither	P_LDx_close	P_LDy_medfar	P_HO_b_close		0.6	0.4	0
P_cSS_neither	P_LDx_close	P_LDy_medfar	P_HO_b_medfar		0.5	0.4	0.1
P_cSS_headed	P_LDx_close	P_LDy_medfar	P_HO_ahead		0.9	0.1	0
P_cSS_headed	P_LDx_close	P_LDy_medfar	P_HO_b_close		0.4	0.3	0.3
P_cSS_headed	P_LDx_close	P_LDy_medfar	P_HO_b_medfar		0.7	0.2	0.1

A4 The Effect of Sailing Behaviour on the Race Course

The following Tables 53 - 56 show the results of the behavioural races that have been simulated with the four different weather scenarios. The outcomes of all three starting position constellations have been averaged and can be found at the right side of the tables.

Table 53: Behavioural races in normal weather conditions

	Normal Weather Setup											
	Starting Position I			Starting Position II			Starting Position III			Averaged Results		
	Behaviour			Behaviour			Behaviour			Behaviour		
Ranking	Risky	Safe	Balanced	Risky	Safe	Balanced	Risky	Safe	Balanced	Risky	Safe	Balanced
1st	12	8	30	20	2	28	16	3	31	32%	9%	59%
2nd	26	7	17	20	14	16	15	21	14	41%	28%	31%
3rd	12	35	3	10	34	6	19	26	5	27%	63%	9%
Avg. Race Time [s]	1434.0	1477.4	1407.5	1418.5	1483.0	1397.2	1424.1	1458.9	1392.7	1425.5	1473.1	1399.1
Avg. Ranking	2	2.54	1.46	1.8	2.64	1.56	2.06	2.46	1.48	1.95	2.55	1.50
T zone entrance [s]	1264.7	1322.3	1250.4	1258.5	1331.8	1244.3	1249.3	1317.3	1225.3	1257.5	1323.8	1240.0
T mark rounding [s]	169.3	155.1	157.1	160.0	151.2	152.9	174.8	141.6	167.4	168.0	149.3	159.1
# of Tacks	3.6	13.0	8.8	3.4	14.0	9.0	3.9	13.2	9.4	3.6	13.4	9.1
# of Limit	0.4	0.0	0.6	0.4	0.1	0.4	0.1	0.0	0.0	0.3	0.0	0.3

Table 53 above shows the results of the races conducted in normal weather conditions. The differences in performance of the sailor setups could be seen when analysing the total race times. They varied between 1392.7 sec and 1407.5 sec for the balanced, between 1418.5 sec and 1434.0 sec for the risky, and between 1458.9 sec and 1483.0 sec for the safe sailors. Based on these numbers, the balanced sailor performed best and left the mark rounding zone around 20 seconds before the risky and around 70 seconds before the safe sailors. Consequently, the balanced sailor won the most and lost the least races. In detail: he/she won 59% of the races, become 2^{nd} in 31% and 3^{rd} in less than 10% of the races in

average. This superior performance led to the best average ranking of around 1.50 that can be explained by the deliberated decision-making process. Therefore, the amount of tacks was moderate and the executed tacks were well timed and in good response to the changing weather conditions.

The risky sailor was 2nd fastest with an average ranking of 1.95. He/she won 32%, become 2nd in 41% and last in 27% of the races. It is worth pointing out that the risky setup needed the longest for rounding the mark independent from the SP. This can be explained by the unfavourable mark zone entrance angle which was caused by a bad positioned yacht which in turn was due to the fact that the yacht hit the outer boundaries several times and therefore could not sail a perfect line towards the mark.

In contrast to that, the safe behaviour had the least amount of hit on the outer boundaries that seems to be logical since the safe sailor was prone to react to weather changes. This behaviour in return caused the highest number of tacks (more than 13 in average) which had a negative effect on the race time. Due to the high number of executed tacks, the yacht was better positioned compared to her two opponents when entering the mark zone leading to the lowest mark rounding times of all yachts independent from the SP.

The balanced behaviour could be considered as the best performing and therefore superior behaviour setup. It presented a good balanced and effective mixture of the safe and risky sailing behaviours in normal weather conditions. This can be seen by the number of performed tacks and hit limits as well as by the mark rounding times which were all between the one of the risky and safe behaviours. The latter two presented extreme behaviours in either direction leading to race signatures with an individual touch, such as a low or high number of performed tacks.

Table 54: Behavioural races in calm weather conditions

	Calm Weather Setup											
	Starting Position I			Starting Position II			Starting Position III			Averaged Results		
	Behaviour			Behaviour			Behaviour			Behaviour		
Ranking	Risky	Safe	Balanced	Risky	Safe	Balanced	Risky	Safe	Balanced	Risky	Safe	Balanced
1st	18	0	32	31	0	19	33	0	17	55%	0%	45%
2nd	32	0	18	19	0	31	17	0	33	45%	0%	55%
3rd	0	50	0	0	50	0	0	50	0	0%	100%	0%
Avg. Race Time [s]	1317.8	1541.5	1312.9	1303.7	1567.8	1313.7	1304.3	1553.0	1316.6	1308.6	1554.1	1314.4
Avg. Ranking	1.64	3	1.36	1.38	3	1.62	1.34	3	1.66	1.45	3.00	1.55
T zone entrance [s]	1172.5	1377.7	1177.8	1170.4	1406.2	1180.9	1167.5	1394.3	1184.9	1170.1	1392.7	1181.2

T mark rounding [s]	145.3	163.8	135.1	133.3	161.6	132.8	136.8	158.8	131.7	138.5	161.4	133.2
# of Tacks	2.1	18.1	2.5	2.1	20.3	3.5	2.0	19.5	3.8	2.1	19.3	3.3
# of Limit	0.9	0.0	1.0	1.0	0.0	1.1	0.9	0.0	0.0	0.9	0.0	0.7

Table 54 above shows the results of the calm weather simulations. They were dominated by the risky and balanced yachts that either became first or second independent from the starting position. Consequently, the safe yacht performed worst and lost all races independent from the starting position. The balanced yacht performed best starting from SP I and won 64% and became 2nd in 36% of the races. The same number but vice visa applied for the risky yacht won 36% and became 2nd in 64% of the races. Regarding SP II and SP III, the risky yacht performed best and won 64% and became 2nd in 36% of all races in average. The same numbers but the other way around applied for the risky yacht won 36% and became 2nd in 64% of the races.

This change of performance towards the risky yacht, the further the SP changed to the right can be explained by the calm weather conditions where a few major wind shifts occurred. Consequently, there was not often the need to tack on the first run. The risky yacht stayed longer on the first tack and the further the SP changed to the right, the longer the risky yacht stayed on the first tack, the more distance could be made towards the mark and the greater her advantage became compared to the other two yachts. This can be seen by analysing the number of executed tacks which decreased from 2.1 to 2.0 the further the SP changed to the right. This fact had a positive effect on the race time which improved from 1317.8 sec (SP I) to around 1304 sec (SP II and SP III). Contrary to this, the number of tacks raised for the balanced yacht the further the SP changed to the right from 2.5 to 3.8. This had a negative effect on the race time which worsened from 1312.9 sec to 1316.6 sec.

The balanced and safe yachts reacted to the major wind shift whereas the safe yacht also responded to medium wind shifts leading to an extremely higher number of tacks. She performed between 18.1 and 20.3 tacks in average which was far more that the other two setups. This high number of tacks was the reason for the bad ranking, the high race time which was around 240 sec higher compared to the other two yachts.

Having analysed these results, the balanced but especially the risky behaviour has to be recommended when sailing in calm weather conditions.

Table 55: Behavioural races in stormy weather conditions

	Stormy Weather Setup											
	Starting Position I			Starting Position II			Starting Position III			Averaged Results		
	Behaviour			Behaviour			Behaviour			Behaviour		
Ranking	Risky	Safe	Balanced	Risky	Safe	Balanced	Risky	Safe	Balanced	Risky	Safe	Balanced
1st	32	5	13	29	4	17	29	4	17	60%	9%	31%
2nd	10	15	25	15	15	20	13	17	20	25%	31%	43%
3rd	8	30	12	6	31	13	8	29	13	15%	60%	25%
Avg. Race Time [s]	1197.9	1286.6	1269.6	1188.9	1276.0	1251.1	1213.3	1310.6	1276.6	1200.0	1291.1	1265.8
Avg. Ranking	1.52	2.50	1.98	1.54	2.54	1.92	1.58	2.50	1.92	1.55	2.51	1.94
T zone entrance [s]	1069.4	1168.2	1149.0	1060.6	1154.3	1127.9	1074.0	1181.5	1146.4	1068.0	1168.0	1141.1
T mark rounding [s]	128.6	118.4	120.6	128.3	121.7	123.2	139.3	129.1	130.2	132.1	123.1	124.7
# of Tacks	2.9	11.9	6.4	2.5	12.1	7.0	2.8	12.6	7.4	2.7	12.2	6.9
# of Limit	0.4	0.0	0.1	0.4	0.0	0.1	0.5	0.0	0.1	0.4	0.0	0.1

Table 55 above shows the results of the races conducted in the stormy weather conditions. The risky yacht performed best by winning 60% and losing 15% of all races. This ranking led to the best overall performance of 1.55. The second best performance with an overall ranking of 1.94 was achieved by the balanced yacht with 31% won races, 43% 2nd places and 25% 3rd places. The safe yacht performed worst by winning the least races (9%), 31% 2nd places and 60% lost races. Consequently, this led to the worst performance with an average ranking of 2.51.

The trends in the ranking were also visible in the total race times leading to the fastest averaged race time of 1200.0 sec achieved by the risky yacht, followed by the balanced yacht with a total race time of 1265.8 sec and the safe yacht with the highest TRT of 1291.1 sec. It is worth pointing out that these total race times were the lowest for all four weather scenarios which should not surprise since the mean wind speed of this weather setup has been the highest with 8.3 ms^{-1}.

The reason for the bad performance of the safe behaviour was, once again, the higher number of tacks leading to the highest race times compared to the other two yachts. In return, the numerous tacks had a positive effect on the position of the yacht when entering the mark rounding zone leading to the least mark rounding times of all three yachts.

The character of the stormy weather setup was similar to the normal one, meaning that the frequency and length of the wind shifts were comparable but the mean wind speed was higher, 8.3 ms^{-1} vs. 5.0 ms^{-1}. Comparing the result of the two weather setups showed a superiority of the balanced yacht in normal and a superiority of the risky yacht in stormy weather conditions. The reason for this discrepancy can be found in the length of the wind

series the yachts saw. Hence, during a stormy weather setup the yachts did not experience as many wind shifts as in the normal setup since they sailed faster to the upwind mark. Therefore, the length of the time period of a stormy weather series used in a race was less leading to a calmer race character. This calmer weather character of the wind shifts has been preferred by the risky yacht that performed best in calm weather conditions (see previous paragraph).

Table 56: Behavioural races in variable weather conditions

	Variable Weather Setup											
	Starting Position I			Starting Position II			Starting Position III			Averaged Results		
	Behaviour			Behaviour			Behaviour			Behaviour		
Ranking	Risky	Safe	Balanced	Risky	Safe	Balanced	Risky	Safe	Balanced	Risky	Safe	Balanced
1st	4	19	27	8	19	23	9	17	24	14%	37%	49%
2nd	7	25	18	11	16	23	11	20	19	19%	41%	40%
3rd	39	6	5	31	15	4	30	13	7	67%	23%	11%
Avg. Race Time [s]	1750.9	1662.7	1653.6	1749.4	1655.8	1650.3	1731.9	1666.4	1627.0	1744.1	1661.6	1643.6
Avg. Ranking	2.7	1.74	1.56	2.46	1.92	1.62	2.42	1.92	1.66	2.53	1.86	1.61
T zone entrance [s]	1548.7	1488.8	1478.5	1549.9	1484.1	1476.7	1523.2	1472.1	1431.6	1540.6	1481.7	1462.3
T mark rounding [s]	202.2	173.9	175.1	199.5	171.7	173.6	208.7	194.3	195.4	203.5	180.0	181.4
# of Tacks	3.7	13.5	13.0	3.9	13.6	12.6	3.8	13.4	12.3	3.8	13.5	12.6
# of Limit	0.0	0.0	0.0	0.0	0.0	0.0	0.0	0.0	0.0	0.0	0.0	0.0

Table 56 above indicates the results of the variable weather races. Similar to the normal weather setup races, the balanced yacht performed best with 49% won races, 40% 2nd places and 11% lost races. This led to an average ranking of 1.61. Contrary to this, the risky yacht performed worst with an average ranking of 2.53. This bad performance was based on 67% lost and 14% won races and 19% 2nd places. The safe yacht performed second best by winning 37% of the races, becoming 2nd in 41% and 3rd in 23% of the races leading to an average ranking around 1.86.

This compared to the other two weather scenarios smaller difference between the balanced and safe behaviour setup can be explained by analysing the number of tacks the two setups executed. The balanced yacht just performed one tack in average less than the safe one. The reason for this could be found in the often changing wind directions and the corresponding responses of the yachts. Due to these variable conditions, the balanced behaviour was forced to tack frequently leading to a behaviour which was similar to the safe one. The risky yacht performed just around a third of the amount of tacks compared to the other two yachts resulting in a passive and inflexible sailing style. This behaviour let to the worst average race time of 1540.6 sec which was around 100 s higher than the fastest setup.

The balanced yacht was well positioned when entering the mark rounding zone due to the higher number of tacks. Nevertheless, the safe yacht was a bit better positioned leading to a two seconds lower mark rounding time. The risky yacht was worst in this category which resulted in a difference between 6 and 30 seconds compared to the other two yachts. Because of her passive sailing behaviour, the risky yacht missed the right time window to tack and stayed on the same tack for too long. Consequently, she could not make much distance towards the mark and lost the link to the other two yachts.

The analyses of the variable race events showed that the balanced behaviour performed best, followed closed by the safe behaviour. Therefore, it is advisable to either sail on a safe or balanced strategy instead of a risky one since this behaviour did not pay off in these variable weather conditions.

A5 The Effect of Sailing Expertise on the Race Course

The following Tables 57 - 64 show the results of the expertise dependent races. The outcome of all three starting position constellations has been averaged and can be found on the right side of each table.

Table 57: Normal weather setup runs with unique applied mark rounding skills

	Normal Weather Setup											
	Starting Position I			Starting Position II			Starting Position III			Averaged Results		
	Expertise			Expertise			Expertise			Expertise		
Ranking	Skilled	Intermed	Expert	Skilled	Intermed	Expert	Skilled	Intermed	Expert	Skilled	Intermed	Expert
1st	9	15	26	8	16	26	8	17	25	17%	32%	51%
2nd	15	20	15	13	21	16	7	24	19	23%	43%	33%
3rd	26	15	9	29	13	8	35	9	6	60%	25%	15%
Avg. Race Time [s]	1420	1400.4	1381.3	1407.8	1392.2	1369.6	1396	1357.6	1348	1407.9	1383.4	1366.3
Avg. Ranking	2.34	2	1.66	2.42	1.94	1.64	2.54	1.84	1.62	2.43	1.93	1.64
T zone entrance [s]	1261.4	1235.5	1219.4	1248	1224.2	1206.3	1220.5	1193	1186.1	1243.3	1217.6	1203.9
T mark rounding [s]	158.6	164.9	161.9	159.8	168	163.3	175.5	164.6	161.9	164.6	165.8	162.4
# of Tacks	9.1	7.8	7.4	9.1	7.8	7	9.1	6.9	6.5	9.1	7.5	7.0
# of Limit	0.4	0.3	0.4	0.2	0.1	0.2	0.2	0.1	0.2	0.3	0.2	0.3

Table 57 shows the results of the simulations where one unique mark rounding expertise level has been applied. Analysing the outcome indicated a superior performance of the expert, a 2nd place for the intermediate and a 3rd place for the skilled sailor. The expert won the most and lost the least races independent from the starting position. The opposite can be observed when analysing the skilled sailor who won the least and lost the most of the races resulting in the worst performance of the three yachts. The intermediate sailor achieved the 2nd best and a balanced performance by winning more races than losing.

The expert had a constantly good performance by winning around 51% and losing 15% of the races almost independent from the starting position leading to an average ranking of 1.64. The intermediate sailor won 32% and lost 25% of the races resulting in an average ranking of 1.92. The skilled sailor performed worst with 17% won and 60% lost races leading to an averaged ranking of 2.44.

The average race time between the expert and the skilled sailors came to around 40 seconds independent from the SP. The intermediate sailor could close the gap and performed between 10 and 22 sec slower that the expert.

The expert's key to success was the small number of well timed tacks. This expertise level needed seven tacks in average to reach and round the mark which was the least compared to the other two sailors (7.5 for the intermediate and 9.1 for the skilled sailors). This piece of information indicated that the higher the level of expertise was, the more effective the sailor became. The higher expertise levelled sailors (intermediate and expert) tried to avoid unnecessary tacks which were achieved by using information about the future. Thereby, the more the sailor knew about the future the better the performance became which can be seen when analysing the expert and intermediate sailors.

The skilled sailor performed worst since he/she did not have any information about the future wind. Hence, the sailor could not postpone, forward or even cancel a tack leading to the highest number of executed tacks of all three sailor expertise setups, i.e. skilled: 9.1, intermediate: 7.5 and expert: 7.0. The limited knowledge about the future wind helped the sailor to avoid unnecessary tacks in the near future (0-30 sec) helping him/her to perform better than the skilled sailor. This had a positive effect on the race times which improved from 1407.9 sec (skilled) to 1383.4 sec (intermediate). The ability of the expert to read the remote future (35-60 sec) had a positive effect on the total average race time that was further improved to 1366.3 sec.

Table 58: Normal weather setup runs with expertise dependent mark rounding skills

	Normal Weather Setup											
	Starting Position I			Starting Position II			Starting Position III			Averaged Results		
	Expertise			Expertise			Expertise			Expertise		
Ranking	Skilled	Intermed	Expert	Skilled	Intermed	Expert	Skilled	Intermed	Expert	Skilled	Intermed	Expert
1st	4	7	39	6	9	35	5	7	38	10%	15%	75%
2nd	8	34	8	11	27	12	4	35	11	15%	64%	21%
3rd	38	9	3	33	14	3	41	8	1	75%	21%	5%
Avg. Race Time [s]	1444.6	1400.4	1359	1431.7	1392.2	1347.5	1422.8	1357.6	1326.8	1433.0	1383.4	1344.4
Avg. Ranking	2.68	2.04	1.28	2.54	2.1	1.36	2.72	2.02	1.26	2.65	2.05	1.30
T zone entrance [s]	1261.4	1235.5	1219.4	1248	1224.2	1206.3	1220.5	1193	1186.1	1243.3	1217.6	1203.9
T mark rounding [s]	183.2	164.9	139.6	183.7	168	141.2	202.3	164.6	140.7	189.7	165.8	140.5
# of Tacks	9.1	7.8	7.4	9.1	7.8	7	9.1	6.9	6.5	9.1	7.5	7.0
# of Limit	0.4	0.3	0.4	0.2	0.1	0.2	0.2	0.1	0.2	0.3	0.2	0.3

The second table, Table 58, shows the results of differently applied expertise levels for rounding the mark (see Chapter 8.2.3). Hence, the mark rounding skills have been updated so that they match the corresponding level of sailing expertise. Consequently, the expert extended his/her lead, whereas the skilled sailor lost more ground in return. The results of the intermediate sailor did not change since the applied mark rounding setup remained the same for this expertise level. Only his/her ranking worsened since the expert extended his/her superiority by needing 21.9 seconds less for rounding the mark compared to the unique mark rounding simulations. In opposite to this, the skilled sailor needed 25.1 seconds more for rounding the mark leading to a worsened average ranking of 2.65, with 10% won and 75% lost races. Contrary to this, the expert improved his/her ranking from 1.64 to 1.30 with 75% won and 5% lost races. Due to the expert's domination, the intermediate sailor worsened his/her performance from 1.93 to 2.05 with 15% won and 21% lost races.

Table 59: Calm weather setup runs with unique applied mark rounding skills

	Calm Weather Setup											
	Starting Position I			Starting Position II			Starting Position III			Averaged Results		
	Expertise			Expertise			Expertise			Expertise		
Ranking	Skilled	Intermed	Expert	Skilled	Intermed	Expert	Skilled	Intermed	Expert	Skilled	Intermed	Expert
1st	15	17	24	13	16	23	9	14	27	25%	31%	49%
2nd	11	23	11	12	21	16	14	21	15	25%	43%	28%
3rd	24	10	15	25	13	11	27	15	8	51%	25%	23%
Avg. Race Time [s]	1318.8	1312.1	1309.6	1317.4	1316.4	1308.4	1321.8	1311.9	1309.8	1319.3	1313.5	1309.3
Avg. Ranking	2.18	1.86	1.82	2.24	1.94	1.76	2.36	2.02	1.62	2.26	1.94	1.73
T zone entrance [s]	1183.6	1180.5	1178.3	1182.3	1181.7	1174.5	1186.3	1178.4	1176.7	1184.1	1180.2	1176.5
T mark rounding [s]	135.2	131.6	131.3	135.1	134.7	133.9	135.5	133.5	133.1	135.3	133.3	132.8
# of Tacks	3.1	2.9	2.6	3.8	3.6	3.5	4.2	4.1	3.8	3.7	3.5	3.3
# of Limit	1	0.7	0.8	1.1	0.9	1	1.2	1	1.1	1.1	0.9	1.0

Table 60: Calm weather setup runs with expertise dependent mark rounding skills

	Calm Weather Setup											
	Starting Position I			Starting Position II			Starting Position III			Averaged Results		
	Expertise			Expertise			Expertise			Expertise		
Ranking	Skilled	Intermed	Expert	Skilled	Intermed	Expert	Skilled	Intermed	Expert	Skilled	Intermed	Expert
1st	1	4	45	1	1	48	1	4	45	2%	6%	92%
2nd	5	40	5	7	42	1	5	40	5	11%	81%	7%
3rd	44	6	0	42	7	1	44	6	0	87%	13%	1%
Avg. Race Time [s]	1337.2	1312.1	1294.3	1337.1	1316.4	1291.5	1338.7	1311.9	1292.9	1337.7	1313.5	1292.9
Avg. Ranking	2.86	2.04	1.1	2.82	2.12	1.06	2.86	2.04	1.1	2.85	2.07	1.09
T zone entrance [s]	1183.6	1180.5	1178.3	1182.3	1181.7	1174.5	1186.3	1178.4	1176.7	1184.1	1180.2	1176.5
T mark rounding [s]	153.6	131.6	116	154.8	134.7	117	152.4	133.5	116.2	153.6	133.3	116.4
# of Tacks	3.1	2.9	2.6	3.8	3.6	3.5	4.2	4.1	3.8	3.7	3.5	3.3
# of Limit	1	0.7	0.8	1.1	0.9	1	1.2	1	1.1	1.1	0.9	1.0

Table 59 shows the results of races in calm weather conditions. Similar to the normal weather setup races, the expert outperformed the intermediate and skilled sailors independent from the starting position. The intermediate performed second best and the skilled sailor became last. It is worth pointing out that the differences in the average race times of the different expertise levels were between two and ten seconds which was far less compared to the 10 and 30 sec difference in the normal weather races. This discrepancy in the race times can be explained by the not often changing major wind conditions and therefore fewer number of executed tacks which were around four less compared to the normal weather setup races. Consequently, the opportunity to avoid unnecessary tacks decreased which was an advantage for the skilled and intermediate sailors. The intermediate, but especially the expert sailor still had the advantage to delay or forward a tack but this skill had a positive effect of secondary order on the total race time which explained the smaller differences between them. Moreover, due to the fact that the major wind direction did not change often, the yachts sailed to the outer limits and hit them twice leading to identical sailing behaviours of the expert and intermediate sailors. Therefore, the yachts finished the races at the same time and achieved the same ranking which explained the higher amount of 50 1st places especially at SP I.

Table 60 shows the results of the simulations where different mark rounding skills have been applied depending on the sailor's level of expertise. The superiority of the expert sailor was very distinctive as he/she won almost every race and lost just one out of the 150 races. The intermediate sailor suffered slightly under the superiority of the expert which decreased his/her average ranking from 1.94 to 2.07. The skilled sailor won 3 out of 150

races and became last in 87% of the races. Hence, his/her ranking worsened from 2.26 to 2.85.

It is worth pointing out that the mark rounding process under these calm weather conditions played an even more important role compared to the normal conditioned weather races since the race times when entering the mark zone differed just between two and ten seconds. In contrast to that, the difference between an effective and ineffective mark rounding was up to 40 sec. Therefore, the ability of rounding the mark could decide whether to win or to lose a race under these calm weather conditions.

Table 61: Stormy weather setup runs with unique applied mark rounding skills

	Stormy Weather Setup											
	Starting Position I			Starting Position II			Starting Position III			Averaged Results		
	Expertise			Expertise			Expertise			Expertise		
Ranking	Skilled	Intermed	Expert	Skilled	Intermed	Expert	Skilled	Intermed	Expert	Skilled	Intermed	Expert
1st	9	15	26	10	15	25	7	14	29	17%	29%	53%
2nd	17	18	15	16	16	18	11	23	16	29%	38%	33%
3rd	24	17	9	24	19	7	32	13	5	53%	33%	14%
Avg. Race Time [s]	1350.9	1325.4	1265.3	1318.4	1264.2	1230.9	1277	1163.9	1144.6	1315.4	1251.2	1213.6
Avg. Ranking	2.3	2.04	1.66	2.28	2.08	1.64	2.5	1.98	1.52	2.36	2.03	1.61
T zone entrance [s]	1215.7	1186.1	1150.9	1198.1	1140.4	1112.7	1158.6	1044.5	1036.8	1190.8	1123.7	1100.1
T mark rounding [s]	135.2	139.3	114.4	120.3	123.8	118.2	118.4	119.4	107.8	124.6	127.5	113.5
# of Tacks	6.9	5.3	4.9	7.2	5.4	5.1	7.9	5.4	5	7.3	5.4	5.0
# of Limit	0	0	0	0	0	0	0	0	0	0.0	0.0	0.0

Table 62: Stormy weather setup runs with expertise dependent mark rounding skills

	Stormy Weather Setup											
	Starting Position I			Starting Position II			Starting Position III			Averaged Results		
	Expertise			Expertise			Expertise			Expertise		
Ranking	Skilled	Intermed	Expert	Skilled	Intermed	Expert	Skilled	Intermed	Expert	Skilled	Intermed	Expert
1st	7	13	30	6	12	32	1	9	40	9%	23%	68%
2nd	15	21	14	17	20	13	17	28	5	33%	46%	21%
3rd	28	16	6	27	18	5	32	13	5	58%	31%	11%
Avg. Race Time [s]	1368.4	1325.4	1251.9	1331.9	1264.2	1218.4	1293.9	1163.9	1131.2	1331.4	1251.2	1200.5
Avg. Ranking	2.42	2.06	1.52	2.42	2.12	1.46	2.62	2.08	1.3	2.49	2.09	1.43
T zone entrance [s]	1215.7	1186.1	1150.9	1198.1	1140.4	1112.7	1158.6	1044.5	1036.8	1190.8	1123.7	1100.1
T mark rounding [s]	152.7	139.3	101	133.8	123.8	105.7	135.3	119.4	94.4	140.6	127.5	100.4
# of Tacks	6.9	5.3	4.9	7.2	5.4	5.1	7.9	5.4	5	7.3	5.4	5.0
# of Limit	0	0	0	0	0	0	0	0	0	0.0	0.0	0.0

Tables 61 and 62 show the results of the simulations conducted in stormy weather conditions. The analysis of the above tables above indicates the same trends as already seen in the normal and calm weather conditioned races. The expert sailor performed best by

winning the most and losing the least races. The second best performance has been achieved by the intermediate sailor who almost won as many races as losing. The weakest performance has been achieved by the skilled sailor who won the least and lost the most races independent from the starting position. The superiority of the expert and the inferiority of the skilled sailor were further increased by applying the same level of expertise for the mark rounding as for the sailing skills.

Similar to the behavioural races in stormy weather conditions, the number of executed tacks varied between the one of the normal and calm weather setups independent from the level of expertise and SP. Again, this can be explained by the calmer character of the stormy weather setup compared to the normal one since the yachts experienced less wind shifts due to their higher sailing speed on the course caused by the higher wind speed. It is worth mentioning that the expert positioned his/her yacht best when entering the mark zone although he/she executed the least tacks overall. This led to the fastest averaged mark rounding times that differed from 113.5 sec (expert) to 124.6 sec (intermediate) to 127.5 sec (skilled). Moreover, the time differences between the three levelled sailors increased for the benefit of the higher skilled sailors. Comparing the mark rounding times of the expert and skilled sailors revealed on difference between 28.1 sec and 51.7 sec depended on the starting position.

Table 63: Variable weather setup runs with unique applied mark rounding skills

	Variable Weather Setup											
	Starting Position I			Starting Position II			Starting Position III			Averaged Results		
	Expertise			Expertise			Expertise			Expertise		
Ranking	Skilled	Intermed	Expert	Skilled	Intermed	Expert	Skilled	Intermed	Expert	Skilled	Intermed	Expert
1st	12	18	20	15	17	18	11	15	24	25%	33%	41%
2nd	17	13	20	9	18	23	16	20	14	28%	34%	38%
3rd	21	19	10	26	15	9	23	15	12	47%	33%	21%
Avg. Race Time [s]	1684.2	1677.8	1670.6	1702.7	1678.2	1663	1691.5	1684.8	1656.6	1692.8	1680.3	1663.4
Avg. Ranking	2.18	2.02	1.8	2.22	1.96	1.82	2.24	2	1.76	2.21	1.99	1.79
T zone entrance [s]	1516.5	1514.9	1509.2	1531	1507.6	1501	1500.7	1490.8	1483.2	1516.1	1504.4	1497.8
T mark rounding [s]	167.7	162.9	161.4	171.7	170.6	162	190.8	194	173.4	176.7	175.8	165.6
# of Tacks	13.8	13.4	13.3	13.8	13.2	12.7	13.4	13.8	12.7	13.7	13.5	12.9
# of Limit	0	0	0	0	0.1	0	0.1	0.1	0	0.0	0.1	0.0

Table 64: Variable weather setup runs with expertise dependent mark rounding skills

	Variable Weather Setup											
	Starting Position I			Starting Position II			Starting Position III			Averaged Results		
	Expertise			Expertise			Expertise			Expertise		
Ranking	Skilled	Intermed	Expert	Skilled	Intermed	Expert	Skilled	Intermed	Expert	Skilled	Intermed	Expert
1st	4	16	30	1	16	33	3	13	34	5%	30%	65%
2nd	14	21	15	15	21	14	19	22	9	32%	43%	25%
3rd	32	13	5	34	13	3	28	15	7	63%	27%	10%
Avg. Race Time [s]	1708.7	1677.8	1648.9	1728.4	1678.2	1642.5	1719.6	1684.8	1634.6	1718.9	1680.3	1642.0
Avg. Ranking	2.56	1.94	1.5	2.66	1.94	1.4	2.5	2.04	1.46	2.57	1.97	1.45
T zone entrance [s]	1516.5	1514.9	1509.2	1531	1507.6	1501	1500.7	1490.8	1483.2	1516.1	1504.4	1497.8
T mark rounding [s]	192.2	162.9	139.7	197.4	170.6	141.5	218.9	194	151.4	202.8	175.8	144.2
# of Tacks	13.8	13.4	13.3	13.8	13.2	12.7	13.4	13.8	12.7	13.7	13.5	12.9
# of Limit	0	0	0	0	0.1	0	0.1	0.1	0	0.0	0.1	0.0

Table 63 shows the results of races in variable weather conditions. Similar to the three other weather setups, the expert performed best but not as superior as before. He/she still won the most and lost the least races but the differences of won races especially for SP II were small, e.g. expert: 18, intermediate: 17, skilled: 15. Nevertheless, the averaged ranking of the expert over all 150 races was the best with a value of 1.79. The second best performance was achieved by the intermediate sailor with and averaged ranking of 1.99 followed by the skilled sailor with 2.21.

This in comparison to the other three weather setups close average ranking can be explained by analysing the number of executed tacks. Due to the variable wind conditions, all three sailor types performed a high number of tacks which was between 12.7 and 13.8. As explained earlier, the number of well timed tacks had a major effect on the race time whereas the ability to postpone or forward a tack can be categorised as secondary order effect since the potential to safe time was smaller compared to the one of a not performed unnecessary tack. This fact and the circumstance that the number of tacks between the sailor setups just varied between 0.8% and 3.8% (SP I), 3.9% and 8.7% (SP II), and 5.5% and 8.7% (SP III) were the reasons that the superiority of the expert sailor was not as distinctive as in the other three weather setups.

Table 64 displays the results of races where an expertise depending mark rounding setup has been applied. Similar to the other three weather setups, the superiority of the expert and consequently the inferiority of the skilled sailor were increased whereas the intermediate could defend its position in the ranking.

A6 Publications

This section also highlights how the present research has contributed and will contribute towards enhancing the modelling and simulation of an advanced yacht-crew-interaction system. The following list gives an overview of realised and possible contributions in journals and conferences:

- Spenkuch, T., Turnock, S.R., Scarponi, M., Shenoi, R.A., 'Development of a sailing simulator environment for assessing and improving crew performance', 7th International Conference on the Engineering of Sport, Biarritz, France, 2008.

- Spenkuch, T., Turnock, S.R., Scarponi, M., Shenoi, R.A., 'The Use of CFD in Modelling Blanketing Effects for Yacht Race Simulations', 11th Numerical Towing Tank Symposium, Brest, France, 2008.

- Spenkuch, T., Turnock, S.R., Scarponi, M., Shenoi, R.A., 'Lifting Line Method for Modelling Covering and Blanketing Effects in Yacht Fleet Race Simulation', 3rd High Performance Yacht Design Conference, Auckland, New Zealand, 2008.

- Spenkuch, T., Turnock, S.R., Scarponi, M., Shenoi, R.A., 'Real time simulation of tacking yachts: how best to counter the advantage of an upwind yacht', 8th International Conference on the Engineering of Sport, Vienna, Austria, 2010.

- Banks, J., Webb A., Spenkuch, T., Turnock, S.R., 'Measurement of dynamic forces experienced by an asymmetric yacht during a Gybe, for use within sail simulation software', 8th International Conference on the Engineering of Sport, Vienna, Austria, 2010.

- Spenkuch, T., Turnock, S.R., Scarponi, M., Shenoi, R.A., ‘Lifting Line Theory Use for Modelling Covering and Blanketing Effects in a Yacht Fleet Race Simulator Environment’, Marine Science and Technology Journal Springer, Tokyo, 2011.

- Spenkuch, T., Turnock, S.R., Scarponi, M., Shenoi, R.A., ‘Simulation of tactical upwind yacht racing: a Bayesian believe network extended Decision Field Theory approach for modelling decision-making of sailors in dynamically changing yacht fleet racing environment’, Psychology of Sport and Exercise Elsevier, submission planned in 2014.